THE ANTIPROLIFERATIVE STUDY OF QUERCUS INFECTORIA GALLS CRUDE AND MICELLE EXTRACT HYDROGEL BEADS AGAINST SELECTED BREAST CANCER CELLS

WAN NUR SUZILLA BT WAN YUSUF

DOCTOR OF PHILOSOPHY

UNIVERSITI MALAYSIA PAHANG
AL-SULTAN ABDULLAH

UNIVERSITI MALAYSIA PAHANG AL-SULTAN ABDULLAH

DECLARATION OF THESIS AND COPYRIGHT

Author's Full Name : WAN NUR SUZILLA BT WAN YUSUF

Date of Birth : 31 JULY 1987

Title : THE ANTIPROLIFERATIVE STUDY OF QUERCUS INFECTORIA GALLS CRUDE AND MICELLE EXTRACT HYDROGEL BEADS AGAINST SELECTED BREAST CANCER CELLS

Academic Session : SEMESTER II 2023/2024

I declare that this thesis is classified as:

☐	CONFIDENTIAL	(Contains confidential information under the Official Secret Act 1997)*
☐	RESTRICTED	(Contains restricted information as specified by the organization where research was done)*
☑	OPEN ACCESS	I agree that my thesis to be published as online open access (Full Text)

I acknowledge that Universiti Malaysia Pahang Al-Sultan Abdullah reserves the following rights:

1. The Thesis is the Property of Universiti Malaysia Pahang Al-Sultan Abdullah
2. The Library of Universiti Malaysia Pahang Al-Sultan Abdullah has the right to make copies of the thesis for the purpose of research only.
3. The library has the right to make copies of the thesis for academic exchange.

Certified by:

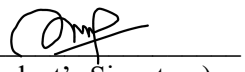

(Student's Signature)

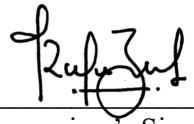

(Supervisor's Signature)

New IC/Passport Number
Date: 31/07/2024

ASSOC. PROF. TS. DR RAIHANA ZAHIRAH BINTI EDROS
Name of Supervisor
Date: 31/07/2024

NOTE: * If the thesis is CONFIDENTIAL or RESTRICTED, please attach a thesis declaration letter.

SUPERVISOR'S DECLARATION

I/~~We~~* hereby declare that I/~~We~~* have checked this thesis/project* and in my/~~our~~* opinion, this thesis/~~project~~* is adequate in terms of scope and quality for the award of the degree of *Doctor of Philosophy/ ~~Master of Science~~.

(Supervisor's Signature)

Full Name : ASSOC. PROF. TS. DR RAIHANA ZAHIRAH BINTI EDROS

Position : ASSOCIATE PROFESOR

Date : 31/07/2024

STUDENT'S DECLARATION

I hereby declare that the work in this thesis is based on my original work except for quotations and citations which have been duly acknowledged. I also declare that it has not been previously or concurrently submitted for any other degree at Universiti Malaysia Pahang Al-Sultan Abdullah or any other institutions.

(Student's Signature)

Full Name : WAN NUR SUZILLA BT WAN YUSUF

ID Number : PET17011

Date : 31/07/2024

THE ANTIPROLIFERATIVE STUDY OF QUERCUS INFECTORIA GALLS CRUDE AND MICELLE EXTRACT HYDROGEL BEADS AGAINST SELECTED BREAST CANCER CELLS

WAN NUR SUZILLA BT WAN YUSUF

Thesis submitted in fulfillment of the requirements

for the award of the degree of

Doctor of Philosophy

Faculty of Chemical and Process Engineering Technology

UNIVERSITI MALAYSIA PAHANG AL-SULTAN ABDULLAH

JULY 2024

ACKNOWLEDGEMENTS

Alhamdulillah, with Allah s.w.t blessing, finally I'm managed to finish my study. First and foremost, I would like to show my gratitude to Universiti Malaysia Pahang Al-Sultan Abdullah (UMPSA), particularly Faculty of Chemical and Process Engineering Technology (FTKKP), Institute of Postgraduate Studies (IPS) and Centre of Excellence for Advanced Research in Fluid Flow (CARIFF) for giving me the opportunity to further my study in Doctor of Philosophy (Engineering Technology) and providing the facilities as well as financial supports (RDU 150379, RDU 170130, RDU 1803181, and PGRS 190396), Graduate Research Assistant (SPPS) and Fellowship Scheme.

My deepest appreciation also goes to my supervisor, Assoc. Prof. Ts. Dr Raihana Zahirah binti Edros, and Dr. Rajaletchumy Veloo Kutty for their guidance, patience, and moral supports in supervising me throughout my journey in completing my research and writing thesis. Not to forget my co-supervisor, Dr Syed Mahmood who also helped me to complete this study. Their passion and determination to science always inspire me to greater efforts. My special appreciation also dedicated to all Universiti Malaysia Pahang Al Sultan Abdullah (UMPSA) staffs, especially lab and technical staff, Mr Fazli, Mr Razhan, Mr Hashim, Mr Zaki, Mr Khairil and all whom I appreciate their great help and services.

Not to forget, many thanks to all my lab collegues for their kind advice and assistance: Mrs Issttifa Iyah Aminuddin, Ms Kong Yee Tong, Dr Rahimah Embong, Dr Rubaiyi Mat Zaid, Mrs Siti Noredyani, Ms Raihan Izzatie and others for their endless moral supports.

Finally, I would like to thank my husband, Mr Mohamad Ridhwan Ruslan for his love, patience, advice, understanding and moral supports until I completed my study. To my beloved parents, late Mr Wan Yusuf Wan Ahmad and Mrs Supiabi Maiden, your love and support have brought me to this level. Lastly, thank you so much for all involved in my journey of completing my study.

ABSTRAK

Manik hidrogel digunakan dalam kajian saintifik untuk menyiasat potensi ekstrak semulajadi dalam menghalang pertumbuhan sel kanser. Mereka menyediakan kestabilan dan pengangkutan dengan memerangkap ekstrak dalam rangkaian hidrogel, bagi memastikan sifat antiproliferasi. Mereka juga boleh direka untuk pelepasan terkawal, bagi memastikan kesan antiproliferatif yang konsisten. Tambahan pula, mereka boleh mencegah penggumpalan dan memastikan penyebaran seragam ekstrak, dan berpotensi meningkatkan keberkesanan. Oleh itu, dalam kajian ini, manik hidrogel *Quercus infectoria* (QI) menggunakan ekstrak QI mentah dan misel telah dibangunkan untuk mengatasi masalah agregasi dan kestabilan misel serta sebagai alternatif baru dalam rawatan kanser. Ekstrak mentah biji QI dihasilkan menggunakan ekstraksi macerasi dengan 70% campuran etanol dan air manakala misel yang mengandungi ekstrak mentah biji QI diformulasi menggunakan kaedah casting pelarut dan kemudian kedua-dua ekstrak dianalisis untuk sifat fizikal dan kimia mereka. Kemudian, ekstrak mentah biji QI dan ekstrak misel dimasukkan ke dalam manik hidrogel melalui tindakan pautan silang antara polimer (pektin) dan penghubung silang (zinc asetat). Semua ekstrak mentah, misel dan manik hidrogel diuji terhadap sel-sel kanser payudara yang terpilih (MCF-7 dan MDA-MB-231) untuk menentukan aktiviti antiproliferatif menggunakan MTT Assay serta untuk aktiviti apoptosis melalui pewarnaan FITC-Annexin V. Daripada penemuan, ia diperhatikan bahawa ekstrak mentah biji QI, misel dan manik hidrogel menunjukkan aktiviti antiproliferatif yang baik terhadap sel kanser payudara (MCF-7 dan MDA-MB-231) tetapi tidak menunjukkan sitotoksisiti terhadap sel normal, L929 selain menginduksi mekanisme kematian sel melalui apoptosis. Semua misel yang diformulasi menunjukkan julat saiz yang baik (di bawah 20 nm), dengan nilai indeks polydispersiti (PDI) antara 0.1-0.4 yang menunjukkan penyebaran sempit dan bercas negatif. Berdasarkan analisis kimia permukaan, ia didapati bahawa semua misel yang dihasilkan, mempunyai nisbah relatif hampir serupa antara ikatan kimia yang disyorkan dan selaras dengan yang dilaporkan dalam vitamin E tulen TPGS. Untuk pemuatan ekstrak, ia menunjukkan bahawa *Quercus infectoria* Vitamin E TPGS (QIT) misel memberikan muatan tertinggi (110.41 µg / ml) berbanding dengan misel lain dan morfologi permukaan oleh Transmission Electron Microscope (TEM), menunjukkan semua misel yang diformulasi adalah dalam keseragaman sederhana dengan bentuk hampir bulat. Profil pelepasan ekstrak terkawal menunjukkan semua misel mempamerkan corak pelepasan biphasik manakala penyerapan selular meningkat dengan masa inkubasi yang lebih panjang. QIT misel menunjukkan aktiviti sitotoksik tertinggi (IC_{50} 8.28±0.82 µg/ml) terhadap sel-sel MCF-7 dengan permulaan tindakan yang lebih cepat berbanding dengan MDA-MB-231 (IC_{50}, 11.09±0.73 µg / ml) dan mekanisme kematian sel apoptotik yang diinduksi tanpa kesan toksik terhadap sel normal, L929. Untuk formulasi manik hidrogel, dua hidrogel yang berbeza telah diformulasikan, menggunakan ekstrak biji QI mentah (QIC) dan misel (QIM). Daripada penemuan, ia menunjukkan kedua-dua formulasi menunjukkan hasil, morfologi, keupayaan mengembang, masa mengembang dan kandungan kelembapan (di bawah 20%) yang baik. Sebagai kesimpulan, manik hidrogel yang baru mengandungi ekstrak mentah dan dan misel biji QI berjaya diformulasikan dengan aktiviti antiproliferatif yang baik terhadap sel-sel kanser payudara yang terpilih dan melindungi ekstrak dengan menambahbaik kestabilan mereka dan secara berkesan mencegah penggumpalan yang tidak diingini.

ABSTRACT

Hydrogel beads are used in scientific studies to investigate the potential of natural extracts in inhibiting cancer cell growth. They provide stability and transportation by enclosing the extract within a network, ensuring its antiproliferative properties. They can also be engineered for controlled release, ensuring consistent antiproliferative effects. Additionally, they prevent agglutination, ensuring uniform distribution of the extract, and potentially enhancing its efficacy. Hence, in this study, *Quercus infectoria* (QI) galls hydrogel beads incorporated with QI galls crude and micelle extracts were developed to overcome the micelle aggregation and stability problem as well as a new alternative in cancer treatment. QI galls crude extract was produced using maceration extraction with 70% aqueous ethanol while QI galls crude extract loaded micelle was formulated using solvent casting method and then both extracts were characterized for their physicochemical properties. Then, the QI galls crude and micelle extract were incorporated into hydrogel beads via crosslinking action between polymer (pectin) and crosslinker (zinc acetate). All crude extract, micelles and hydrogel beads were tested against selected breast cancer cells (MCF-7 and MDA-MB-231) to determine the antiproliferative activity using MTT Assay as well as for apoptosis activity via FITC-Annexin V staining. From the findings, it was observed that the QI galls crude extract, micelles and hydrogel beads exhibited good antiproliferative activity against breast cancer cells (MCF-7 and MDA-MB-231) but showed no cytotoxicity against normal cell line, L929 apart from induced the cell death mechanism through apoptosis. All formulated micelles showed a good size range (below 20 nm), with polydispersity index (PDI) value between 0.1-0.4 indicating narrow distribution and negatively charged. Based on the surface chemistry analysis, it was observed that all formulated micelles, had almost similar relative ratio amongst the suggested chemical bonds and in accordance with those reported in pure vitamin E TPGS. For extract loading, it was showed that *Quercus infectoria* Vitamin E TPGS (QIT) micelle gave highest loading (110.41 µg/ml) as compared to other micelles and the surface morphology by Transmission Electron Microscope (TEM), showed all formulated micelles were in moderate uniformity with nearly spherical shape. Controlled drug release profile showed all micelles demonstrated biphasic release pattern while the cellular uptake was increased with prolonged incubation time. QIT micelle showed highest cytotoxic activity (IC_{50} 8.28±0.82 µg/ml) against MCF-7 cells with faster onset of action as compared to MDA-MB-231 (IC_{50} 11.09±0.73 µg/ml) and induced apoptotic cell death mechanism with no toxicity effect against normal cells, L929. For the hydrogel beads formulation, two different hydrogel beads were formulated, using QI crude (QIC) and micelle (QIM) extract. From the findings, it was showed both formulated beads, demonstrated good yield, morphology, swelling ability, swelling time and moisture content (below 20%). As conclusion, a novel polymeric hydrogel beads incorporated with QI galls crude and micelle extract with good antiproliferative activity against selected breast cancer cells were successfully formulated and presents a promising strategy for safeguarding the integrity of extracts by improving their stability and effectively preventing undesirable aggregation.

TABLE OF CONTENT

LIST OF TABLES

LIST OF FIGURES

LIST OF SYMBOLS

%	Percentage
<	Less than
>	Higher than
±	About
≤	Less and equal to
≥	Higher and equal to
˚C	Degree Celsius
µg	Microgram
µl	Microlitre
µg/ml	Microgram per millilitre
µm	Micrometre
cells/ml	Cells per millilitre
cm	Centimetre
cm^3	Cubic centimetre
g	Gram
kDa	Kilodalton
L	Litre
M	Molar
mg	Milligram
mg/g	Miligram per gram
mg/ml	Milligram per millilitre
ml	Millilitre
mm	Millimetre
ng/ml	Nanogram per millilitre
nm	Nanometre
U/ml	Units per millilitre
v/v	Volume per volume
w/v	Weight per volume
xg	Relative centrifugal force

LIST OF ABBREVIATIONS

ADME	Absorption, distribution, metabolism, and elimination
$AlCl_3$	Aluminium chloride
ANOVA	One-way analysis of variance
API	Active pharmaceutical ingredients
ATCC	American Type Culture Collection
CMC	Carboxymethyl cellulose
CMC	Critical micelle concentration
DCM	Dichloromethane
DISC	Death-inducing signalling complex
DLS	Dynamic light scattering
DMEM	Dulbecco's Modified Eagle Medium
DMSO	Dimethylsulfoxide
DNA	Deoxyribonucleic acid
DPPH	2,2-diphenylpicrylhydrazyl
EPR	Enhanced permeability and retention
ER	Estrogen receptors
ESCA	Electron spectroscopy for chemical analysis
QIT	*Quercus infectoria* Vitamin E TPGS micelle
TAT	Tannic acid Vitamin E TPGS micelle
GAT	Gallic acid Vitamin E TPGS micelle
TGT	Tannic and Gallic acid Vitamin E TPGS micelle
QIC	*Quercus infectoria* crude extract hydrogel beads
QIM	*Quercus infectoria* micelle extract hydrogel beads
GAE	Gallic acid equivalent
RE	Rutin equivalent
FADD	Fas-associated death domain
FBS	Fetal Bovine Serum
FC	Folin-Ciocalteu
FDA	Food and Drug Administration
GA	Gallic Acid
HER2	Human epidermal growth factor receptor 2
HLB	Hydrophile–lipophile balance

HPLC	High Performance Liquid Chromatography
L929	Normal fibroblast cell line
MCF-7	Michigan Cancer Foundation-7 breast cancer cells
MDA-MB-231	Triple negative breast cancer cell line
MDR	Multidrug resistance
MTT	3-(4,5-dimethylthiazol-2-yl)-2,5-diphenyl-2H-tetrazolium bromide
Na_2CO_3	Sodium carbonate
$NaNO_2$	Sodium nitrite
NCR	National Cancer Registry of Malaysia
NDDS	Novel drug delivery systems
NP	Nanoparticles
PBS	Phosphate buffer saline
PEG	Poly-ethylene glycol
P-gp	P-glycoprotein
PI	Propidium iodide
PR	Progesterone receptor
PS	Phosphatidylserine
PUFA	Polyunsaturated fatty acid
QI	Quercus infectoria
RES	Reticuloendothelial system
SEM	Standard Error of Mean
SPSS	Statistical Package of Social Science
TA	Tannic Acid
TEM	Transmission Electron Microscope
TFC	Total Flavanoid Content
TNBC	Triple negative breast cancers
TNF	Tumor necrosis factor
TPC	Total Phenolic Content
TPGS	D-α-tocopheryl polyethylene glycol succinate
TRADD	TNF receptor-associated death domain
USA	United State of America
USFDA	United State Food and Drug Administration
XPS	X-ray Photoelectron Spectroscopy

CHAPTER 1

INTRODUCTION

1.1 Background of study

Breast cancer is the most common cancer type among women worldwide (Shen et al., 2018). Approximately 1.5 million of new breast cancer cases are reported each year, accounting for 25% of all cancer cases. In 2022, roughly 1.9 million people will be diagnosed with cancer in the United States (Madewell et al., 2020). An estimated 287,850 women and 2,710 men will be diagnosed with breast cancer, which makes it the most common cancer diagnosis. Breast cancer has now overtaken lung cancer as the world's mostly commonly-diagnosed cancer, and is responsible for one in six of all cancer deaths among women, according to statistics released by the International Agency for Research on Cancer (IARC) in December 2020 (Muthu et al. 2021). Just in United State of America (USA) alone, breast cancer is expected to cause about 40, 000 deaths of women in 2017(Khurana et al., 2018)

According to estimates, there are about 100,000 people in Malaysia living with cancer at any one time. The National Cancer Registry of Malaysia (NCR) records 21,773 Malaysians being diagnosed with cancer every year (Wu et al. 2017). In Malaysia, the total number of new cancer cases diagnosed from 2012 to 2016 increased by 11,731 cases when compared to cancer cases diagnosed from 2007 to 2011. The five most common cancers among male in Malaysia are colorectal, lung, nasopharynx, lymphoma, and prostate. Among Malaysian females, the five most common cancers are breast, colorectal, cervical, ovarian and lung (Ministry of Health Malaysia, 2017). Generally, the three most common cancers in Malaysia are breast followed by colorectal and lung (Ministry of Health Malaysia, 2017).

Breast cancer has complex classifications. As for today, breast cancer is often classified based on histopathologic type. The majority of breast cancer cases are invasive ductal carcinoma, but other sub-types still getting attention because of their aggressiveness and occurrence in different patient subpopulations (MacPherson et al., 2019). Currently, patient diagnosed with breast cancer are often given standard treatment that involves surgery, radiation therapy and drug therapy (MacPherson et al., 2019). Usually, the surgery and radiation therapy are used mainly for eradicating the primary breast tumour and loco regional cancerous tissues (Greenlee et al., 2017). Their value tends to decline as cancer progresses and metastasizes. In this current study, the focus is the drug therapy. Drug therapy serves to reduce the tumour burden and prevent, control or treat cancer metastasis (Greenlee et al., 2017). Breast cancer drug therapy often consists of hormonal therapy and chemotherapy. Hormone therapy is the use of hormone-like drugs to suppress cancer cell proliferation, whereas chemotherapy is the use of cytotoxic compounds to kill cancer cells (Greenlee et al., 2017). However, chemotherapy have limited survivability and possess various negative side effect as well as drug resistance problem. Hence, current available therapies are inadequate and spur demand for improve technologies (Rasha et al., 2019). Therefore, there is a continuous search for novel therapeutic agents with fewer side effects. Rapid growth in nanotechnology towards the development of nanomedicine products holds greats promise to improve therapeutic strategies against cancer (Rasha et al., 2019). Nanomedicine represents an opportunity to achieve sophisticated targeting strategies and multi-functionality (Rasha et al., 2019).

Nanomedicine refers to the biomedical application of materials with at least one dimension below 100nm (Lu et al., 2018). Examples of nanomedicine range from liposomes, micelles, nanoparticles, dendrimers and nanotubes (Lu et al., 2018). They can be made of diverse materials including lipids, phospholipids, polymers, protein, inorganic materials and a combination of them (Lu et al., 2018). Some of the nanomedicine, such as liposomes (e.g: Doxil, Titusville) and nanoparticles (e.g: Abraxane) are already widely used for clinical treatment of breast cancer with success (Thapa & Kim, 2023). Nanomedicine can serve a broad range of functions for cancer patients besides treatment including tissue repairing, disease detection, cancer imaging and theranostic (Thapa & Kim, 2023). Among the novel drug delivery systems using nanoparticles, micelles are an important one. Micelles are microscopic spheres formed by amphiphilic molecules

(having both water-loving and water-hating parts) that self-assemble in an aqueous environment. The water-hating tails cluster inwards, forming a core, while the water-loving heads face outwards, interacting with the water. This structure allows micelles to solubilize hydrophobic (water-insoluble) compounds like some bioactive components found in natural products. Micelles also can be used to target herbal medicine to the cancer sites which improve the selectivity, drug delivery effectiveness and safety thereby reduce doses and increases patient compliance . (Thapa & Kim, 2023).

However, micelles were formulated using wet synthesis and stored under aqueous environment in the form of liquid suspension (Mahasawat et al., 2019). Particles suspended in liquids tend to aggregate, which ultimately results in their separation and settling due to gravity. However, aggregation is considered a significant mechanism that is responsible for the increased thermal conductivity observed in nanofluids. Some level of consolidation in a nanofluid may be advantageous. (Liyanage et al., 2016). This can cause the micelles become aggregated during storage and at the same time will lose their nanoscale-associated physical and chemical properties (Mahasawat et al., 2019). One promising strategy that can be used to prolong the shelf life of the nanoparticle is by encapsulating the nanoparticles into a polymer matrix where this matrix can serve as a stabilizing agent for the nanoparticles (Mahasawat et al., 2019). Various natural polymer such as pectin, chitosan, alginate as well as synthetic polymer such as polyvinyl alcohol that can be used as the encapsulating agent for the nanoparticles. This encapsulating system of the micelle and the crude plant extract is known as the hydrogel beads, which was formulated by using crosslinking method between the polymer and crosslinker (Surini & Diandra, 2017).

In recent decades, the use of herbal drugs has significantly increased which is evident from the increased global market for herbal medicines (Thapa & Kim, 2023). The usage of herbal medicines has grown because of their therapeutic advantages. However, the use of novel drug delivery systems for the formulation of herbal medicines is slow when compared to the complexity of the active constituents (Bilia et al., 2018). Although several formulations for herbal drugs have been developed and they have demonstrated efficacy similar to that of chemically synthesized modern drugs, a lot of studies need to be conducted (Bilia et al., 2018).

In this current study, a common local herb, namely *Quercus infectoria* (QI) galls has been selected due to its wide usage and medicinal benefit in traditional practices worldwide, particularly among Malaysian women (Jiayu Gao et al., 2018). *Quercus infectoria* galls, also known as Aleppo galls or gallnuts, are a natural source of tannins, with gallic acid being the most abundant. Tannins have been shown to possess various biological properties, including antiproliferative and anticancer effects. In addition, several scientific evidences have demonstrated a broad range of pharmacological properties associated with this plant, including anti-inflammatory, antioxidant, antidiabetic, larvicidal, antibacterial, antifungal and anticancer properties (Jiayu Gao et al., 2018). Several studies have investigated the antiproliferative effects of *Quercus infectoria* galls extracts against various cancer cell lines. However, there is limited research on the efficacy of *Quercus infectoria* galls extracts in micelle and hydrogel bead form for drug delivery to target cancer cells and the comparison of the antiproliferative activity of crude, micelle extract and hydrogel beads of *Quercus infectoria* galls against cancer cells. This research aims to address these gaps by investigating the antiproliferative effects of crude and micelle extract of *Quercus infectoria* galls encapsulated in hydrogel beads against selected breast cancer cells. This approach also could lead to a novel drug delivery system for *Quercus infectoria* galls extracts with improved stability and efficacy against breast cancer cells.

1.2 Problem statement

Cancer is a major public health issue in most developed countries; however, there have been significant improvements in patient survival rates over the last three decades because of early detection and advancements in medical treatment (Jantamat et al., 2019). A significant number of cancer patients receive chemotherapy or chemoradiotherapy and benefit from anticancer drug treatment. However, due to their toxic effects on normal cells/tissues, anticancer drugs cause a wide range of side effects, including nausea, vomiting, anorexia, diarrhea, oral mucositis, and numbness. These side effects frequently impair patients' quality of life (QOL) and make it difficult to continue with chemotherapy or chemoradiotherapy (Bourhia et al., 2019). Although many valuable strategies for treating or preventing these side effects have been developed, they are still insufficient (Bourhia et al., 2019). As a result, a novel or alternative approach to treating or preventing these side effects is required.

However, there are limitations for herbal or natural products extract because most of the herbal active constituents are poorly water-soluble because of their hydrophobic nature. This property leads to decreased bioavailability and increased systemic clearance thus necessitating repeated administration or increased dose, and thus limits the clinical use of herbal medicines (Thapa & Kim, 2023). Therefore, nanoparticles can be utilized to increase the herbal drug solubility and help to localize the drug at a specific site and resulting in better efficacy and improved patient compliance (Thapa & Kim, 2023).

The extremely large surface area-to-volume ratio of nanocarriers provides an opportunity to manipulate their surface properties for improved treatment, for example, cancer targeting, extended circulation, increased endocytosis and transcytosis, in order to gain more efficient access into tumour sites, metastatic sites and cancer cells (Korin et al., 2018). Moreover, by entrapping in or binding onto nanocarriers, the therapeutic agents can also gain better stability, increased solubility, and controlled release kinetics. Drug combinations may also be co-delivered for increased synergistic or additive anticancer effects (Korin et al., 2018). However, the nanoparticles can be aggregated during the storage time thus will reduce in stability. In order to overcome this, this formulated nanoparticles may be encapsulated into a polymer matrix to improve the stability as well as the shelf life (Mahasawat et al., 2019). This system or also known as hydrogel beads have been widely used in applications such as biomedical materials, drug delivery system and also food packaging (Mahasawat et al., 2019).

Hence, by using QI galls as the natural source, this study aimed to develop a novel natural drug delivery system in the forms of hydrogel beads. This formulated hydrogel beads were incorporated with QI galls nanoparticle and crude extract that will selectively deliver the therapeutic agent into the breast cancer cells and simultaneously provide a continuous monitoring of the effectiveness of the therapeutic agent. Besides that, a study into the molecular event on the cellular uptake and the behaviour of the chemotherapeutic agent intracellular would reveal the killing mechanisms possessed by the QI galls extract. The use of this extract as the anticancer agent should improve the therapeutic effect while reducing the unwanted side effects to the healthy cells.

1.3 Research objectives

This study was composed of few objectives which are:

1. To investigate the phytochemicals profiling and the cytotoxic effect of the QI galls crude extract against selected breast cancer cells.

2. To develop a novel system of QI-loaded Vitamin E TPGS micelles (QIM) followed by the characterization of micelle physicochemical properties such as particle size, surface chemistry, surface morphology, drug loading, drug release an antiproliferative effect against selected breast cancer cells.

3. To formulate hydrogel beads incorporated with QI galls nanoparticle and crude extract for a better stability followed by the characterization of the hydrogel beads physicochemical properties.

1.4 Research hypothesis

It is hypothesised that the development of hydrogel beads incorporated with QI galls-loaded Vitamin E TPGS micelle (QIM) and crude extract (QIC) will improve the stability of the micelle and solubility of the crude extract as well as delivery into cancer cells, thus improving the antiproliferative activity against selected breast cancer cells.

1.5 Scope of research work

This research is primarily focused on evaluating the antiproliferative properties of *Quercus infectoria* galls crude and micelle extract incorporated in hydrogel beads on the cancer cells, specifically targeting breast cancer cells. The scope encompasses the following key dimensions which the first phase of the study related to the first research objective involved the phytochemical screening of bioactive compounds (phenolics and flavonoids), antiproliferative activity, and apoptosis assay of the QI galls crude extract. The phenolic contents were determined by using Total Phenolic Content (TPC) method while for the flavonoid content by using Total Flavonoid Content (TFC) method. The antioxidant activity of the QI gall crude extract was analysed by the 2,2-diphenylpicrylhydrazyl (DPPH) scavenging method. The antiproliferative activity of the crude extract against breast cancer cells was determined by 3-(4,5-dimethylthiazol-2-yl)-2,5-diphenyl-2H-tetrazolium bromide (MTT) assay. Cell death mechanism of cells is

determined by using FITC-Annexin V staining apoptosis assay. Two types of breast cancer cells utilised in antiproliferative and cell death mechanism assay which were MCF-7 and MDA-MB-231 cell lines.

The second phase of the study related to the second research objective, which involved the characterization of the physicochemical properties followed by the antiproliferative activity and apoptosis assay of the micelle. Particle size and size distribution of the micelle was measured by dynamic light scattering in aqueous medium. The surface charge was determined by Zetasizer. The shape and surface morphology of the micelles were visualized using Transmission Electron Microscope (TEM). The surface chemistry of the micelles was analysed by X-ray Photoelectron Spectroscopy (XPS). For the drug loading and drug release profile, both was determined by High Performance Liquid Chromatography (HPLC). Then, the molecular event of the cellular uptake behaviour and cytotoxicity study of the developed nanoparticles in *vitro* that was determined by quantitative study. The antiproliferative activity of the micelle against breast cancer cells was determined by MTT assay and apoptosis was determined by using FITC-Annexin V staining.

Next, the third phase of the study related to the third research objective which involved the physicochemical characterization followed by the antiproliferative activity of the hydrogel beads. The physicochemical properties that were evaluated was the yield, shape and morphology, particle size distribution, swelling ability, swelling time, moisture content, encapsulation efficiency and antiproliferative activity against breast cancer cells (MCF-7 and MDA-MB-231). However, some limitations were acknowledged for this research which the use of only in vitro models, and the potential need for further in vivo investigation. Besides that, the safety and efficacy of the extract or delivery system in humans are not addressed within this research scope. This current study was focused on the formulation ad the antiproliferative potential of the QI galls crude and micelle extract hydrogel beads regardless of its final dosage formulation.

CHAPTER 2

LITERATURE REVIEW

2.1 Introduction

Breast cancer is cancer that develops from breast tissue (Sun et al., 2017). It is the most common invasive cancer in women. 1 in 8 women in the United States was diagnosed with breast cancer in her lifetime. In 2024, an estimated 310,720 women and 2,800 men will be diagnosed with invasive breast cancer. Breast cancer commonly develops in cells lining in the milk ducts and the lobules that supply the ducts with milk.

Medical treatment of breast cancer with anticancer drugs such as tamoxifen or raloxifene may prevent breast cancer in those who are at high risk of developing it (Waks & Winer, 2019). Recent breakthroughs have improved early detection, diagnosis, treatment, and survival of breast cancer, leading to substantial advancements in the field. One of the promising approaches that might improve the therapy's option and efficacy is nanoparticles. Nanoparticles have a variety of features, including a tiny size, the capacity to carry different medicines, a high surface area, and the potential to enhance conjugated absorption. As a result, nanoparticle are thought to be effective tumour-targeting vehicles (Tong et al., 2018). Nanomedicine is an attractive field of translational medicine that can be used against metastatic breast cancer (Afzal et al., 2021). Various forms of tumour or metastases-targeting nanomedicine have been attempted to address this need and this field is expected to drive therapeutic research forward (Afzal et al., 2021). Nanomedicine offers numerous benefits over other options, which include targeted delivery to the desired sites, the capability to load single or more therapeutic agents and, and the ability to overcome solubility and stability issues (Tran et al., 2017). However, one of the limitations of using nanoparticles is the stability in colloidal suspension. This problem can be overcome through encapsulation of this nanoparticle in hydrogel beads. Hydrogel

beads offer a versatile platform for delivering nanoparticles with improved efficacy, safety, and targeting compared to free nanoparticles. This makes them a valuable tool in various applications such as drug delivery.

Besides, this approach also can channel the active constituents of the herbal or plant drug to the site of action (Prof. Shriniwas Mane et al., 2023). There are many advantages of encapsulating this herbal or plant crude and nanoparticle extract in hydrogel beads including enhancement of solubility and bioavailability, protection from toxicity, enhancement of pharmacological activity, improvement in stability, improving tissue macrophages distribution, sustained delivery and protection from physical and chemical degradation (Prof. Shriniwas Mane et al., 2023). Furthermore, this system also can carry the optimum amount of the drug to the site of interest bypassing all the biological barriers and increased prolonged circulation of the drug in the blood stream due to their small size (Prof. Shriniwas Mane et al., 2023).

One of the potential herbs, *Quercus infectoria* (QI) or locally known as "manjakani" was utilized in this study. *Quercus infectoria* galls, or gallnuts, are growths on oak trees triggered by insects. Traditionally the QI galls used in medicinal practice, but recent research suggests they hold promise as antiproliferative agents. This gall extract is rich in tannins, flavonoids, and gallic acid, compounds with antioxidant and potential cell growth inhibitory properties. These compounds might act by reducing free radical damage or interfering with cancer cell division or survival. Hence, in this current study the galls crude and micelle extract were incorporated into hydrogel beads and analysed for their antiproliferative activity.

2.2 *Quercus infectoria* (QI)

Quercus infectoria (QI) is a small tree or shrub belonging to *Fagaceae* (*Quercaceae*) family (Fateh et al., 2017). The plant is found in Turkey, Syria, Persia, Cyprus, and Greece. The various QI species originated in Iran, Iraq and Turkey, but now widespread and particularly common in Asia, Europe and North Africa (Fateh et al., 2017). Galls are irregular plant growth, which is stimulated by the reaction between plant hormones and powerful growth regulating chemicals produced by insects or mites (Fateh et al., 2017). The QI galls are produced by the insect, *Cynips quercufolii*, for depositing its egg (Fateh et al., 2017).

The stem are crooked, shrubby looking with smooth and bright-green leaves borne on short petioles of 1 to 1.5 inches long (Salleh et al., 2015). The leaves are bluntly mucronate, rounded, smooth, unequal at the base and shiny on the upper side. The galls shape is rounded, hard body with 1-1.5cm in diameter. The numerous horny protuberances on the external surface giving it a rough touch (Salleh et al., 2015). Appear as greyish brown to brownish black on its external and yellow in colour of the inner surface. The present of pores on its uneven surface indicates infection (Figure 2.1).

Quercus infectoria (QI) galls have been used in traditional medicine in Asia for centuries (Jiayu Gao et al., 2018). For millennia, QI galls have been utilized as traditional remedies in Western and Eastern cultures to treat inflammatory conditions such as dysentery and diarrhea, stomachaches, toothaches, and tooth decay. They have also been used in postpartum care, to fight metabolic abnormalities, and to treat diseases related to oxidative stress. In recent years, there has been an increased interest in natural products for disease prevention and treatment. QI galls have been studied for their biological effects in vitro and in vivo, attributed to their high antioxidant phenolic content. Compared to medications, QI galls have the potential to be more effective and have fewer negative effects and adverse responses while also being less expensive for the public due to their significant antioxidant phytochemicals.

Figure 2.1: The physical morphology of QI galls

Source: Suzilla (2017)

2.2.1 Phytochemical and bioactive components of *Quercus infectoria* (QI) galls

The main constituents found in the galls of QI are tannic acid (50-70%) and a small amount of free gallic and ellagic acid (Fateh et al., 2017). The galls major compound is tannin which is also known as gallotannic acid. This is a complex mixture of phenolic acid glycosides varying greatly in composition (Ismail et al., 2021). The galls also contain sugar, gum, and essential oil. The previous study revealed that the ethanolic extract of QI galls gave positive results for tannin, flavonoids, saponins, triterpenes, anthraquinones, and coumarin. The various phytochemical compounds detected are known to have beneficial importance in medicinal science. Furthermore, QI gall contains trace amounts of beta-sitosterol, amenoflavone, hexamethyl ether, isocryptomerin, calcium oxalate, methyl oleanolate, gum, sugar, and essential oil (Kamarudin, Muhamad, et al., 2021).

2.2.1.1 Tannic acid

Tannins are polyphenolic compounds with carbohydrates as their backbone. Tannins are divided into two types: hydrolyzable and non-hydrolyzable, often known as condensed tannins. Hydrolysable tannins are made up of a central core polyhydric alcohol, such as hydroxyl groups, that are partially or completely esterified with gallic acid (gallotannins) or hexahydroxydephenic acid (ellagitannins). The hydrolysis of gallotannins produces glucose and gallic acid. Tannic acid is a particular tannin made up of ten galloyl (3, 4, 5-trihydroxyphenyl) units surrounding a glucose core. However, natural tannic acid is composed of 2-12 galloyl moieties. Tannic acid, which is a combination of glucose gallic acid esters, is a common ingredient in many meals. Tannic acid, one of the plant's most abundant reserves, is a gall tannin made up of gallic acid and glucose esters, with galloyl groups immediately esterified to the glucose molecule. Tannic acid is beneficial to health because of its chemopreventive effects on carcinogenesis and mutagenesis (Ismail et al., 2021).

Tannic acid has been discovered to reduce cancers generated by chemical carcinogens in the skin, stomach, and lungs. Tannic acid activity has been linked to decreased carcinogen activation via cytochrome P450 inhibition, electrophilic trapping, and arachidonic acid metabolism modification. Tannic acid has previously been shown to directly impede the formation of cancer cells, in addition to acting as a possible

chemopreventive option. Tannic acid is also thought to increase the efficacy of herbal medications. Tannic acid has been shown in vitro to suppress proliferation in various types of cancer cells and induce apoptosis. Tannic acid has been found in an animal model study to have a chemopreventive effect against cancer, including hairless mice, and to be able to block around 70% of the development of ultraviolet-induced skin tumors. Tannic acid shows anticancer action and cancer defense against several cancer forms, including the disease produced by chemical insulation. Tannic acid was also discovered to be a powerful chemosensitizer to counteract multidrug resistance (Ismail et al., 2021).

Furthermore, tannic acid inhibits cancer promotion and progression by inducing cell cycle arrest and apoptosis of cancer cells, as well as inhibiting cancer cell proliferation, angiogenesis, migration, invasion, and colony formation. Furthermore, tannic acid acts as a carrier element in an anticancer drug delivery system, influencing chemo sensitization, multidrug resistance, and inhibiting epithelial-to-mesenchymal transition. Numerous studies have shown that tannic acid suppresses growth in multiple types of cancer cells in vitro and that apoptosis causes cancer cell death. In another study, in mice, tannic acid prevented skin, lung, and stomach cancers produced by polycyclic aromatic carcinogens and N-methyl-N-nitrosourea. Tannic acid also caused cell death by apoptosis and cell cycle arrest, which reduced colony formation and size, as well as cell migration and adhesion. Tannic acid also has an anti-glioma impact in vivo, as it reduces tumour volume while increasing intra-tumoural necrosis and lymphocyte infiltration without producing systemic harm (Ismail et al., 2021).

Besides that, tannins are reported to possess physiological astringent and hemostatic properties, which hasten wound healing and ameliorate inflamed mucus membranes and also inhibit the growth of microorganisms by precipitating microbial protein and making nutritional proteins unavailable for them (Ismail et al., 2021). Tannins have also been shown to exert various physiological effects, such as accelerating blood coagulation, lowering blood pressure, decreasing serum cholesterol levels, producing liver necrosis, modulating immune responses, and exhibiting significant antioxidant potential (Kamarudin, Muhamad, et al., 2021). Tannic acid, the most abundant phytochemical found in QI galls, is closely associated with the biological consequences caused by QI galls, as previously shown(Kamarudin, Nik Salleh, et al., 2021).

2.2.1.2 Gallic acid

Gallic acid (3,4,5-trihydroxy benzoic acid), a naturally occurring polyphenol found primarily in plant-based foods such as tea, grapes, berries, nuts, and wine, is infamous for its anticarcinogenic effects against multiple types of cancerous cells, including cervical cancer, making this compound an important biomolecule for therapeutic purposes. Gallic acid inhibits cell growth and death in HeLa cells in a dose-dependent manner, with an IC50 of 80 μM using MTT assay. It also induces apoptosis, as evidenced by an increase in annexin-positive cells and caspase inhibitor-tested results (Ismail et al., 2021).

Besides that, after 24 and 72 hours of treatment, gallic acid caused a decrease in mitochondrial membrane potential (MMP) in HeLa cells. Exposure to 100 μM gallic acid for 24 hours resulted in a 75% reduction in MMP levels relative to the control group. Further investigation revealed that gallic acid-induced cell death was accompanied with an increase in reactive oxygen species (ROS) levels and glutathione (GSH) depleted cells in HeLa cells. Subsequent study by Zhao and Hu further validated its anti-cancer potential by drastically reducing the viability of cervical cancer cells (HeLa and HTB-35) in a dose-dependent manner at 5, 10, and 15 μg/ml concentrations, with 92%, 84%, and 66% growth inhibition, respectively. Gallic acid at doses of 10, 15, and 20 μg/ml inhibited cell migration by 73%, 40%, and 34% in HeLa cells and 45%, 22%, and 17% in HTB-35 cells, respectively, compared to the control group(Ismail et al., 2021).

Gallic acid demonstrates anticancer efficacy by targeting multiple pathways involved in oncogenesis. Gallic acid regulates apoptosis through two key pathways: death receptor-mediated (extrinsic) and mitochondrial-mediated (intrinsic). Caspases are protease enzymes that play an important role in both apoptosis routes. When activated, caspases cause cell death by deactivating anti-apoptotic proteins, inhibiting DNA replication, and reorganizing the cytoskeleton. Caspase-3, the most significant caspase executioner, interacts with caspase-8 and caspase-9 to regulate the extrinsic and intrinsic apoptosis pathways, respectively(Ismail et al., 2021).

2.2.1.3 Ellagic acid

Ellagic acid (2,3,7,8-tetrahydroxy-chromeno[5,4,3-cde] chromene-5,10-dione) has been proposed as a cancer chemopreventive drug for colon, breast, prostate, cutaneous, esophageal, and osteogenic sarcoma. Other properties, such as radical scavenging activities and antiviral activities, have been described for ellagic acid. Early investigation on the cytotoxic and anti-proliferative properties of ellagic acid in cancer cells, including HUVEC, HEL 299, Caco-2 colon, MCF-7 and Hs 578T breast, and DU 145 human prostate cancer cells revealed that ellagic acid caused specific cytotoxicity against the cell lines in a dose-dependent manner. After 24 hours of incubation, treatment with ellagic acid at concentrations ranging from 10-100 µmol/L had no effect on normal fibroblast cells. Instead, an increase in adenosine triphosphate (ATP) bioluminescence of 18-21% was detected, indicating enhanced mitochondrial activity. In contrast, ellagic acid at 1-100 µmol/L concentration showed anti-proliferative effects against Caco-2, MCF-7, Hs 578T, and DU 145 cancer cells, with IC50 values of 37 µmol/L, 72 µmol/L, 59 µmol/L, and 42 µmol/L, respectively. At this concentration, ATP levels were reduced by about 50%, which was related with a loss in cell viability as seen by morphological alterations in cells exposed to the high concentration of ellagic acid. In addition, ellagic acid inhibited angiogenesis by lowering the levels of angiogenic factors MMP-2, MMP-9, and VEGF165 (Ismail et al., 2021).

According to reports, ellagic acid at 50 µmol/L significantly reduced MMP-2 and MMP-9 activity in all cells to less than 50% compared to the control. As the concentration climbed to 100 µmol/L, their activity decreased to less than 40% of the control. Low VEGF165 levels were seen in all cells treated with 100 µmol/L of ellagic acid. The findings convincingly revealed ellagic acid's chemopreventive effects, suggesting that it might be employed as a natural anticancer agent in cancer treatment. Furthermore, regulation of apoptosis by ellagic acid was demonstrated via caspase-3 activation and a shift in Bax/Bcl-2 balance where an increased in Bax pro-apoptotic protein level resulting in the decrease of Bcl-2 anti-apoptotic protein, a key event in the mitochondrial-mediated (intrinsic) apoptosis pathway.

A recent study by Guo et al. found that ellagic acid had a dose-dependent anti-invasive and anti-proliferative action on human cervical carcinoma (HeLa) cells. The study found that ellagic acid treatment at 2.5, 5.0, and 10.0 µM doses reduced the invasion

rate of HeLa cells by 76.43%, 65.54%, and 56.44%. In addition to increasing the rate of apoptosis, ellagic acid administration boosted and lowered the expression of the IGFB7 gene and the AKT/mammalian target of the rapamycin (mTOR) signaling pathway. This data indicates that ellagic acid has anti-cervical cancer activity and hence is a possible candidate for cervical cancer treatment(Ismail et al., 2021).

2.2.2 Pharmacological properties of *Quercus infectoria* (QI) galls

The gall of QI is described in detail in ethnobotanical and literature to possess various pharmacological properties such as analgesic, antidote, anti-inflammatory, antipyretic, antiseptic, anti stomatitis, deodorant, derivative, desiccant, germicidal, hypoglycaemic, astringent, sedative, tonic to teeth and gum, and wound healing. Galls of QI have also been documented to possess antitremorine, anticancer, antibacterial, antifungal, larvicidal, antiviral, and local anesthetic (Ismail et al., 2021).

The ability of QI galls to act as a chemotherapeutic agent has been discovered by previous researchers. Based on *in vitro* study by Hasmah *et al*., (2010) has shown the different antiproliferative activity of different QI gall extracts against cervical cancer (HeLa)and ovarian cancer (Caov-3). Furthermore, another study showed that acetone extract of QI galls demonstrated anticancer activity in 1, 2-dimethyl hydrazine-induced colon cancer (Ramesh, 2013). Besides that, the previous study revealed that QI extract can inhibit melanogenesis in non-toxic concentration (Jamshidzadeh et al., 2017). In traditional Asian medicine, it has been extensively applied for the treatment of infectious diseases, skin disorders, and inflammatory ailments (Chokpaisarn et al., 2017). Several scientific researchers have demonstrated the biological properties of QI galls confirming the traditional use of broad-spectrum antibacterial, anti-inflammatory, and antioxidant (Chokpaisarn et al., 2017).

Another study revealed that the ethanolic extract of QI galls displayed a competent antibacterial activity against most important skin pathogens causing wound infections and can also interfere with the formation of staphylococcal biofilm (Chokpaisarn et al., 2017). It was also reported that QI galls exhibited antioxidant effect through its ability to scavenge free radicals such as DPPH, nitric oxide (NO), superoxide ($O_2^{-)}$, hydrogen peroxide (H_2O_2), and hydroxyl (OH). A recent study also showed that QI gall extract could enhance the wound-healing process of diabetic ulcers by promoting cell

proliferation, re-epithelialization, and granulation tissue formation (Ismail et al., 2021). Therefore, it can be used as a novel alternative treatment for the diabetic wound.

Another study showed that acetone extract of QI galls demonstrated anticancer activity in 1, 2-dimethyl hydrazine-induced colon cancer (Sharba et al., 2020). It is suggested that the anticancer activity of the extracts might be influenced by its antioxidant effect. Previous studies have reported that QI galls exhibited antioxidant effect through its ability to scavenge free radicals such as DPPH, nitric oxide (NO), superoxide (O_2^-), hydrogen peroxide (H_2O_2) and hydroxyl (OH) (Jiayu Gao et al., 2018). Therefore, in this study, QI galls crude extract was tested for their cytotoxic potential against breast cancer cells and then further developed into nanomedicine for a better solubility and bioavailability. Other studies assessed the efficacy of the QI galls in inhibiting the growth of new blood vessels (antiangiogenic activity). The treatments demonstrated that the extract could suppress the formation of new blood vessels, known as angiogenesis. This inhibitory impact is primarily achieved by reducing the levels of key molecules involved in angiogenesis, such as VEGF and MMPs (Taib et al., 2020).

Furthermore, the powder derived from gallnuts of QI galls is utilized to reinstate the flexibility of the uterine wall, as well as to remedy aphthous ulcers (Taib et al., 2020). Additionally, they are frequently employed in Malay traditional medicine to address postpartum wound infections. In India, they are traditionally used for dental applications, such as treating toothaches and gingivitis (Taib et al., 2020). Throughout Asia, it has been extensively employed for the management of infectious infections, dermatological conditions, and inflammatory disorders. In Korean traditional medicine, these herbs are commonly utilized for their therapeutic properties in treating dysentery, diarrhea, and dermatitis (Taib et al., 2020).

However, this QI galls crude extract as well as several plant and herbal extracts have restricted therapeutic efficacy because they are not well soluble in water. Nanomedicine provides a solution through the manipulation of substances at the nanoscale. Nanomedicine enhances solubility by increasing the surface area by the breakdown of particles into nanoparticles, allowing for greater interaction with water. In addition, extracts can be enclosed in water-soluble carriers such as micelles, which protect them and facilitate their distribution throughout the body. Occasionally, the chemical composition of the extract can be altered to enhance its ability to dissolve in

water. The enhanced solubility results in increased absorption by the body, which may result in more effective therapeutic effects with smaller doses. Moreover, nanoparticles can be engineered to provide precise delivery to tissues, thereby minimizing adverse effects and enhancing the overall effectiveness of treatment. Nanomedicine has potential in maximizing the efficacy of herbal treatments, but additional research is required to comprehensively comprehend the enduring safety and efficacy of these pioneering delivery systems.

2.3 Nanomedicine

Nanotechnology is a rapidly expanding field, encompassing the development of materials within 5-200 nanometres (nm) in size. It has a wide range of applications in the fields of engineering, medicine and life science (Germain et al., 2020). Advanced in nanotechnology were utilized in medicine known as nanomedicine for therapeutic drug delivery and treatment for a variety of diseases and disorders. In this mean, the drug is dissolved and entrapped into a biodegradable carrier which is specially designed to absorb drug and protecting it against chemical and enzymatic degradation (Germain et al., 2020). The objective in designing these nanostructures as the delivery system is to release pharmacologically active molecules for site-specific action with accurate dose (Ghotekar et al., 2019). In current years, several biodegradable polymeric nanostructures have attracted the notice with their inherent capacity to target organ/tissue to deliver the drug. These properties in tissue targeting, accessing deep molecular targets and controlling drug release have created a revolution in the field of pharmaceutical sciences (Ghotekar et al., 2019).

As for today, only few nanomedicine products have gained United State Food and Drug Administration (USFDA) approval. Doxil and Abraxane are the two most successful nanoformulations which are widely used for breast cancer treatment in clinical settings (Zhang et al., 2018). Their development and the ways how they are incorporated into the standard drug therapy for cancer treatment also provide good lessons for the nanomedicine researchers and clinicians (Zhang et al., 2018). Doxil® was the first Food and Drug Administration (FDA) approved nanomedicine against metastatic ovarian cancer and AIDS-related Kaposi's sarcoma in 1995, which was formulated to improve the efficacy and reduce the toxicity of doxorubicin therapy (van der Meel et al., 2019). In 2005, Abraxane® was approved to treat metastatic breast cancer and has been shown to

improve tumour uptake of paclitaxel (Jeevanandam et al., 2018). Nanomedicine is also used in the diagnosis of cancer metastasis.

Various nanotechnology has been investigated to increase the bioavailability of the herbal and plant extract due to their poor solubility, stability, and bioavailability. Certain substances can experience both physical and chemical deterioration, resulting in a decrease in their therapeutic effectiveness. Nanotechnology-based herbal medicinal formulations have gained significant interest in recent decades because of their heightened efficacy and ability to address the challenges associated with herbal medicine. Nanotechnology-based delivery methods utilizing biocompatible, biodegradable materials such as lipids, polymers, or nano emulsions can enhance the solubility, stability, bioavailability, and pharmacological action of herbal substances.

2.3.1 Nanotechnology and drug delivery system for plant extract

Herbal medicines are gaining popularity worldwide and show remarkable potential for treating, maintaining, and enhancing health, as well as preventing and treating many diseases. This is due to the presence of beneficial phytochemicals in herbal or plant extract. Phytochemicals, commonly referred to as secondary metabolites, are compounds synthesized by plants and have significant significance in traditional medicine (Dewi et al., 2022). Secondary metabolites have demonstrated diverse biological actions, establishing a scientific rationale for the utilization of herbs in traditional medicine. These substances exhibit pharmacological properties that can be utilized for the treatment of bacterial and fungal infections, as well as chronic degenerative disorders including diabetes and cancer. They are regarded safe compared to current conventional pharmaceuticals and are also more cost-effective (Dewi et al., 2022).

Nevertheless, the majority of these biologically active phytochemical elements suffer from constraints, such as poor absorption and distribution, as well as inadequate target specificity. Consequently, their bioavailability is diminished, leading to a drop-in biological activity. Furthermore, substantial quantities are necessary to elicit the effects of these phytochemical substances (Dewi et al., 2022). Additionally, certain phytochemical compounds are vulnerable to acidic environments and have limited stability. These restrictions impede its practical use in a therapeutic setting. Hence,

phytotherapeutics need a scientific approach to deliver the components in a sustained manner to increase patient compliance and avoid repeated administration (Yuan et al., 2017). This can be achieved by designing novel drug delivery systems for herbal or plant constituents. This system will not only reduce the repeated administration but also can help to increase the therapeutic value by reducing toxicity and increasing bioavailability (Eltayeb et al., 2017).

The effectiveness of medicinal plant species or herbal medicine depends on the supply of the active compounds. Therefore, the nanocarrier should deliver the active constituent at a sufficient concentration during the entire treatment period, and direct it toward the desired target tissue (Chaturvedi et al., 2021). However, partial, or total loss of a specific activity can be observed when an active compound of an extract is isolated or purified. Moreover, some components are highly sensitive to the acidic pH of the stomach, which causes their degradation and loss of the desired effect after ingestion (Chaturvedi et al., 2021).

All these limitations can be overcome by using different drug delivery systems based on nanotechnology, such as polymeric nanoparticles, solid lipid nanoparticles, liquid crystal systems, liposomes, micelles, and microemulsions. This is an interesting approach to improve formulation's most desirable properties. Furthermore, nanoparticle drug delivery system for herbal or plant extract may represent a future where activity is ensured, and the problems associated with using medicinal plants are overcome (Chaturvedi et al., 2021). Besides, the use of herbal or plant remedies in a novel drug delivery system will enhance the improvement in the use of medicinal plants that will come forth to treat various chronological diseases (Chaturvedi et al., 2021). Nanotechnology-based delivery methods for herbal medicines offer significant promise and distinctive qualities. They can transform compounds that are less soluble, poorly absorbed, and unstable into promising pharmaceuticals. Thus, nanotechnology-based delivery methods offer a great opportunity to enhance the effectiveness of herbal medicine and address the challenges connected with it.

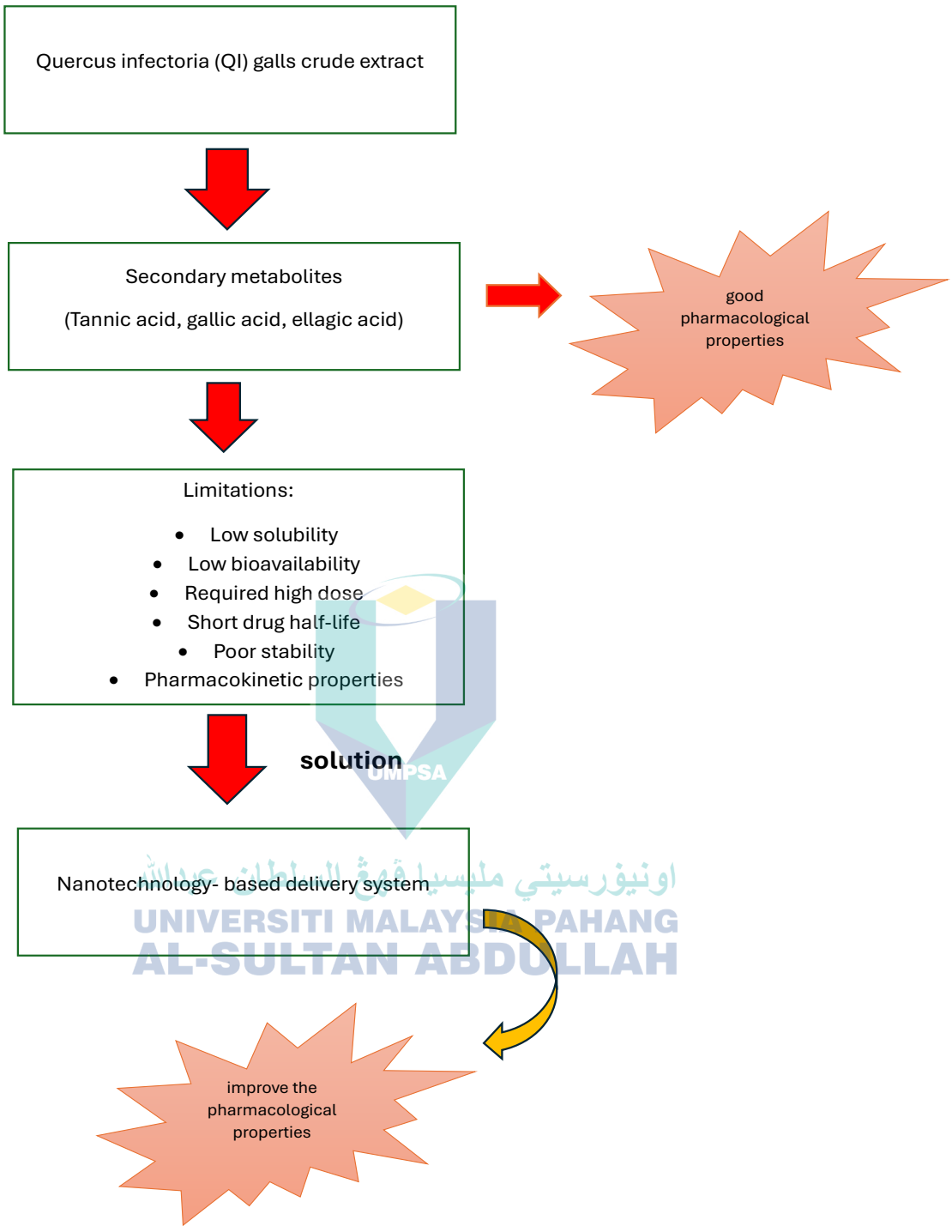

Figure 2.2: Schematic showing the deficiencies of the phytochemicals that limit their clinical application. Nanotechnology-based delivery system methods can overcome these limitations, mostly by increasing their bioavailability and absorption, thereby increasing their activity.

Delivering therapeutic compounds to the target site is a major problem in the treatment of disease. A conventional application of drugs is characterized by limited effectiveness, poor biodistribution, and lack of selectivity (Wu et al., 2017). These limitations can be overcome by a controlled drug delivery system. In this system, the drug is directly transported to the site of action, thus its effects on normal tissue and undesirable side effects can be minimized (Weng et al., 2018). Besides, this system also can protect drugs from rapid degradation or clearance and may enhance drug concentration in target tissues, hence, lower doses of drugs are required (Patra et al., 2018). Through the drug delivery system also, cell-specific targeting can be achieved by attaching or encapsulating drugs into individually designed carriers. Recent developments in nanotechnology reveal that nanoparticles have great potential as drug carriers. Due to their small sizes, nanoparticles exhibited unique physicochemical and biological properties (Patra et al., 2018).

Nanocarriers with optimized physicochemical and biological properties are taken up by cells more easily than larger molecules (Patra et al., 2018). The way the drug is to the nanocarrier is important for targeted therapy. A drug may be adsorbed or covalently attached to the nanocarriers surface or else it can be encapsulated into it. Covalent linking has the advantage over other ways as it can control the number of drug molecules connected to the nanocarrier (Minzanova et al., 2018) . The primary goals of the drug delivery system include more specific drug targeting and delivery, reduction in toxicity while maintaining the therapeutic effect, greater safety and biocompatibility, and faster development of new safe medicines. There are two mechanisms involved in the drug delivery system which are passive and active targeting (Minzanova et al., 2018).

2.3.1.1 Passive and active targeting mechanism in drug delivery system

The passive targeting effect in the drug delivery system is the Enhanced Permeability and Retention (EPR) effect. Materials of small size can accumulate in tumors over normal tissues because of the leaky vasculature and poorly developed lymphatic drainage in tumor tissue (Yang et al., 2018) (Figure 2.3). EPR can enhance the drug delivery specificity for solid malignant diseases such as cancer. In this mechanism, nanoparticles bearing drug will reach targeting sites by natural uptake of the reticuloendothelial system (RES) (Yang et al., 2018).

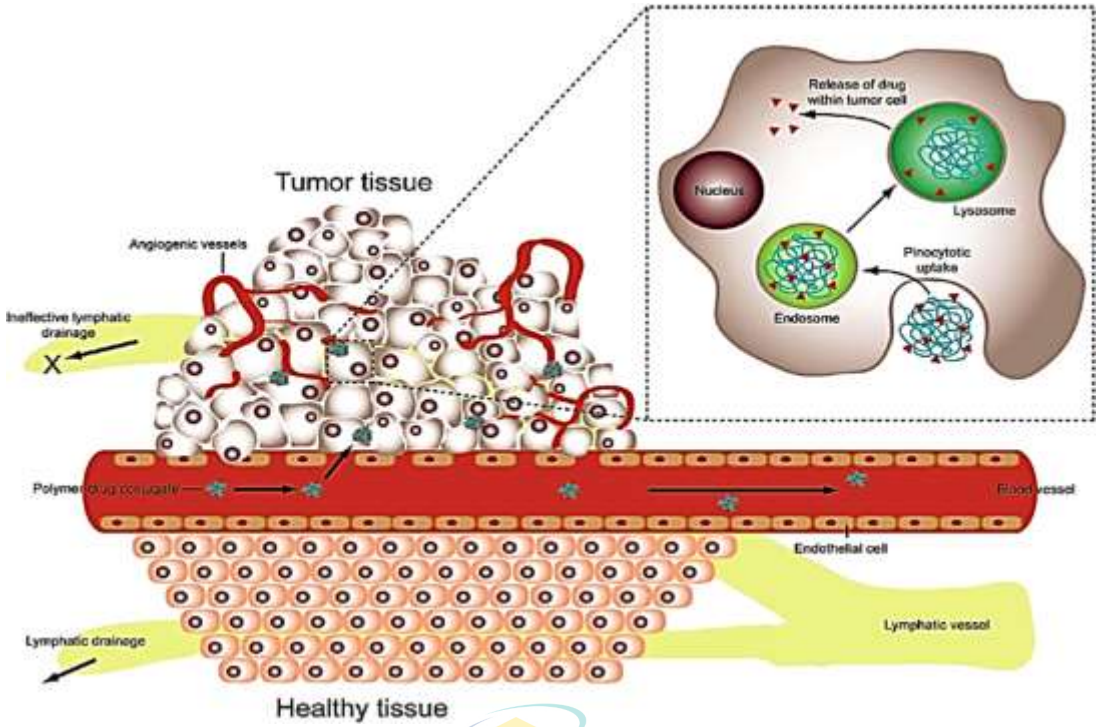

Figure 2.3: Schematic diagram of passive targeting of tumor tissues associated with the EPR effect

Source: Fox et al., (2009)

In addition to EPR, nanocarriers may improve the efficiency of their loaded drug at the cellular level. This is due to, nanocarriers can enter the tumor sites by passive endocytosis mechanisms to potentiate the efficacy of drugs that act on intracellular targets (e.g: RNA drugs, paclitaxel and doxorubicin) (Yang et al., 2018).

For an active targeting mechanism, nanocarriers are attached with affinity ligands on their surface through ligand-receptor interactions so that the nanocarriers can bind and accumulate at the target cells (Patra et al., 2018). Active targeting can be further divided into three different targeting levels which are first-order targeting, second-order targeting, and third-order targeting. In first-order targeting, the drug is distributed to capillary beds of target sites-organ or tissue (e.g.: lymphatic tissue, peritoneal cavity, pleural cavity, cerebral ventricles, eyes, and joints) (Jahangirian et al., 2017). In second-order targeting, drugs are targeted to specific sites such as tumor cells (e.g.: Kupfer cells in the liver). In third-order targeting, the drug is localized intracellularly at the target site via endocytosis or through receptor-based ligand-mediated (Jahangirian et al., 2017). The mechanisms for passive and active targeting are illustrated in Figure 2.4 below. Exceptional progress

has been achieved in the development of new drug delivery methods for encapsulating plant active metabolites, including organic, inorganic, and hybrid nanoparticles, over the last few decades. In terms of solubility, bioavailability, toxicity, and pharmacokinetics the improved formulations have been proven to outperform traditional and previously utilized methods.

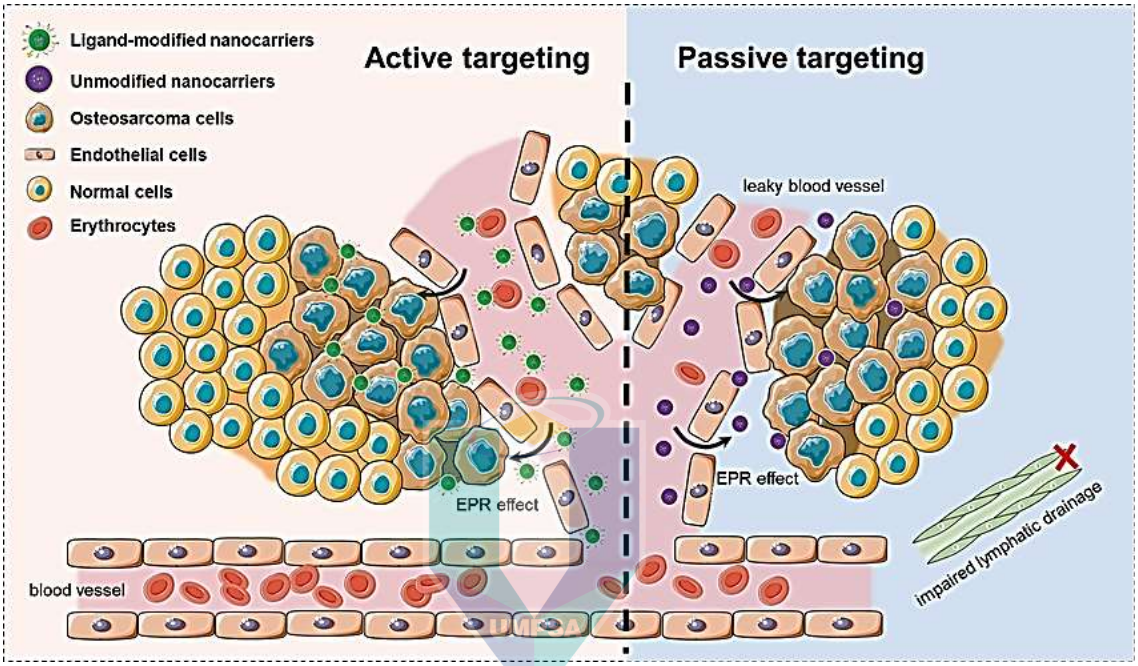

Figure 2.4: Schematic diagram of passive and active targeting mechanism in drug delivery system.
Source: Shi et al., (2023)

2.3.2 Design of nanoparticles in drug delivery system for plant extract

Based on the literature, 70% of the active compounds derived from plants are hydrophobic. Nanotechnology has been employed as a tactic to enhance the bioavailability and bioactivity of phytochemical substances. The capacity to design appropriate formulations for medication delivery is crucial for the development of innovative nanotechnology-based therapeutics. Efficient distribution of phytochemicals is crucial for the successful prevention and treatment of diseases. The delivery systems mentioned include lipid-based and polymer-based. These systems can enhance the bioactivity of phytochemical substances (Dewi et al., 2022).

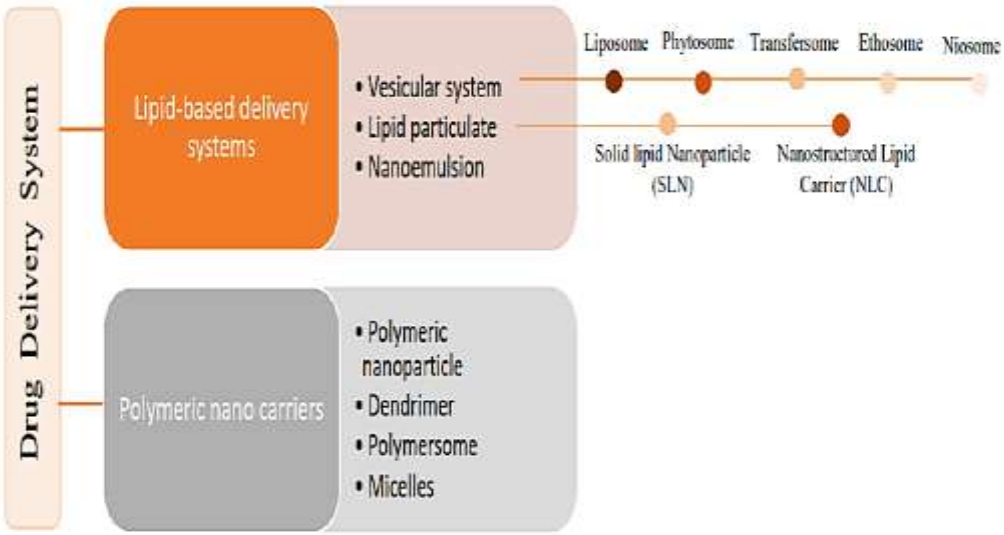

Figure 2.5: The nanotechnology-based delivery system for phytochemical constituents

Source: Dewi et al., (2022)

Nanoparticles for drug delivery can be prepared from a variety of materials such as proteins, polysaccharides and synthetic polymers (Ghotekar et al., 2019). The selection of material depends on many factors such as the size of nanoparticles, inherent properties of the drug, surface characteristics such as charge and permeability, the degree of bioavailability and many more (Ghotekar et al., 2019). After selection, these nanoparticles will be prepared most often by three methods; dispersion of preformed polymers, polymerization of monomers and ionic gelation of hydrophilic polymers (van der Meel et al., 2019). The other methods such as supercritical fluid technology and particle replication in non-wetting have also been exploiting. At the end of preparation, an ideal nanostructure system should have a high drug-loading capacity and reduce the number of matrix materials for administration (Ghotekar et al., 2019). Particle size and size distribution are the most significant characteristics of nanoparticles (Ghotekar et al., 2019).

Efficient herbal medication delivery devices have been created using nanotechnology. Lipid-based carrier systems, including vesicular systems such as micelles, liposomes, phytosomes, transfersomes, ethosomes, and niosomes, as well as lipid particulates like SLN and NLC, and nanoemulsions, have attracted significant

attention for delivering phytochemicals. These systems aim to enhance the bioactivity and bioavailability of phytochemical compounds while improving their stability.

When developing a new drug delivery system and carriers for herbal drugs, it is important to meet certain requirements. These include delivering the drug at a rate that is appropriate for the body's needs throughout the treatment period and ensuring that the active components of the herbal drug reach the intended site of action (Rahman et al., 2020). Various strategies have been employed to enhance the solubility, stability, availability, and capacity to pass through the gastrointestinal tract of drugs. Nanocarrier has garnered significant interest in the advancement of novel pharmaceutical carriers and delivery systems. An effective approach to counter this issue is enclosing natural plant metabolites within biodegradable and biocompatible nanoparticles (Rahman et al., 2020).

Nanoparticles are often manufactured with a guided bottom-up method, in which engineered macromolecular components are guided by external stimuli to interact with each other and self-assembled into a complex structure that otherwise would not be possible. Drugs can be either encapsulated within the nanoparticle or attached to the surface (Jin et al., 2020). A typical drug delivery with nanoparticles starts with a nanoplatform which includes liposomes, polymeric nanoparticles, micelles, drug-conjugated polymers, and dendrimers. To design effective nanoparticles, the combined effects of size, shape, surface chemistry, and other parameters need to be understood (Jin et al., 2020).

Furthermore, modifying the key characteristics of nanocarriers, including their composition (organic, inorganic, or hybrid), dimensions (small, medium, or large), shapes (spherical, cylindrical, or cubic), and surface properties (charge, functional groups, PEGylation, or attachment of targeting molecules), is recognized as a primary method for adjusting the physical and chemical properties of nanocarriers. The primary objective of utilizing nanocarriers in drug delivery is to efficiently cure a medical condition while minimizing adverse effects and potential consequences. Several newly developed nanostructures are illustrated in Figure 2.6.

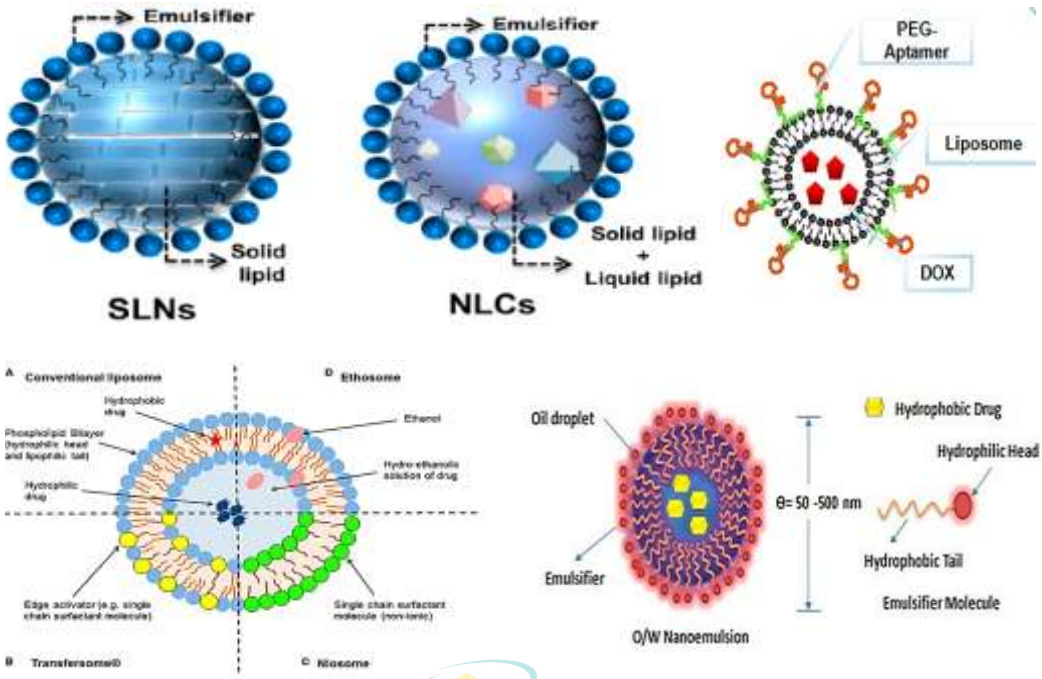

Figure 2.6: Various types of nanoparticles
Source: Rahman et al., (2020)

While there are many self-assembled nanoparticles, the most studied can be broadly sorted by the structure. For example, amphiphilic nanoparticles (the most common type used as drug carriers), dendrimers, polyrotaxanes, carbon nanotubes, graphene, and metal solid core nanoparticles. All these nanoparticles can be functionalized to target specific sites on tumor cells actively (Jin et al., 2020). One of the common amphiphilic nanoparticles used in drug delivery systems for herbal extract is micelles. The amphiphilic nanoparticles contain macromolecules with both hydrophobic and hydrophilic regions. In an aqueous environment such as blood or cellular fluid, the hydrophobic region will cluster together to be shielded from the surrounding polar water, forming a micelle (Malysa-Pasko et al., 2018). Synthetic micelles have hydrophobic cores while more complex, amphiphiles can form liposomes with a double-layer macromolecular wall and hydrophilic core with the same or different properties from the surrounding fluid (Figure 2.5). Drugs can be captured either in the core or on the surface of these particles, depending on their properties. Novel drug delivery systems (DDS) are currently commercialized to improve hydrophobic drug biodistribution, pharmacokinetics, stability and simultaneously increase their absorption at cancerous sites while excluding unwanted effects (Malysa-Pasko et al., 2018). For this study, the

nanoparticles of interest are micelles due to the structure being composed of a solitary core shell, formed by the self-assembly of synthetic amphiphilic di- or tri-block copolymers. These copolymers have both hydrophobic and hydrophilic segments, and the self-assembly occurs in aqueous conditions. The resulting assembly is characterized by its narrow and compact size (Rahman et al., 2020).

2.3.2.1 Micelle

Micelles is a nanosized (10–100 nm) polymer particle or colloidal dispersion is composed of a single core-shell structure (Figure 2.7). It is formed by the self-assembly of synthetic amphiphilic di- or tri-block copolymers in aqueous media. These copolymers have both hydrophobic and hydrophilic segments, and the self-assembly results in a narrow and small-sized structure (Rahman et al., 2020). The internal side of the micelle is hydrophobic which can help in the encapsulation of hydrophobic drugs or plant extract that will then be released based on the drug delivery action. Micelle is composed of a hydrophilic head on the outer layer which can help in the mobilization in an aqueous environment. Micelles are used the most as carriers for hydrophobic drugs and can be used directly intravenous (Khan et al., 2018).

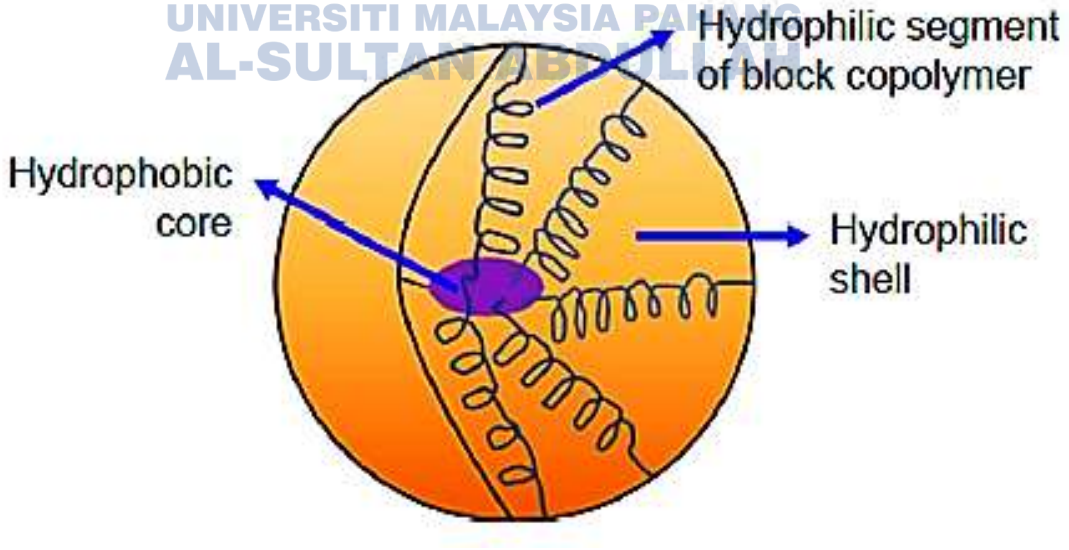

Figure 2.7: Schematic diagram of micelles.
Source: Rahman et al., (2020)

Micelles formed from amphiphilic di- or tri-block copolymers have gained popular attention in nanomedicine research for their multifunction properties (Ghosh & Biswas, 2021). Such building blocks of polymers are physiological-friendly and can be chosen to formulate micelles with prolonged shelf-life and controlled drug release in the human body (Ghosh & Biswas, 2021). The size of micelles is the optimal molecule size for passive targeting through the enhanced permeability and retention (EPR) effect of the leaky vascular and lymphatic system of cancer site (Ghosh & Biswas, 2021).

The molecular weight of polymer micelles is often high thus will enable prolonged storage in the cancerous tissue. Micelles can be absorbed easily at the tumor sites as compared to other tissue due to the high concentration in the surrounding area. The drugs or extract can be dissolved in the hydrophobic core or inbound chemically with the biodegradable carrier (Khan et al., 2018). The formulation of micelle is simple, but it is complicated to control the drug release from the micelle. Hence, surface modification of the micelle is usually incorporated to achieve the controlled drug release. The activation of the micelle always occurs at the cancerous site and thus can prevent the drug release in the blood circulation and simultaneously reduce the toxicity against normal cells (Bilia et al., 2018). Micelles need to be well-stabilized in the body to increase drug accumulation at the tumor site and extend blood circulation. There are two ways to attain this appropriate stability: thermodynamic stability, which relies on the polymeric micelles' ability to resist dilution, and dynamic stability, which involves the micelle breaking down into a single polymer chain (Rahman et al., 2020).

Another benefit of using micelles in drug delivery is the narrow size distribution. This is obtained through a self-assembled core-shell structure mainly depending on the thermodynamic equilibrium that can be achieved by the particular reaction condition during the synthesis process (Deshmukh et al., 2017). As a result, the micelles synthesize process is very crucial to the critical micelle concentration (CMC) of the polymeric molecules constituting micelles. This is the most critical part when selecting the materials to formulate micelle for drug delivery purposes. If the concentration falls below the CMC, the hydrolysis of the micelles into a free chain due to the thermodynamic instability will take place, thus posing a risk during the intravenous administration of cancer drugs. Besides that, the sudden dilution of micelles by the bloodstream and body fluid can also stimulate the immediate release of the encapsulated drug, which can lead to severe toxicity to the nearby cells (Deshmukh et al., 2017).

There are several previous studies conducted by formulating micelle as the carrier of the drugs for medicinal purposes. Qiu *et al*. reported formulated luteolin polymeric micelles with monomethoxy poly (ethylene glycol)-poly (3 caprolactone) (MPEG-PCL) by self-assembled method and tested them on C-26 colon carcinoma cells. In this study, the pharmacokinetics of free luteolin and the encapsulated luteolin in rats were studied, and the results revealed that there is a higher concentration of MPEG-PCL micelles. The in vitro cytotoxicity studies showed the lower IC_{50} for the MPEG-CL luteolin micelles suggesting that the incorporation of luteolin into MPEG-PCL micelles can potentially improve the bioavailability and cytotoxic effect against cancer cells (X.-M. Li et al., 2018). Blanco et al., synthesize PEG-PLGA polymeric micelles of β- lapachone using film hydration method and tested it on mice with subcutaneous A549 lung cancer. The findings revealed that this nanoformulation can prolong the circulation of the micelles in blood. Besides that, the in vitro administration of the micelles to lung cancer causes DNA damage and PARP-1 hyperactivation.

Self-assembled micelle can act as a carrier to deliver hydrophobic drugs and therapeutic substances with an increased solubility also prolonged circulation in the human body. Although micelles are recognized as one of the excellent agents for novel drug delivery systems due to their unique properties such as small size and improved pharmacokinetics, the poor stability of micelles remains a significant challenge (Gregoriou et al., 2020). Several factors affect the micelle stability in terms of thermodynamic and kinetic stability. One of the parameters that can be applied to determine the stability of the micelle is the CMC. Lower CMC indicates greater thermodynamic stability of the micelle (Gregoriou et al., 2020). The CMC value relies on the length of the hydrophobic chain, where an increase in hydrophobicity of the polymer will increase the cohesion of the hydrophobic core resulting in a decrease in CMC. Another factor that can affect the thermodynamic stability of the micelle is the drug-core binding ability. The hydrophobicity of a drug incorporated in the micelle will increase the degree of hydrophobicity of the polymer and decrease the CMC (Gregoriou et al., 2020).

The other crucial factor is the interaction between the polymer chains on the outer layer surface with the aqueous environment. For example, an increase in the polyethylene glycol (PEG) chain length and surface density on the surface of micelles will increase the protection of the hydrophobic core against exposure to an aqueous environment and

prevent micellar destabilization (Gregoriou et al., 2020). Finally, the microenvironment plays an important function in micellar formation and stability. Small changes in the temperature, solvent, and preparation techniques may manipulate the CMC and the size of micelles formed (Gregoriou et al., 2020). Therefore, it is very important to select the correct preparation techniques and solvent to get smaller micelles with a uniform size distribution. For example, the micelles formed from the solvent evaporation technique have been found to possess a smaller size (~30 nm) compared to those from dialysis techniques which yielded much bigger and non-uniform micelles (~110 nm) (Lu et al., 2018).

Kinetic stability reflects the stability of micelles in an aqueous solution over time. It is important to determine the kinetic stability to ensure that the encapsulated drug or extract is not released prematurely. Kinetic stability is dependent on several parameters: CMC, the ratio of the hydrophilic-hydrophobic segments of the polymers, and the incorporated drugs. As regards CMC, the kinetic stability increases when the hydrophobic length in block copolymers increases (Lu et al., 2018). The molecular weight ratio between hydrophilic-hydrophobic segments allows it to resist destabilization by the environment. Polyethylene glycol (PEG)-block-poly3caprolactone (PCL), PEG-b-polylactide-coglycolide, and PEG-b-poly-c-benzyl L-glutamate are the most researched block copolymers for application in micelle production. Because of its acceptable qualities, which include safety, biodegradability, and high loading for lipid-soluble biomaterials, PEGPCL is the most preferred among them (Rahman et al., 2020). In this study, D-α-tocopheryl polyethylene glycol succinate also known as vitamin E TPGS was used to synthesize micelles for encapsulation of QI galls nanoparticle and crude extract. Vitamin E TPGS is composed of both lipophilic alkyl tail and hydrophilic polar head, which can be promoted to micelles formation above its critical micelle concentration (CMC) of 0.02 % wt (Gregoriou et al., 2020).

2.3.2.2 Vitamin E TPGS

D-α-tocopheryl polyethylene glycol succinate (Vitamin E TPGS or simply TPGS) is a water-soluble by-product of natural Vitamin E, which is synthesized from esterification of Vitamin E succinate with PEG (Yang et al., 2018). It is a molecule with a molecular weight of approximately 1513 (Figure 2.8 and Figure 2.9). TPGS is a white or slightly yellowish, waxy solid with a melting point of 37–41°C (Guo et al., 2013). The

amphiphilic nature of TPGS results in a hydrophile–lipophile balance (HLB) of 13.2, rendering it an effective surfactant. HLB is a parameter used to estimate the emulsification stability of a non-ionic surfactant, with a higher value signifying a higher degree of hydrophilicity in the molecular structure and enhanced emulsifier function (Yang et al., 2018). USFDA has permitted TPGS as a safe pharmaceutical substance used in drug formulation.

Moreover, TPGS can form micelles upon dissolving in water at a concentration above its CMC value of 0.02 wt%, and other liquid-like crystalline phases when the concentration keeps increasing but well below 20 wt% (H. Li et al., 2019). In recent years, TPGS has been widely used as an emulsifier, solubilizer, absorption enhancer, and stabilizer. In terms of pharmaceutical application, TPGS has been mostly applied in the development of various drug delivery systems (Yang et al., 2018). The composition of PEG and vitamin E has been found to improve the half-life of drugs in plasma by preventing opsonization and enhancing cellular uptake of the drug molecules. TPGS also possesses advantages such as inhibiting membrane transporters; and P-glycoprotein (P-gp) for improving the oral bioavailability of chemotherapeutic drugs, preventing MDR, and augmenting intestinal permeability and bioavailability of certain drugs. TPGS has also been used for prodrug fabrication to improve chemotherapy (Korin et al., 2018). Furthermore, TPGS has also been applied in the formulation of nanomedicine, given its ability to increase the permeability and solubility of hydrophobic drugs and to afford controlled and sustained delivery of drugs, as exemplified by TPGS-based prodrugs in the form of micelles, liposomes, and TPGS-based copolymers nanoparticles (Yang et al., 2018).

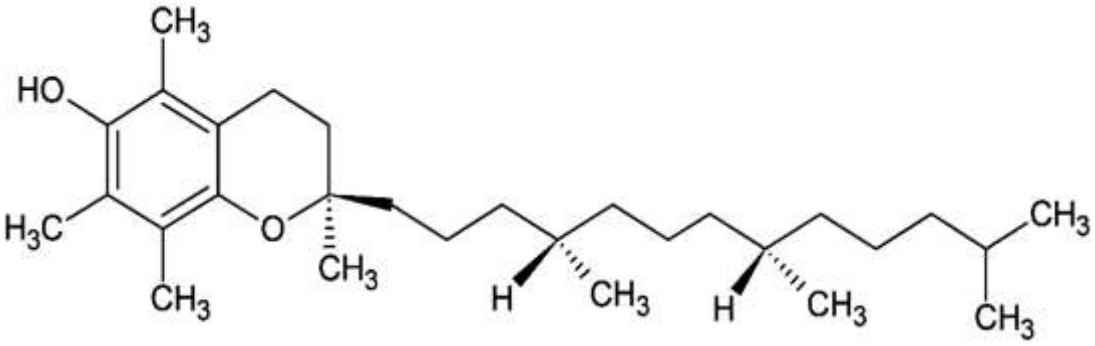

Figure 2.8 Molecular structure of D-α-tocopherol (Vitamin E)

Source : Kutty & Feng, (2013)

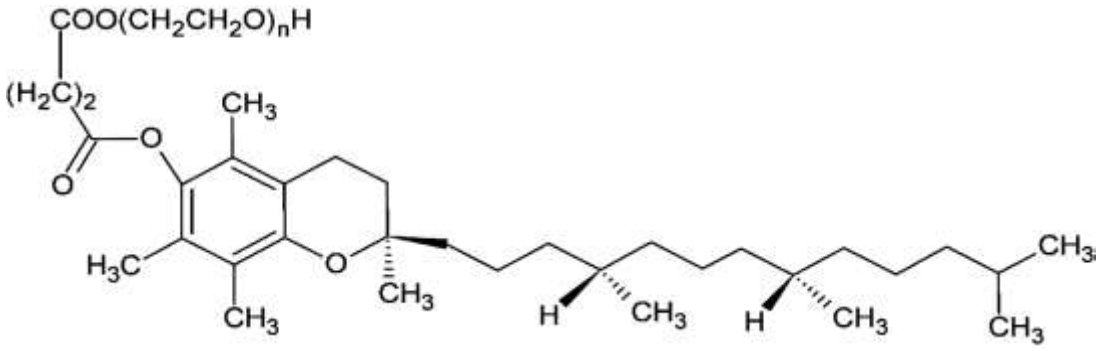

Figure 2.9 Molecular structure and various segments of TPGS

Source : Kutty & Feng, (2013)

However, most developed nanoparticles were formulated by solvent or wet synthesis and stored in the form of liquid suspension. This can lead the nanoparticles to agglomerate during storage, losing their nanoscale-related physical and chemical properties during prolonged storage. Thus, to overcome this limitation, the use of hydrogel materials for the encapsulation of the nanoparticle and crude plant extract can be carried out (Hussain et al., 2018). Their special properties and large water content provide an environment that suits most biological and drug molecules. Their crosslinked properties also can give better protection of encapsulated nanoparticles or crude plant extract against degradation and immune recognition (Hussain et al., 2018).

2.4 Hydrogels and their application in drug delivery

Hydrogels is a hydrophilic polymeric linkage that can absorb huge volumes of water and swellable (Narayanaswamy & Torchilin, 2019). These hydrogels can undergo swelling and shrinkage suitably to facilitate controlled drug release (Narayanaswamy & Torchilin, 2019). Their porosity and hydrophilic properties make them incredibly attractive drug-delivery vehicles that are biocompatible (Narayanaswamy & Torchilin, 2019). These hydrogels are widely used especially in biomedical fields as they can be transformed into varieties of physical shapes such as nanoparticles, microcapsules, slabs, films, and coatings (Narayanaswamy & Torchilin, 2019).

Hydrogel beads are a spherical dosage form containing herbal extract or drugs (Surini & Diandra, 2017). By encapsulating the herbal extract or drug inside, the

bioavailability and stability of the herbal extract and drugs can be enhanced. Hydrogel beads can expand in water because of the hydrophilic polymer is cross-linked with its cross-linker (Surini & Diandra, 2017). The unique physical features of the hydrogels, especially their porosity, give an advantage in drug delivery applications such as sustained release of the encapsulated drug or extract (Narayanaswamy & Torchilin, 2019). A high amount of encapsulated drug or extract is maintained quite sometimes via a controlled release mechanism either by diffusion, swelling, chemical, or based on surrounding factor (Lai & Rogach, 2017).

There are two pathways involved in diffusion-control drug delivery in hydrogel systems which are by reservoir or matrix. Both pathways allow the release of encapsulated drug or extract through a water-filled hydrogel mesh or pores (Narayanaswamy & Torchilin, 2019). For the reservoir, the hydrogel membrane is coated with a drug-containing core that forms capsules, spheres, or slabs that have high concentrations of drugs and will allow a sustained release of drug or extract. While for the matrix system will operate through the macromolecular pores on the hydrogel beads (Narayanaswamy & Torchilin, 2019). This type of release is time-dependent where the initial rate of release is following the square root of time rather than constant (Figure 2.10).

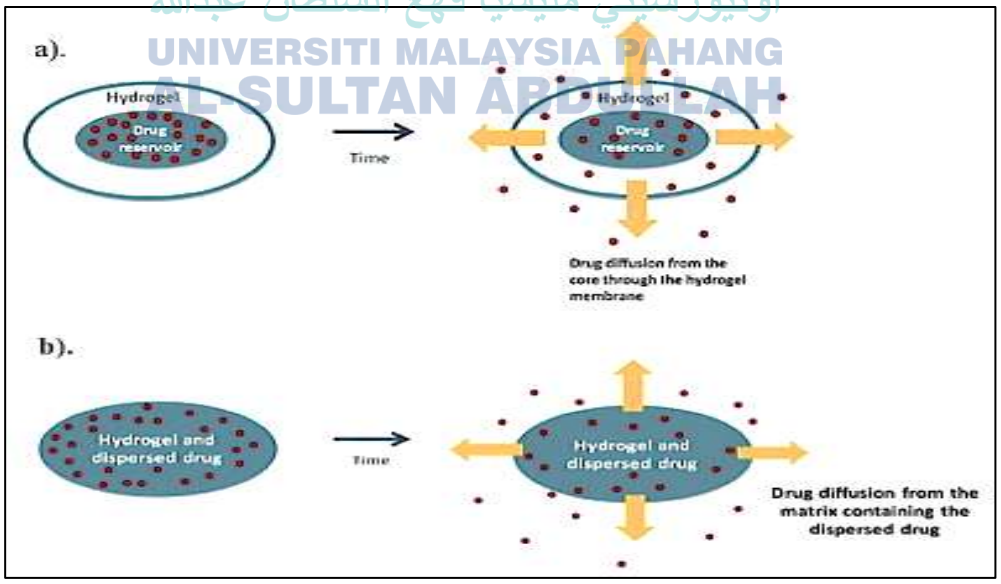

Figure 2.10 : Diffusion-controlled drug delivery with hydrogels. a) matrix device b) reservoir device.

Source: Narayanaswamy & Torchilin, (2019)

Hydrogel beads can be formulated using natural or synthetic polymers. A lot of previous studies have been conducted on the formulation of hydrogel beads using natural polymer and herbal or natural plant extract, as both have good solubility in water, high swelling ability, low toxicity level, and high biodegradability (Amiri et al., 2021). Hydrogels provide a flexible medium for the treatment of a variety of ailments including cancer and diabetes. For drug delivery purposes, the hydrophilic properties of hydrogels and their swelling or shrinking ability are appealing (Rajmohan & Bellmer, 2019). Besides that, the hydrogel applications are not strictly limited to targeted drug delivery, with a physical structure highly susceptible to alteration in many ways (Surini & Diandra, 2017).

Recent advances in hydrogels have been enormous in the area of selective drug delivery (Lai & Rogach, 2017). They are modified by attaching to target ligands and various types of polymers that give them an attractive drug delivery property. The application of pH-responsive hydrogels for cancer therapy and glucose-responsive hydrogels for diabetes is noteworthy (Narayanaswamy & Torchilin, 2019). To date, an attractive technique for drug delivery is developed by using modified stem cell membranes for controlled delivery (Narayanaswamy & Torchilin, 2019). These drug-loaded hydrogel-coated membranes (nanogels) are highly specific to the cancer site and highly biocompatible. In cancer therapy, immunotherapy platforms using hydrogel are crucial. Promising drug delivery carriers for cancer therapy are hydrogels which enable the targeted delivery of antibodies and other immune-regulatory molecules at the cancer site (Amiri et al., 2021). This makes hydrogels special not only for controlled drug delivery of extract but also as a good carrier for therapeutic use. Thus, in this present study, we are focusing on the development of hydrogel-based materials as carriers for herbal nanoparticles and crude extracts to ensure a successful drug delivery purpose.

2.4.1 Formulation of hydrogel-based for delivery of herbal medicines

Herbal medicine is one of the main components of traditional medicine. The therapeutic potential of herbal medicine has been recognized worldwide, contributing to the drug development from medicinal herbs. To date, nutraceutical products have been widely used in treating disease as well as in maintaining community health (Surini & Diandra, 2017). Nutraceutical products can be food or food-related, such as dietary supplements, herbal products, cereals, soups and healthy drinks (Surini & Diandra, 2017).

The therapeutic areas covered by nutraceutical products include cancers, osteoporosis, hypertension, cholesterol, depression and diabetes (Lai & Rogach, 2017). A key factor that contributes to the rapid growth of these herbal-related products is the growing knowledge and confidence of consumers in natural products or medicine (Chan et al., 2010). However, the chemopreventive properties of herbal medicines have been limited by certain factors such as lack of targeting capacity and poor bioavailability (Lai & Rogach, 2017). In addition, the effectiveness of the absorption and cellular internalization of these bioactive, which are the crucial parts of the herbal treatment, can vary greatly due to the changes in structures and physicochemical properties of the various bioactive in herbal medicines thus reducing the efficacy of the treatment (Lai & Rogach, 2017).

A carrier to facilitate the delivery of these active constituents can be used to overcome this limitation. For this purpose, various materials including lipids and polymers have been used in the past years to formulate hydrogel beads (Lai & Rogach, 2017). Hydrogel beads are spherical dosage forms containing active constituents such as plant extract or drugs (Surini & Diandra, 2017). By formulating these beads, the bioavailability and stability of the drugs or extract can be improved, providing a uniform distribution of drugs and having an attractive dosage form (Surini & Diandra, 2017). A previous study showed that the hydrogel beads made of mulberry leaf (Morus alba L.) extract using cross-linked pectin had a spherical shape with an unsmooth surface, had good swelling ability in water, and were able to maintain their form (Surini & Diandra, 2017). Another study revealed that encapsulation of herbal galactagogue extract in chitosan coated-alginate microcapsules using the gelation method in optimum conditions, led to the formation of spherical microcapsules with good morphological properties and encapsulation efficiency (Khorshidian et al., 2019).

As shown by the previous studies and research, formulation and development of hydrogel-based materials as carriers for herbal medicines or extracts can improve the efficacy of herbal treatments in both clinical and pre-clinical studies (Lai & Rogach, 2017). This can reveal the potential of advances in microfabrication technologies, which encourage hydrogel manipulation and make future combinations of herbal extract and established anticancer drugs into one single treatment (Lai & Rogach, 2017).

2.4.2 Modulation of hydrogel properties for drug delivery

One of the important factors to be monitored when formulating carriers for herbal medicines is the loading quantity, which is largely affected by the affinity of the herbal components to the hydrogel matrix (Lai & Rogach, 2017). In traditional medicine, several herbs were used to form a formulation. Therefore, for the treatment to be successful, several components must be administered simultaneously. Technically, this is difficult, since most of the delivery mechanisms reported in the literature are specifically intended for single-drug therapies to be used (Narayanaswamy & Torchilin, 2019). A hydrogel-based system that can hold herbal components with different degrees of hydrophilicity is required to resolve this problem. The affinity of the components to the hydrogel matrix would be low if the loaded components were hydrophobic. Hence, before the loading process is complete, the components can simply diffuse out of the matrix, reducing the final loading yield (Lai & Rogach, 2017).

To overcome this limitation, the hydrophobic extract or drug can be first encapsulated into a carrier that has a higher affinity to the hydrogel matrix before it is loaded into a hydrogel (Nadzri et al., 2019). This method has been conducted in situ gel-forming system, which is composed of curcumin-loaded micelles and thermosensitive hydrogel. Curcumin is an active constituent in turmeric and is commonly used as a spice or as a remedy to treat various illnesses and chronic diseases. However, the clinical use of curcumin has been restricted due to its low aqueous solubility and affinity to the hydrogel matrix. Thus, to overcome this problem, curcumin has first been loaded in a carrier to form polymeric micelles followed by loading into hydrogels for sustained release. This research showed an alternative way to increase the loading efficiency by first encapsulating a herbal ingredient in another system before hydrogel formulation (Lai & Rogach, 2017). The other alternative to improve the loading efficiency is by modulating hydrogel properties to improve the affinity of the hydrogel matrix to hydrophobic components (Lai & Rogach, 2017). This has been revealed in previous research, in which an alginate-based hydrogel has been formulated to load the herbal extract of *Piper sarmentosum*. Hydrogels formulated using alginate with a higher mannuronate and guluronate content have been shown to give higher loading efficiency. This finding revealed that the chemical composition of polymers can be one of the leading

factors that facilitate the encapsulation of drugs or herbal medicines into hydrogels (Amiri et al., 2021).

In addition to the encapsulating efficiency, when a carrier is developed, the other important factor to be observed is the release sustainability (Lai & Rogach, 2017). This controlled release can be achieved by adjusting the polymer composition to regulate the mesh size of the polymer chain, the barrier of the polymer network to drug absorption, and the swellable property of a hydrogel (Lai & Rogach, 2017). A previous study by Patenaude and Hoare, showed functionalized natural polymers such as carboxymethyl cellulose (CMC), dextran and hyaluronic acid, and PNIPAM–based synthetic oligomers with hydrazide or aldehyde functional groups to generate a series of in situ gelation, hydrazine-cross-linking hydrogels (Ahmed, 2015). This study was accomplished by adjusting the number and proportion of different reactive oligomers or polymer precursors, hydrogels with different swelling abilities, and degradation kinetic properties (Ahmed, 2015). Finally, high biodegradability and low toxicity are crucial parameters to be considered if a carrier is to be used in a biological body. This parameter is particularly a major concern in the chemical hydrogel. However, this limitation can be overcome by using biodegradable chemical components or natural polymer in the formulation as showed in the previous study where dextran has been copolymerized with lactic acid oligomers. This formulated hydrogel has been reported to be fully degradable under physiological conditions (Lai & Rogach, 2017).

Based on the research purpose, either for food enrichment or drug-based formulation, different encapsulation methods can be used. In this study, the polymeric hydrogel beads were synthesized through an ionic gelation method between pectin and zinc acetate, the crosslinker. The QI galls nanoparticle and crude extract were incorporated into hydrogel beads to increase their stability as well as to protect their pharmaceutical attributes. Pectin hydrogels are being recognized as a highly promising substance for the controlled release of pharmaceuticals in the rapidly evolving field of drug delivery (Kapoor et al., 2024).

2.4.3 Pectin-based polymeric hydrogel beads and their medicinal used

Pectin is a complex polysaccharide with main constituents as a linear chain polymer of 1,4-D-galacturonic acid whose carboxylic groups are naturally more or less methyl-esterified (Jiande Gao et al., 2020). Pectin is a biopolymer with wide usage because of its structural diversity and complexity. Although pectin from different sources has some common structural characteristics, many aspects of the common structure change according to the species and the physiological stage of the plant. In addition, the application of pectin is determined by its chemical features, including galacturonic acid content, methoxyl content, and degree of acetylation.

Pectin is a polysaccharide with a core consisting of _-1,4-linked D-galacturonic acid and -1,2-L-rhamnose units in turn, as well as a large number of neutral sugars, including arabinose, galactose, and lesser amounts of other sugars (Minzanova et al., 2018). Pectin has a linear anionic backbone with regions having no side chains known as "smooth regions", and regions with non-ionic side chains known as "hairy regions" (Minzanova et al., 2018). The structural classification of pectin includes: homogalacturonan (HG), rhamnogalacturonan I (RG-I), and substituted galacturonic such as rhamnogalacturonan II (RG-II) (Figure 2.11)

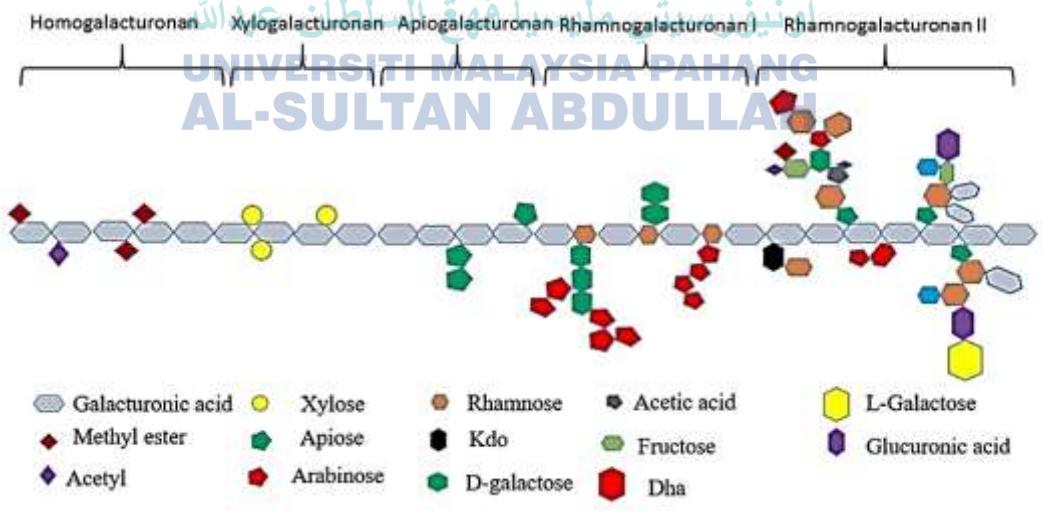

Figure 2.11: Structural characteristics of pectin molecules.

Source: Kedir et al., (2022)

Pectin hydrogel beads are used to encapsulate drugs or plant extract for oral drug delivery. This polysaccharide is not digested in the upper intestinal tract but its digestion in the lower stomach which is the colon will release the oligomers or drugs with the potential bioactivity (Mala & Anal, 2021). Pectin hydrogels exhibit versatility in various fields, including oral and transdermal drug administration, wound healing, tissue engineering, and ongoing clinical trials. Despite the limitations of standardization and regulatory compliance, the future of pectin hydrogels seems promising, as it offers new opportunities for enhanced drug delivery systems (Kapoor et al., 2024). Studies have indicated that pectin may help prevent metastasis; this is particularly the case for pectin which has been reduced in size and absorbed by the body into smaller, less molecularly heavy pieces. The anticancer effects of pectin that have been modified by heat, radiation, chemicals, and enzymes are more potent than those of unmodified pectin (Kedir et al., 2022).

Previous studies showed that calcium-pectin beads, some of them further reticulated by polyethyleneimine and/or chitosan were incubated in simulated gastric, intestinal, or colonic media in the presence or absence of pancreatin or pectinases. Pectin oligomers were released only in simulated colonic media (*i.e.*, in the presence of pectinase) but the fragments were not longer than dimers which is much shorter than previously reported for pectin incubated with human feces. The *in vitro* study of pectin digestion will therefore need simulated digestion media with much lower pectolytic enzyme concentrations (Minzanova et al., 2018).

Another study showed that pectin-based hydrogel beads incorporated with mulberry leaf extract had a spherical shape with an unsmooth surface, good swelling ability and time, and were able to maintain their form after the drying process (Surini & Diandra, 2017). The other study revealed that there is excellent potential in the manipulation of polymer concentration and crosslinker influence particle size of hydrogel beads, sphericity, and flow property. From this study, it was showed that high amylopectin containing bora rice, a natural polysaccharide exhibits promising effects for controlled release colon targeting drug delivery (Mala & Anal, 2021).

Pectin hydrogels have gained popularity in cancer therapy due to their biocompatibility and capacity to incorporate anticancer drugs. These hydrogels offer tailored drug delivery, which improves therapeutic efficacy while reducing systemic side effects. Their potential in localized cancer treatment offers hope for better patient outcomes (Kapoor et al., 2024). Yin et al. (2023) provided a famous example, effectively creating a biodegradable hydrogel by adding silibinin into a pectin-OCMC blend. Silibinin, an anti-lung cancer drug, specifically inhibits the TMEM16A ion channel. As a result, the scientists explored the therapeutic efficacy of encapsulating silibinin in a pectin-OCMC hydrogel in a mouse lung cancer model. The CCK-8 assay revealed that a pectin-OCMC hydrogel containing silibinin (100 mg/L and 200 mg/L) reduced LA795 cell viability by 73.25% and 31.25%, respectively. Furthermore, An et al. (2021) developed pectin-based, injectable, and biodegradable hydrogels, paving the way for advanced enhanced anticancer therapy. A hydrogel was created utilizing biodegradable pectin aldehyde (pectin-CHO) and a polymer blend called poly(N-isopropylacrylamide-stat-acylhydrazide). Injectable hydrogels can efficiently encapsulate and distribute anticancer medicines, such as DOX hydrochloride and combretastatin A4 disodium phosphate (CA4), to tumor locations. Incorporating DOX into hydrogels can greatly inhibit the development of CT-26 cells.

In addition, prior research has shown the in vitro anti-cancer effects of several rutin formulations enclosed in low methoxyl pectin beads. The rutin, encapsulated in 3NA15Sor1Bica (a mixture of 3% Non-amidated LMP, 15% sorbitol, and 1% NaHCO3), exhibited superior anti-cancer action compared to rutin that was not encapsulated. This effect was particularly pronounced in human colon adenocarcinoma (HT-29) and human mouth epidermal carcinoma (KB) cells (Jantrawut et al., 2014). Another study revealed that hydrogel and nanoparticles made from pectins, which are polysaccharides originating from plants, were created by adjusting the number of free carboxyl groups (DE) and the concentration of the polymer. Pectin-based films possess a favorable structure, physico-chemical characteristics, biocompatibility, and the capacity to impede the growth of the U87MG human glioblastoma cell line. These biomaterials show great potential for use in intraoperative procedures for the surgical removal of brain tumors. The ion gelation approach was utilized in conjunction with a straightforward injection of biopolymer into cross-linker agent pectin-based NPs. This process was thoroughly examined and analyzed. Nanoparticles (NPs) exhibited no toxicity when evaluated on a human glioma

cell culture, which is actually advantageous and appropriate for encapsulating a selective anticancer medication. The form, average size, surface charge, and nanomechanical properties of NPs were examined and demonstrated to be appropriate for non-invasive drug delivery systems (Chai et al., 2023) .

Nevertheless, there is a scarcity of research regarding the antiproliferative effect against breast cancer cells. Therefore, this work aims to investigate the inhibitory effect of pectin- based hydrogel beads containing pectin and QI gall loaded micelles on the growth of breast cancer cells. This research investigated the antiproliferative activity of pectin-based hydrogel beads and their ability to induce apoptosis in certain breast cancer cells.

2.5 Apoptosis

Apoptosis is a physiological process of cell death where a population damaged, infected, or potentially neoplastic cells are removed in response to a variety of signals. These signals include receptor-mediated signals, withdrawal of growth factors, anti-tumour drugs and under certain conditions, damage to DNA.

Apoptosis is essential for normal development and tissue homeostasis; perturbations in its regulation contribute to numerous pathological conditions including cancer, autoimmune and degenerative diseases (Sánchez-Carranza et al., 2017). The term apoptosis is derived from the Greek words, ‘apo’ meaning away from and ‘ptosis’ meaning falling off and it refers to the falling of leaves from trees in autumn. It is used to describe the situation in which a cell actively pursues a course toward death upon receiving certain stimuli (Sánchez-Carranza et al., 2017).

Generally, apoptosis can be identified by cell morphological and biochemical changes. Morphological alterations of apoptotic cell death that concern both nucleus and cytoplasm are remarkably similar across cell types and species. Morphological hallmarks of apoptosis in the nucleus are chromatin condensation and nuclear fragmentation, which accompanied by rounding up of the cell, reduction of cellular volume (pyknosis) and retraction of pseudopods (Darvin et al., 2017). At later stage of apoptosis, morphological features include plasma membrane blebbing, ultrastructural modification of cytoplasmic organelles, and loss of membrane integrity, budding and formation of apoptotic bodies (Figure 2.12) (Darvin et al., 2017). As for the biochemical changes, three main changes

can be observed in apoptosis which are activation of caspases, membrane changes and recognition by phagocytic cells, also deoxyribonucleic acid (DNA) and protein breakdown (Kopustinskiene et al., 2020). Early in apoptosis, there will be membrane translocation known as phosphatidylserine (PS) in the outer layers of cell membrane, which been "flipped out" from the inner layers (Kopustinskiene et al., 2020).

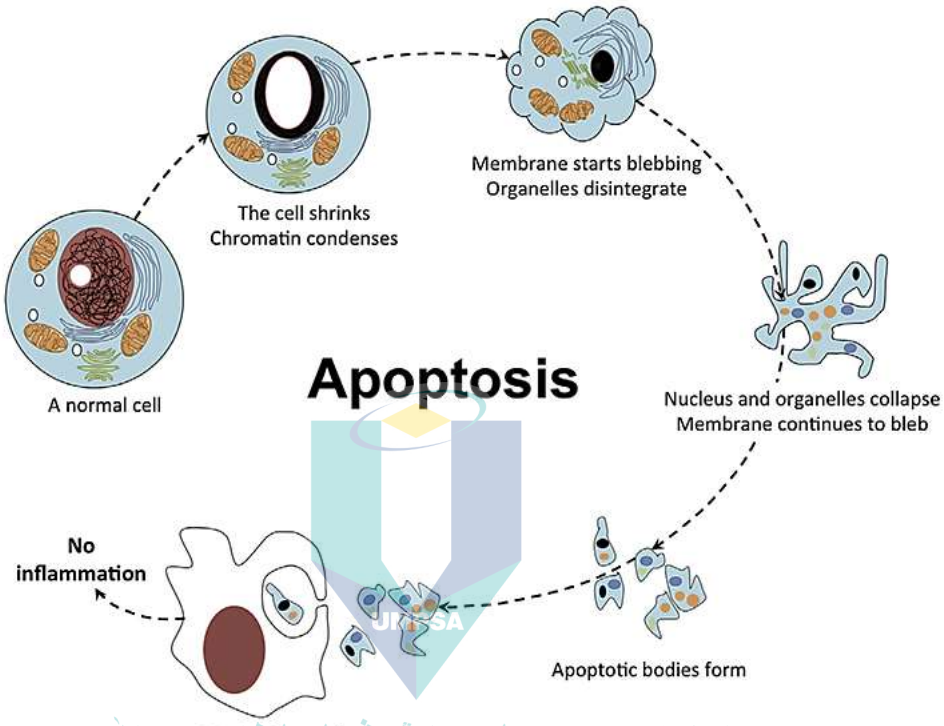

Figure 2.12: The sequence of morphological changes in apoptosis process

Source : Vetrivel et al., (2019)

2.5.1 Targeting apoptosis in cancer treatment

Apoptosis represents a major causative factor in the development and progression of cancer. The ability of tumour cells to evade engagement of apoptosis can play significant role in their resistance to conventional therapeutic regimens. Defect in apoptosis has been implicated with cancer pathogenesis. As the tumour mass enlarge, evasion of apoptosis permits the survival of neoplastic cells over the intended lifespan, destabilisation of the exogenous survival factors requirement and protection against oxidative stress and hypoxia, thereby results in accumulation of genetic alterations that

deregulate cells proliferation, interfere with cellular differentiation, facilitate angiogenesis and increase invasiveness (Ye et al., 2017).

Mechanism of apoptosis has large impact in the development of cancer treatment. Evidence have shown that apoptosis function deficiency can contribute to the treatment resistance associated with conventional therapies (e.g.: chemotherapy and radiotherapy), in which higher doses of anticancer drugs are required to kill the tumour masses due to increase threshold for cell death. For example, apoptosis inhibition in oxidant-induced carcinogenesis in lung cells (V79) lead to cisplatin resistance. It was shown that low activities of apoptotic proteins had lower apoptotic cell death, thereby reduced the sensitivity of V79 to cisplatin treatment (Mangal et al., 2017).

Furthermore, apoptosis plays a vital role in the response of cancer to anticancer agents. Previously, it has been demonstrated that successful application of cancer treatment by nonsurgical method has been achieved by induction of apoptosis (Darvin et al., 2017). Hence, an understanding of underlying mechanism of apoptosis in cancer treatment is reasonable to figure out the pathway involve in apoptosis.

2.5.2 Mechanisms of apoptosis

Understanding the mechanisms of apoptosis is important to understand the pathogenesis conditions because of dysregulation of it. Caspases are the central mechanism of apoptosis as they play major role in the apoptotic event. The two commonly described pathways are the intrinsic (mitochondrial) and extrinsic (death receptor) pathways of apoptosis (Figure 2.11). Apoptosis occurs on a cell-by-cell basis. For each affected cell, two primary phases are observed: one of initiation and a second of execution. The resulting cell remnants are processed for reuse. Both phases are complex and require exquisite organization of multiple cellular systems, including interactions between proteins and cellular membranes (Ye et al., 2017).

Apoptotic signaling mechanisms primarily operate through two major pathways: the intrinsic pathway, which is mediated by mitochondria, and the extrinsic system, which involves death receptors. The extrinsic apoptotic pathway is characterized by its dependence on caspases, while the intrinsic apoptotic pathway can be activated by either caspase-dependent or caspase-independent signals (Vetrivel et al., 2019).

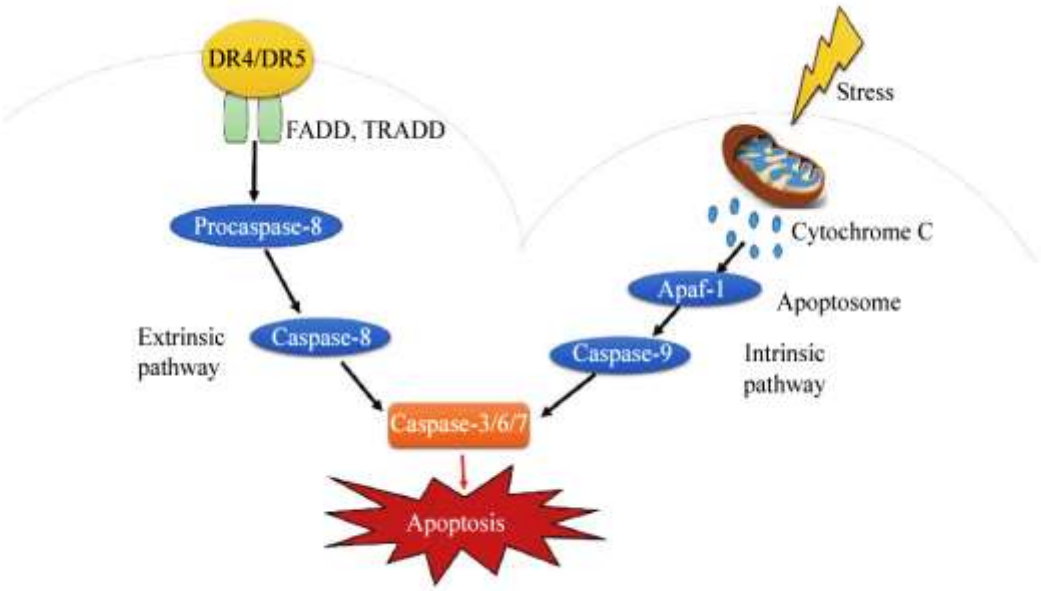

Figure 2.13: Schematic representation of the key events in the mechanism of apoptosis

Source: Vetrivel et al., (2019)

The extrinsic death receptor pathway begins when death ligands bind to a death receptor. Although several death receptors have been described, the best-known death receptors is type 1 TNF receptor (TNFR1) and a related protein called Fas (CD95) and their ligands are called tumor necrosis factor (TNF) and cell surface death receptor (Fas) ligand and (FasL) respectively (Pfeffer & Singh, 2018). These death receptors have an intracellular death domain that recruits adapter proteins such as TNF receptor-associated death domain (TRADD) and Fas-associated death domain (FADD) as well as cysteine protease like caspase 8 (Pfeffer & Singh, 2018). Binding of the death ligand to the death receptor results in the formation of binding site for an adaptor protein and the whole ligand-receptor-adaptor protein complex are known as the death-inducing signalling complex (DISC) (Darvin et al., 2017). DISC then initiates the assembly and activation of pro-caspase 8. The activated form of the enzyme, caspase-8 is an initiator caspase, which initiates apoptosis by cleaving other downstream or executioner caspase (Darvin et al., 2017).

The intrinsic pathway is initiated within the cell. Internal stimuli such as irreversible genetic damage, hypoxia, extremely high concentration of cytosolic Ca^{2+} and severe oxidative stress are some triggers of the initiation of the mitochondrial pathway (Id & Chaudhry, 2019). Regardless of the stimuli, this pathway is the result of increased mitochondrial permeability and the release of pro-apoptotic molecules such as cytochrome-c into the cytoplasm (Id & Chaudhry, 2019). This pathway is regulated by a group of protein belonging to Bcl-2 family, named after the Bcl-2 gene, observed at chromosomal breakpoint of the translocation of chromosomes 18 to 14 in follicular non-Hodgkin lymphoma (Id & Chaudhry, 2019).

There are two main groups of Bcl-2 proteins, namely pro-apoptotic proteins (e.g., Bax, Bak, Bad, Bcl-X_s, Bid, Bik, Bim and Hrk) and the anti-apoptotic proteins (e.g. Bcl-2, Bcl-X_L, Bcl-W, Bfl-1, and Mcl-I) (Pfeffer & Singh, 2018). The anti-apoptotic proteins regulate apoptosis by blocking the mitochondrial release of cytochrome-c while the pro-apoptotic proteins act by promoting such release. Other apoptotic factors that are released from the mitochondrial intermembrane space into the cytoplasm include apoptosis inducing factor (AIF), second mitochondria-derived activator of caspase (Smac), direct IAP binding protein with low pI (DIABLO) and Omi/high temperature requirement protein A(HtrA2). Cytoplasmic release of cytochrome-c activates caspase-3 via the formation of complex known as apoptosome which is made up of cytochrome-c, Apaf-1 and caspase-9. On the other hand, Smac/DIABLO or Omi/HtrA2 promotes caspase activation by binding to inhibitor of apoptosis protein (IAPs) which subsequently lead to disruption in the interaction of IAPs with caspase-3 or caspase-9 (Pfeffer & Singh, 2018).

CHAPTER 3

METHODOLOGY

3.1 Introduction

In this study, galls of *Quercus infectoria* (QI) have been chosen for the development of nanomedicine. The first phase of this study involved the extraction of QI gall extract, phytochemical screening, and the cytotoxicity study of the QI gall extract. Preparation of the QI gall extract was carried out using the maceration extraction method with 70% aqueous ethanol as the solvent. Then, the filtration of the QI gall extract was conducted. The extract then was concentrated by the rotary evaporation process. The concentrated extract was stored in a -80˚C freezer overnight. After 24 hours, the extract was freeze-dried to obtain the powder extract and stored at 4˚C before use. The QI gall extract was analyzed for the phytochemical constituents, tannic and gallic acid content by High Performance Liquid Chromatography (HPLC). Then, the antioxidant activity of the QI gall extract was analyzed by using the DPPH Scavenging method. The QI gall extract also was analyzed for the Total Phenolic and Total Flavonoid content. Cytotoxicity study was carried out using QI galls extract against selected breast cancer cells, MDA-MB-231 and MCF-7. Besides, the QI galls extract also will be tested against normal cell lines as control which are L929 cell lines. This cytotoxicity study of the QI galls crude extract against selected breast cancer and normal cell lines was analyzed using MTT assay standard protocol in which the optical density at 570nm will be determined by a microplate reader.

The second phase of this study is the development of QI galls extract as micelles and the properties characterization of the developed micelles. The nanoparticles bearing QI gall extract were synthesized using the solvent casting method where the nanocarrier used to encapsulate the QI gall extract is Vitamin E TPGS. Then the developed micelles were

characterized for their properties such as the particle size and size distribution, surface charge, surface morphology, surface chemistry, drug loading, and drug release profile. The particle size and size distribution of the micellar samples were measured using dynamic light scattering in an aqueous medium. The surface charge was determined by Zetasizer at room temperature. The shape and surface morphology of the micelles was visualized by using a Transmission Electron Microscope (TEM). The surface chemistry of the micelles was analyzed by X-ray Photoelectron Spectroscopy (XPS). For the drug loading and in vitro drug release profiles, both were analyzed using High-Performance Liquid Chromatograpy (HPLC). The next step in this research involved the *in vitro* quantitative of cellular uptake of the micellar formulation. Besides, this phase also was focused on the cytotoxic activity of the micellar formulations against breast cancer (MDA-MB-231 and MCF-7) and normal cell lines (L929). The quantitative study of cellular uptake of the micellar formulation was assessed by the microplate reader. The cytotoxic activity of the micellar formulation against selected breast cancer and normal cell lines was analyzed using the MTT assay standard protocol in which the optical density at 570nm will be determined by a microplate reader.

The third and final phase of this research is the formulation and characterization of hydrogel beads incorporated with QI gall nanoparticles and crude extract. The QI galls hydrogel beads were formulated using the ionic gelation method between polymer, pectin, and the crosslinker, zinc acetate. The synthesized hydrogel beads then were characterized for their physical and chemical properties such as yield, shape and morphology, particle size distribution, swelling ability and time, moisture content, encapsulation efficiency, and the cytotoxicity effect against breast cancer cells; MCF-7 and MDA-MB-231 as well as normal cells, L929. The experimental design of this study was summarized in the flowchart as shown in Figure 3.1.

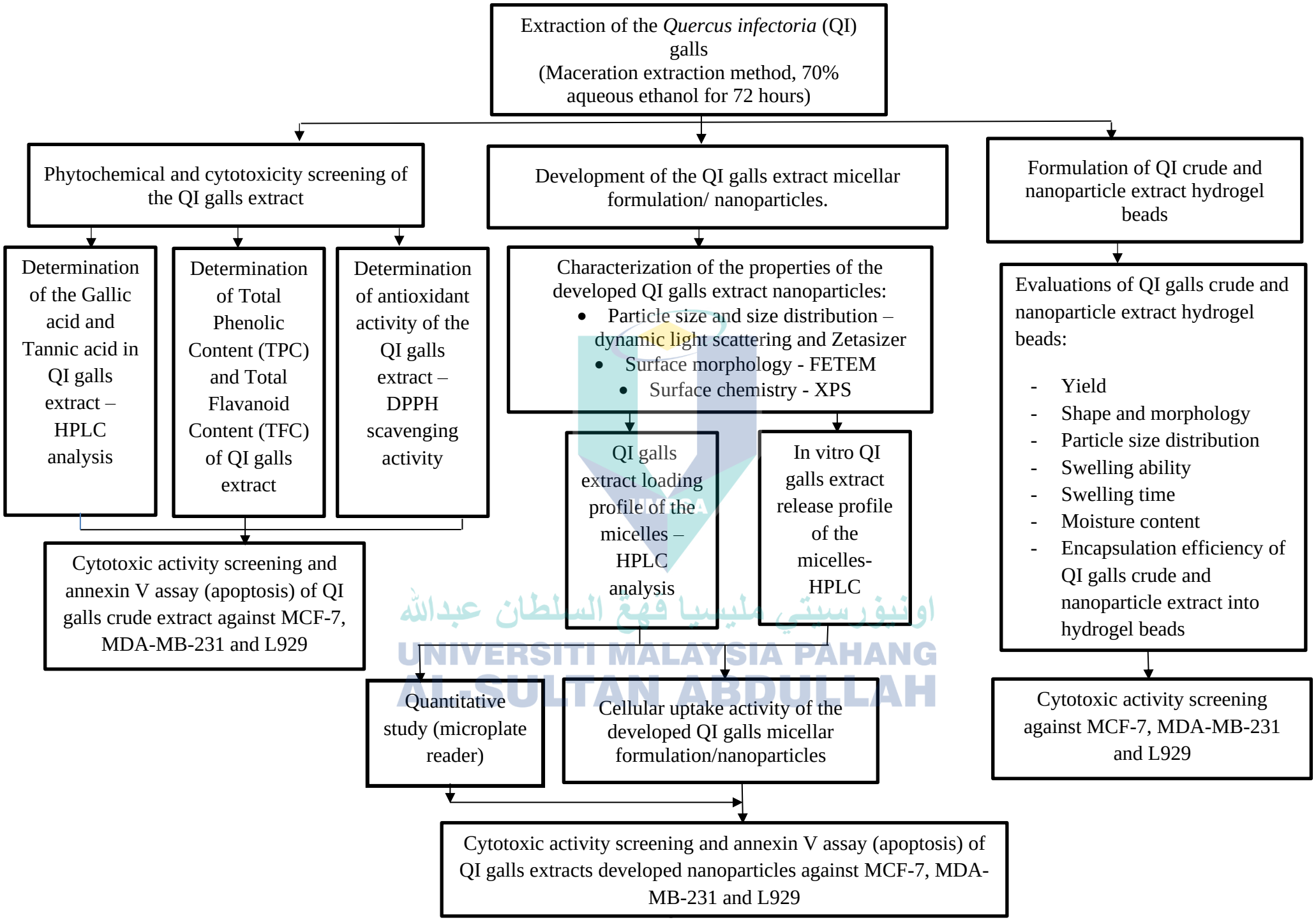

Figure 3.1: Research flowchart

3.2 Materials

Table 3.1: List of chemical and reagents

No	Chemicals and reagents	Supplier
1	0.25% Trypsin-EDTA	Gibco, Life Technologies, USA
2	Pectin	Merck, Germany
3	Absolute ethanol	Roche Diagnostic GmbH, USA
4	Chloroform	Merck, Germany
5	Doxetacel	Calbiochem, Germany
6	DMEM powder	Invitrogen, USA
7	DMSO	Sigma-Aldrich, USA
8	EDTA	Amresco, USA
9	Zinc acetate	Sigma-Aldrich, USA
10	Fetal Bovine Serum (FBS)	Gibco, Life Technologies, USA
11	Gallic acid	Sigma-Aldrich, USA
12	Rutin	Sigma-Aldrich, USA
13	Tannic acid	Sigma-Aldrich, USA, USA
14	HCl	Merck, Germany
15	Ethanol	Sigma-Aldrich, USA
16	Potassium hydroxide	Sigma-Aldrich, USA
17	Sodium carbonate (Na_2CO_3)	Merck, Germany
18	Methanol	Merck, Germany
20	Sodium chloride (NaCl)	Amresco, USA
21	Sodium nitrite ($NaNO_2$)	Merck, Germany
22	Paraformaldehyde	Sigma-Aldrich, USA

Table 3.1 continued

23	Penicillin-streptomycin	Invitrogen, USA
24	Phosphate Buffer Saline (PBS) tablet	Sigma-Aldrich, USA
25	Triton-x	Sigma-Aldrich, USA
26	Trypan blue	Invitrogen, USA
27	Folin Ciocalteu	Roche Diagnostic GmbH, USA

Table 3.2: List of laboratory apparatus/consumables

No	**Apparatus/consumables**	**Supplier**
1	25 cm^3 tissue culture flask	Nunc, Denmark
2	96-wells plate	Nunc, Denmark
3	Beaker (500ml and 1L)	Asahi Techno Glass, Japan
4	Centrifuge tube	Greiner Bio-One, Austria
5	Filter paper	GE Healthcare, Life Science, Malaysia
6	Flow cytometry tube	BD Bioscience, USA
7	Haemocytometer	Assistant, Germany
8	Multichannel pipette	Eppendorf, New York
9	Petri dish	Nunc, Denmark
11	Poly-L-Lysin slide	Sigma-Aldrich, USA
12	Schott Duran bottle (500ml and 1L)	Duran Group GmbH, Germany
13	Stericup Filter Units (0.22µm)	Millipore, Singapore

Table 3.3: List of kit and antibodies

No	Kit and antibodies	Supplier
1	FITC Annexin V Apoptosis Detection Kit I	BD Bioscience, US
2	MTT Kit	BD Bioscience, US

Table 3.4: List of laboratory instruments

No	Equipments	Supplier
1	BD Facs Canto II flowcytometer	BD Bioscience, USA
2	Biosafety Cabinet class II	Erla Technologies, Malaysia
3	Centrifuge Universal 320	Hettich, USA
4	CO_2 Incubator	Shel Lab, USA
5	Fluorescence microscope	LEICA, Germany
6	Fume Hood	Levtech Sdn Bhd, Malaysia
7	Hot plate and magnetic stirrer	Erla Technologies, Malaysia
8	Microscope Axiostar Plus	LEICA, Germany
9	pH meter	Hanna Instruments, US
11	Rotamax 120	Heidolph, Germany
12	Rotavac Heidolph Laborate 4000	Heidolph, Germany
13	Spectrophotometer	Thermo Scientific, US
14	Vacuum pump	Heidolph, Germany
15	Water bath	Memmert, Germany
16	Weighing apparatus	Shimadzu, USA

Table 3.4 continued

17	HPLC apparatus	Agilent LC1100
18	UV Visible Spectrophotometer	Thermo Scientific, US
19	Dynamic Light Scattering (DLS)	90 Plus, Brookhaven Instruments Co., TX, and USA
20	Zetasizer	Malvern Nano ZS, Malvern Instruments Ltd., Worcestershire, UK
21	Transmission Electron Microscope (TEM)	JEM-2200FS, JEOL, Japan
22	X-ray photoelectron spectroscopy (XPS)	Kratos Ultra DLD, Shimadzu, Japan

3.3 *Quercus infectoria* (QI) galls extracts preparation.

Galls of *Quercus infectoria* (QI) were purchased from a local Indian herbal store. The galls were identified based on their morphology parameters such as external color, size, surface, texture, odor, taste, and thickness. Firstly, 1kg of galls was ground into powder before the extraction procedure was carried out. Then 50g of QI galls powder was homogenized in a beaker containing 500 ml of 70% ethanol and placed in an incubator shaker for 72 hours with the temperature maintained at 50˚C and frequent agitation. Then, the solution was filtered using Whatman No. 1 filter paper. The solvent was evaporated under reduced pressure to dryness by a rotary evaporator. Then, the extracts were freeze-dried for 48 hours to get powder extract. Finally, the powder extract was weighed and the percentage of yields was calculated based on the formula below and stored at 4˚C before used (Wan Yusof & Abdullah, 2020).

$$\text{Extraction yield (\%)} = \frac{\text{Final weight (g)}}{\text{Initial weight (g)}} \times 100 \qquad 3.1$$

3.4 Quantification of gallic and tannic acid in *Quercus infectoria* (QI) extract

The concentration of tannic and gallic acid from the QI gall extract was determined by High-Performance Liquid Chromatography (HPLC) analysis. HPLC was performed by reversed-phase HPLC on the C18 column through a binary gradient elution consisting of an aqueous methanol eluent at low pH as a mobile phase. The gradient system consisted of solvent A (25ml acetic acid and 975ml distilled water) and solvent B (99.8% methanol) pump at 1ml/min. The gradient starts with 100% solution B at 30 minutes. The column temperature was maintained at 30˚C. The sample peaks were identified by comparing them with standard solutions of tannic and gallic acid at 280nm. The quantity of gallic and tannic acid will be determined using the appropriate calibration curve (Hasmida et al., 2015).

3.5 Determination of the Total Phenolic Content (TPC) in *Quercus infectoria* (QI) galls extract

The TPC of the QI gall extract was quantified using a Folin-Ciocalteu (FC) assay. An aliquot (1 ml) of diluted (0.8 mg/ml) extract solution was dissolved with 5 ml of FC reagent, which is pre-diluted 10 times with distilled water. The mixture was kept for 5 minutes at room temperature, followed by adding 4ml of sodium carbonate solution (Na_2CO_3, 7.5% w/v). The solutions were shaken and stood for 1 hour at room temperature. The absorbance of the resulting blue color was recorded at 765nm using a UV-Vis Spectrophotometer. 25, 50, 100, 200, and 400 µg/ml Gallic acid dissolved in methanol was used as the standard for making a calibration curve to determine the TPC. The result was expressed as mg GA equivalent/g of freeze-dried crude extract (mg GAE/ g CE) (Sepahpour et al., 2018).

3.6 Determination of Total Flavanoid Content (TFC) in *Quercus infectoria* (QI) galls extract

The colorimetric assay was used for the determination of the TFC in QI gall extract. 500 µl of diluted extract (0.8mg/ml) was dissolved in 2.5 ml of distilled water followed by the addition of 150 µl of 5% (w/v) sodium nitrite ($NaNO_2$) to the solution. After 5 minutes, 300 µl of 10% (w/v) aluminum chloride ($AlCl_3$) was mixed and the solution was allowed to stand for 5 minutes before the addition of 1 ml of 1M NaOH solution. The mixture was diluted with 550 µl of distilled water and shaken vigorously.

The solution absorbance was read at 510nm using a UV-visible spectrophotometer. Rutin was used as the standard at concentrations of 25, 50, 100, 200, and 400 µg/ml. The results were reported as mg Rutin equivalent/g of freeze-dried crude extract (mg Rutin/g) (Sepahpour et al., 2018).

3.7 Determination of antioxidant activity of *Quercus infectoria* (QI) galls extract by DPPH free radical-scavenging assay.

The antioxidant capacity of the QI galls extract was measured using 1,1-diphenyl-2-picrylhydrazyl (DPPH) radical scavenging assay. An aliquot (1ml) of QI galls extract was mixed with 3.9 ml of 0.1 mM methanolic DPPH solution. The mixture was thoroughly mixed and allowed to stand in the dark for 30 minutes at room temperature. The absorbance of the solution was read at 517nm. Results was expressed as the percentage of inhibition of the DPPH radical which was calculated according to the following equation:

$$\% \text{ of inhibition} = \frac{A_{control} - A_{sample}}{A_{control}} \times 100 \text{ , where} \qquad 3.2$$

$A_{control}$ is the absorbance of the DPPH and A_{sample} is the absorbance of the DPPH after adding extracts. All tests will be done in triplicate (Sepahpour et al., 2018).

3.8 Cell culture

Different types of cancerous and non-cancerous cells were used in this study, namely, breast cancer (MCF-7 and MDA-MB-231) and normal fibroblast (L929). These cell lines were purchased from the American Type Culture Collection (ATCC, Manassas, Virginia, USA). The growth medium used was Dulbecco's Modified Eagle Medium (DMEM) (Invitrogen, USA) supplemented with 10% Fetal Bovine Serum (FBS) (Gibco, Life Technologies, USA) and 1% penicillin-streptomycin (Invitrogen, USA).

Firstly, the cryovial containing frozen cells was thawed by gentle agitation in a 37˚C water bath or rubbing with palms. Then, cryovial contents were transferred to a centrifuge tube containing 10 ml growth medium and spun at 125 *x*g for 5 minutes. The supernatant was discarded, and the cell pellet was gently resuspended in a complete growth medium and dispensed into a 25 cm^3 sterile culture flask (Nunc, Denmark). The

cell culture was maintained in a 37˚C humid incubator with an air mixture containing 5% (v/v) CO_2. All procedures involved were performed under controlled aseptic conditions.

3.8.1 Subculture of cell lines

Subculture is necessary to maintain the healthy growth of the cultured cells. It is preferable to perform subculture at the top end of the log phase where the growth rate is higher, and the recovery time (lag phase) is shorter (Freshney, 2006). Therefore, subculture was carried out once cells had 80% occupied the surface area of the cultured flask. Firstly, the culture medium was discarded, and cells were washed thrice with phosphate buffer saline (PBS). Then 1 ml of 0.25% (v/v) trypsin-EDTA (Sigma- Aldrich, USA) was added to the flask and incubated in a 5% CO_2 incubator at 37˚C for 5-10 minutes to detach the cells. Next, 5 ml of fresh culture medium was added, and cells were aspirated by gently pipetting the medium. Cells suspension was then transferred into the centrifuge tube and spun for 5 minutes at 300 *x*g. The supernatant was discarded and cells were divided in ratios 1:2 to 1:6 into a new culture flask and maintained in a 5% CO_2 incubator (Shel Lab, USA) at 37˚C for 72 hours (Wan Yusof & Abdullah, 2020).

3.8.2 In vitro cytotoxicity study of the breast cancer cells using QI gall crude extract

Cells were washed thrice with PBS and trypsinized. The cells were counted by using a hemocytometer. Then, 100µl of cell suspension was seeded at a concentration of 5 x 10^4 cells/ml into a 96-well plate (Nunc, Denmark) and incubated in a 5% CO_2 incubator until reached 80% confluent. Then, the medium was discarded and replaced with 200µl of fresh medium in each well. Before treatment, 10mg of QI extracts or docetaxel drug were dissolved in 1 ml dimethyl sulfoxide (DMSO) to obtain 10 mg/ml of stock solution. Starting from 10 mg/ml of prepared stock solution, serial dilutions were then performed to prepare different ranges of concentrations. Next, 2µl of QI gall extracts or docetaxel (control drug) of different concentrations were added into each well. Cells treated with 1% DMSO served as negative control. It has been demonstrated that at this recommended concentration, DMSO does not affect cell viability (Lope Pihie *et al*., 2012). The cells were incubated in a 5% CO_2 incubator at 37˚C for 72 hours. All treatments were performed in triplicates.

After treatment, an MTT assay (BD Bioscience, USA) was then carried out to evaluate the cytotoxic activity of the extracts against cancerous (MCF-7, MDA-MB-231) and normal (L929) cell lines. Docetaxel was used as a control drug. Firstly, 50 µl of MTT solution (BD Bioscience, USA) was added to each well and incubated in a 5% CO_2 incubator for 4 hours. MTT solution was removed, and the purple formazan crystal formed at the bottom of the wells was dissolved with 200 µl DMSO for 20 minutes. The result was read using the ELISA (Bio-Rad Microplate Reader Model 680, USA) at 570 nm. The resulting color intensity is directly proportional to the number of living cells. The relative percentage of living cells was determined by the following formula:

$$\frac{\text{Optical Density (OD) average of samples}}{\text{Optical Density (OD) average of control}} \times 100\% \qquad 3.3$$

The IC_{50} value was determined from the dose-response curve of living cells percentage against the final concentration of the treatment agent. In this study, the crude extract that inhibits cancer cell proliferation with $IC_{50} \leq 20\mu g/ml$ was considered as a good antiproliferative agent and potent to inhibit cancer cell proliferation. The most potent extract was selected for further study of cell death mechanism via apoptosis and screened for phytochemical constituents. The IC_{50} value was used as concentration for consecutive experiments (Wan Yusof & Abdullah, 2020).

3.8.3 In vitro apoptosis activity in breast cancer cells using QI galls crude extract

Cells with 80% confluency were treated with QI galls crude extract and incubated for 72 hours in a 5% CO_2 incubator at 37˚C. Untreated cells were used as negative control and cells treated with docetaxel were the control drug. After incubation, cells were trypsinized and centrifuged at 300 *x*g for 5 minutes.

According to the manufacturer's instructions, the AV/PI staining was carried out using FITC Annexin V Apoptosis Detection Kit I (BD Biosciences, USA). Briefly, cells were washed twice with cold PBS before resuspended in 1X binding buffer at a concentration of $1x10^6$ cells/ml. Then, 100µl of $1x10^5$ of cell suspension (cells/ml) were transferred into a 5ml flow cytometry tube and mixed with 5µl of FITC Annexin V and 5µl propidium iodide (PI). After 15 minutes of incubation at room temperature in the dark, 400 µl of binding buffer was added into the tube and analyzed with BD FACS Canto

II flow cytometer within 1 hour. BD FACSDiva version 6.1.2 software was used to analyze the data (Wan Yusof & Abdullah, 2020).

3.9 Preparation of *Quercus infectoria* (QI) galls and phenolics extract loaded micelles.

QI gall extract and phenolics; tannic acid, gallic acid and combination of tannic and gallic acid-loaded nanoparticles were prepared according to the solvent-casting method. Briefly, QI gall extract (2 mg) will be added to a chloroform solution of TPGS (50 mg). The organic solvent was removed by rotary vacuum evaporation (water bath temperature set to 40˚C). The thin film formed was further dried in a vacuum overnight and hydrated in 1×PBS buffer. The mixture was incubated at 37˚C under constant agitation and then sonicated for a few minutes. The resultant mixture was filtered through a 0.2 mm polyether sulfone syringe to remove the excess amount of QI gall extract (Kutty, Chia, et al., 2015). The formulated micelles are known as; QI galls extract (QIT), tannic acid (TAT), gallic acid (GAT) and combination of tannic and gallic acid (TGT).

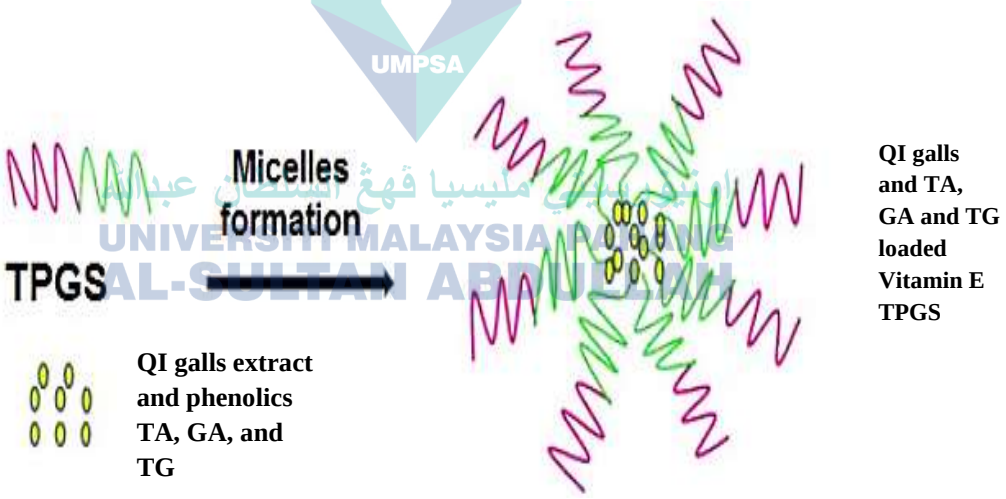

Figure 3.2: Schematic diagram for the formulation of QI galls-loaded Vitamin E TPGS

3.9.1 Characterization of particle size, size distribution, and surface charge

The particle size and size distribution of the formulated micelles (QIT, TAT, GAT, and TGT) nanoparticle samples were measured by dynamic light scattering (DLS) (90 Plus, Brookhaven Instruments Co., TX, and USA) in an aqueous medium. The surface charge was determined by Zetasizer (Malvern Nano ZS, Malvern Instruments

Ltd., Worcestershire, UK) at room temperature. The nanoparticles were diluted with deionized water to a count rate of 300-500 kcps and sonicated for 5 min before measurement to ensure that the nanoparticles were well dispersed (Kutty, Chia, et al., 2015).

3.9.2 Characterization of surface morphology

The shape and surface morphology of the formulated micelles (QIT, TAT, GAT, and TGT) were visualized using a transmission electron microscope (TEM, JEM-2200 FS, JEOL, Japan). The sample was prepared by placing one drop of micelles solution on a copper grid and then dried under vacuum pressure (Kutty, Chia, et al., 2015).

3.9.3 Characterization of surface chemistry

The surface chemistry of the formulated micelles (QIT, TAT, GAT, and TGT) micelles were analyzed by X-ray photoelectron spectroscopy (XPS) (Kratos Ultra DLD, Shimadzu, Japan) under fixed transmission mode with pass energy of 80 mV and the binding energy range of 0-1100 eV. The nanoparticle samples were prepared by dropping the solution onto glass slides and drying under vacuum pressure (Kutty, Chia, et al., 2015).

3.9.4 Drug encapsulation of the micelles

The amount of QI gall extract and phenolics encapsulated in the micelles was measured by high-performance liquid chromatography (HPLC) (Agilent LC1100). A reversed-phase Inertsil ODS-3 column (150×4.6 mm, particle size 5 mm, GL Science Inc., Tokyo, Japan was used. 1 ml micelles were freeze-dried and dissolved in 1 ml dichloromethane (DCM). After evaporating DCM, 1 ml mobile phase consisting of acetonitrile and water solution (50:50 v/v) was added to dissolve the drugs. After centrifugation at 13,000 rpm for 5 min, a supernatant of the suspension was collected, and the solution was then filtered through a 0.45 mm PVDF syringe filter for HPLC analysis. The column effluent was detected at 230 nm with a UV/VIS detector, and the flow rate was set to 1.0 ml/min (R.V. Kutty *et al*., 2015).

The drug loading is calculated as:

$$\text{Drug loading (\%)} = \frac{\text{weight of drug used (g)}}{\text{weight of micelles + drug used (g)}} \times 100 \qquad 3.4$$

3.9.5 In vitro drug release profile of the micelles

5ml of QI galls extract loaded micelle was placed in a dialysis bag (molecular weight cut-off 10kda) with 0.1% (w/v) Tween 80. The dialysis bag was incubated in 10ml PBS (0.1M, pH 7.4) containing 0.1% (v/v) Tween 80 at 37˚C with gentle shaking at 90 rpm. The incubation buffer was collected and replaced with a fresh incubation buffer at every designated time point. The collected buffer, including the released drug, was centrifuged at 13,000 rpm for 20 minutes at 4˚C. The supernatant was drained, and the pellet was resuspended with a mobile phase consisting of acetonitrile and water solution (50:50) (v/v). The amount of drug released was quantified using High-Performance Liquid Chromatography (HPLC) using the method described in drug loading before (Kutty, Chia, et al., 2015).

3.9.6 In vitro cytotoxicity study of breast cancer cells using QI gall and phenolics loaded micelle

Cell lines were seeded in 96-well transparent plates (Costar, IL, USA) at 5×103 cells/well (0.1 ml), and after 12 hours, the medium was replaced by micelle suspensions with designated concentrations for 24 hours. The micelles were sterilized with UV irradiation overnight before the experiment. Cell viability was measured using the MTT assay standard protocol in which the optical density at 570 nm will be determined by a microplate reader (Genios, Tecan, Männedorf, Switzerland) (Kutty, Chia, et al., 2015).

3.9.7 In vitro apoptosis activity in breast cancer cells using QI galls and phenolics loaded micelle

Cells with 80% confluency were treated with micelles extract and incubated for 24 hours in 5% CO_2 incubator at 37˚C. Untreated cells were used as negative control and cells treated with docetaxel were the control drug. After incubation time, cells were trypsinized and centrifuged at 300 *x*g for 5 minutes. The AV/PI staining was carried out using FITC Annexin V Apoptosis Detection Kit I (BD Biosciences, USA) according to the manufacturer's instructions. Briefly, cells were washed twice with cold PBS before

resuspended in 1X binding buffer at a concentration of $1x10^6$ cells/ml. Then, 100µl of $1x10^5$ of cell suspension (cells/ml) were transferred into a 5ml flow cytometry tube and mixed with 5µl of FITC Annexin V and 5µl propidium iodide (PI). After 15 minutes of incubation at room temperature in the dark, 400 µl of binding buffer was added into the tube and analyzed with BD FACS Canto II flow cytometer within 1 hour. BD FACSDiva version 6.1.2 software was used to analyze data (Wan Yusof & Abdullah, 2020).

3.9.8 In vitro quantitative study of the cellular uptake of the *Quercus infectoria* (QI) galls micelle

In vitro quantitative study of cellular uptake of the QI galls micellar formulations was assessed by the microplate reader. After reaching confluence, cells were detached, counted, and seeded in a 96-well black plate at $2x10^4$ cells/ well (0.1ml). After 24 hours of incubation, the medium was replaced by QI gall micelles suspensions with a concentration of 0.125 mg/ml. After 0.5 hours or 2 hours of incubation, the QI gall extract suspension was removed. Cells were washed twice with 1x PBS and immersed in 50ml of 0.5% Triton-X-100 in 0.2 N NaOH solutions. After 15 minutes of incubation under gentle shaking, the fluorescent intensities were measured with a microplate reader at an excitation wavelength of 430nm and an emission wavelength of 485nm (Kutty, Chia, et al., 2015).

3.10.1 Formulation of *Quercus infectoria* (QI) galls crude and micelle extract hydrogel beads

QI galls crude (QIC) and micelle extract (QIM) hydrogel beads were synthesized via the ionic gelation method. Pectin and QI gall extracts (crude or micelle) were solubilized in distilled water and then stirred until the mixture became homogenous. After that, the mixture was dropped into the zinc acetate solution via a hose with a diameter of 2.5 mm. The cross-linking time was 15 minutes with mechanical stirring, after which the beads were filtered and washed with distilled water. Finally, the hydrogel beads were dried using a freeze drier (Surini & Diandra, 2017).

(a)

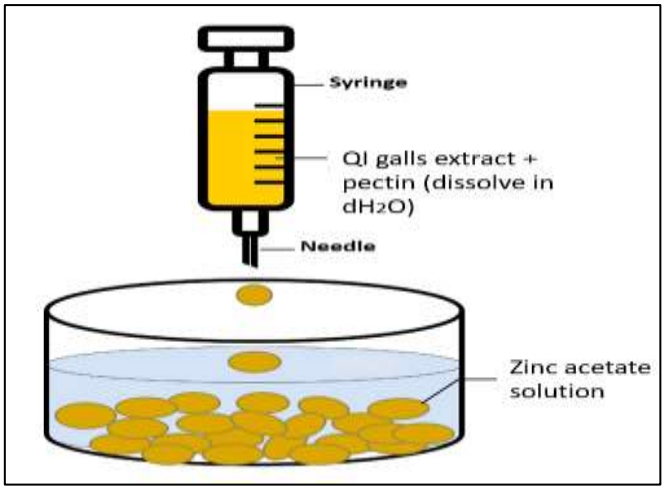

(b)

(c)

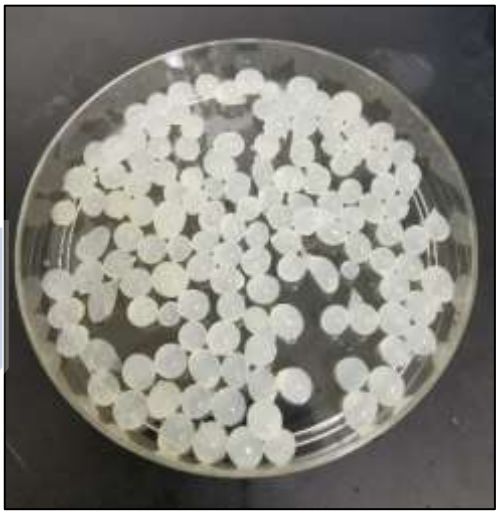

Figure 3.3: (a) Schematic diagram for the formulation of hydrogel beads; (b) QI gall crude hydrogel beads; (c) QI gall micelle hydrogel beads

3.10.1 Determination of yield

The yield was calculated using the following equation:

$$Wp=Wm\ /Wt \times 100\%\ (1) \qquad 3.5$$

Where Wp is the yield, Wm is the total weight of the beads after formulation, and Wt is the total weight of the mixture being prepared for the formulation (Surini & Diandra, 2017).

3.10.2 Determination of hydrogel beads shape and morphology

An optical microscope was used for the shape and morphology examination. Beads were observed using an optical microscope with several magnifications (4x, 10x and 40x) (Surini & Diandra, 2017).

3.10.3 Particle size distribution of the hydrogel beads

The diameters of 300 randomly selected beads from each formula were measured using a Vernier caliper. The results of the measurement of the average diameter of the beads for each formula then calculated and recorded (Surini & Diandra, 2017).

3.10.4 Swelling ability of the hydrogel beads

The 100mg beads from each formula were placed in weighing dishes. After, 10 mL of distilled water was added. Then, the swelling of the beads in room temperature was observed. Beads were weighed using an analytical balance at 5, 10, 15, 30, 60, 90, and 120 minutes, and swelling ability was calculated by the following equation:

$$\text{Swelling ability (\%)} = W2\text{-}W1 \,/\, W1 \times 100\% \qquad 3.6$$

Where W2 is the beads weight after swelling, and W1 is the initial beads weight (Surini & Diandra, 2017).

3.10.5 Swelling time of the hydrogel beads

The 10 mL of distilled water was added to the 100mg beads from each formula that were placed in weighing dishes. Then, the swelling of the beads was observed in terms of time. Swelling time was determined by measuring the time it took for the beads to swell for the first time in distilled water. The swelling time test was performed visually by observing the beads as they began to sink into the distilled water from their original floating position (Surini & Diandra, 2017).

3.10.6 Moisture content of the hydrogel beads

Moisture content was determined using a moisture analyzer. The equipment was prepared to reach a temperature of 105°C before use. Then, 1g beads were spread on a plate, and the moisture analyzer was turned on to show the beads' moisture content (Surini & Diandra, 2017).

3.10.7 Encapsulation efficiency of extract into hydrogel beads

Encapsulation efficiency of the QI galls crude and nanoparticle extracts was estimated by Nunes *et al*. (2015) method. In this method, at first, the amount of surface phenolic compounds, or nonencapsulated compounds, was calculated. For this purpose, 100 mg of hydrogel beads was added to 1 mL of ethanol–methanol solution (ratio of 1: 1) by vortex for 1 min to lyse the hydrogel beads. After filtration, its phenolic content was determined by the Folin– Ciocalteu method. Finally, the encapsulation efficiency was calculated using following equation:

$$\text{Encapsulation Efficiency (EE \%)} = \frac{(Ci - Cf)}{Ci} \times 100 \qquad 3.7$$

EE stands for encapsulation efficiency, Ci stands for initial total phenolic content (TPC), and Cf stands for encapsulated phenolic content inside hydrogel beads.

3.10.8 Cytotoxic activity of QI galls micelle and crude extract hydrogel beads.

The cytotoxicity of hydrogel beads was evaluated on breast cancer cells; MCF-7 and MDA-MB-231 and normal cell line, L929 using the MTT assay. The cells were cultured in DMEM supplemented with 10% FBS, penicillin (100 U/ml) and streptomycin (100 µg/ml) at 37°C and 5% CO2. The cells (1 x 10^5 cells/ml) were incubated with QI galls nanoparticle and crude extract loaded hydrogel beads for 24, 48 and 72 h. The MTT solution (0.5 mg/ml) was added and incubated for 4 h. Formazan crystals were then dissolved with DMSO. A change in color was detected by a UV-Visible spectrophotometer at 570 nm. The cell viability (%) of treated cells was calculated as percentages of the untreated cells (control) (Mahasawat et al., 2019).

3.11 Statistical analysis

Data were expressed as mean ± SEM (Standard Error of Mean) of three independent experiments. Data analysis for the results were performed using the Statistical Package of Social Science (SPSS) Software, version 20. The Shapiro-Wilk test was used for normality. The statistical significances of differences was determined using One-way analysis of variance (ANOVA) and probability values of $p < 0.05$ were considered to be statistically significant.

CHAPTER 4

RESULTS AND DISCUSSION

4.1 Introduction

The antiproliferative activity of the QI galls crude and micelle extract hydrogel beads and the research findings were discussed in this chapter. To provide a clear picture of this study, the following order arranged the results and discussion: the beginning of this chapter was focused on the findings of the physicochemical properties, cytotoxicity study, and the apoptosis activity of the QI gall crude extract. The yield of the extraction of the QI gall was also highlighted. The organoleptic properties of QI gall also were investigated through visual inspection. The parameters of the organoleptic inspection were external color, size, surface, texture, and odor.

The next findings were focused on the formulation and characterization of the QI gall-loaded micelle. The micelles were formulated using a solvent casting method between Vitamin E TPGS as the nanocarrier and the crude extracts. There are four types of formulated micelles which are micelle incorporated with QI gall crude extract (QIT), micelle incorporated with tannic acid (TAT), micelle incorporated with gallic acid (GAT), and micelle incorporated with a combination of tannic and gallic acid (TGT). This study was conducted to examine the antiproliferative effects of various micelle formulations containing QI gall crude extract and certain phenolics that are abundant in QI gall crude extract such as tannic and gallic acid. This approach could help to analyze the QI gall crude extract cytotoxic activity and gain insights into the specific effects of individual phenolics that are contained in the crude extract. By subjecting a micelle containing the QI gall crude extract to an antiproliferative study, the comprehensive inhibitory effect on cell proliferation caused by the natural mixture can be determined. By comparing this to micelles that are solely loaded with tannic and gallic acid, or each

one individually, the primary active components and their mechanisms of action can be figured out. Through this approach, more effective composition can be discovered. The formulated micelles were then characterized for their physicochemical properties such as the particle size and size distribution, surface charge, surface chemistry, surface morphology, in vitro drug release and loading as well as the quantitative cellular uptake. The physicochemical properties and cytotoxicity results were discussed for all the formulated micelles.

After the micelle formulation and characterization, the next findings were focused on the formulation of the hydrogel beads incorporated with QI gall crude (QIC) and micelle (QIM) extracts. Hydrogel beads were formulated through the ionic gelation method which involves the crosslinking action between polymer pectin and crosslinker zinc acetate was carried out. The findings such as the yield, particle size, moisture content, swelling time, swelling ability, encapsulation efficiency, and cytotoxicity study of the QI galls crude and micelle hydrogel beads were discussed. From the findings, it was revealed that the formulation of the hydrogel beads can improve the cytotoxicity of the extract as compared to the crude extract.

4.2 Organoleptic properties of *Quercus infectoria* (QI) galls

The parameters of organoleptic properties of QI galls investigated were external color, size, surface, texture, and odor. All of these parameters are important as the morphological identification (Wan Yusof & Abdullah, 2020). The picture of the powder form and crude extract of the QI gall is shown in Figure 4.1 below. The results of the organoleptic properties obtained are summarized in Table 4.1 below.

(a) (b)

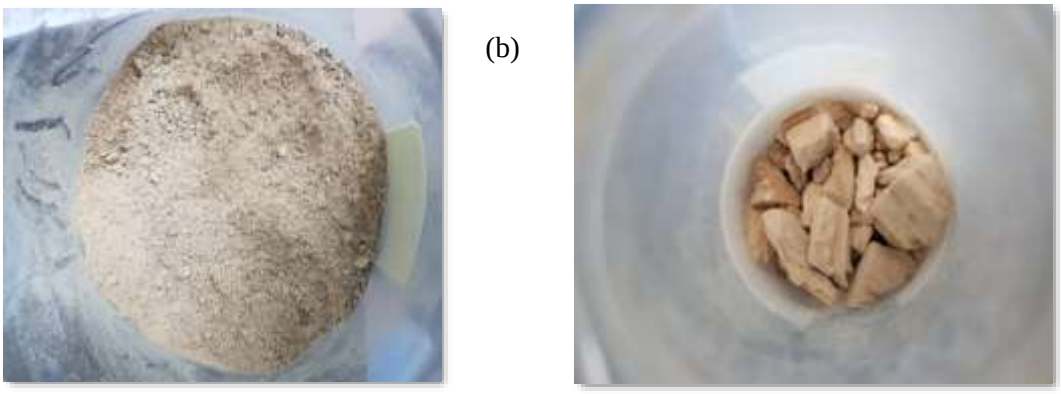

Figure 4.1: Picture of: a) powder form of QI gall b) crude extract of QI gall

Table 4.1: Organoleptic properties of QI galls

No	Parameter	Results
1	External colour	Dark yellowish
2	Texture	Hard and woody
3	Surface	Rough and horny
4	Odour	Pungent odour
5	Size	Small (diameter 1-1.5cm)

4.3 Extraction yield of *Quercus infectoria* (QI) galls

The extraction of QI galls powder with 70% ethanol produced a high yield with the weight of extract obtained is 23.77 ± 0.38g and a percentage yield is 47.54%. The QI powder used for the extraction is 50 g. Determination of percentage yield is important to help in the organic solvent selection for the future extraction process. The results obtained are summarized in Table 4.2 below.

Table 4.2: Extraction yield of QI galls

Solvent	Weight of extract (g)	Yield of extract (%)
70 % ethanol	23.77 ± 0.38	47.54 ± 0.62

The extraction yield was strictly dependent on the nature of extracting solvents and the method of extraction due to the presence of different availability of bioactive compounds, resulting from the various chemical characteristics and polarities that may or not be soluble in a particular solvent (Hamad et al., 2017). Besides, the extraction yield of the plant depicted that polar compounds in herbal or plant samples were easier to extract with polar solvent. In the previous study, it was reported that methanol extracts

the most components from the plant, followed by ethanol and water respectively (Hamad et al., 2017). The ability of a solvent to dissolve different solutes is determined by the solvent's polarity. This is known as the 'like dissolves like' principle in chemistry. As a result, polar and non-polar solvents can dissolve polar and non-polar compounds (Zarrinmehr et al., 2022). The presence of various antioxidant compounds with varying chemical properties and polarities may or may not make a particular solvent soluble. Polyphenols are frequently recovered from plant matrices using polar solvents. Aqueous mixtures containing ethanol, methanol, acetone, and ethyl acetate are the best solvents. Methanol is generally more efficient in extracting lower molecular weight polyphenols, whereas aqueous acetone is effective in extracting higher molecular weight flavanols. Ethanol is a well-known solvent for polyphenol extraction that is also safe for human consumption (Ho et al., 2018).

Previous studies also revealed that the mixture of organic solvents with water gives a higher yield as compared to the pure organic solvent alone (El Maaiden et al., 2022). The suitable solvent for extracting target compounds should be selected carefully because the extracted compound will be based on the types of solvent used. A polar solvent will extract a polar compound and a non-polar solvent will extract a non-polar compound thus different solvents will yield different extract composition (El Maaiden et al., 2022). The highest yield is commonly achieved by using methanol or ethanol and their mixture with water. However, ethanol and water mixtures are widely used due to their low toxicity and high extraction yield. In advance, their polarity can be modulated by mixing them at a selected ratio. This current finding can be supported by the previous study of isolation of phenolic compounds from cherry liquor pomace where they found that a 70% ethanol and water mixture is more effective compared to the pure solvent did (El Maaiden et al., 2022).

4.4 Total Phenolic Content (TPC) and Total Flavanoid Content of *Quercus infectoria* (QI) galls crude extract

The total phenolic content of the *Quercus infectoria* galls extract was expressed as gallic acid (GA) equivalent as presented in Table 4.3. This total phenolic content was determined by using the Folin-Ciocalteu colorimetric method. Gallic acid was used as the standard phenolic compound. The result showed total phenolic content of the QI gall extract is 672.22 ± 0.55 µg/mg gallic acid (GA) equivalent. The results obtained in this

study are much higher than those reported by (Nur Syukriah et al., 2014) who reported the total phenolic content from 70% aqueous-ethanolic extract of QI galls extract was only 99.43 µg/mg GAE.

Table 4.3: Total Phenolic and Total Flavanoid Content in QI galls extract

Sample	**Total Phenolic Content (µg/mg GA equivalent)**	**Total Flavanoid Content (µg/mg Rutin equivalent)**
Quercus infectoria (QI) extract	672.22 ± 0.55	4.8 ± 0.25

Phenols are very important plant constituents because of their radical scavenging ability due to their hydroxyl groups. The Folin-Ciocalteu assay gives an estimation of the total phenolic content in the herbal and plant extracts (Aryal et al., 2019). Besides that, some components in the plant extract such as sugars, ascorbic acid, and some phenols may also react with the Folin reagents and this will contribute to the increment of the total phenolic detected (Aryal et al., 2019).

According to a previous study by (Shahin, 2014), the highest amount of phenolic was found in QI galls extract which is 635.25 µg/mg GA equivalent. This can support the findings in the current study as the total phenolic content is not much different. The other findings revealed that the QI galls extract contains a higher amount of phenolic content (Hamad et al., 2017). The analysis revealed that phenolic compounds are the major phytochemicals in the QI gall extract. This finding is similar to the results obtained by (Khurana et al., 2018) who found that the QI galls extract had a large number of polyphenols and had a potent reducing power. Another study revealed that the QI gall extracts highest total phenolic content (TPC) was measured at 1756 mg of gallic acid equivalents (mGAE). This extract was obtained using the supercritical fluid extraction with carbon dioxide (SCFE-CO2) technique, with methanol as the co-solvent. The reason for this is comprehensible since the co-solvent methanol can form complexes with phenolic chemicals, resulting in a higher extraction yield (Purbowati et al., 2023). According to (Choudhry & Akhtar, 2023), the TPC result was determined by utilizing a

distinct absorbance versus concentration curve specifically created for gallic acid. The outcome was thereafter stated in terms of gallic acid equivalents (GAE). The QI extract utilized in this study possesses a total phenolic content of 56.1 mg GAE/g.

The total flavonoid content obtained in this finding is 4.8 ± 0.25 µg/mg Rutin equivalents. This total flavonoid content of the QI gall extract was determined using the aluminium chloride colorimetric method in terms of Rutin equivalents. Our current findings are supported by the previous findings by (Hamad et al., 2017) where only a small amount of flavonoid content was detected. According to the previous study, the QI galls extract comprises a small number of various flavonoids such as hyperoside, hesperidin, rutin, and quercetin as well as other types of flavonoid compounds (Hamad et al., 2017). In this current study, rutin was used standard for the determination of total flavonoid content in QI gall extract. A previous study also reported that the total flavonoid content (TFC) of the QI gall extract sample was measured in micrograms of quercetin equivalents (QE) per milligram (mg) of dry weight. The investigation revealed that the product contained a total of 35.32 mg of quercetin per gram, along with QI extracts and other flavonoids (Choudhry & Akhtar, 2023).

Flavonoids and phenolic compounds are produced by plants as bioactive secondary compounds. Flavonoids are polyphenolic compounds found in plants that are classified into six groups: isoflavonoids, flavanones, flavanols, flavonols, flavones, and anthocyanidins (Kopustinskiene et al., 2020). Flavonoids have been shown to have a wide range of anticancer properties, including the ability to modulate reactive oxygen species (ROS)-scavenging enzyme activities, participate in cell cycle arrest, induce apoptosis and autophagy, and suppress cancer cell proliferation and invasiveness. Flavonoids have a dual action in terms of ROS homeostasis: under normal conditions, they act as antioxidants, but in cancer cells, they are potent pro-oxidants, activating apoptotic pathways and downregulating pro-inflammatory signaling pathways (Kopustinskiene et al., 2020).

4.5 Antioxidant activity of the *Quercus infectoria* (QI) galls crude extract

The DPPH method was first introduced about 50 years ago by Blois (Proestos et al., 2013). Nowadays, this method is widely used to determine the ability of a compound to act as a hydrogen donor or free radical scavenger to figure out its antioxidant activity (Chaves et al., 2020). For this method, the parameter inhibitory concentration known as IC_{50} is used for the data interpretation. This IC_{50} value refers to the concentration of the drug/extract that caused a 50% loss of the DPPH activity (purple color intensity). Most of the natural products, such as plant extract and essential oils were evaluated concerning their IC_{50} value while others were determined for their antioxidant capacity (Chaves et al., 2020).

For this current study, the QI gall extract was tested for its antioxidant activity by the DPPH method. Ascorbic acid is used as the standard for the calibration curve. From the experiment, it was revealed that the IC_{50} value obtained for the sample QI galls extract was 44.5 µg/ml (Figure 4.2). The value obtained for the sample QI gall extract is much higher than the standard, ascorbic acid. The value of the IC_{50} for ascorbic acid is 76.3 µg/ml (Figure 4.2). Previous study by (Shahin, 2014), reported that *Quercus infectoria* extract exhibited the highest antioxidant capacity which was 89.19% of DPPH inhibition. The antioxidant compound will reduce DPPH, a purple-colored stable free radical to a colorless ơ-ơ- diphenyl-picryl hydrazine. The scavenging ability of free radicals is an important marker to evaluate the antioxidant capacity of a compound. From another study, it was showed that the IC_{50} value obtained from *Quercus infectoria* galls oil is 170.5 µg/ml (A. El-Agbar et al., 2018). However, when compared to the current study, the IC_{50} value is much lower. The QI galls oil can also act as a potent antioxidant because of the presence of α-tocopherol, phenolics compounds, flavonoids, and numerous fatty acid compounds (A. El-Agbar et al., 2018).

Another previous study revealed that the antioxidant activity of QI gall extract was 81% in comparison with the reference (ascorbic acid). The QI gall extract is reported to include phenolic and flavonoid components that have antioxidant properties(Choudhry & Akhtar, 2023).

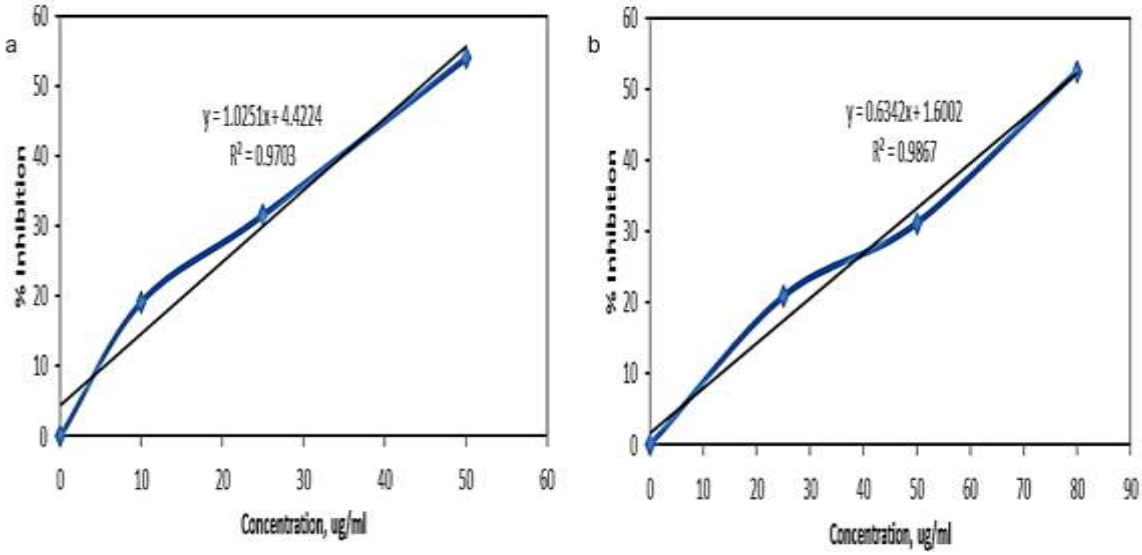

Figure 4.2: Scavenging activity of: a) Standard ascorbic acid b) *Quercus infectoria* (QI) galls extract

The DPPH method was commonly used to test any compound or extract for its free radical scavenging activity (De et al., 2017). The antioxidant compound works by donating an electron or hydrogen to DPPH when it reacts with it and at the same time neutralizing its free radical (De et al., 2017). A lot of other factors can contribute to the antioxidant activity like polyunsaturated fatty acid (PUFA), levels of α-tocopherol and β-carotene bleaching ability that can be used to determine the capacity of active components in inhibiting lipid peroxidation (Mrid et al., 2019).

4.6 Quantification of gallic and tannic acid in *Quercus infectoria* crude extract

HPLC was used to quantify the gallic and tannic acid in QI gall extract. The concentration of the targeted bioactive constituents was identified based on the peak area from the calibration curve. From the findings, it was shown that QI gall extract contains a high concentration of tannic acid and a small amount of gallic acid which were 1794.18 ± 0.71 mg/gm and 76.22 ± 0.44 mg/gm respectively. From the results, it was revealed that tannic acid is the major bioactive constituent in QI extract. Due to its high concentration, most of the pharmacological properties exhibited by the gall extract can be attributed to tannic acid (Liu et al., 2019). Figure 4.3 shows the chromatogram of the standard and sample of gallic and tannic acid. These phenolics have been determined in

QI gall extract based on their retention times against standards as well as spiking the samples with standard (Liu et al., 2019). Based on the previous study it was revealed that the aqueous extract of QI galls contains higher concentrations of gallic acid (101.55 mg/g) and tannic acid (2975.11 mg/g). This result showed that water is a better extraction for both gallic and tannic acid. The higher yield of both compounds might contribute to the pharmaceutical properties such as antioxidant and anticancer activity (Liu et al., 2019).

Previous studies reported lower concentrations of gallic acid and tannic acid in ethanolic extract of QI galls which are 37.22 mg/gm and 954.03 mg/gm respectively. However, these findings were also supported by previous data from past research, which showed the presence of tannic acid and gallic acid in QI gall extract (Husna et al., 2018).

Another study showed that the QI gall extract comprises seven bioactive constituents, namely tannic acid (67.18%), quinic acid (7.99%), gallic acid (2.57%), maleic acid (0.02%), ellagic acid (0.22%), salicylic acid (0.03%), chlorogenic acid (0.09%), benzoic acid (0.01%), caffeic acid (0.02%), and aconitic acid (0.02%). Identifying other compositions can be challenging because the acquired peaks are highly reproducible (Purbowati et al., 2024). Additional qualitative investigation of the QI gall extract using LC-MS/MS uncovers several chemicals present in the extract. The extract obtained by the SCFE-CO2 process with methanol as the co-solvent had the highest TPC compound, measuring 1756 mGAE. The supercritical CO2 or SCFE-CO2 extraction technique, using methanol as a co-solvent, successfully achieved a high-quality gall extract with significant yields of tannic acid. The extraction process also resulted in a high total phenolic content (TPC) and showed non-toxic properties. Moreover, the extract contained more than 20 different chemicals (Purbowati et al., 2023).

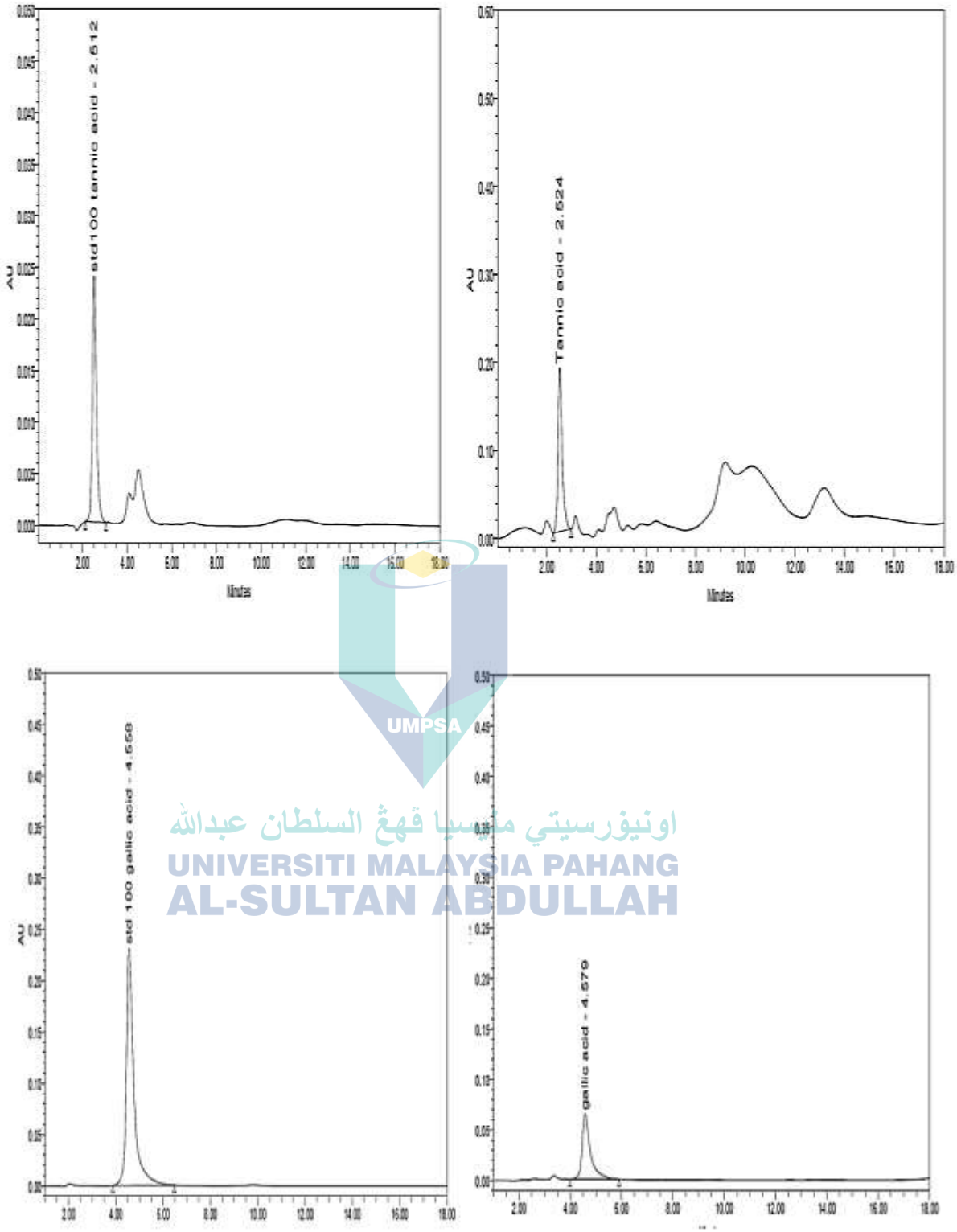

Figure 4.3: HPLC chromatogram with retention time (Rt); a) standard gallic acid, Rt: 4.558; b) gallic acid in QI galls extract, Rt: 4.579; c) standard tannic acid, Rt: 2.512; d) tannic acid in QI galls extract, Rt: 2.524.

4.7 Cytotoxic activity of *Quercus infectoria* (QI) crude extract

MTT assay was applied to assess the effect of QI gall extract and phenolics tannic acid (TA) and gallic acid (GA) and a mixture of (TA and GA) against breast cancer cell lines (MCF-7 and MDA-MB-231). To determine the cell viability, the cells were treated with various concentrations of QI gall extract and phenolics for 24, 48, and 72 hours. Docetaxel was used as a control drug. The use of the control drug in this study is for evaluating the cytotoxicity and potency of commercial anticancer drugs in comparison with the QI galls extract using selected breast cancer cells, MCF-7 and MDA-MB-231. This docetaxel serves as the positive control. A previous study reported the efficacy of the docetaxel drug in triple-negative breast cancer cells. MDA-MB-231 and breast cancer cells, MCF-7 (Kutty & Feng, 2013). The IC_{50} values obtained referred to 50% of the cells population killed or retarded by plant extract or drug (Ayob et al., 2014). There are four categories of extracts which are very active ($IC_{50} \leq 20$ µg/ml), moderately active ($IC_{50} >$ 20–100 µg/ml), weakly active ($IC_{50} >$ 100–1000 µg/ml) and inactive ($IC_{50} >$ 1000 µg/ml). For pure compounds or drug, an IC_{50} value less than 4 µg/mL is considered potent (Nordin et al., 2018).

Table 4.4 shows the IC_{50} values of QI galls extract and phenolic; TA and GA against MCF-7 cell line for 24,48- and 72-hour treatment. From the results, it was revealed that QI gall extract exhibited a good cytotoxic effect against the MCF-7 cell line after 72 hours of treatment with IC_{50} values of 0.961 ± 3.3 µg/ml. For 24 and 48 hours of treatment, QI gall extract showed a moderately active effect against the MCF-7 cell line (IC_{50} 74.25 µg/ml). For the phenolics, TA and GA, both expressed positive results only after 72 hours of exposure. The IC_{50} value obtained for TA was 9.61 ± 2.3 µg/ml while for GA was 4.03 ± 5.3 µg/ml (Figure 4.4). As comparing both TA and GA it was showed that GA possessed a better cytotoxic effect against MCF-7 cell line as the IC_{50} value was higher. As compared to control docetaxel (IC_{50} value 0.828 ± 0.99 µg/ml), QI gall crude extract exhibits good cytotoxic activity against MCF-7 cells ($p < 0.05$). A previous study showed that QI gall ethyl acetate extract (QIEA) exhibits cytotoxicity towards MDA-MB-231, MCF-7, and Hep G2 cell line with IC_{50} values 90.0 ± 16.9 µg/ml (MDA-MB-231), 20.5 ± 1.23 µg/ml (MCF-7) and 23.6 ±2.14 µg/ml (HePG2) (Wan Yusof & Abdullah, 2020).

Table 4.4: IC_{50} values of QI galls extract, and phenolics for 24,48- and 72-hours treatment against MCF-7 cell line, *$p < 0.05$ was taken as significantly different from control drug (docetaxel).

Extract	IC_{50} values (µg/ml)		
	24 hours	48 hours	72 hours
Docetaxel	31.25 ± 3.9	21.88 ± 2.5	0.828 ± 0.99
QI galls extract	74.25 ± 9.3	74.25 ± 7.4	0.961 ± 3.3*
Tannic Acid	> 100	> 100	9.61 ± 2.3*
Gallic Acid	86.63 ± 4.3	86.63 ± 5.8	4.03 ± 5.3*
Tannic/ Gallic Acid	> 100	> 100	2.81 ± 0.42

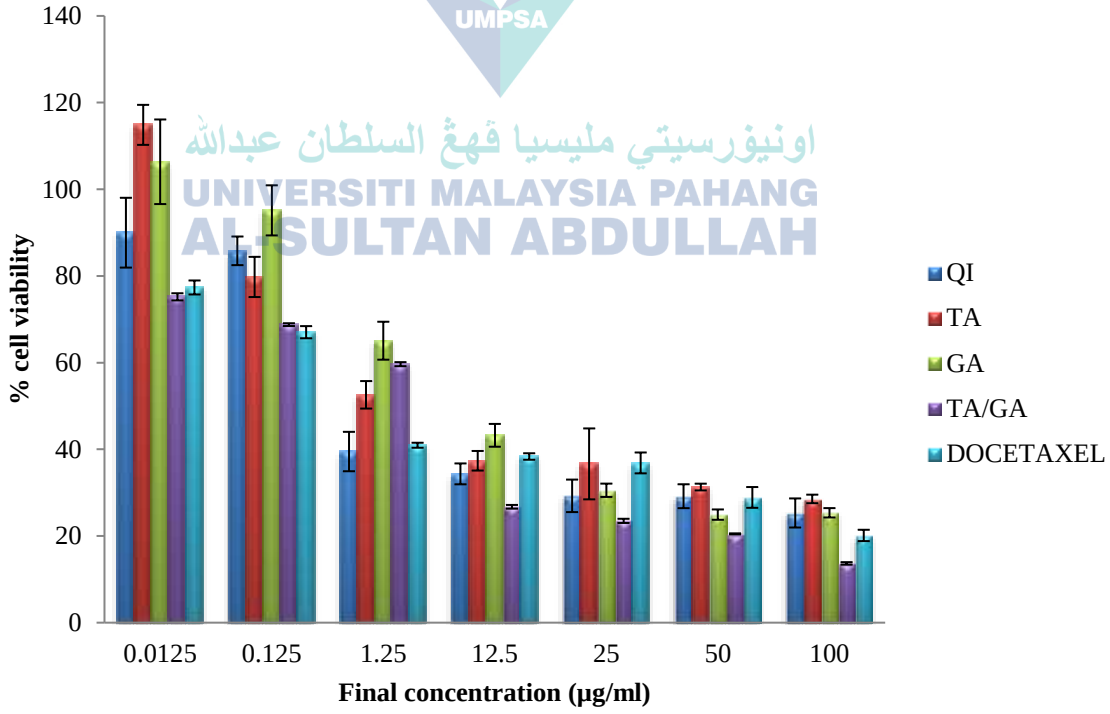

Figure 4.4: Cytotoxic activity of QI galls extracts and phenolics against MCF-7 cell lines after 72 hours of treatment. The graph represents means ± SEM µg/ml of three independent experiments (n=3).

Table 4.5 shows the IC_{50} values of QI gall extract and phenolic; TA and GA against the MDA-MB-231 cell line for 24, 48, and 72 hours of treatment. After 24 hours of treatment, all QI galls extract and phenolics; TA, GA and in combination exhibited weakly active (IC_{50} > 100 µg/ml) cytotoxic activity against MDA-MB-231 cells. Followed by 48 hours of treatment, QI galls and all phenolics showed higher IC_{50} values (IC_{50} < 100 µg/ml). QI galls extract and positive control, Docetaxel gave the lowest IC_{50} value after 48 hours of treatment with IC_{50} 50 ± 0.11 µg/ml and 68.75 ± 1.38 µg/ml respectively. However, after 72 hours of incubation, it was observed that QI galls extract exhibited a very active (IC_{50} ≤ 20 µg/ml) cytotoxic activity against the MDA-MB-231 cell line with the value of IC_{50} 9.61 ± 8.9 µg/ml as well as the positive control, docetaxel with IC_{50} 8.28 ± 1.79 µg/ml (p > 0.05). TA and GA showed moderately active cytotoxic activity with the IC_{50} values 74.25 ± 5.7 µg/ml and 43.33 ± 4.4 µg/ml respectively (Figure 4.5).

Table 4.5: IC_{50} values of QI galls extract, and phenolics for 24,48- and 72-hours treatment against MDA-MB-231 cell line, *p < 0.05 was taken as significantly different from control drug (docetaxel).

Extract	IC_{50} values (µg/ml)		
	24 hours	48 hours	72 hours
Docetaxel	> 100	68.75 ± 1.38	8.28 ± 1.79
QI galls extract	> 100	50 ± 0.11	9.61 ± 8.9
Tannic Acid	> 100	86.63 ± 2.2	74.25 ± 5.7*
Gallic Acid	> 100	74.25 ± 2.1	43.33 ± 4.4
Tannic/ Gallic Acid	> 100	99 ± 0.85	37.5 ± 0.44*

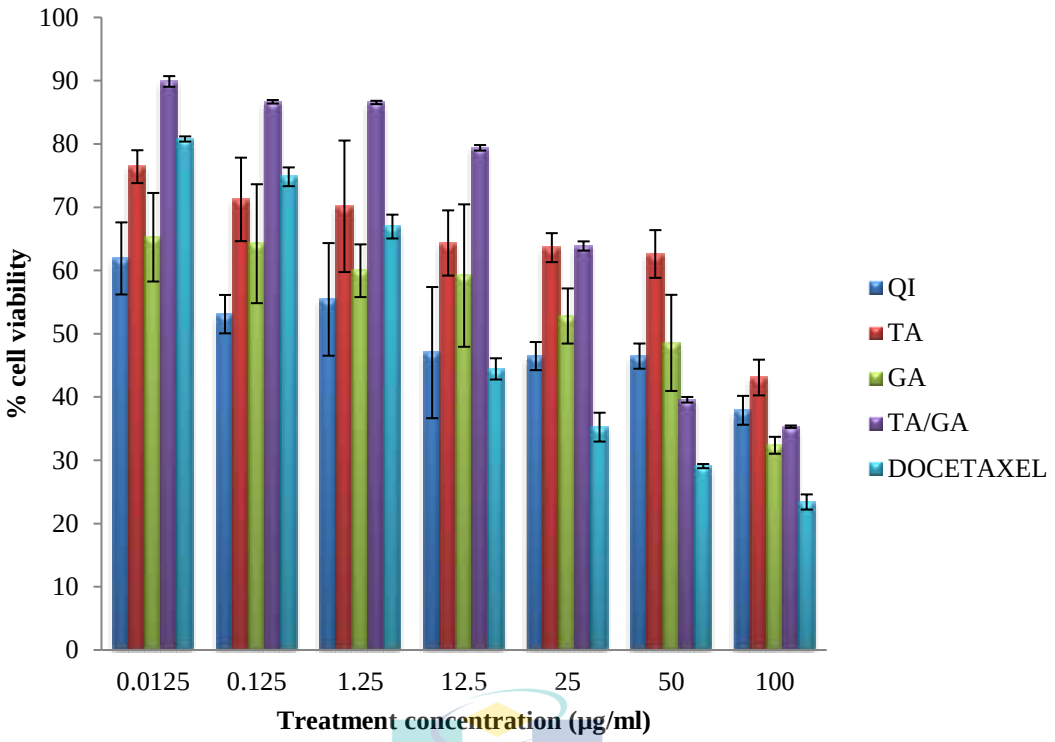

Figure 4.5: Cytotoxic activity of QI gall extracts and phenolics against MDA-MB-231 after 72 hours of treatment. The graph represents means ± SEM µg/ml of three independent experiments (n=3).

Due to the promising results exhibited by TA and GA alone in cytotoxicity against MCF-7 and MDA-MB-231 cell lines, hence, the combination of TA and GA was used to treat MCF-7 and MDA-MB-231 cell lines. TA and GA were combined per their ratio (1:24) found in the crude extract. MCF-7 and MDA-MB-231 cells were incubated with various concentrations of TA/GA for 24, 48, and 72 hours. From the results, it was shown that for 24 and 48 hours, the combination of TA and GA seems to have no cytotoxic effects against both cell lines as the IC_{50} > 100 µg/ml. These results were unexpected since the single GA already showed higher IC_{50} (86.63 µg/ml) after 24- and 48-hour incubation against MCF-7 cells. For MDA-MB-231 cells, single GA and TA gave IC_{50} values of 86.63 ± 2.2 µg/ml and 74.25± 2.2 µg/ml. Hence, the IC_{50} of the TA and GA combination was expected to be higher than these values. These results reveal that the single GA and TA work better against both cell lines as compared to the combination of TA and GA. TA seems to exhibit antagonistic effects when combine with GA because it retarded the effect of GA against both cell lines. After 72 hours, the combination of TA and GA showed a promising cytotoxic effect against the MCF-7 cell line with the IC_{50}

obtained was 2.81 ± 0.42 µg/ml (Table 4.4). For MDA-MB-231, the IC_{50} value after 72 hours of treatment was 37.5 ± 0.44 µg/ml (Table 4.5). This lower value may be due to the nature of this triple-negative breast cancer cell which is already known to have a poorer prognosis and is hard to treat even with established anticancer drugs and therapy (Ilaghi et al., 2021). The higher IC_{50} value obtained after 72 hours of treatment may be due to the hydrolyzation of TA where the ester bond is broken down to produce gallic and ellagic acid, resulting in increased cytotoxic activity (Ilaghi et al., 2021). These results were supported by the previous research, which, also showed the higher cell viability for the TNBC cell lines indicates lower therapeutic effects in comparison with the other types of breast cancer cells such as ER and PR overexpressed MCF-7 cells (Amna et al., 2019). These findings revealed that docetaxel was less effective against TNBC cells as compared to other types of breast cancer cells.

From the results, it was revealed that the cytotoxic effects of QI gall extract, phenolics, and docetaxel against breast cancer cells were decreased in a dose-dependent manner and by the prolonged treatment duration (Figure 4.5). This can be supported by the previous study, which showed that gallic acid (GA) inhibited cell growth dose-dependently (Moghtaderi et al., 2018). The IC_{50} of GA was approximately 150 µM in 24 hours and 50 µM in 48 hours (Moghtaderi et al., 2018). For tannic, and a combination of tannic and gallic acid against MDA-MB-231, it was shown that the IC_{50} values obtained were significantly lower as compared to the positive control, docetaxel ($p < 0.05$). These results revealed that QI gall extract was more effective as an anticancer agent compared to the individual phenolic compound. There are a lot of natural products known to have anticancer effects such as gallic acid and tannic acid which can be extracted from plants and herbs (Amna et al., 2019). Both of these phenolics are commonly applied in folk and traditional medicine to treat various diseases (Moghtaderi et al., 2018).

Another recent study showed that tannic acid and gallic acid showed good cytotoxic effects against cancer cell lines, prostate, and leukemia. However, the IC_{50} value obtained for breast cancer cells, MCF-7 is much lower as compared to the current study (IC_{50} > 50 µg/ml) (Alaklabi et al., 2018). Deiab *et al*. showed that 1,2,3,4,6-tetra-*O*-galloyl-D-glucose compound from QI galls extracts demonstrated significant antiproliferative effects on human MDA-MB-231 breast cancer cells with IC_{50} value as low as 1.2 M (Shen et al., 2018). Five compounds, including gallic acid, tannic acid,

methyl gallate, 1,2,3,4,6-tetra-*O*galloyl-D-glucose, and amentoflavone of QI galls have been broadly reported to possess anticancer effects against cancerous cells through apoptosis, cell cycle, angiogenesis, or metastasis mechanism of action (Qadir et al., 2017).

The anticancer activity of phenolics and polyphenols is related to their antioxidant and anti-inflammatory activity which can be associated with cell proliferation and survival (Moghtaderi et al., 2018). Previous data showed that gallic acid and tannic acid independently possess anticancer effects on several types of cancer (Nordin et al., 2018). Regarding the previous research, several compounds extracted from the QI galls have been proven to have anticancer effects (Nordin et al., 2018). Among them, gallic acid is the common compound revealed to have good anticancer activity against animal models and *in vitro* cancerous cell lines (Shen et al., 2018). Ellagic acid is another polyphenol that has been used in anticancer studies and has already shown a good anticancer effect against various cancer cells.

As a control, the QI galls crude extract was also tested against a normal cell line, L929 cells. From the results, it was shown that QI galls crude extract was cytoselective because it does not have a toxic effect against normal cell lines after 72 hours of incubation (Figure 4.6). A previous study also showed that the lowest IC_{50} of QI galls extract was tested against MDCK (control cell line) and the findings revealed that the extract showed very low toxicity towards normal cell (Ismail et al., 2021).

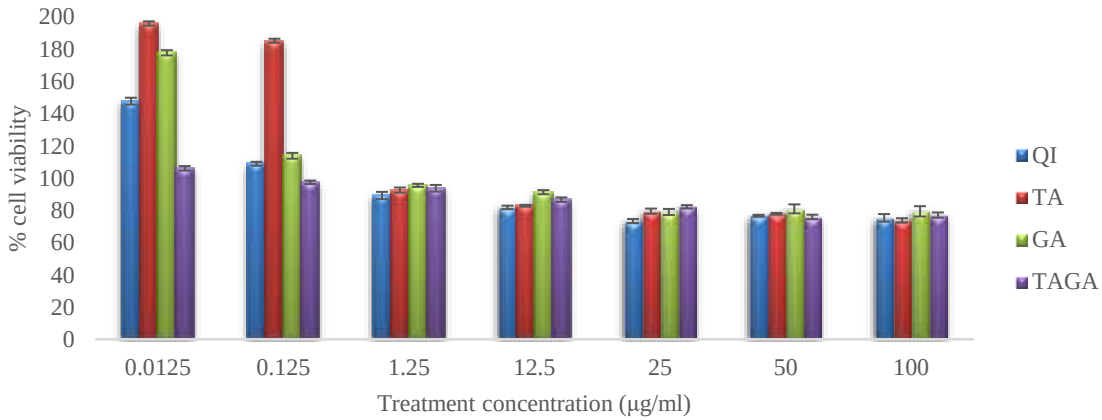

Figure 4.6: Cytotoxic activity of QI gall extracts and phenolics normal cell line, L929 after 72 hours treatment. The graph represents means ± SEM µg/ml of three independent experiments (n=3).

4.8 Cell death mechanisms of *Quercus infectoria* (QI) crude extract against breast cancer cells by FITC-Annexin V Assay

To determine whether the cytotoxicity of the QI galls extract, and docetaxel drug involved the induction of apoptosis, MCF-7 and MDA-MB-231 cells were treated with the corresponding IC_{50} concentrations of the QI galls extract and drug. The cells used were from the same batch of cells for cytotoxicity study. Then these cells were stained with Annexin V- fluorescein isothiocyanate (FITC), followed by the flow cytometric analysis. This staining procedure is based on the ability of Annexin V (AV) to bind to PS. Before the apoptosis event, PS becomes translocated from the inner side to the outer side of the plasma membrane and becomes exposed, to allow the binding of AV. Staining with propidium iodide (PI) enables viable cells (AV^-/PI^-), early apoptotic cells (AV^+/PI^-), late apoptotic cells (AV^+/PI^+), and dead cells (AV^-/PI^+) to be identified.

From the results, it was revealed that the QI galls extract, and docetaxel drug-induced cell death mechanisms through apoptosis. For MCF-7 cells, it was shown that when treated with QI galls extract, the percentage of early apoptosis cells was significantly higher ($p < 0.05$) than the untreated which was 50.33±0.38 % (Table 4.6). For the docetaxel drug, the percentage of early apoptosis cells was 12.53±0.24 % which is lower than the percentage of early apoptosis cells treated with QI galls extract and the untreated cells ($p < 0.05$) (Table 4.6). As compared to the untreated cells, the percentage of early apoptosis cells was just only 2.27±0.09 % (Table 4.6).

Extracts/ Treatment duration	Without treatment	Docetaxel treatment	Treatment with QI galls crude extract
72 hours	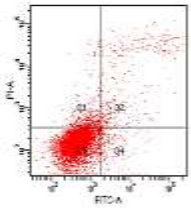	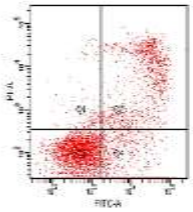	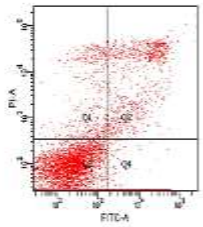
Extracts/ Treatment duration	**Without treatment**	**Docetaxel treatment**	**Treatment with QI galls crude extract**
72 hours	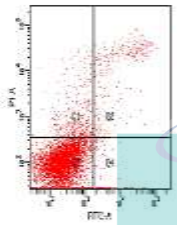	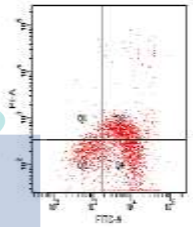	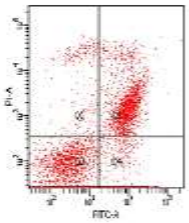

Figure 4.7: Scatter plot of FITC-AV/PI double staining in quadrant analysis. Q1: dead cells, Q2: late apoptotic cells, Q3: viable cells, and Q4: early apoptotic cells, n=3.

Table 4.6: Percentage of cells based on event of apoptosis in MCF-7 cell line. *$p < 0.05$ was taken as significantly different from the untreated group

Event of apoptosis	% of cells in the quadrant		
	untreated	QI galls extract	Docetaxel
Viable cell	89.4±0.83	31.33±0.33*	80.4±0.31*
Early apoptosis	2.27±0.09	50.33±0.38*	12.53±0.24*
Late apoptosis	4.7±0.07	11.5±0.29*	4.6±0.03
Dead/necrotic	3.8±0.06	8.03±0.09*	2.53±0.03*

For MDA-MB-231, when treated with QI galls extract, the percentage of early apoptosis cells was 48.2±0.2 % (Table 4.7). This is lower when compared to the percentage of early apoptosis cells of MCF-7 treated with QI gall extract. As compared to the untreated cells, this value was significantly higher ($p < 0.05$). For the cells treated with docetaxel drug, the percentage of early apoptosis cells was lower which was only 9.8±0.06 % (Table 4.7). For untreated cells, the percentage of early apoptosis cells was 8.4±0.06% (Table 4.7). These findings indicated that QI galls extract, and docetaxel drug stimulates cell death through the apoptosis mechanism because these two extracts exhibited more Annexin V-FITC staining than control cells (Figure 4.9). The percentage of dead/necrotic cells was low in each treatment.

For the percentage of viable cells, it was shown that the percentage of MCF-7 cells treated with QI galls extract was significantly lower ($p < 0.05$) as compared to the untreated where the value was only 31% (Table 4.6). For the cells treated with docetaxel, the percentage of viable cells after 72 hours of treatment was high with the percentage 80% ($p < 0.05$). This value was not much different from the untreated, where the percentage of viable cells for the untreated was 89%. These results showed a great killing effect of QI gall extract against MCF-7 cells. For the MDA-MB-231 cell line, the results showed the same pattern where the percentage of viable cells for the cells treated with QI galls extract was significantly lower ($p < 0.05$) as compared to the untreated cells. The percentage of the viable cells was 45.7% (Table 4.7). This value however is a little bit higher as compared to the percentage of viable cells in MCF-7 cells treated with QI galls extract. This may be due to the nature of the MDA-MB-231 cells which are also known as triple-negative breast cancer cells due to the lack of estrogen receptor, progesterone receptor, and HER2 protein. This type of cell does not respond to hormonal therapy medicines or medicines that target HER2 protein receptors. For the cells treated with docetaxel, the percentage of viable cells was 77.7% which is not much different compared to the percentage of viable cells in untreated cells. The percentage of viable cells in untreated cells was 89.2% (Table 4.7).

Table 4.7: Percentage of cells based on the event of apoptosis in the MDA-MB-231 cell line. *$p < 0.05$ was taken as significantly different from the untreated group

Event of apoptosis	% of cells in the quadrant		
	untreated	QI galls extract	Docetaxel
Viable cell	89.0±0.09	45.8±0.12*	77.43±0.22*
Early apoptosis	8.4±0.06	48.2±0.2*	9.8±0.06*
Late apoptosis	1.6±0.03	4.6±0.03*	5.1±0.03*
Dead/necrotic	0.73±0.03	1.2±0.03*	7.63±0.03*

The results from this study revealed that the QI galls extract led to an increased number of apoptotic cells compared to the untreated cells without significantly increasing the percentage of necrotic cells. These findings support the cytotoxicity data which suggests that QI gall extract exerts antiproliferative activities through the mechanism of apoptosis (Figure 4.8). Induction of apoptosis is one of the important markers of cytotoxicity of the anticancer agent (Moradi et al., 2016). During the apoptosis events, the integrity of the cell membrane is lost and the phosphatidylserine membrane becomes externalized on the cell surface, where it can be stained by FITC-tagged anticoagulant Annexin V (Zhou et al., 2018). Propidium iodide (PI) will stain late apoptotic or necrotic cells whose membrane integrity has been lost (Zhou et al., 2018). The orthogonality of this dye binding and fluorescence allows for the simultaneous detection of early apoptosis and late apoptosis/necrotic (Moradi et al., 2016). The percentages of cells analyzed by flow cytometry following Annexin V and PI staining could be classified into four categories (Khazaei et al., 2017). The populations of cells residing in the Annexin V+/PI- and the Annexin V+/PI+ quadrants were determined as early and late apoptotic cells. The Annexin V−/PI - and the Annexin V−/PI+ quadrants were determined as living cells and necrotic cells respectively (Pumiputavon et al., 2017).

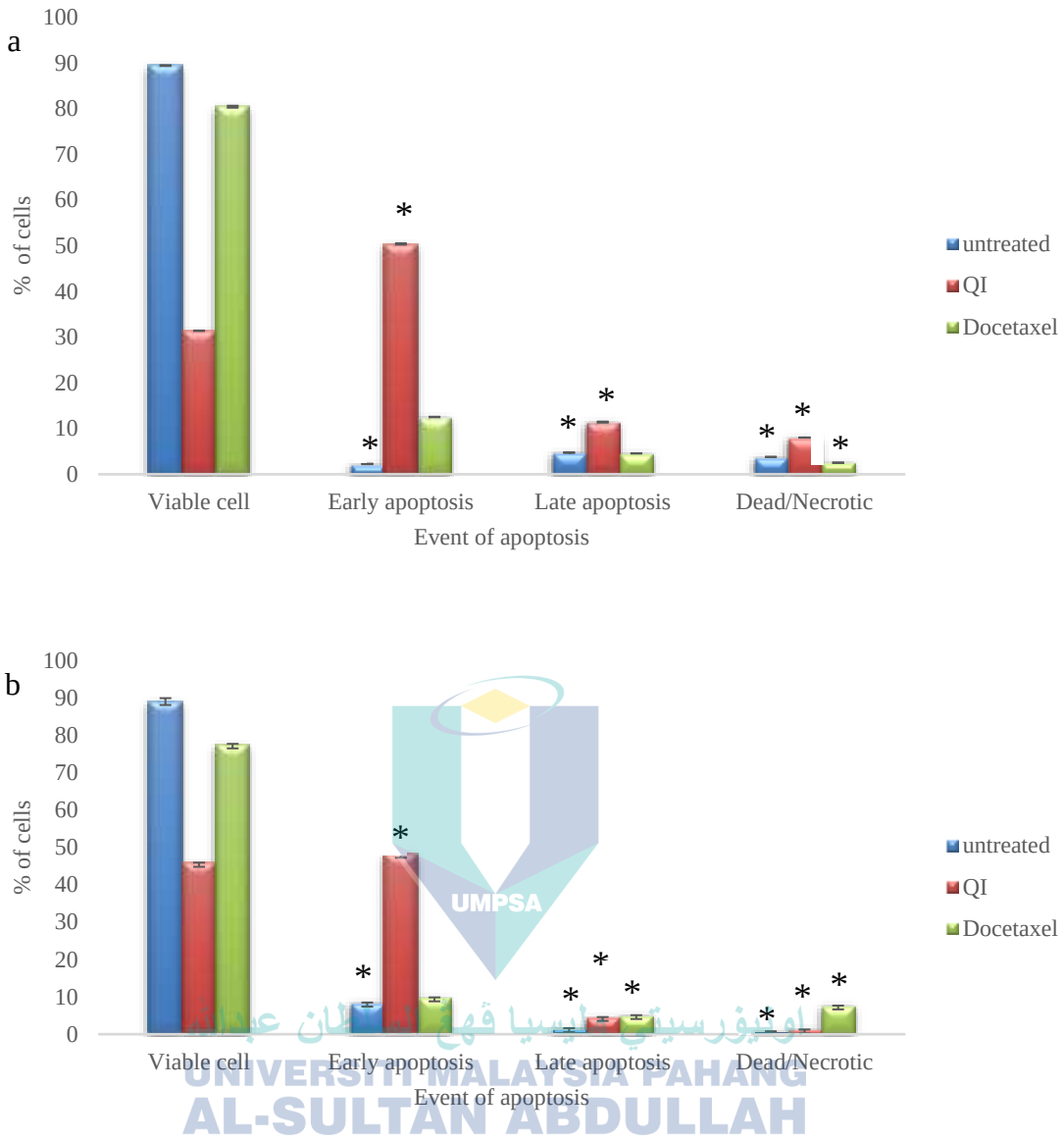

Figure 4.8: Annexin V-FITC staining of untreated, QI galls crude extract and Docetaxel (positive control) against a) MCF-7 cell lines; b) MDA-MB-231 after 72 hours treatment. The graph is representing means ± SEM µg/ml of three independent experiments.

4.9 Characterization of micelles

4.9.1 Micelles size, size distribution, and surface charge properties

Micelles were prepared according to the solvent casting method. Micelle suspension prepared consistently formed a transparent yellowish-clear solution with invisible precipitation. This indicates that extracts were well encapsulated within the micelle. There were four types of micelles formulated QI gall- vitamin E TPGS (QIT), tannic acid- vitamin E TPGS (TAT), Gallic acid- vitamin E TPGS (GAT), and Tannic/Gallic acid- vitamin E TPGS (TGT). These micelles were formulated to achieve maximum solubility and bioavailability of encapsulated extracts (Gaonkar et al., 2017). All micelles were prepared through a solvent solvent-casting technique using vitamin E TPGS as the nanocarrier. The size, size distribution, and zeta potential measured by the dynamic light scattering (DLS) (Kutty, Chia, et al., 2015). The results obtained are shown in Table 4.8, from which it can be found that the mean size of QI-loaded TPGS micelles is distributed from 8 nm to 14 nm. The mean size for the other formulated micelles such as TA, GA, and TA/GA-loaded TPGS also ranges below 20 nm (Fig. 4.9).

Table 4.8 Characterization of the micelles. Particle size, size distribution, and zeta potential of the micelles.

Micelles	Size (nm)	Polydispersity index (pdi)	Zeta potential (mV)
QIT	19.54 ± 2.97	0.344± 0.04	-18.57±1.46
TAT	11.3± 2.02	0.363±0.01	-19.83±3.48
GAT	14.31±1.38	0.142± 0.05	-14.73± 0.99
TGT	10.32 ± 1.15	0.38±0.1	-11.27±0.91

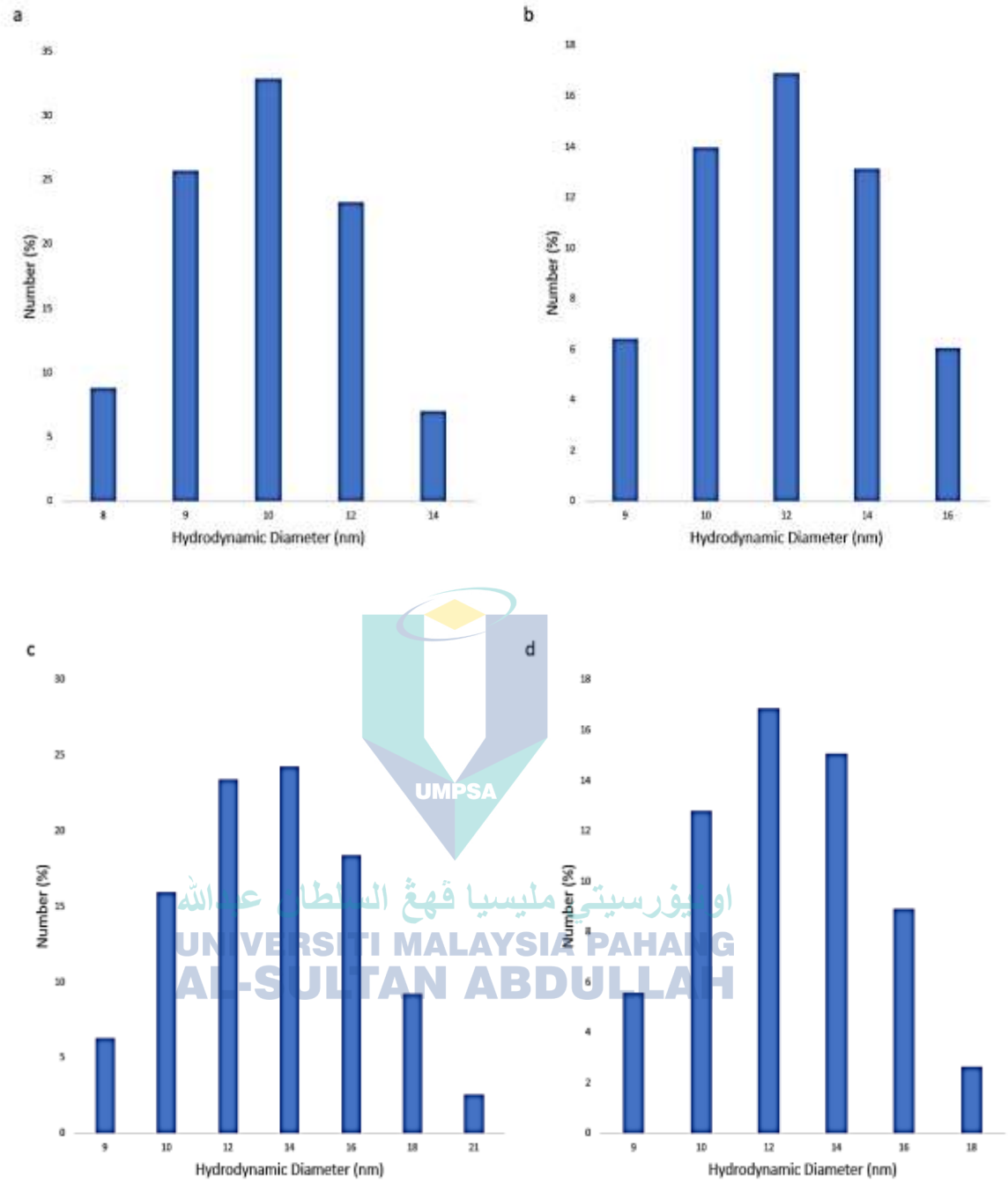

Figure 4.9 Particle size and size distribution of the micelles. a) QI-loaded vitamin E TPGS micelle (QIT), b) TA-loaded vitamin E TPGS micelle (TAT), c) GA-loaded vitamin E TPGS micelle (GAT), and d) TA+GA-loaded vitamin E TPGS micelle (TGT).

This size range (below 20 nm), ensures the micellar nature of the synthesized nanosuspensions (Khurana et al., 2018). The use of vitamin E TPGS enables the reduction of the interfacial tension and stabilizes the micelles thus resulting in the formation of smaller nanoparticles (Khurana et al., 2018). Besides, the smaller size of the micelles can be due to the cosolvent ability to promote the effectiveness of emulsification of the oil-surfactant mixture (Khurana et al., 2018). A previous study showed that a novel Garcinol (GAR) loaded PLGA-based nanoparticles using vitamin E TPGS produced nanoparticles of approximately 88 nm in size which is optimal for the ability of the micelles to be used for intravenous administration and cancer passive targeting. As compared to the previous study, it was revealed that our formulated micelles were smaller in size and thus could promote passive diffusion into the targeting site effectively. Micelles size within the range of 10-100 nm has been reported to be suitable for drug delivery purposes in cancer therapy (Kutty & Feng, 2013). The nanocarrier in such size can improve the permeability and retention effect (EPR) at the cancer site (Kutty & Feng, 2013).

One of the benefits of micelles as nanocarriers is their smaller size (10-100 nm) which is bigger than the free drug molecules (1 nm). Thus this nanocarrier will secure the drugs from rapid clearance by our body's immune system (Kutty, Chia, et al., 2015). This can be achieved with the rise of the circulatory half-life of the drugs and ease the diffusion of nanoparticles through the leaky vasculature at the tumor site (Kutty, Chia, et al., 2015). Particle size and size distribution are a significant marker of nanoformulations since particles with smaller sizes accumulate more at the cancer site. Particle size plays an important marker in determining the bio-distribution and circulation times of the nanoparticles in vivo. Particle size also is one of the major factors for the efficiency of the nanocarrier (Meng et al., 2017). Smaller particle size (<200 nm) can prevent the rapid clearance and uptake by the reticuloendothelial system (RES) and can increase the circulation of the micelles in the blood system thus leading to passive targeting (Meng et al., 2017).

The polydispersity index (PDI) of all the micelles ranges between 0.1-0.4 which indicates a narrow size distribution (Table 4.8). An effective nanocarrier should provide a suitable particle size with a narrow distribution for drug release (Cheng et al., 2016). The surface charge of the micelles plays a significant role in both its colloidal stability in suspension and interaction with cells. Formulating nanomedicine with suitable zeta

potential is an essential but challenging task. Formulations with a minimum ±30 mV zeta potential are considered stable (Németh et al., 2022). Nanoparticles with zeta potentials between -10 and +10 mV are thought to be approximately neutral, whereas nanoparticles with zeta potentials greater than +30 mV or less than -30 mV are thought to be strongly cationic and strongly anionic, respectively (Bilia et al., 2018). Because most cellular membranes are negatively charged, zeta potential can influence a nanoparticle's ability to permeate membranes, with cationic particles generally exhibiting greater toxicity due to cell wall disruption (Bilia et al., 2018). The magnitude of a nano formulation's zeta potential can predict its stability. High zeta potential indicates highly charged particles that prevent aggregation and ensure redispersion due to repulsive electric forces, whereas low zeta potential indicates coagulation (Németh et al., 2022). In general, absolute values of 30 mV and 60 mV are considered to have good and excellent stability, respectively. Zeta potentials of 30 mV indicate monodisperse formulations with no aggregates, while 20 mV indicates only short-term stability, and 5 mV indicates rapid aggregate formation (Németh et al., 2022).

Table 4.8 above shows the zeta potential for all formulated micelles as being negatively charged (-11 mv to -20 mv), which increases colloidal stability in the blood and promotes cellular uptake via endocytosis (Kutty, Chia, et al., 2015). Furthermore, the PEG molecules on the micelle's surface can improve the evasion of the immune system thus reducing the loss of nanoparticles due to accumulation in the mononuclear phagocytic system (MPS) located in the liver and spleen (Kutty, Chia, et al., 2015). These characteristics can improve the targeting ability of nanoparticles in cancer and eliminate systematic toxicity (Kutty, Chia, et al., 2015). Zeta potential value straight indicates the stability of micelles, with a higher value typically showing higher stability (Cheng et al., 2016). Micelles containing polymer are usually negatively charged (Cheng et al., 2016). In this study, the zeta potential value obtained for all nanoformulations showed that the micelles had short-term stability and easily aggregated during storage.

4.9.2 Surface chemistry analysis of the micelles

The surface analysis of nanoparticles is important for the internal body drug delivery as this will greatly affect their toxicity, and connections with the surroundings, and at the same time will control the amount and pathway of the micelles uptake by tissues and cells (Korin et al., 2017). Therefore, obtaining information regarding their surface composition is important to get more information on surface chemistry relationships and to improve the properties of the nanoparticles so that they can be a good delivery carrier (Korin et al., 2017). In this study, the formulated nanoparticles (QIT, TAT, GAT, and TGT) were examined for their surface chemistry properties by X-ray photoelectron spectroscopy (XPS) (Fig. 4.10).

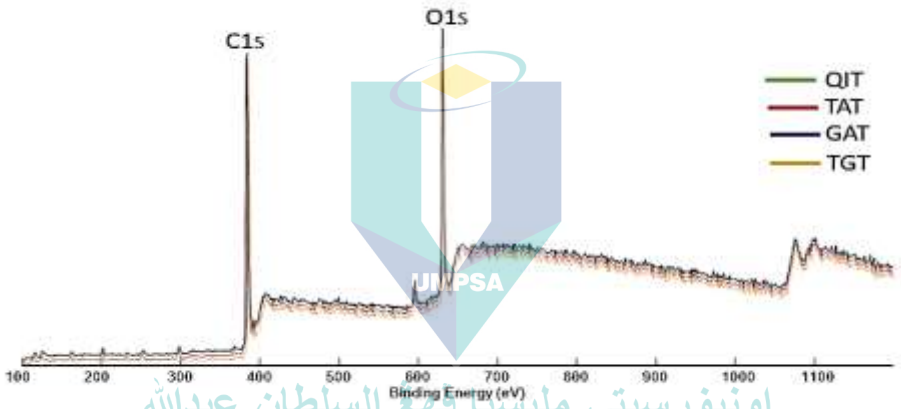

Figure 4.10 Representative X-ray photoelectron spectroscopy (XPS) spectrum of wide scan spectrum for the micelles.

XPS, also known as electron spectroscopy for chemical analysis (ESCA), is a highly sensitive quantitative spectroscopic method for examining the surface properties of a material (Korin et al., 2017). From the results, it was shown that all the formulated micelles had almost similar relative ratios amongst the suggested chemical bonds and followed those reported in pure vitamin E TPGS. Hence, it can be concluded that the TPGS was well distributed over the surface of the formulated micelles. This condition revealed that TPGS can be a good surface stabilizer in drug delivery. Previous studies showed that, when formulation involves the use of vitamin TPGS as the matrix material, it was shown that as more TPGS is used, the proportion of C-C/C-H bonds increases, while the proportion of O-C=O bonds decreases (Mu & Feng, 2013). This is due to the

during the formulation process, there were more TPGS molecules distributed on the micelles' surface.

From these current findings, it was also revealed that TPGS not only can serve as an emulsifier but also be a novel kind of nanocarrier that has self-emulsifying effects (H. Li et al., 2019). Due to the amphiphilic properties of vitamin E TPGS, repeated washing would be able to remove the TPGS from the micelle surface.

4.9.3 Encapsulation of the *Quercus infectoria* (QI) galls extract and phenolics into micelles

Drug loading is determined as the weight of the drug (μg) per mg of the drug-loaded nanocarriers. The QI galls crude and phenolics extract loaded into the micelles were measured using HPLC and the results are shown in Table 4.9. From the results, it was shown that the drug loading for QI galls crude extract was the highest as compared to other phenolics. Drug loading for QIT was 110.41 μg/mg followed by GAT 87.47 μg/mg, TAT 83.39 μg/mg, and TGT 81.92 μg/mg (Table 4.9). From this study, it was found that the drug loading of the formulated micelles was following the size of the micelles. This is because the QIT has the largest micelles size, and it also showed the highest drug loading. This was also applicable to other formulated micelles which were TAT. GAT and TGT. Previous studies showed that drug loading efficiency is dependent on many factors including the size of the micelles or nanoparticles, specific interactions between the extract/drug with core, and the method of micelles preparation (Mishra, 2013). In this current study, it was revealed that the size of the micelles influences the drug loading of the micelles. A larger hydrophobic block leaves a bigger core structure and therefore will increase the ability to entrap the QI galls crude and phenolic extract (Mishra, 2013).

Table 4.9 Drug loading of the QI galls extract and phenolics into micelles

Micelles	Drug loading (µg/mg)
QIT	110.41
TAT	83.39
GAT	87.47
TGT	81.92

Among the influencing factors on the efficiency of drug loading are preparation methods, additives (e.g., stabilizers, bioadhesives including mucoadhesives, solvent), nature of the drug or extract used, nature of the polymer, their respective solubilities, and pH. Formulation variables can be modified to improve the drug loading in nanoparticles (Deshmukh et al., 2017). Depending on the both preparation process and the physicochemical properties of both in drug molecule and the nanocarrier, the drug or extract encapsulation can be either by entrapment within the nanocarrier and/or by surface adsorption onto this nanocarrier (Deshmukh et al., 2017).

Any kind of preparation process, polymerization of monomers or dispersion of preformed polymer, entrapment within non-porous nanoparticles require the solubility of drug molecules in the macromolecular material, whereas porous nanoparticles may encapsulate the drug or extract molecule by adsorption either onto the surface or within the macromolecular network (Bilia et al., 2018). Besides that, the other factor that may influence the drug loading efficiency is the electrical charges on both the extract and nanocarrier. A previous study by Gaonkar et al., (2016) showed that Garcinol encapsulated into vitamin E TPGS emulsified PLGA-NPs exhibit relatively high drug loading capacity and encapsulation efficiency, which might be due to the strong interaction between garcinol and polymer. Hence, the interaction between the drug and the nanocarrier also can be a crucial factor that contributes to a better drug-loading capacity in formulated micelles.

4.9.4 Surface morphology of the micelles

The shape and surface morphology of the formulated micelles (QIT, TAT, GAT, and TGT) were visualized under a Transmission Electron Microscope (TEM). Through this analysis, a high-resolution image of the micelles was obtained. As shown in Figure 4.11 below, the QIT, TAT, GAT, and TGT micelles were in moderate uniformity with a nearly spherical shape. Particle size measurements obtained were consistent with the results of the DLS analysis, where the micelles size was below 100 nm and uniformly distributed.

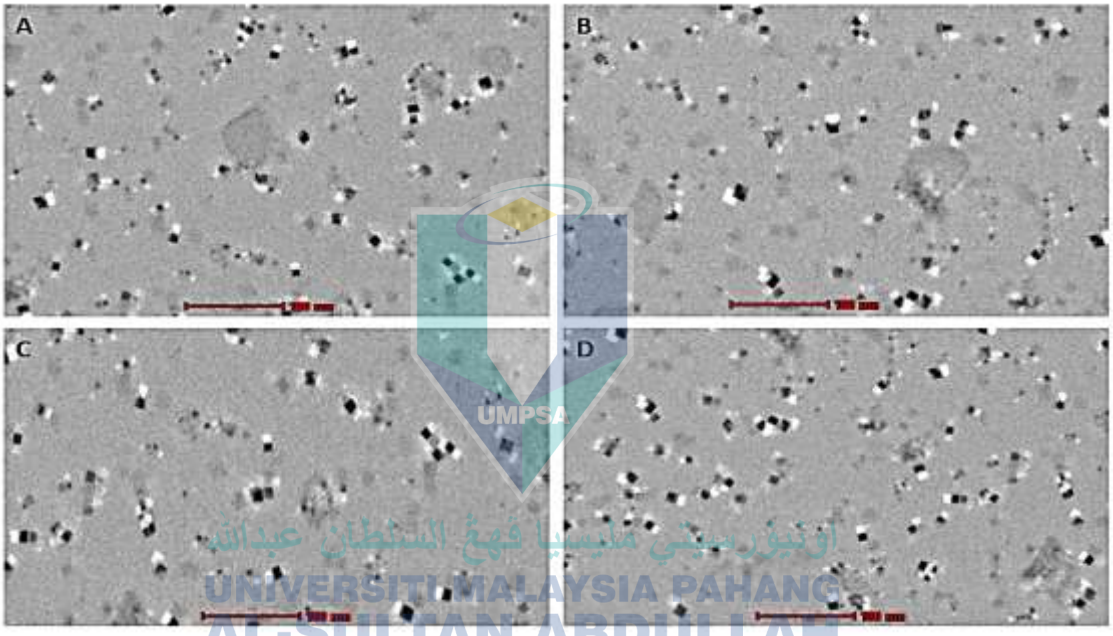

Figure 4.11 Representative Transmission electron microscope (TEM) images of the micelles. a) Quercus infectoria-loaded vitamin E TPGS (QIT), B) Tannic acid-loaded vitamin E TPGS micelles (TAT), C) Gallic acid-loaded vitamin E TPGS micelles (GAT) and D) Tannic acid+Gallic acid-loaded vitamin E TPGS micelles (TGT)

Previous study showed that the micelles are generally spherical in shape, but the size of the micelles shown by TEM analysis figure was slightly bigger than that tested from DLS. This may due to low melting point of vitamin E TPGS (~ 38 °C) and the micelles suffer from melting and expansion in certain extent under the high electron beam in TEM which make them seem bigger than in DLS analysis (Korin et al., 2018). However, from the current and previous study, showed that the vitamin E TPGS micelles still have the average diameter under 100 nm and this will be superior to escape the

biological barrier elimination and entering the cancer site by penetrating leaky vasculature (Korin et al., 2017).

4.9.5 In vitro drug release of the micelles

Controlled drug release is the leading advantage of polymeric micelles from the pharmaceutical point of view. Both the structure of nanocarrier and the chemical properties of polymeric micelles can influence the drug release rate (Savaser et al., 2018). Figure 4.12 shows the in vitro drug release profiles of the formulated micelles (QIT, TAT, GAT, and TGT), where all micelles exhibited a biphasic release pattern characterized by an initial burst then followed by a slow, sustained release until the 10 days of the experiment been conducted.

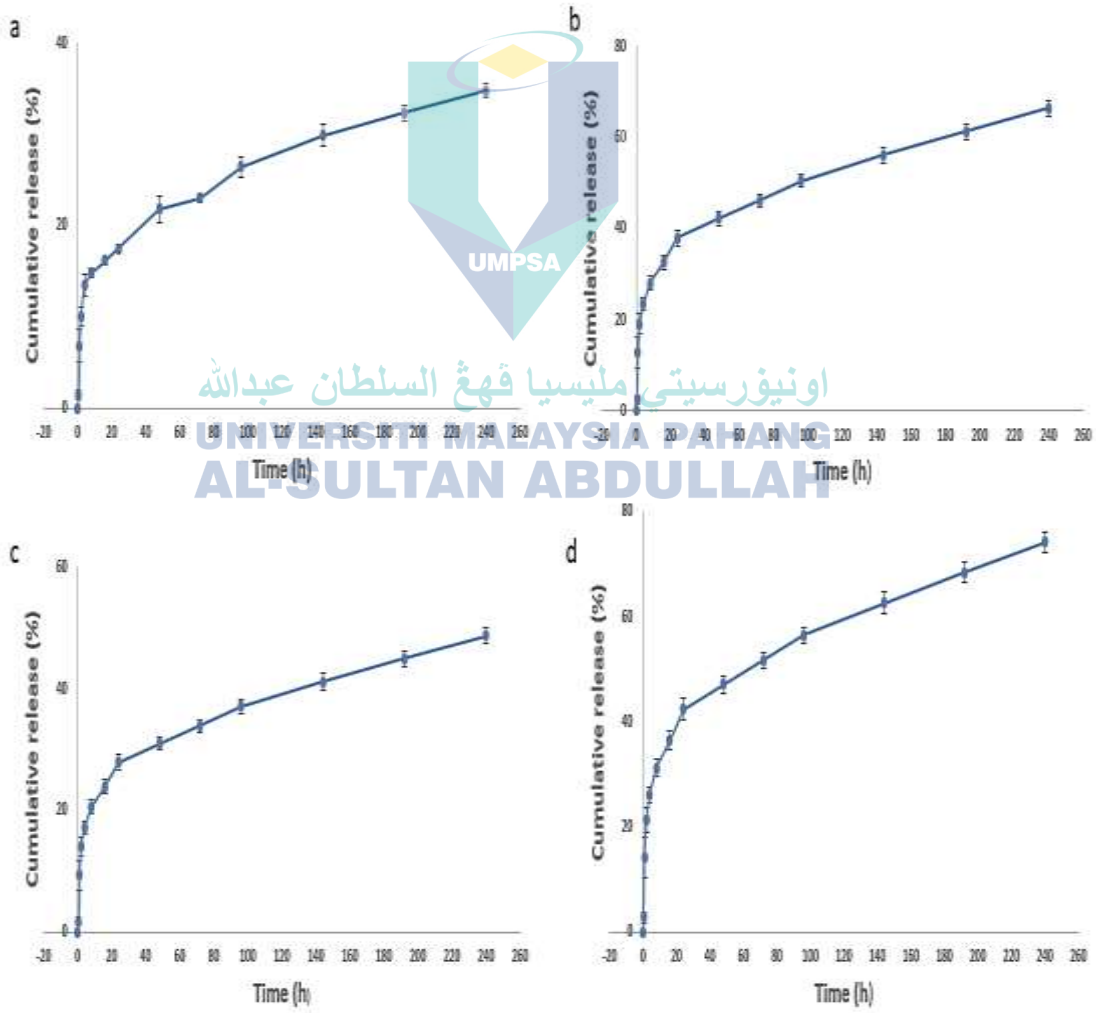

Figure 4.12 In vitro drug release profile of a) QIT, b) TAT, c) GAT and d) TGT micelles at pH=7.4. Data represent mean ± SEM, n=3.

In many cases, drug release from nanoparticles was observed to be biphasic- an initial burst then followed by a rather slow (thus controlled) release. This condition occurred most for micelles prepared by the emulsification solvent evaporation method. With single emulsions, the solvent elimination concentrates the incorporated substance towards the surface while for multiple emulsions, it makes holes in the polymeric walls near the surface resulting in the initial burst release (Wang et al., 2017). The rest of the incorporated drug is released under the dual influence of diffusion within the matrix and polymer degradation.

Besides that, drug release from polymeric micelles is dependent on the type of encapsulation process used to load the drug. For a chemically conjugated drug, bulk degradation or surface erosion of the polymer slowly releases the drug. Conversely, for a physically entrapped drug, diffusion is the main mechanism for drug release (Kutty, Tay, et al., 2015). It has been shown that drugs incorporated into micelles have superior properties such as higher bioavailability and targeted release compared to the free drug (Wang et al., 2017). Formulation of micelles also can help to decrease the toxicity of a drug towards normal cells compared to free-form (Muthu et al., 2015).

4.9.6 Cytotoxicity of the micelles

Cytotoxicity of the QI-loaded vitamin E TPGS micelles against breast cancer cells was determined by MTT assay. From the results, it was showed a faster onset of action within 24 hours for both cell lines. As compared to the results obtained from the use of QI galls crude extract, the effect of the extract only showed after 72 hours of treatment. From this, it was revealed that the QI galls nanoparticle extracts showed a faster effect against breast cancer cells as compared to the crude extract. The results obtained are shown in Figure 4.13 below. From the results, it was observed that the cell viability decreased as the concentration of the QI galls nanoparticle extract increased. However, the percentage of cell viability in MCF-7 is higher as compared to the MDA-MB-231 cell line. This could be attributed to the higher accumulation of QI galls and phenolics-loaded vitamin E TPGS micelles in MCF-7 than in MDA-MB-231 cells. A previous study also showed a higher accumulation of Mgf-SPNMS micelles in MCF-7 than in MDA-MB-231 cells (Khurana et al., 2018). This is due to the nature of the MDA-MB-231 cells which are known to express P-gp efflux transporters (Khurana et al., 2018). The higher

expression of P-gp receptors on MDA-MB-231 cells will contribute to the lower accumulation of micelles in these cells (Khurana et al., 2018).

Table 4.10 below shows the IC_{50} values of QI galls and phenolics nanoparticle extract for 24-hour treatment against breast cancer cell lines, MCF-7 and MDA-MB-231. From the results, it was revealed that for QI galls nanoparticle extract, IC_{50} for MCF-7 is higher than for the MDA-MB-231 cells. The IC_{50} obtained for QI galls nanoparticle (QIT) extract is 8.28±0.82 µg/ml while for the MDA-MB-231 cells is 11.09±0.73 µg/ml. TAT, GAT, and TGT also showed IC_{50} but the value is quite low where the value obtained was higher than 20 µg/ml except for the TGT against MCF-7 (14.06±1.24 µg/ml).

Table 4.10 IC_{50} values of QI gall nanoparticle extract for 24-hour treatment against breast cancer cell lines (MCF-7 and MDA-MB-231), *$p < 0.05$ was taken as significantly different from control drug (docetaxel micelles).

Micelles	**IC50 (µg/ml)**	
	MCF-7	MDA-MB-231
QIT	8.28±0.82	11.09±0.73
TAT	43.75±0.71*	46.88±0.85*
GAT	81.25±1.1*	75±1.05*
TGT	14.06±1.24	37.5±1.03*
Docetaxel	6.875±1.59	9.688±0.94

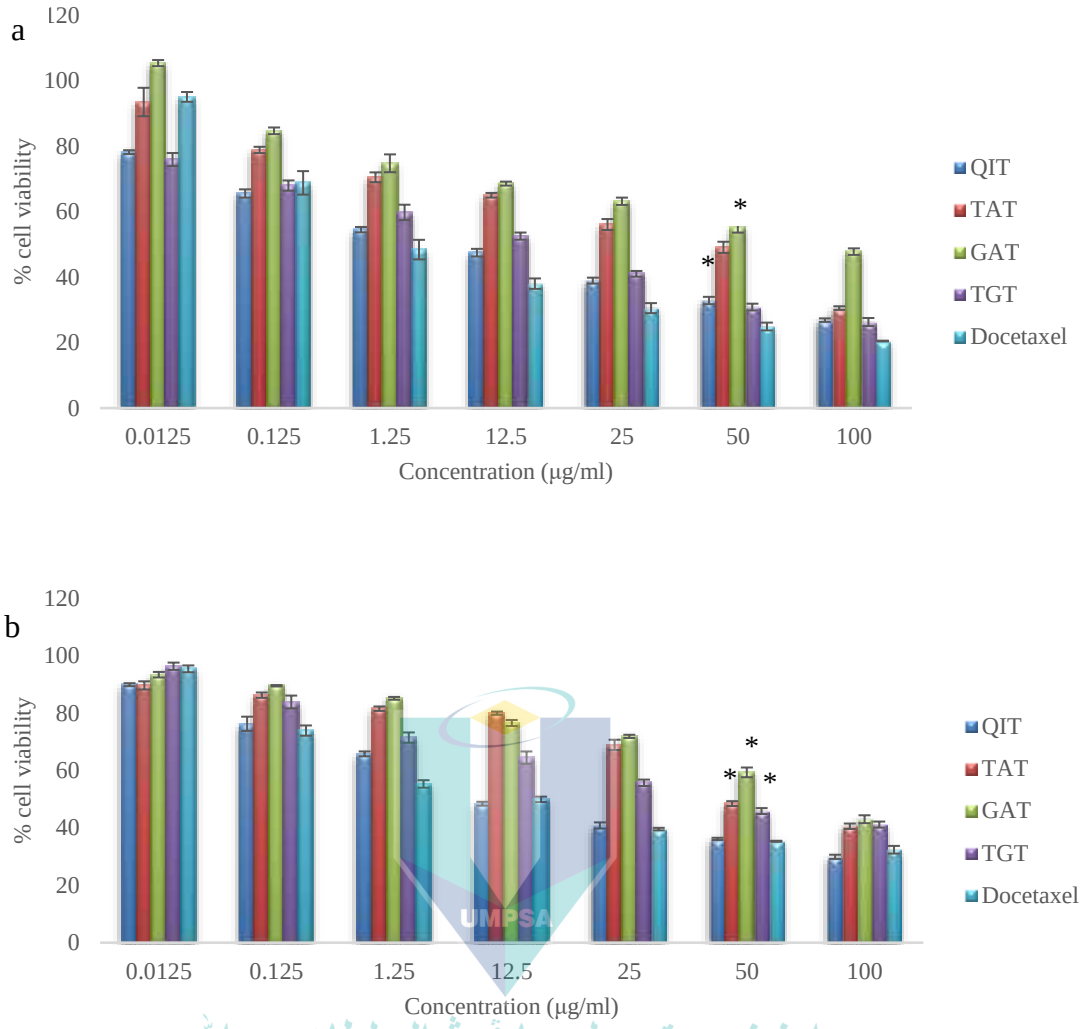

Figure 4.13 Cytotoxic activity of QIT, TAT, GAT, and TGT micelles against a) MCF-7 and b) MDA-MB-231 cell lines for 24-hour treatment duration. Data represent mean ± SEM. n=3.

However, as compared to the other phenolic micelles (TAT, GAT, and TGT), QIT exhibited the highest and most potent IC_{50} value. The data obtained revealed that the extract works better on MCF-7 as compared to MDA-MB-231 cells. Previous studies also showed higher cell viability for MDA-MB-231 cells indicating lower therapeutic effects in comparison with overexpressed MCF-7 cells (Kutty & Feng, 2013). Moreover, MDA-MB-231 also known as triple-negative breast cancer cells, always showed an aggressive phenotype and commonly will have a slower response to the treatment as compared to the less aggressive, estrogen receptor-positive, MCF-7 breast cancer cells (Khurana et al., 2018).

As a control, the micelles also were tested against a normal cell line, L929. From the results, it was shown that the QIT, TAT, GAT, and TGT micelles did not show any toxicity effect against normal cell line (Figure 4.14)

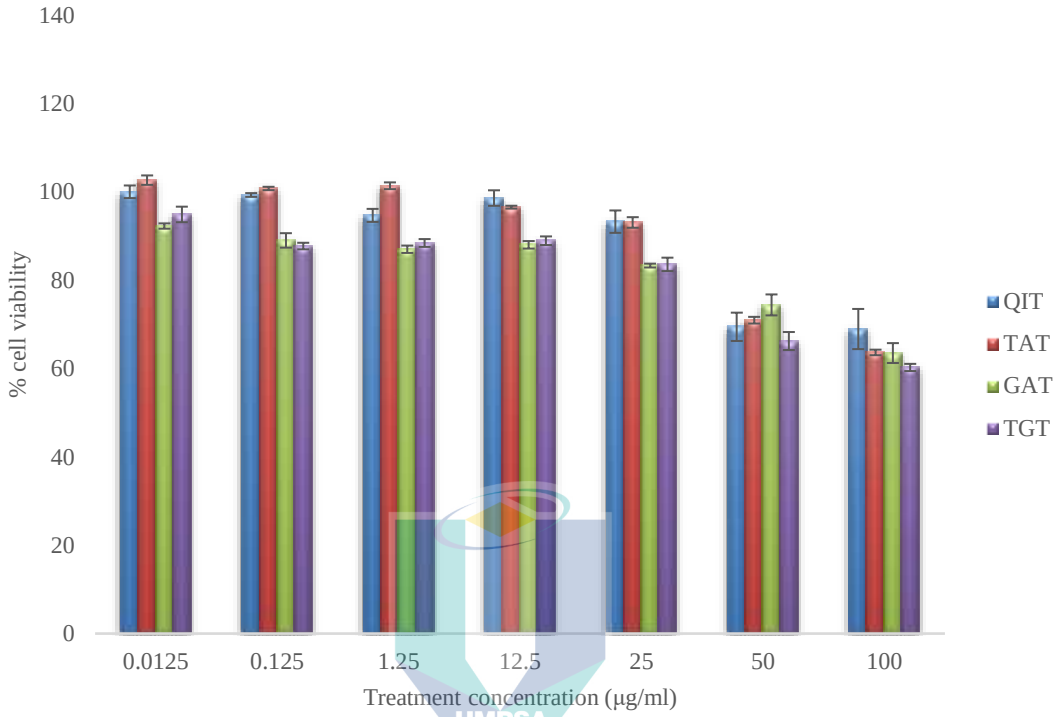

Figure 4.14 Cytotoxic activity of QIT, TAT, GAT, and TGT micelles against L929 cell lines for 24-hour treatment duration. Data represent mean ± SEM. n=3.

4.9.7 Cell death mechanisms of *Quercus infectoria* (QI) micelle extract against breast cancer cells by FITC-Annexin V Assay

Due to the good cytotoxicity of QIT, further study was carried out to determine the cell death mechanism of the breast cancer cells (MCF-7 and MDA-MB-23). For this purpose, flow cytometric analysis of Annexin V-FITC and PI double staining was employed to determine the effect of the QIT micelles extract on the apoptosis of breast cancer cells. The results showed that QIT induced the cell death mechanism of breast cancer cells through apoptosis. The results are shown in Figure 4.15 below.

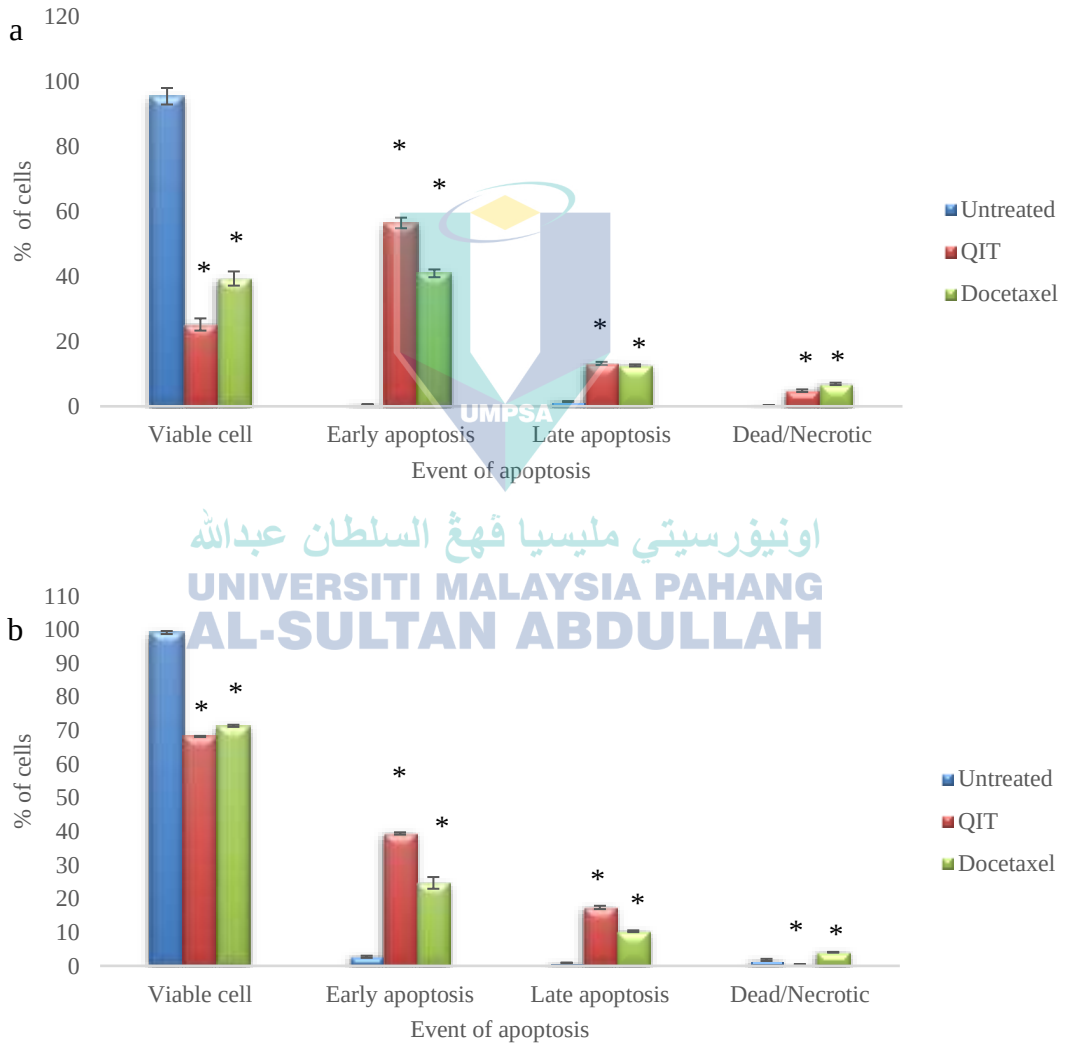

Figure 4.15 Apoptotic activity of untreated, QIT and Docetaxel (positive control) loaded micelles against a) MCF-7 and b) MDA-MB-231 cell lines for 24-hour treatment duration. Data represent mean ± SEM. n=3.

Table 4.11 shows the percentage of cells based on the event of apoptosis in MCF-7 cells. From the table, it was shown that QIT can induce apoptosis in both cell lines, MCF-7 and MDA-MB-231. However, the percentage of early apoptosis in MCF-7 is higher than in MDA-MB-231. The percentage of early apoptosis is 56.40±1.63% as compared to MDA-MB-231, 39.37±0.34%. This present data revealed that QIT has a higher accumulation and better therapeutic effect on MCF-7 cells than MDA-MB-231. MDA-MB-231 cells is a triple-negative breast cancer (TNBC) cells that unable to express estrogen receptors, progesterone receptors, and HER2 protein. Therefore, this present data is due to the nature of the MDA-MB-231 which hardly responds and is less sensitive to the treatment.

Extracts/ Treatment duration	Without treatment	Docetaxel treatment	Treatment with QI galls crude extract
24 hours	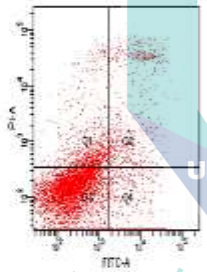	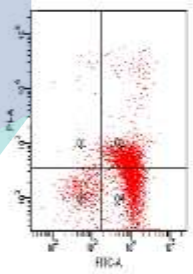	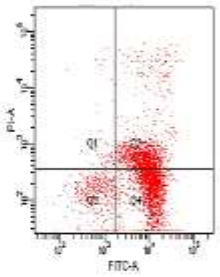
Extracts/ Treatment duration	Without treatment	Docetaxel treatment	Treatment with QI galls crude extract
24 hours	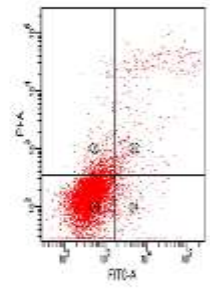	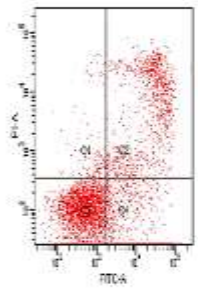	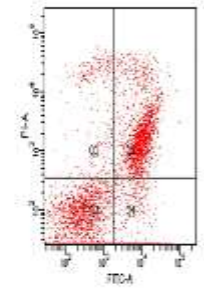

Figure 4.16: Scatter plot of FITC-AV/PI double staining in quadrant analysis. Q1: dead cells, Q2: late apoptotic cells, Q3: viable cells, and Q4: early apoptotic cells, n=3.

Table 4.11: Percentage of cells based on the event of apoptosis in MCF-7 cell line. *$p <$ 0.05 was taken as significantly different from the untreated group

Event of apoptosis	% of cells in the quadrant		
	untreated	QI galls micelle extract	Docetaxel
Viable cell	95.37±2.54	25.17±1.88*	39.30±2.18*
Early apoptosis	0.55±0.13	56.40±1.63*	40.90±1.19*
Late apoptosis	1.47±0.09	13.20±0.47*	12.57±0.33*
Dead/necrotic	0.27±0.12	4.8±0.40*	6.90±0.36*

Table 4.12 shows the percentage of cells based on the event of apoptosis in MDA-MB-231 cells. As compared to the control drug, docetaxel micelle, the percentage of early apoptosis is lower than QIT where the percentage is 40.90±1.19%. For MDA-MB-231 cells, it also showed a lower percentage of early apoptosis cells, 24.67±1.75% of the control drug, docetaxel, as compared to the QIT. From the results, it was revealed that QIT has better results and higher accumulation than docetaxel micelle in both breast cancer cells. The percentage of dead/necrotic cells was low in each treatment. In comparison with the previous study of apoptosis using QI galls crude extract, it was revealed that the nanoparticle form of extract showed a higher percentage of apoptotic cells, and the effect can be seen in a shorter period of incubation which is within 24 hours. For the crude extract, it takes up to 72 hours for the action. Previous studies also showed that curcumin-loaded vitamin E TPGS is also more effective than free curcumin at inducing apoptosis of HT-29 cells (Ji et al., 2018). This could be due to by encapsulation of the extracts as nanoparticles will manipulate the particle size of the extracts and allow it to diffuse through the cells effectively by endocytosis and act synergistically with TPGS (H. Li et al., 2019). Besides that, this encapsulation also will increase the drug's bioavailability (H. Li et al., 2019).

Table 4.12: Percentage of cells based on the event of apoptosis in the MDA-MB-231 cell line. *$p < 0.05$ was taken as significantly different from the untreated group

Event of apoptosis	% of cells in the quadrant		
	untreated	QI galls nanoparticle extract	Docetaxel
Viable cell	99.1±0.45	68.20±0.17*	71.37±0.32*
Early apoptosis	2.70±0.32	39.37±0.34*	24.67±1.75*
Late apoptosis	0.9±0.11	17.4±0.49*	10.3±0.26*
Dead/necrotic	1.77±0.32	0.40±0.05*	4.03±0.12*

4.9.8 *In vitro* quantitative cellular uptake of the *Quercus infectoria* (QI) vitamin E TPGS (QIT) micelle

Cellular uptake of QI galls loaded vitamin E TPGS (QIT) micelles was determined to see the uptake characteristic into the breast cancer cells MCF-7 and MDA-MB-231. The therapeutic ability of the micelles is commonly affected by the uptake and accumulation of extract/drugs in the cancerous or targeted site. In this study, coumarin 6 was encapsulated as a fluorescent dye during micelles formulation to study the cellular uptake of the nanoparticle in MCF-7 and MDA-MB-231 cell lines. Then, the cellular uptake was further quantified by the fluorescent mode assessed by the microplate reader. The level of extract of drug accumulation in cells usually depends on the cellular internalization and release profile of the formulated micelles (Xiong & Wei, 2016).

The results of the cellular uptake are shown in Figure 4.17 below. From the results, it was revealed that the cellular uptake was increased with the prolonged incubation time. However, the uptake for the MDA-MB-231 is lower than MCF-7. For MCF-7, at 0.5 hours, the cellular uptake was 36.11 ± 4.89 %. After 2 hours, the cellular uptake was increased to 70.69 ± 2.84%. These results showed that the coumarin-6 micelles were accumulated at higher concentrations in MCF-7 cells. As compared to MDA-MB-231 cells, the cellular uptake at 0.5 hours is 19.85 ± 1.4 %. Then, after 2 hours

of incubation, the cellular uptake was increased to 55.32 ± 2.04 %. These results showed that coumarin-6 micelles were internalized into the MDA-MB-231 cells, but the accumulation rate was lower as compared to MCF-7 cells.

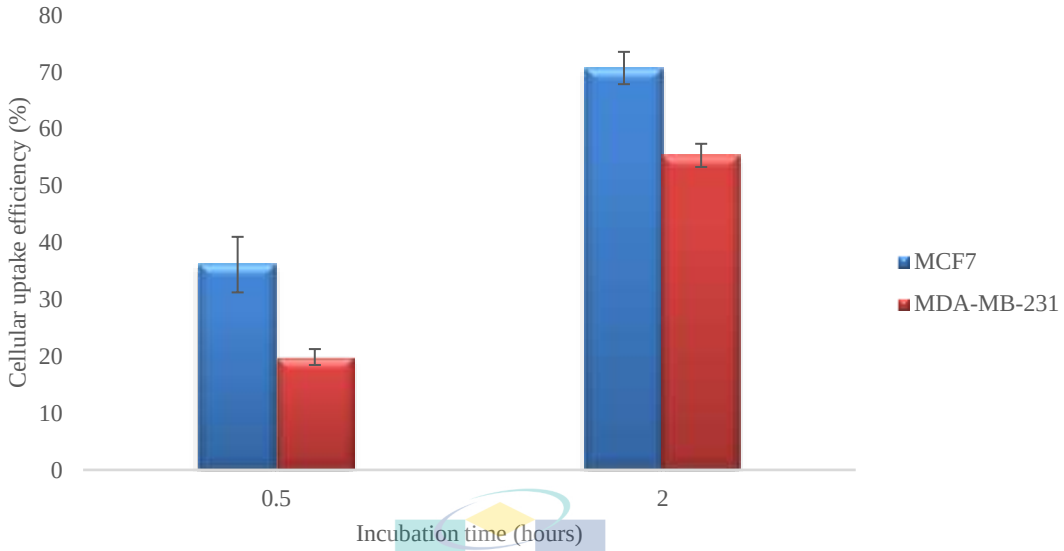

Figure 4.17 Cellular uptake efficiency of the coumarin-6 loaded vitamin E TPGS micelles (TPC6). TPC6 micelles were incubated in MCF-7 and MDA-MB-231 breast cancer cell lines for 0.5- and 2-hour incubation time at 37°C. Data represent mean ± SEM. n=3.

A previous study also revealed that nanoparticle uptake in breast cancer cells is effective and the uptake for MCF-7 cells was higher than MDA-MB-231 (Gregoriou et al., 2020). Another showed that the accumulation of micelles was observed to be much higher for MCF-7 cells than MDA-MB-231 suggesting that the micelles were diffused easily into MCF-7 as compared to MDA-MB-231 (Khurana et al., 2018). Besides that, it is reported that the higher cellular uptake is due to the presence of surfactants, vitamin E TPGS that enhance the permeability and can manipulate the cell integrity (Khurana et al., 2018).

4.10 Characterization of hydrogel beads formulation using *Quercus infectoria* (QI) galls crude and micelle extracts

4.10.1 Formulation of the hydrogel beads formulations

The results showed that the optimum concentration of the cross-linker which is zinc acetate was 2.5% and 5% because these concentrations will produce sphere shapes of the beads without tailing. The spherical shape of the beads was due to the crosslinking process between polymer, pectin and crosslinker, zinc acetate (Surini & Diandra, 2017). Besides that, for the selection of the extract, the dry extract was selected as it will create much more attractive beads with a bright brown color whereas the wet extract produces less attractive beads with a darker color. The best extract-to-polymer ratio was 1:2 and 1:3 as this proportion can make a good flow in the hose and form good shapes of beads. 15 minutes was selected as the best crosslinking duration as it resulted in beads with greater swelling ability. The best drying method for the produced hydrogel beads was freeze-drying as this can help the beads retain their original shape and size before drying. The beads before and after drying are shown in Figure 4.18 below. The parameters of formula optimization and formula to produce QI galls crude and micelle extracts hydrogel beads are shown in Table 4.13 and Table 4.14.

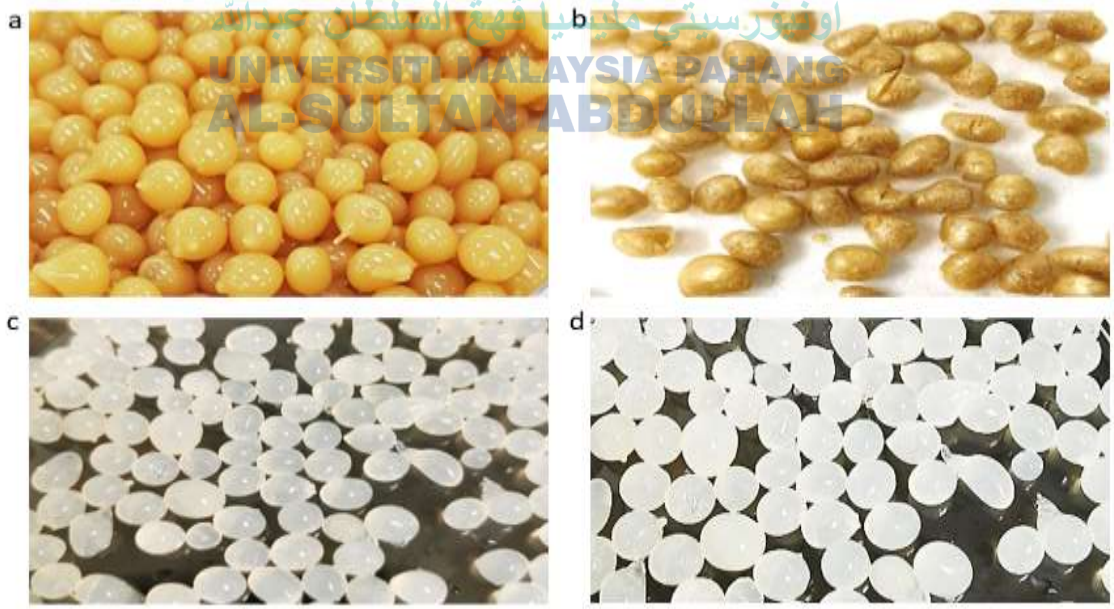

Figure 4.18 Hydrogel beads made of *Quercus infectoria* (QI) galls crude (QIC) and micelle extract (QIM); a) QIC beads (before drying), b) QIC beads (after drying), c) QIM beads (before drying), d) QIM beads (after drying).

Table 4.13 Parameters for hydrogel beads formulation

Parameter	**Variables**
Zinc Acetate concentration (%)	2.5
Nature of Quercus infectoria (QI) gall extract	Dry and wet extract
Extract to pectin ratio	1:1, 1:2, 1:3
Cross-linking duration (minutes)	15,30, 45, and 60
Beads drying method	Freeze dryer and room temperature

Table 4.14 Formulation of QIC and QIM extract hydrogel beads

Materials	**F1**	**F2**	**F3**
QI galls crude or nanoparticle extract (g)	1.2	1.2	1.2
Pectin (g)	1.2	2.4	3.6
Distilled water (Ml)	48	48	48
Zinc acetate concentration (%)	2.5	2.5	2.5

4.10.2 Yield of the *Quercus infectoria* (QI) galls crude and micelle extract hydrogel beads

The formulated QI crude (QIC) and micelle (QIM) hydrogel beads were characterized for the yield of production. From the results, it was shown that the yield of QIC and QIM were in the range of 64.33% to 92.13%. It was also observed that the yield for QIM was higher than QIC due to the use of nanoparticle extract. This shows that the types of extract used either crude or nanoparticle extract can also affect the yield of produced beads. From these findings, it is revealed that nanoparticle extract will give a higher yield of hydrogel beads as compared to the crude extract. Besides that, the results did not reach 100% yield may be due to the loss of water during the drying process of the hydrogel beads using the freeze dryer. The yield of each formulated hydrogel beads is shown in Table 4.15 below.

Table 4.15 Yield of QI crude and micelle extract hydrogel beads

Formulation	Yield (%)	
	QIC	QIM
F1	75.28 ± 0.17	88.75± 1.13
F2	80.17 ± 0.38	92.13± 1.00
F3	64.33 ± 0.18	79.43± 1.20

4.10.3 Shape and morphology of the *Quercus infectoria* (QI) galls crude and micelle extract hydrogel beads

Beads were observed visually, and it was observed that before the drying process, QIC beads were in sphere shape with smooth surfaces and light yellow. For the QIM beads, it was observed that beads are also in sphere shape but smaller in size as compared to the QIC beads. This may be due to the smaller particle size of QI nanoparticle extract and this extract had better encapsulation into beads as compared to the crude extract. After the drying process, it was observed that both QIC and QIM beads still maintained the sphere shape and color but had a slightly deflated texture. This occurs due to the drying mechanism of freeze-drying which water was lost during the process will produce space inside the beads (Surini & Diandra, 2017). These findings can be supported by a

previous study, where the mulberry leaf extract hydrogel beads also maintained the original shape and color after the drying process but the bead's texture was slightly deflated (Surini & Diandra, 2017).

4.10.4 Size distribution of the *Quercus infectoria* (QI) galls crude and micelle extract hydrogel beads

The size distribution was determined by measuring the diameters of each bead in every single batch of production (100-150 beads per batch). The measurement was carried out by using a vernier caliper. The results of the measurement of the bead's average diameter are in Table 4.16 below. From the results, it was shown that the size of QIC is larger than QIM. This can be caused by the dimensions of the integrated substance and the existence of supplementary constituents. Micelles, employed in the micelle-extracted form, are essentially little spheres that enclose the bioactive chemicals. These micelles are considerably smaller in comparison to the full crude extract. This facilitates a more uniform dispersion inside the hydrogel, reducing swelling and yielding smaller beads. Furthermore, crude extracts consist of a broader spectrum of constituents in addition to the targeted bioactive compounds. These can encompass more substantial components such as sugars and starches. As these voluminous elements take up more room within the hydrogel network, the beads expand and increase in size. On the other hand, micelle extraction separates the bioactive components, leading to a higher concentration and smaller amount that occupies less volume within the hydrogel bead.

Table 4.16 Average diameter of QI crude and micelle extract hydrogel beads

Formulation	**Average diameter (mm)**	
	QIC	QIM
F1	2.57 ± 0.06	1.84 ± 0.06
F2	2.39 ± 0.06	1.5 ± 0.05
F3	2.75 ± 0.05	2.17 ± 0.05

4.10.5 Swelling ability of the *Quercus infectoria* (QI) galls crude and micelle extract hydrogel beads

A swelling ability test was carried out as this property is important to monitor how much and for how long the hydrogel beads could swell in water. This feature is important as the beads would be consumed using water by consumers. The swelling ability results are shown in Figure 4.19 below. From the results, it was shown that F3 had the greatest swelling ability while F1 had the least swelling ability for both QIC and QIM hydrogel beads. This result can be explained by the extract-to-polymer ratio (1:3) in F3, which gives a greater amount of crosslinking between polymer, pectin, and crosslinker, zinc acetate. Due to this, there will be a larger network of hydrogen bonds in F3 thus will increase the ability of the beads to swell in water. The previous study showed that a formulation with a higher amount of extract to polymer ratio also produces a greater swelling ability (Surini & Diandra, 2017). However, when compared to the study conducted by Das et al., the swelling ability of the hydrogel beads is <100%. This showed that QIC and QIM both had good swelling ability.

a

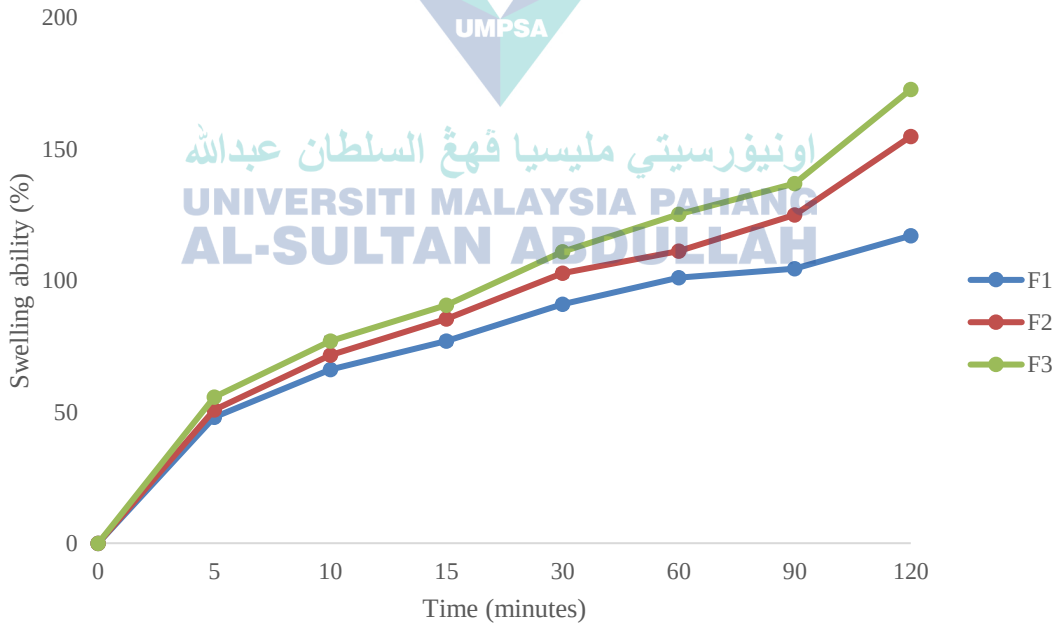

b

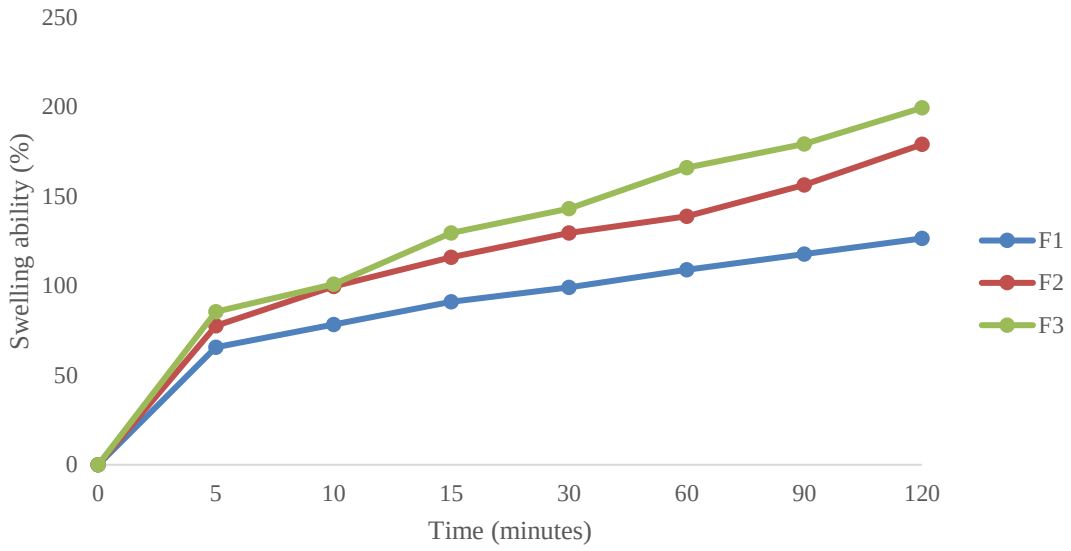

Figure 4.19 Swelling ability of; a) *Quercus infectoria* (QI) crude hydrogel beads (QIC), b) *Quercus infectoria* (QI) micelle hydrogel beads (QIM)

4.10.6 Swelling time of the *Quercus infectoria* (QI) galls crude and micelle extract hydrogel beads

Swelling time was determined to know the time taken for the beads to swell the first time when exposed to water. This is one of the important factors as the beads must swell well when soaked in the water for consumer use. The swelling time was measured visually by observing the beads as they sank in the water from their original position floating at the water's surface.

Table 4.17 shows the results of the swelling times for QIC and QIM hydrogel beads for each formula. From the results, it was shown that Formula 3 (F3) had the fastest swelling time for both QIC and QIM beads. This is due to the bigger extract-to-polymer ratio (1:3) and there will be more polymer cross-linked with an extract. This will lead to more formation of hydrogen bonds thus will increase the capability of the beads to bind with water molecules and swell faster. However, from the findings, it was observed that all formulations had a swelling time of less than 1 minute. These results were due to the shorter crosslinking time applied (15 minutes), hence, the swelling became faster for all formulations. Previous studies also showed that the swelling time for mulberry leaf extract was less than 1minutes due to the use of pectin as the polymer (Surini & Diandra,

2017). Pectin was used as the polymer and its hydrophilic nature will cause the beads to absorb water and swell.

Table 4.17 Swelling time of QI crude and micelle extract hydrogel beads

Formula	Swelling time (s)	
	QIC	QIM
F1	30±2	27±1
F2	19.7±1.53	17.3±0.58
F3	15.3 ±0.58	14±1

4.10.7 Moisture content of the *Quercus infectoria* (QI) galls crude and micelle extract hydrogel beads

Moisture content is the number of water molecules that are entrapped within a product. Moisture can be incorporated into products in several ways such as from the production process, atmospheric moisture, and from the packaging material or process. Moisture content is very important to be considered especially in food product production since it can affect the product's stability, shelf-life, freshness, quality, and resistance to bacterial contamination.

In this study, the moisture content of the hydrogel beads was determined, and the results are shown in Table 4.18 below. From the results, it was revealed that the moisture content of the QIC and QIM hydrogel beads was below 20% which indicates that these beads had low and acceptable moisture content. A range of 5 to 12 % moisture content is considered optimal and reading up to 17% is generally considered moderate moisture content and acceptable (Vera Zambrano et al., 2019). This range of moisture content was obtained in this study due to the use of pectin as the polymer that can absorb water and has high humidity. A previous study also showed the mulberry leaf extract hydrogel beads had high moisture content which was 21.09% to 26.52% due to the use of pectin as the polymer (Surini & Diandra, 2017).

Table 4.18 Moisture content of QI crude and micelle extract hydrogel beads

Formula	Moisture content (%)	
	QIC	QIM
F1	12.1 ± 0.9	10.9 ± 0.7
F2	13.9± 0.73	13.1 ± 0.68
F3	17.1 ± 0.69	16.0 ± 0.16

4.10.8 Encapsulation efficiency of the *Quercus infectoria* (QI) galls crude and micelle extract hydrogel beads

Encapsulation is a method where the active compound or drugs are encapsulated into a biodegradable matrix forming a system. Encapsulation of bioactive natural products and medicinal herbs is commonly used in food, agricultural, pharmaceuticals, and cosmetics industries for protection purposes and to improve the bioavailability of the constituents (Kurozawa & Hubinger, 2017). Encapsulation efficiency (EE%) refers to the concentration of the encapsulated extract or drugs in the formulation over the initial concentration used to produce the formulation.

In this study, the EE% for QIC and QIM hydrogel beads was determined. The results are shown in Table 4.19 below. From the results, it was revealed that the EE% for QIM was higher than QIC for all formulations. This result is due to the use of QI galls nanoparticle extract in this formulation where the nanoparticle extract is smaller in size and will contribute to a better loading into the wall matrix as compared to the crude extract. Besides that, in QIC, the crude extract was used, and the property of this crude extract is hydrophobic hence the affinity of the extract to the hydrogel beads matrix will be low. In this condition, the extract may diffuse out of the matrix before the encapsulation process is complete hence reducing the EE% in QIC hydrogel beads.

As for the QIM, the nanoparticle extract was made of vitamin E TPGS as the carrier for the QI galls crude extract to form the nanoparticle system (micelles). Hence, the surface is already modulated, and the hydrophobic properties of the crude extract have already been improved. This will increase the affinity of the components to the hydrogel

matrix and facilitate the loading of the nanoparticle extract into the hydrogel. Previous research mentioned that one of the methods to improve the affinity and hydrophilicity of the extracts/drugs is by encapsulating them into a system that has a higher affinity to the hydrogel matrix before the encapsulation process (Lai & Rogach, 2017). This method has already been implemented in an in-situ gel-forming system, which uses curcumin-loaded micelles to formulate thermosensitive hydrogel (Sarıyer et al., 2020).

Table 4.19 Encapsulation efficiency of QI crude and micelle extract hydrogel beads

Formula	Encapsulation efficiency (%)	
	QIC	QIM
F1	29.76±5.96	40.28±2.55
F2	60.0±5.83	66.10±3.14
F3	48.06 ±3.47	55.83±4.41

4.10.9 Cytotoxicity study of the *Quercus infectoria* (QI) galls crude and micelle extract hydrogel beads

The cytotoxic effects of QI gall nanoparticle and crude extract hydrogel beads were determined by using an MTT assay. This cytotoxic assay was investigated on human breast cancer cells; MCF-7 and MDA-MB-231. To assess the threshold for the hydrogel beads materials used in this research, the cell viability assays were conducted using increasing concentrations of the beads for 24 to 72 h incubation periods. From the result, it was observed that both hydrogel beads showed cytotoxic effects against the tested breast cancer cell line, but the effect differs depending on the types of beads and breast cancer cells tested. For this analysis, hydrogel beads (F2) for both QIC and QIM were used due to the greatest encapsulation efficiency.

For the MCF-7 cell line, it was revealed that QIM hydrogel beads showed more effective cytotoxicity where the IC_{50} value was obtained only after 24 hours of incubation period (Figure 4.20). As compared to the QIC hydrogel beads, the cytotoxic effect can only be observed after 48 hours of exposure. This indicates that the micelle extract works better as compared to the crude extract. The IC_{50} value obtained for QIM hydrogel beads

is 6.88 ± 2.7 µg/ml, whereas for QIC hydrogel beads is 5.7 ± 3.1 µg/ml (Figure 4.20). These results can be caused by the size of the QIT micelles being smaller than the QI galls crude extract as the size of the QIT was in nanoscale. This can improve the efficiency of the release of the extract and can promote better uptake of the extract by targeting breast cancer cells. A previous study showed that S-AgNPs/alginate hydrogel beads tended to cause higher cytotoxicity than L-AgNPs/alginate hydrogel beads. Size-dependent cytotoxicity of AgNPs has also been reported in this study (Mahasawat et al., 2019). FA-AML1 cells were more sensitive to 7nm AgNPs than 50nm AgNPs. Treatment of FA-AML1 with 50 µg/ml of 7nm AgNPs and 50nm AgNPs for 24 h resulted in 69% and 30% cell death, respectively (Mahasawat et al., 2019).

Even though this present study did not perform the release profiles of QIM and QIC hydrogel beads, smaller nanoparticle extract incorporated in QIM hydrogel beads have been shown to have higher toxicity to MCF-7 cell line than larger QI galls crude extract in QIC hydrogel beads. Two proposed mechanisms have been discussed. First, smaller QI galls nanoparticle extract from QIM hydrogel beads might penetrate the cells easier than larger QI galls crude extract. Second, smaller QI galls nanoparticle extract from QIM hydrogel beads, which have a higher surface area to volume ratio, might lead to a greater amount of extract released from the surface of QIM hydrogel beads. This will then result in nuclear damage and eventually cause cell death.

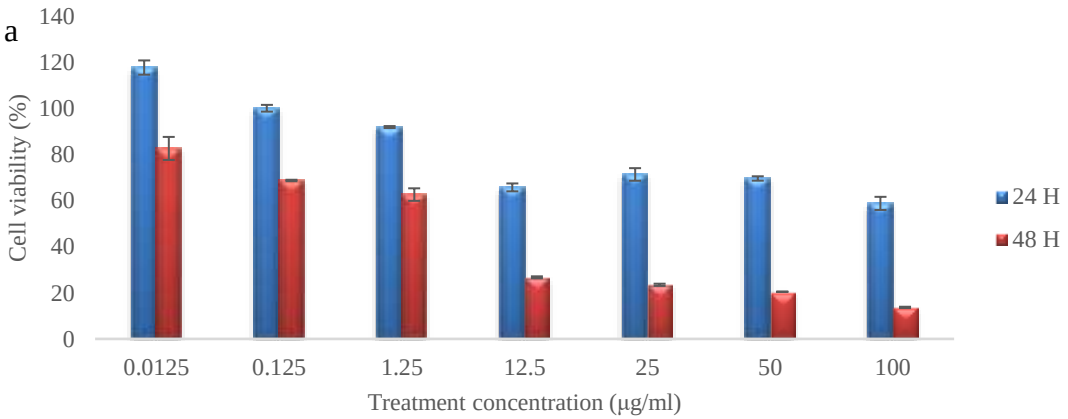

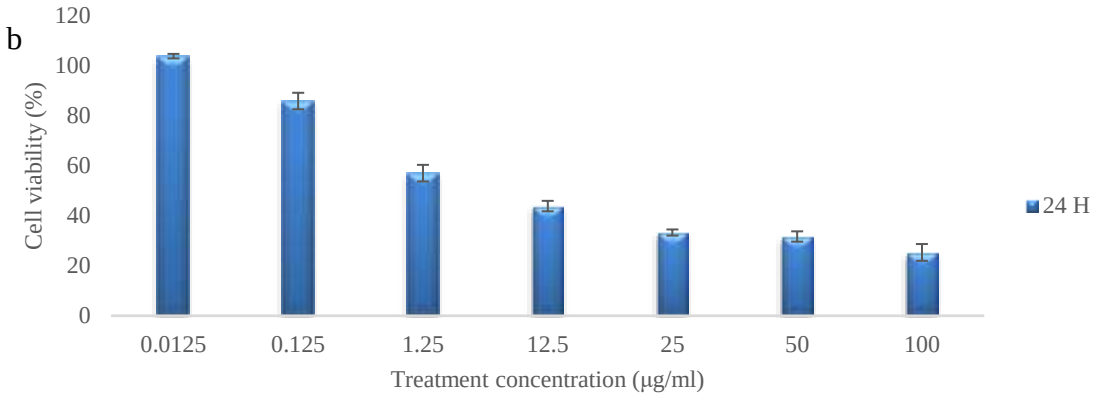

Figure 4.20 Cytotoxic activity of; a) QIC hydrogel beads, b) QIM hydrogel beads against MCF-7 cell lines. Data represent mean ± SEM. n=3.

For MDA-MB-231, it was observed that both QIM and QIC showed toxic effects only after 48 and 72 hours of exposure (Figure 4.21). As compared to MCF-7, the effect of the hydrogel beads on tested cells is slower maybe due to the nature of the triple-negative breast cancer cells that are hardly responsive to the treatment. Triple-negative breast cancer (TNBC), a specific subtype of breast cancer that does not express estrogen receptor (ER), progesterone receptor (PR), or human epidermal growth factor receptor 2 (HER-2), has clinical features that include high invasiveness, high metastatic potential, proneness to relapse (Yin et al., 2020). Triple-negative breast cancer is considered to be more aggressive and has a poorer prognosis than other types of breast cancer, mainly because fewer targeted medicines treat triple-negative breast cancer (Kurozawa & Hubinger, 2017). Previous studies have shown that triple-negative breast cancer is more likely to spread beyond the breast and more likely to reoccur after treatment (Kurozawa & Hubinger, 2017). Hence, this may reflect the results obtained from this present study.

The IC_{50} obtained for QIC beads was 9.61± 1.1 µg/ml while for the QIM hydrogel beads was 4.06 ± 1.7 µg/ml (Figure 4.21). From the results, it can be observed that the smaller size of the micelles extract incorporated in the QIM beads works better as it gives the higher IC_{50} value, and the results were obtained only after 48 hours of incubation time. As for the QIC beads, the IC_{50} was obtained after 72 hours of incubation time. This may be due to the larger molecule size of the QI galls crude extract encapsulated inside the QIC hydrogel beads making it harder to be released out during the treatment duration. Previous studies also revealed that the size of the molecule and the size of the beads can affect the cytotoxic effect against the tested cells. From this study, it was shown that

smaller-sized AgNPs/alginate hydrogel beads can be used as an antibacterial biomaterial with low cytotoxicity and genotoxicity to human cells (Mahasawat et al., 2019).

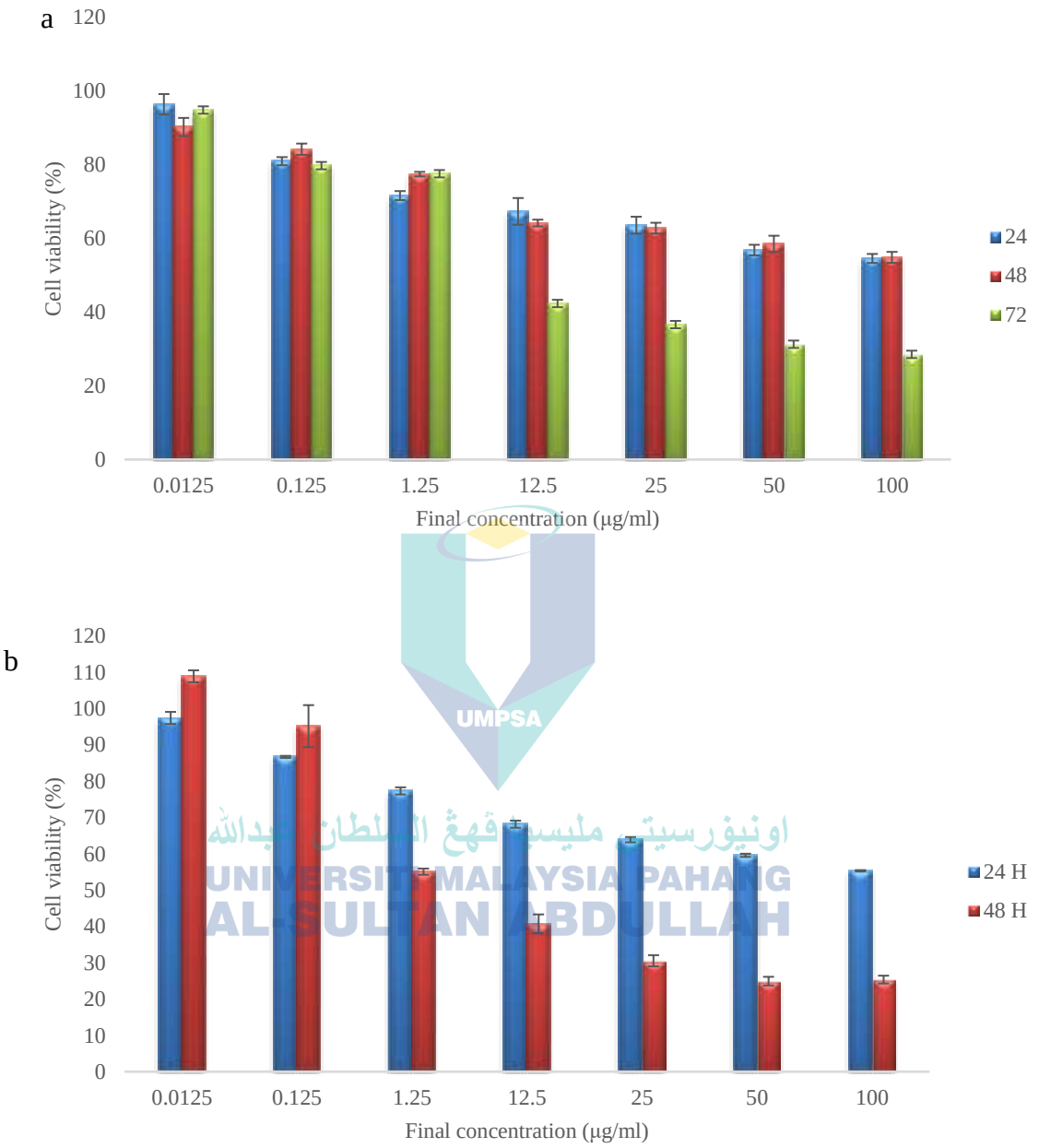

Figure 4.21 Cytotoxic activity of; a) QIC hydrogel beads, b) QIM hydrogel beads against MDA-MB-231 cell lines. Data represent mean ± SEM. n=3.

As a control, the QI galls hydrogel beads were also tested against a normal cell line, L929 cells. From the results, it was observed that both QIM and QIC hydrogel beads were cytoselective because it was showed no toxic effect against normal cell lines after 72 hours of incubation (Figure 4.22). Previous study also revealed that AgNPs/alginate

hydrogel beads showed low cytotoxicity and genotoxicity to normal cells (Mahasawat et al., 2019).

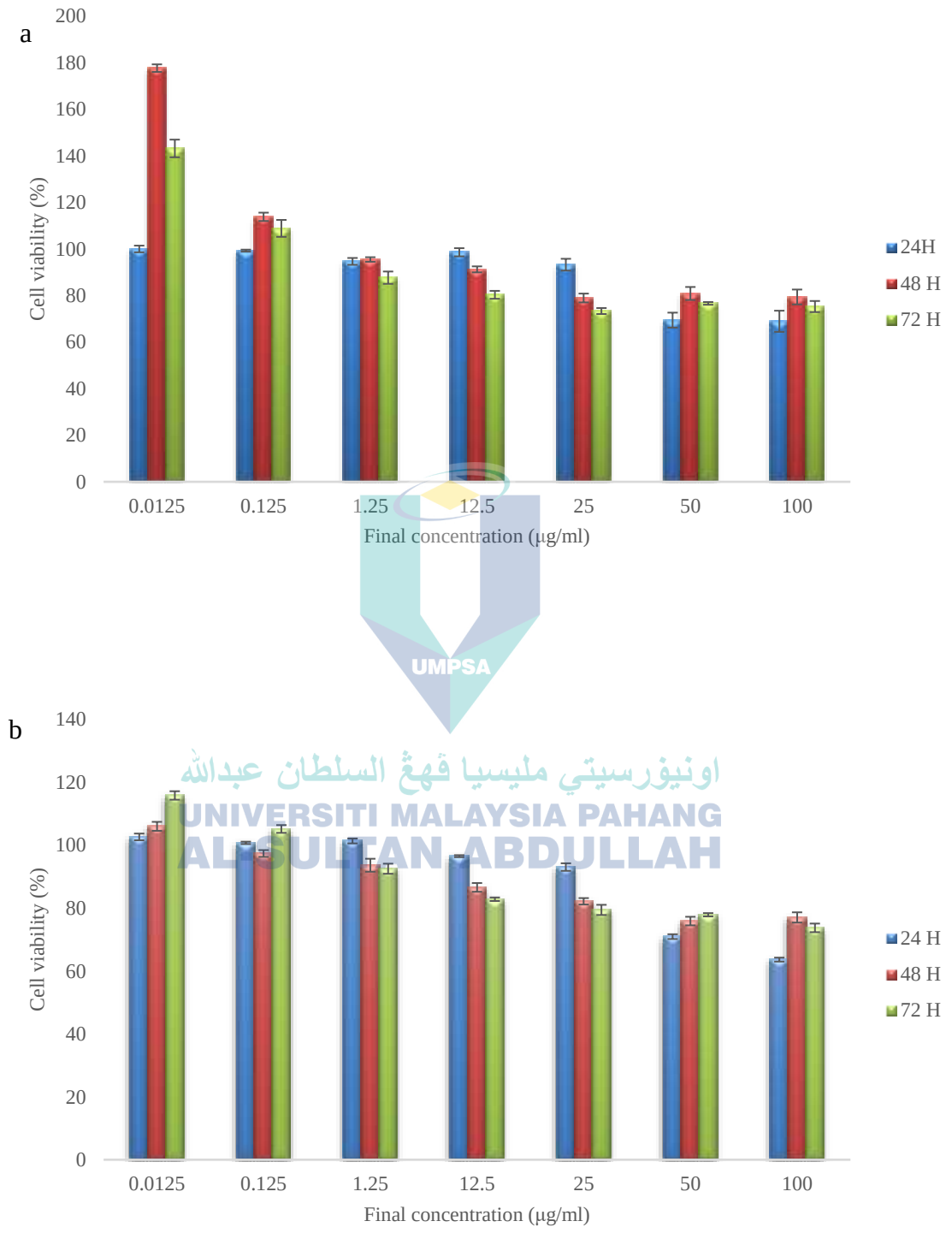

Figure 4.22 Cytotoxic activity of; a) QIC hydrogel beads, b) QIM hydrogel beads against L929 cell lines for 24,48 and 72 h of treatment duration. Data represent mean ± SEM. n=3.

CHAPTER 5

CONCLUSION AND RECOMMENDATIONS

This chapter summarizes the major findings about the effects of QI galls crude and micelle extract against breast cancer cells. The major conclusion of this research is itemized under the three components related to the research objectives: (1) the phytochemical screening and *in vitro* cytotoxicity of QI galls crude extract against breast cancer cells, (2) the physicochemical properties of the QI gall micelle the cytotoxicity effectiveness of QI galls micelle extract against breast cancer cells, and (3) the physicochemical characterization and cytotoxicity study of the polymeric hydrogel beads incorporated with QI gall crude and micelle extract against breast cancer cells. Finally, the recommendations for future studies are given.

5.1 Conclusion

This chapter presents a brief overview of the results and discussion, a summary of the experiments, and a conclusion to all the details that had been presented previously in every chapter. Generally, a drug delivery system made of polymeric hydrogel beads incorporated with QI galls nanoparticles and crude extracts for the delivery of QI galls extracts into breast cancer cells was successfully developed.

This study started with the extraction of the QI gall using the maceration extraction technique followed by the phytochemical screening of the crude extract. From the phytochemical screening, it was revealed that the crude extract had a good TPC (672.22 ± 0.55 mGAE) and TFC (4.8 ± 0.25 RE) content as well as antioxidant activity (IC_{50} 44.5 µg/ml). Besides that, the crude extract also comprises a large amount of tannic acid (1794.18 ± 0.71 mg/gm) and a small amount of gallic acid (76.22± 0.44 mg/gm). For the cytotoxicity result, it was shown that QI galls crude extract exhibits a good result where the IC_{50} obtained was 0.961 ± 3.3 µg/ml against MCF-7 and 9.61 ± 8.9 µg/ml

against MDA-MB-231 cells after 72 hours of incubation. Interestingly, this QI gall crude extract also showed cytoselective properties as this extract exhibited no cytotoxic effect against the normal cell line, L929. The cell viability was also found to decrease with prolonged incubation time. For the apoptosis study, it was observed that QI galls crude extract induced cell death mechanism through induction of apoptosis.

A drug delivery system known as the micelle of QI galls loaded vitamin E TPGS (QIT) was developed for a sustainable and controlled delivery of the extract into breast cancer cells. Besides that, this nanoparticle was developed to reduce the particle size of QI gall crude extract for better delivery to the cancer site. The size and the solubility of the crude extract were manipulated, and their uptake efficiency was evaluated on the MCF-7 and triple-negative breast cancer cells (MDA-MB-231). From the results, it was shown that the QIT improves the therapeutic effect on the breast cancer cells whereas the cytotoxic effect can be observed only after 24 hours of exposure. The IC_{50} obtained for MCF-7 was 8.28 ± 0.82 µg/ml while for MDA-MB-231 was 11.09 ± 0.82 µg/ml. This QIT micelle also induced cell death mechanisms through the induction of apoptosis. Besides that, the physicochemical properties of the formulated micelle showed good data, where this formulated micelle had a good particle size (below 20 nm), narrow size distribution (PDI between 0.1-0.4), and good surface charge (zeta potential ranges from -11 mv to -20 mv). The findings on the surface chemistry of the micelle revealed that all formulated micelles had almost similar relative ratios amongst the suggested chemical bonds in those reported for pure Vitamin E TPGS. The drug loading showed QIT had the highest load (110.41 µg/ml) and exhibited a biphasic release pattern characterized by an initial burst then followed by a slow and sustained release until the 10th day of the experiment. QIT micelle also showed increased cellular uptake with prolonged incubation time.

The polymeric hydrogel beads incorporated with QI galls crude (QIC) and micelle (QIM) extract were formulated using the ionic gelation method between pectin as the polymer and zinc acetate as the crosslinker. This hydrogel beads formulation also aimed to increase the stability of the micelle which easily agglomerate in liquid suspension as well as the solubility of the crude extract. However, in this current study, the stability of the micelle in the hydrogel beads system is not determined. These hydrogel beads showed good antiproliferative activity against breast cancer cells where the onset can be observed

faster. The IC_{50} of MCF-7, for QIM, was obtained only after 24 hours of incubation time (6.88 ± 2.7 μg/ml) while the QIC was obtained after 48 hours of incubation (IC_{50} 5.7 ± 3.1 μg/ml). For MDA-MB-231, it showed a slower onset where the IC_{50} was obtained after 48 hours for QIM (IC_{50} 9.61 ± 1.1 μg/ml) and for QIC after 72 hours of incubation (IC_{50} 4.06 ± 1.7 μg/ml) This finding proves that the manipulation of the size and carrier of the crude extract and micelle enhanced the therapeutic efficacy compared to the free drug itself. The administration of vitamin E TPGS and polymer caused no toxicity to normal cells, attesting to the biocompatibility of the nanocarrier. For the physicochemical characterization of QIC and QIM, it was shown that both had good yield (highest yield in F2 for both QIC and QIM - > 80%), size distribution, swelling ability, swelling time, moisture content, and encapsulation efficiency (%EE). Out of three formulations (F1, F2, and F3), F2 was selected as the best formulation as it provided the highest yield and the %EE for both QIC and QIM. All these three formulations differ in terms of extract-to-polymer (pectin) ratio; F1 (1:1), F2(1:2), and F3 (1:3). Through this invention, it was hoped that this novel drug delivery system could be utilized pharmaceutically as an early prevention and alternative approach to combat breast cancer.

5.2 Recommendation and future perspectives

The evidence and findings from the results shown above strongly suggest that the developed hydrogel beads formulations of QI gall crude and micelle extract give a good cytotoxic effect on the breast cancer cells and at the same time it showed a very low cytotoxic effect against normal cells. These findings suggest that QI gall crude extracts, particularly when encapsulated in micelle-loaded hydrogel beads, offer promise as a novel breast cancer therapeutic strategy. However, in this study, we are focused only on passive targeting in QIT micelle drug delivery. For the future, it was recommended to develop the active targeting drug delivery system by manipulating the micelle surface with suitable ligands to target the breast cancer cells. It was known that targeted nanomedicine plays an essential role in cancer therapy by delivering the drug to the cancer site directly. Conjugation of antibodies to drugs and carriers will enhance the selective accumulation of antiproliferative drugs in tumour sites which enable tumour-associated surface markers.

In this study, we only focused on single-modality treatments i.e., chemotherapy. Since none of the single-modality treatments can cure cancer effectively, it is proven that

multimodality treatment improves the therapeutic effects in cancer cells. It is believed that the co-delivery of various therapeutic agents by nanocarriers can further enhance killing effects. Besides that, it was recommended to test these developed hydrogel beads on other types of cancer cells such as cervical cancer cells. This is due to some previous studies; it was revealed that this QI gall extract was very potent and exhibited a very good killing effect against cervical (Wan Yusof & Abdullah, 2020) and ovarian cancer cells (Hasmah et al., 2010). In addition, it is also important to study the effect of these polymeric micelles and hydrogel beads after intravenous administration *in vivo* to understand the pharmacokinetics of the developed hydrogel beads and micellar formulations.

It is also strongly recommended to conduct the drug release study for the QIC and QIM hydrogel beads. Conducting drug release studies is crucial in the development of a hydrogel-based delivery system for effectively and safely targeting breast cancer cells. These analyses enable researchers to ascertain the rate and duration of release of the QI gall extract from the hydrogel beads. This information is crucial for optimizing the delivery system. An optimized release profile guarantees that the extract achieves therapeutic levels at the desired location while reducing the likelihood of inadequate or excessive dosage. By employing a controlled release mechanism, the occurrence of harmful side effects can be minimized as it prevents a sudden release and decreases overall exposure to the body. Moreover, the release profile can be modified to specifically target tissues, such as the acidic tumor microenvironment. The study also aids in forecasting the behavior of the system within the body and evaluating the enduring stability of the QI gall extract within the beads. Ultimately, a drug release study offers useful insights for enhancing the hydrogel system to provide targeted and controlled distribution, so maximizing the therapeutic advantages against breast cancer while minimizing any adverse consequences. In addition, the study on the stability of the micelle encapsulated in the hydrogel beads also can be conducted in future. Micelles are crucial in the process of encapsulating and releasing therapeutic compounds in medication delivery using hydrogel beads. Their stability is of utmost importance. Stable micelles guarantee regulated medication release, shield the drug from deterioration, and preserve its efficacy during storage. To assess the stability of micelles within these beads, key characteristics such as critical micelle concentration, particle size, entrapment

efficiency, drug release profile, and the influence of environmental variables such as pH and temperature on the micelles can be analyzed.

Besides that, it is also recommended to formulate hydrogel beads incorporated with free and nanoparticle forms of established anticancer drugs such as docetaxel, cisplatin, or tamoxifen so that we can compare the effectiveness of the breast cancer treatment with this current formulated hydrogel beads (QIC and QIM hydrogel beads). Finally, it is also recommended to carry out the optimization of the hydrogel beads formulation. By optimizing the formulation, it is possible to create hydrogel beads with functionalities that are well suited for drug delivery. Imagine beads engineered to release medications gradually, selectively target certain body regions, or flawlessly merge with the body's tissues. This optimization not only enhances overall performance but also introduces sophisticated features. Furthermore, optimization can lead to cost savings by reducing material use and eliminating unnecessary processes. Therefore, further studies in these research fields are strongly recommended for future work.

REFERENCES

A. El-Agbar, Z., R. Naik, R., & K. Shakya, A. (2018). Fatty Acids analysis and Antioxidant activity of Fixed oil of Quercus Infectoria, Grown in Jordan. *Oriental Journal of Chemistry*, *34*(3), 1368–1374. https://doi.org/10.13005/ojc/340324

Afzal, M., Ameeduzzafar, Alharbi, K. S., Alruwaili, N. K., Al-Abassi, F. A., Al-Malki, A. A. L., Kazmi, I., Kumar, V., Kamal, M. A., Nadeem, M. S., Aslam, M., & Anwar, F. (2021). Nanomedicine in treatment of breast cancer – A challenge to conventional therapy. *Seminars in Cancer Biology*, *69*(July), 279–292. https://doi.org/10.1016/j.semcancer.2019.12.016

Ahmed, E. M. (2015). Hydrogel : Preparation , characterization , and applications : A review. *Journal of Advanced Research*, *6*(2), 105–121. https://doi.org/10.1016/j.jare.2013.07.006

Alaklabi, A., Arif, I. A., Ahamed, A., Surendra Kumar, R., & Idhayadhulla, A. (2018). Evaluation of antioxidant and anticancer activities of chemical constituents of the Saururus chinensis root extracts. *Saudi Journal of Biological Sciences*, *25*(7), 1387–1392. https://doi.org/10.1016/j.sjbs.2016.12.021

Amiri, M., Khazaeli, P., Salehabadi, A., & Salavati-Niasari, M. (2021). Hydrogel beads-based nanocomposites in novel drug delivery platforms: Recent trends and developments. *Advances in Colloid and Interface Science*, *288*, 102316. https://doi.org/10.1016/j.cis.2020.102316

Amna, U., Halimatussakdiah, Wahyuningsih, P., Saidi, N., & Nasution, R. (2019). Evaluation of cytotoxic activity from Temurui (Murraya koenigii [Linn.] Spreng) leaf extracts against HeLa cell line using MTT assay. *Journal of Advanced Pharmaceutical Technology and Research*, *10*(2), 51–55. https://doi.org/10.4103/japtr.JAPTR_373_18

Aryal, S., Baniya, M. K., Danekhu, K., Kunwar, P., Gurung, R., & Koirala, N. (2019). Total Phenolic content, Flavonoid content and antioxidant potential of wild vegetables from western Nepal. *Plants*, *8*(4). https://doi.org/10.3390/plants8040096

Ayob, Z., Mohd Bohari, S. P., Abd Samad, A., & Jamil, S. (2014). Cytotoxic Activities against Breast Cancer Cells of Local Justicia gendarussa Crude Extracts . *Evidence-Based Complementary and Alternative Medicine*, *2014*, 1–12. https://doi.org/10.1155/2014/732980

Bilia, A. R., Piazzini, V., Asprea, M., Risaliti, L., Vanti, G., & Bergonzi, M. C. (2018). Plants extracts loaded in nanocarriers: An emergent formulating approach. *Natural Product Communications*, *13*(9), 1157–1160. https://doi.org/10.1177/1934578x1801300914

Bourhia, M., Abdelaziz Shahat, A., Mohammed Almarfadi, O., Ali Naser, F., Mostafa Abdelmageed, W., Ait Haj Said, A., El Gueddari, F., Naamane, A., Benbacer, L., & Khlil,

N. (2019). Ethnopharmacological Survey of Herbal Remedies Used for the Treatment of Cancer in the Greater Casablanca-Morocco. *Evidence-Based Complementary and Alternative Medicine*, *2019*. https://doi.org/10.1155/2019/1613457

Chai, A., Schmidt, K., Brewster, G., Xiong, L. S. P., Church, B., Wahl, T., Sadabadi, H., Kumpaty, S., & Zhang, W. (2023). Design of Pectin-Based Hydrogel Microspheres for Targeted Pulmonary Delivery. *Gels*, *9*(9). https://doi.org/10.3390/gels9090707

Chan, E. S., Yim, Z. H., Phan, S. H., Mansa, R. F., & Ravindra, P. (2010). Encapsulation of herbal aqueous extract through absorption with ca-alginate hydrogel beads. *Food and Bioproducts Processing*, *88*(2–3), 195–201. https://doi.org/10.1016/j.fbp.2009.09.005

Chaturvedi, M., Kumar, M., Sinhal, A., & Saifi, A. (2021). Recent development in novel drug delivery systems of herbal drugs. *International Journal of Green Pharmacy*, *5*(2), 87–94. https://doi.org/10.4103/0973-8258.85155

Chaves, N., Santiago, A., & Alías, J. C. (2020). Quantification of the antioxidant activity of plant extracts: Analysis of sensitivity and hierarchization based on the method used. *Antioxidants*, *9*(1). https://doi.org/10.3390/antiox9010076

Cheng, X., Yan, H., Jia, X., & Zhang, Z. (2016). Preparation and in vivo / in vitro evaluation of formononetin phospholipid/Vitamin E TPGS micelles. *Journal of Drug Targeting*, *24*(2), 161–168. https://doi.org/10.3109/1061186X.2015.1064435

Chokpaisarn, J., Chusri, S., Amnuaikit, T., Udomuksorn, W., & Voravuthikunchai, S. P. (2017). Potential wound healing activity of Quercus infectoria formulation in diabetic rats . *PeerJ*, *5*, e3608. https://doi.org/10.7717/peerj.3608

Choudhry, A., & Akhtar, N. (2023). Formulation, characterization of Quercus infectoria (Olivier) emulsions, and in vitro, in vivo evaluation as cosmeceutical formulation. *Journal of Cosmetic Dermatology*, *22*(12), 3480–3490. https://doi.org/10.1111/jocd.15865

Darvin, P., Joung, Y. H., Kang, D. Y., Sp, N., Byun, H. J., Hwang, T. S., Sasidharakurup, H., Lee, C. H., Cho, K. H., Park, K. Do, Lee, H. K., & Yang, Y. M. (2017). Tannic acid inhibits EGFR/STAT1/3 and enhances p38/STAT1 signalling axis in breast cancer cells. *Journal of Cellular and Molecular Medicine*, *21*(4), 720–734. https://doi.org/10.1111/jcmm.13015

De, S., Das, D. C., & Mandal, T. (2017). Isolation and Characterization of Flavonoid Compound Extracted Cardanthera Difformis Druce and Study of Its Antibacterial and Antioxidant Activities in Vitro. *International Research Journal of Pharmacy*, *8*(2), 44–49. https://doi.org/10.7897/2230-8407.080223

Deshmukh, A. S., Chauhan, P. N., Noolvi, M. N., Chaturvedi, K., Ganguly, K., Shukla, S. S., Nadagouda, M. N., & Aminabhavi, T. M. (2017). Polymeric micelles: Basic research to clinical practice. *International Journal of Pharmaceutics*, *532*(1), 249–268. https://doi.org/10.1016/j.ijpharm.2017.09.005

Dewi, M. K., Chaerunisaa, A. Y., Muhaimin, M., & Joni, I. M. (2022). Improved Activity of Herbal Medicines through Nanotechnology. *Nanomaterials*, *12*(22). https://doi.org/10.3390/nano12224073

El Maaiden, E., Bouzroud, S., Nasser, B., Moustaid, K., El Mouttaqi, A., Ibourki, M., Boukcim, H., Hirich, A., Kouisni, L., & El Kharrassi, Y. (2022). A Comparative Study between Conventional and Advanced Extraction Techniques: Pharmaceutical and Cosmetic Properties of Plant Extracts. *Molecules*, *27*(7). https://doi.org/10.3390/molecules27072074

Eltayeb, N. M., Eltayeb, G. M., & Salhimi, S. M. (2017). Malaysian journal of analytical sciences anti-proliferative effect of aerva javanica extracts on mcf7 and mda-mb-231 breast cancer cell lines (Kesan Anti-proliferatif Ekstrak Aerva Javanica Ke Atas Titisan Sel Kanser Payudara MCF7 dan MDA-MB-231). *Malaysian Journal of Analytical Sciences*, *21*, 1028–1035. https://doi.org/10.17576/mjas-2017-2105-04

Fateh, A. R. F. M., Elamin, I. E., Shayoub, M. E., & Salah, E. O. H. (2017). Preliminary Phytochemical Screening of Quercus infectoria Olievier Fagaceae. *International Journal of Advances in Pharmacy, Biology and Chemistry*, *2*(2), 346–350. https://doi.org/10.20959/wjpps20181-10775

Fox, M. E., Szoka, F. C., & Fréchet, J. M. J. (2009). Soluble polymer carriers for the treatment of cancer: The importance of molecular architecture. *Accounts of Chemical Research*, *42*(8), 1141–1151. https://doi.org/10.1021/ar900035f

Gao, Jiande, Fan, D., Song, P., Zhang, S., & Liu, X. (2020). Preparation and application of pH-responsive composite hydrogel beads as potential delivery carrier candidates for controlled release of berberine hydrochloride. *Royal Society Open Science*, *7*(11). https://doi.org/10.1098/rsos.200676

Gao, Jiayu, Yang, X., Yin, W., & Li, M. (2018). *Gallnuts: A Potential Treasure in Anticancer Drug Discovery*. https://doi.org/10.1155/2018/4930371

Gaonkar, R. H., Ganguly, S., Dewanjee, S., Sinha, S., Gupta, A., Ganguly, S., Chattopadhyay, D., & Chatterjee Debnath, M. (2017). Garcinol loaded Vitamin E TPGS emulsified PLGA nanoparticles: Preparation, physicochemical characterization, in vitro and in vivo studies. *Scientific Reports*, *7*(1). https://doi.org/10.1038/s41598-017-00696-6

Germain, M., Caputo, F., Metcalfe, S., Tosi, G., Spring, K., Åslund, A. K. O., Pottier, A., Schiffelers, R., Ceccaldi, A., & Schmid, R. (2020). Delivering the power of nanomedicine to patients today. *Journal of Controlled Release*, *326*(July), 164–171. https://doi.org/10.1016/j.jconrel.2020.07.007

Ghosh, B., & Biswas, S. (2021). Polymeric micelles in cancer therapy: State of the art. *Journal of Controlled Release*, *332*(September 2020), 127–147. https://doi.org/10.1016/j.jconrel.2021.02.016

Ghotekar, S., Pansambal, S., Pawar, S. P., Pagar, T., Oza, R., & Bangale, S. (2019). Biological activities of biogenically synthesized fluorescent silver nanoparticles using Acanthospermum hispidum leaves extract. *SN Applied Sciences*, *1*(11). https://doi.org/10.1007/s42452-019-1389-0

Greenlee, H., Hershman, D. L., Shi, Z., Kwan, M. L., Ergas, I. J., Roh, J. M., & Kushi, L. H. (2017). BMI, lifestyle factors and taxane-induced neuropathy in breast cancer patients: The pathways study. *Journal of the National Cancer Institute*, *109*(2), 1–8. https://doi.org/10.1093/jnci/djw206

Gregoriou, Y., Gregoriou, G., Yilmaz, V., Kapnisis, K., Prokopi, M., Anayiotos, A., Strati, K., Dietis, N., Constantinou, A. I., & Andreou, C. (2020). Resveratrol loaded polymeric micelles for theranostic targeting of breast cancer cells. *Nanotheranostics*, *5*(1), 113–124. https://doi.org/10.7150/ntno.51955

Guo, Y., Luo, J., Tan, S., Otieno, B. O., & Zhang, Z. (2013). The applications of Vitamin e TPGS in drug delivery. *European Journal of Pharmaceutical Sciences*, *49*(2), 175–186. https://doi.org/10.1016/j.ejps.2013.02.006

Hamad, H. O., Alma, M. H., Gulcin, İ., Yılmaz, M. A., & Karaoğul, E. (2017). Evaluation of phenolic contents and bioactivity of root and nutgall extracts from iraqian Quercus infectoria olivier. *Records of Natural Products*, *11*(2), 205–210.

Hasmah, A. ., Nurazila, Z., Chow, C., Rina, R., & Rafiquzzaman, M. (2010). Cytotoxic Effects of Quercus Infectoria Extracts towards Cervical (Hela) and Ovarian (Caov-3) Cancer Cell Lines. *Health and the Environment Journal*, *1*(2), 17–23. http://hej.kk.usm.my/pdf/HEJVol.1No.2/Article03.pdf

Hasmida, M. N., Liza, M. S., Nur Syukriah, A. R., Harisun, Y., Mohd Azizi, C. Y., & Fadzilah Adibah, A. M. (2015). Total phenolic content and antioxidant activity of Quercus infectoria galls using supercritical CO<inf>2</inf> extraction technique and its comparison with Soxhlet extraction. *Pertanika Journal of Science and Technology*, *23*(2), 287–295.

Ho, L. H., Ramli, N. F., Tan, T. C., Muhamad, N., & Haron, M. N. (2018). Effect of extraction solvents and drying conditions on total phenolic content and antioxidant properties of watermelon rind powder. *Sains Malaysiana*. https://doi.org/10.17576/jsm-2018-4701-12

Husna, M., Nabilah, I., & Wan Nor Amilah, W. A. W. (2018). Anti-microbial activity of aqueous Quercus infectoria gall extract against pathogenic Leptospira. *Malaysian Journal of Medical Sciences*, *25*(4), 42–50. https://doi.org/10.21315/mjms2018.25.4.4

Hussain, S. A., Hameed, A., Nazir, Y., Naz, T., Wu, Y., Suleria, H. A. R., & Song, Y. (2018). Microencapsulation and the characterization of polyherbal formulation (PHF) rich in natural polyphenolic compounds. *Nutrients*, *10*(7). https://doi.org/10.3390/nu10070843

Id, R. J., & Chaudhry, G. (2019). Understanding Apoptosis and Apoptotic Pathways Targeted

Cancer Therapeutics. *Tabriz University of Medical Sciences*, *7*(3), 113–117. https://doi.org/10.15171/jcvtr.2015.24

Ilaghi, M., Sharifi, I., Sharififar, F., Sharifi, F., Oliaee, R. T., Babaei, Z., Meimamandi, M. S., Keyhani, A., & Bamorovat, M. (2021). The potential role and apoptotic profile of three medicinal plant extracts on Leishmania tropica by MTT assay, macrophage model and flow cytometry analysis. *Parasite Epidemiology and Control*, *12*. https://doi.org/10.1016/j.parepi.2021.e00201

Ismail, I., Kasiraja, V., Abdullah, H., Sultan, U., Abidin, Z., Campus, G. B., Programme, B., & Campus, H. (2021). *A review on anticancer potential of Quercus infectoria and its bioactive compounds*. *41*(4), 701–705.

Jahangirian, H., Lemraski, E. G., Webster, T. J., Rafiee-Moghaddam, R., & Abdollahi, Y. (2017). A review of drug delivery systems based on nanotechnology and green chemistry: Green nanomedicine. *International Journal of Nanomedicine*, *12*, 2957–2978. https://doi.org/10.2147/IJN.S127683

Jamshidzadeh, A., Shokri, Y., Ahmadi, N., Mohamadi, N., & Sharififar, F. (2017). Quercus infectoria and Terminalia chebula decrease melanin content and tyrosinase activity in B16/F10 cell lines. *Journal of Pharmacy & Pharmacognosy Research*, *5*(5), 270–277. http://jppres.com/jppres/pdf/vol5/jppres16.195_5.5.270.pdf%5Cnhttp://jppres.com/jppres/depigmentation-effect-of-quercus-infectoria-and-terminalia-chebula/

Jantamat, P., Weerapreeyakul, N., & Puthongking, P. (2019). Cytotoxicity and apoptosis induction of coumarins and carbazole alkaloids from Clausena harmandiana. *Molecules*, *24*(18), 1–14. https://doi.org/10.3390/molecules24183385

Jantrawut, P., Akazawa, H., & Ruksiriwanich, W. (2014). Anti-cancer activity of rutin encapsulated in low methoxyl pectin beads. *International Journal of Pharmacy and Pharmaceutical Sciences*, *6*(3), 199–202.

Jeevanandam, J., Barhoum, A., Chan, Y. S., Dufresne, A., & Danquah, M. K. (2018). Review on nanoparticles and nanostructured materials: History, sources, toxicity and regulations. *Beilstein Journal of Nanotechnology*, *9*(1), 1050–1074. https://doi.org/10.3762/bjnano.9.98

Ji, S., Lin, X., Yu, E., Dian, C., Yan, X., Li, L., Zhang, M., Zhao, W., & Dian, L. (2018). Curcumin-Loaded Mixed Micelles: Preparation, Characterization, and in Vitro Antitumor Activity. *Journal of Nanotechnology*, *2018*. https://doi.org/10.1155/2018/9103120

Jin, A., Wang, Y., Lin, K., & Jiang, L. (2020). Nanoparticles modified by polydopamine: Working as "drug" carriers. *Bioactive Materials*, *5*(3), 522–541. https://doi.org/10.1016/j.bioactmat.2020.04.003

Kamarudin, N. A., Muhamad, N., Salleh, N. N. H. N., & Tan, S. C. (2021). Impact of solvent selection on phytochemical content, recovery of tannin and antioxidant activity of quercus

infectoria galls. *Pharmacognosy Journal*, *13*(5), 1195–1204. https://doi.org/10.5530/pj.2021.13.153

Kamarudin, N. A., Nik Salleh, N. N. H., & Tan, S. C. (2021). Gallotannin-enriched fraction from quercus infectoria galls as an antioxidant and inhibitory agent against human glioblastoma multiforme. *Plants*, *10*(12). https://doi.org/10.3390/plants10122581

Kapoor, D. U., Garg, R., Gaur, M., Pareek, A., Prajapati, B. G., Castro, G. R., Suttiruengwong, S., & Sriamornsak, P. (2024). Pectin hydrogels for controlled drug release: Recent developments and future prospects. *Saudi Pharmaceutical Journal*, *32*(4), 102002. https://doi.org/10.1016/j.jsps.2024.102002

Kedir, W. M., Deresa, E. M., & Diriba, T. F. (2022). Pharmaceutical and drug delivery applications of pectin and its modified nanocomposites. *Heliyon*, *8*(9), e10654. https://doi.org/10.1016/j.heliyon.2022.e10654

Khan, T., Gurav, P., & Efferth, T. (2018). *PhytoNanotechnology : Enhancing Delivery of Plant Based Anti-cancer Drugs*. *8*(February). https://doi.org/10.3389/fphar.2017.01002

Khazaei, S., Abdul Hamid, R., Ramachandran, V., Mohd Esa, N., Pandurangan, A. K., Danazadeh, F., & Ismail, P. (2017). Cytotoxicity and Proapoptotic Effects of Allium atroviolaceum Flower Extract by Modulating Cell Cycle Arrest and Caspase-Dependent and p53 -Independent Pathway in Breast Cancer Cell Lines . *Evidence-Based Complementary and Alternative Medicine*, *2017*, 1–16. https://doi.org/10.1155/2017/1468957

Khorshidian, N., Mahboubi, A., Kalantari, N., Hosseini, H., Yousefi, M., Arab, M., da Cruz, A. G., Mortazavian, A. M., & Mahdavi, F. S. (2019). Chitosan-coated alginate microcapsules loaded with herbal galactagogue extract: Formulation optimization and characterization. *Iranian Journal of Pharmaceutical Research*, *18*(3), 1180–1195. https://doi.org/10.22037/ijpr.2019.1100776

Khurana, R. K., Gaspar, B. L., Welsby, G., Katare, O. P., Singh, K. K., & Singh, B. (2018). Improving the biopharmaceutical attributes of mangiferin using vitami E-TPGS co-loaded self-assembled phosholipidic nano-mixed micellar systems. *Drug Delivery and Translational Research*, *8*(3), 617–632. https://doi.org/10.1007/s13346-018-0498-4

Kopustinskiene, D. M., Jakstas, V., Savickas, A., & Bernatoniene, J. (2020). Flavonoids as anticancer agents. *Nutrients*, *12*(2), 1–25. https://doi.org/10.3390/nu12020457

Korin, E., Froumin, N., & Cohen, S. (2017). Surface Analysis of Nanocomplexes by X-ray Photoelectron Spectroscopy (XPS). *ACS Biomaterials Science and Engineering*, *3*(6), 882–889. https://doi.org/10.1021/acsbiomaterials.7b00040

Korin, E., Froumin, N., Cohen, S., Mishra, A. K., Cheng, X., Yan, H., Jia, X., Zhang, Z. Z., Peter Christoper, G. V., Vijaya Raghavan, C., Siddharth, K., Siva Selva Kumar, M., Hari Prasad, R., Lamprecht, A., Lv, S., Wu, Y., Cai, K., He, H., Li, Y., … Singh, B. (2018). Surface

Analysis of Nanocomplexes by X-ray Photoelectron Spectroscopy (XPS). *Biomaterials*, *438*(2), 1–12. https://doi.org/10.1002/9781118636299

Kurozawa, L. E., & Hubinger, M. D. (2017). ScienceDirect Hydrophilic food compounds encapsulation by ionic gelation. *Current Opinion in Food Science*, *15*, 50–55. https://doi.org/10.1016/j.cofs.2017.06.004

Kutty, R. V., Chia, S. L., Setyawati, M. I., Muthu, M. S., Feng, S. S., & Leong, D. T. (2015). In vivo and ex vivo proofs of concept that cetuximab conjugated vitamin E TPGS micelles increases efficacy of delivered docetaxel against triple negative breast cancer. *Biomaterials*, *63*, 58–69. https://doi.org/10.1016/j.biomaterials.2015.06.005

Kutty, R. V., & Feng, S. S. (2013). Cetuximab conjugated vitamin E TPGS micelles for targeted delivery ofdocetaxel for treatment of triple negative breast cancers. *Biomaterials*, *34*(38), 10160–10171. https://doi.org/10.1016/j.biomaterials.2013.09.043

Kutty, R. V., Tay, C. Y., Lim, C. S., Feng, S. S., & Leong, D. T. (2015). Anti-migratory and increased cytotoxic effects of novel dual drug-loaded complex hybrid micelles in triple negative breast cancer cells. *Nano Research*, *8*(8), 2533–2547. https://doi.org/10.1007/s12274-015-0760-8

Lai, W. F., & Rogach, A. L. (2017). Hydrogel-Based Materials for Delivery of Herbal Medicines. *ACS Applied Materials and Interfaces*, *9*(13), 11309–11320. https://doi.org/10.1021/acsami.6b16120

Li, H., Yan, L., Tang, E. K. Y., Zhang, Z., Chen, W., Liu, G., & Mo, J. (2019). Synthesis of TPGS/Curcumin Nanoparticles by Thin-Film Hydration and Evaluation of Their Anti-Colon Cancer Efficacy In Vitro and In Vivo. *Frontiers in Pharmacology*, *10*(July), 1–12. https://doi.org/10.3389/fphar.2019.00769

Li, X.-M., Liu, J., Shi, D.-D., Wen, Z.-G., & Yang, P.-L. (2018). *Quercetin and aconitine synergistically induces the human cervical carcinoma HeLa cell apoptosis via endoplasmic reticulum (ER) stress pathway , Fang-Fang Pan*. 1–12. https://doi.org/10.1371/journal.pone.0191062

Liu, S., Li, S., Lin, G., Markkinen, N., Yang, H., Zhu, B., & Zhang, B. (2019). Anthocyanin copigmentation and color attributes of bog bilberry syrup wine during bottle aging: Effect of tannic acid and gallic acid extracted from Chinese gallnut. *Journal of Food Processing and Preservation*, *43*(8), 1–13. https://doi.org/10.1111/jfpp.14041

Liyanage, D. D., Thamali, R. J. K. A., Kumbalatara, A. A. K., Weliwita, J. A., & Witharana, S. (2016). An Analysis of Nanoparticle Settling Times in Liquids. *Journal of Nanomaterials*, *2016*. https://doi.org/10.1155/2016/7061838

Lu, Y., Zhang, E., Yang, J., & Cao, Z. (2018). Strategies to improve micelle stability for drug delivery. *Nano Research*, *11*(10), 4985–4998. https://doi.org/10.1007/s12274-018-2152-3

MacPherson, I. R., Spiliopoulou, P., Rafii, S., Saggese, M., Baird, R. D., Garcia-Corbacho, J., Italiano, A., Bonneterre, J., Campone, M., Cresti, N., Posner, J., Takeda, Y., Arimura, A., & Spicer, J. (2019). A phase I/II study of epertinib plus trastuzumab with or without chemotherapy in patients with HER2-positive metastatic breast cancer. *Breast Cancer Research*, *22*(1), 1–9. https://doi.org/10.1186/s13058-019-1178-0

Madewell, Z. J., Yang, Y., Jr, I. M. L., Halloran, M. E., & Dean, N. E. (2020). NOTE: This preprint reports new research that has not been certified by peer review and should not be used to guide clinical practice. 1. *MedRxiv*, *165*, 1–13.

Mahasawat, P., Mudtaleb, S., & Eaidprap, P. (2019). The Influence of Silver Nanoparticle Sizes on Antibacterial Activity, Cytotoxicity and Genotoxicity of Alginate Hydrogel Beads Containing Silver Nanoparticles. *Applied Mechanics and Materials*, *886*, 70–77. https://doi.org/10.4028/www.scientific.net/amm.886.70

Mala, T., & Anal, A. K. (2021). Protection and Controlled Gastrointestinal Release of Bromelain by Encapsulating in Pectin–Resistant Starch Based Hydrogel Beads. *Frontiers in Bioengineering and Biotechnology*, *9*(October), 1–14. https://doi.org/10.3389/fbioe.2021.757176

Malysa-Pasko, M., Lukasiewicz, M., Ziec, G., Slusarz, E., & Jakubowski, P. (2018). Micellar Extraction of Active Ingredients of Plant Raw Materials as a Tool for Improving the Quality of Diet Supplements and Additional Substances. *Proceedings*, *9*(1), 59. https://doi.org/10.3390/ecsoc-22-05789

Mangal, S., Gao, W., Li, T., & Zhou, Q. T. (2017). Pulmonary delivery of nanoparticle chemotherapy for the treatment of lung cancers : challenges and opportunities. *Nature Publishing Group*, *38*(6), 782–797. https://doi.org/10.1038/aps.2017.34

Meng, X., Liu, J., Yu, X., Li, J., Lu, X., & Shen, T. (2017). Pluronic F127 and D-α-Tocopheryl Polyethylene Glycol Succinate (TPGS) Mixed Micelles for Targeting Drug Delivery across The Blood Brain Barrier. *Scientific Reports*, *7*(1), 1–12. https://doi.org/10.1038/s41598-017-03123-y

Ministry of Health Malaysia. (2017). *National strategic plan for cancer control programme 2016-2020*.

Minzanova, S. T., Mironov, V. F., Arkhipova, D. M., Khabibullina, A. V, Mironova, L. G., Zakirova, Y. M., & Milyukov, V. A. (2018). *Biological Activity and Pharmacological Application of Pectic Polysaccharides : A Review*. 1–31. https://doi.org/10.3390/polym10121407

Mishra, A. K. (2013). Nanomedicine for Drug Delivery and Therapeutics. *Nanomedicine for Drug Delivery and Therapeutics*. https://doi.org/10.1002/9781118636299

Moghtaderi, H., Sepehri, H., Delphi, L., & Attari, F. (2018). Gallic acid and curcumin induce cytotoxicity and apoptosis in human breast cancer cell MDA-MB-231. *BioImpacts*, *8*(3), 185–194. https://doi.org/10.15171/bi.2018.21

Moradi, M. taghi, Karimi, A., & Alidadi, S. (2016). In vitro antiproliferative and apoptosis-inducing activities of crude ethyle alcohole extract of Quercus brantii L. acorn and subsequent fractions. *Chinese Journal of Natural Medicines*, *14*(3), 196–202. https://doi.org/10.1016/S1875-5364(16)30016-4

Mrid, R. Ben, Bouchmaa, N., Bouargalne, Y., Ramdan, B., Karrouchi, K., Kabach, I., Karbane, M. El, Idir, A., Zyad, A., & Nhiri, M. (2019). Phytochemical Characterization, Antioxidant and In Vitro Cytotoxic Activity Evaluation of Juniperus oxycedrus Subsp. Oxycedrus Needles and Berries. *Molecules*. https://doi.org/10.3390/molecules24030502

Mu, L., & Feng, S. S. (2003). A novel controlled release formulation for the anticancer drug paclitaxel (Taxol®): PLGA nanoparticles containing vitamin E TPGS. *Journal of Controlled Release*, *86*(1), 33–48. https://doi.org/10.1016/S0168-3659(02)00320-6

Muthu, M. S., Kutty, R. V., Luo, Z., Xie, J., & Feng, S. S. (2015). Theranostic vitamin E TPGS micelles of transferrin conjugation for targeted co-delivery of docetaxel and ultra bright gold nanoclusters. *Biomaterials*. https://doi.org/10.1016/j.biomaterials.2014.11.008

Nadzri, M. N. Bin, Majeed, S., Sami, F., Tabish, M., & Ansari, M. T. (2019). Preparation and evaluation of hydrogels containing methanolic extract of brassica oleracea ver. italic. *Journal of Global Pharma Technology*, *11*(1), 140–146.

Narayanaswamy, R., & Torchilin, V. P. (2019). Hydrogels and their applications in targeted drug delivery. *Molecules*, *24*(3). https://doi.org/10.3390/molecules24030603

Németh, Z., Csóka, I., Semnani Jazani, R., Sipos, B., Haspel, H., Kozma, G., Kónya, Z., & Dobó, D. G. (2022). Quality by Design-Driven Zeta Potential Optimisation Study of Liposomes with Charge Imparting Membrane Additives. *Pharmaceutics*, *14*(9). https://doi.org/10.3390/pharmaceutics14091798

Nordin, M. L., Abdul Kadir, A., Zakaria, Z. A., Abdullah, R., & Abdullah, M. N. H. (2018). In vitro investigation of cytotoxic and antioxidative activities of Ardisia crispa against breast cancer cell lines, MCF-7 and MDA-MB-231. *BMC Complementary and Alternative Medicine*, *18*(1), 1–10. https://doi.org/10.1186/s12906-018-2153-5

Nur Syukriah, A. R., Liza, M. S., Harisun, Y., & Fadzillah, A. A. M. (2014). Effect of solvent extraction on antioxidant and antibacterial activities from quercus infectoria (Manjakani). *International Food Research Journal*, *21*(3), 1031–1037.

Patra, J. K., Das, G., Fraceto, L. F., Campos, E. V. R., Rodriguez-Torres, M. D. P., Acosta-Torres, L. S., Diaz-Torres, L. A., Grillo, R., Swamy, M. K., Sharma, S., Habtemariam, S., & Shin, H. S. (2018). Nano based drug delivery systems: Recent developments and future prospects

10 Technology 1007 Nanotechnology 03 Chemical Sciences 0306 Physical Chemistry (incl. Structural) 03 Chemical Sciences 0303 Macromolecular and Materials Chemistry 11 Medical and He. *Journal of Nanobiotechnology*, *16*(1), 1–33. https://doi.org/10.1186/s12951-018-0392-8

Pfeffer, C. M., & Singh, A. T. K. (2018). Apoptosis: A target for anticancer therapy. *International Journal of Molecular Sciences*, *19*(2). https://doi.org/10.3390/ijms19020448

Proestos, C., Lytoudi, K., Mavromelanidou, O., Zoumpoulakis, P., & Sinanoglou, V. (2013). Antioxidant Capacity of Selected Plant Extracts and Their Essential Oils. *Antioxidants*, *2*(1), 11–22. https://doi.org/10.3390/antiox2010011

Prof. Shriniwas Mane, Dr. S. K. Bais, & A. B. Trigune. (2023). An Update Review on Novel Drug Delivery System. *International Journal of Advanced Research in Science, Communication and Technology*, *8*(1), 640–648. https://doi.org/10.48175/ijarsct-7926

Pumiputavon, K., Chaowasku, T., Saenjum, C., Osathanunkul, M., Wungsintaweekul, B., Chawansuntati, K., Wipasa, J., & Lithanatudom, P. (2017). Cell cycle arrest and apoptosis induction by methanolic leaves extracts of four Annonaceae plants. *BMC Complementary and Alternative Medicine*, *17*(1), 1–11. https://doi.org/10.1186/s12906-017-1811-3

Purbowati, R., Rozafia, A., Taufiqurohmah, T., & Syahrani, A. (2024). *Quantitative analysis of Quercus infectoria gall extract from supercritical fluid extraction CO2 using LC-MS/MS*. https://doi.org/10.1063/5.0207030

Purbowati, R., Taufikurohmah, T., & Syahrani, A. (2023). Green extraction of Quercus infectoria gall with supercritical CO2 and methanol co-solvent. *Environmental Science and Pollution Research*, *30*(55), 116952–116959. https://doi.org/10.1007/s11356-023-28047-1

Qadir, M. A., Shahzadi, S. K., Bashir, A., Munir, A., & Shahzad, S. (2017). *Evaluation of Phenolic Compounds and Antioxidant and Antimicrobial Activities of Some Common Herbs*. https://doi.org/10.1155/2017/3475738

Rahman, H. S., Othman, H. H., Hammadi, N. I., Yeap, S. K., Amin, K. M., Samad, N. A., & Alitheen, N. B. (2020). Novel drug delivery systems for loading of natural plant extracts and their biomedical applications. *International Journal of Nanomedicine*, *15*, 2439–2483. https://doi.org/10.2147/IJN.S227805

Rajmohan, D., & Bellmer, D. (2019). Characterization of spirulina-alginate beads formed using ionic gelation. *International Journal of Food Science*, *2019*. https://doi.org/10.1155/2019/7101279

Ramesh, S. R. and G. (2013). Preliminary Phytochemical Screening of Quercus infectoria Olievier Fagaceae. *International Journal of Advances in Pharmacy, Biology and Chemistry*, *2*(2), 346–350. http://www.ijapbc.com/files/12-2222.pdf

Rasha, F., Ramalingam, L., Gollahon, L., Rahman, R. L., Rahman, S. M., Menikdiwela, K., & Moustaid-Moussa, N. (2019). Mechanisms linking the renin-angiotensin system, obesity, and breast cancer. *Endocrine-Related Cancer*, *26*(12), R653–R672. https://doi.org/10.1530/ERC-19-0314

Salleh, L. M., Abel, S. E. R., Zahedi, G., Rahman, R. A., Nasir, H. M., & Faua'ad, S. A. S. (2015). Optimization of supercritical carbon dioxide extraction of quercus infectoria oil. *Jurnal Teknologi*, *74*(7), 79–86. https://doi.org/10.11113/jt.v74.4703

Sánchez-Carranza, J. N., Alvarez, L., Marquina-Bahena, S., Salas-Vidal, E., Cuevas, V., Jiménez, E. W., Veloz, G. R. A., Carraz, M., & González-Maya, L. (2017). Phenolic compounds isolated from Caesalpinia coriaria induce S and G2/M phase cell cycle arrest differentially and trigger cell death by interfering with microtubule dynamics in cancer cell lines. *Molecules*, *22*(4). https://doi.org/10.3390/molecules22040666

Sarıyer, S., Duranoğlu, D., Doğan, Ö., & Küçük, İ. (2020). *Journal of Drug Delivery Science and Technology pH-responsive double network alginate / kappa-carrageenan hydrogel beads for controlled protein release : Effect of pH and crosslinking agent*. *56*(January). https://doi.org/10.1016/j.jddst.2020.101551

Savaser, A., Esim, O., Kurbanoglu, S., Ozkan, S. A., & Ozkan, Y. (2018). Current perspectives on drug release studies from polymeric nanoparticles. In *Organic Materials as Smart Nanocarriers for Drug Delivery* (pp. 101–145). Elsevier. https://doi.org/10.1016/B978-0-12-813663-8.00003-8

Sepahpour, S., Selamat, J., Manap, M. Y. A., Khatib, A., & Razis, A. F. A. (2018). Comparative analysis of chemical composition, antioxidant activity and quantitative characterization of some phenolic compounds in selected herbs and spices in different solvent extraction systems. *Molecules*, *23*(2), 1–17. https://doi.org/10.3390/molecules23020402

Shahin, S. (2014). Antioxidant Properties and Total phenolic content of herbs used in post partum diet therapy in Patna (Bihar), India. *IOSR Journal of Pharmacy and Biological Sciences*, *9*(2), 17–20. https://doi.org/10.9790/3008-09231720

Sharba, Z. A., Hasoon, B. A., Maeah, R. K., & Hussein, N. N. (2020). Cytotoxicity, antioxidant, and antimicrobial activities of crude extract of quercus infectoria plant. *Plant Archives*, *20*(January), 227–230.

Shen, H., Gao, Q., Ye, Q., Yang, S., Wu, Y., Huang, Q., Wang, X., & Sun, Z. (2018). Peritumoral implantation of hydrogel-containing nanoparticles and losartan for enhanced nanoparticle penetration and antitumor effect. *International Journal of Nanomedicine*, *13*, 7409–7426. https://doi.org/10.2147/IJN.S178585

Shi, P., Cheng, Z., Zhao, K., Chen, Y., Zhang, A., Gan, W., & Zhang, Y. (2023). Active targeting schemes for nano-drug delivery systems in osteosarcoma therapeutics. *Journal of Nanobiotechnology*, *21*(1), 1–28. https://doi.org/10.1186/s12951-023-01826-1

Sun, Y. S., Zhao, Z., Yang, Z. N., Xu, F., Lu, H. J., Zhu, Z. Y., Shi, W., Jiang, J., Yao, P. P., & Zhu, H. P. (2017). Risk factors and preventions of breast cancer. *International Journal of Biological Sciences*, *13*(11), 1387–1397. https://doi.org/10.7150/ijbs.21635

Surini, S., & Diandra, D. M. (2017). Formulation of mulberry leaf (morus alba l .) Extract hydrogel beads using cross-linked pectin. 1–4.

Suzilla, Y. (2017). Cytotoxic activity of quercus infectoria galls extracts on selected cancer cells and mechanism of apoptosis on hela cells by wan nur suzilla bt wan yusuf . *Thesis submitted in fulfilment of the requirements for the degree of Master of Science*. *August*.

Taib, M., Rezzak, Y., Bouyazza, L., & Lyoussi, B. (2020). Medicinal Uses, Phytochemistry, and Pharmacological Activities of Quercus Species. *Evidence-Based Complementary and Alternative Medicine*, *2020*. https://doi.org/10.1155/2020/1920683

Thapa, R. K., & Kim, J. O. (2023). Nanomedicine-based commercial formulations: current developments and future prospects. *Journal of Pharmaceutical Investigation*, *53*(1), 19–33. https://doi.org/10.1007/s40005-022-00607-6

Tong, C. W. S., Wu, M., Cho, W. C. S., & To, K. K. W. (2018). Recent advances in the treatment of breast cancer. *Frontiers in Oncology*, *8*(JUN). https://doi.org/10.3389/fonc.2018.00227

Tran, S., DeGiovanni, P.-J., Piel, B., & Rai, P. (2017). Cancer nanomedicine: a review of recent success in drug delivery. *Clinical and Translational Medicine*, *6*(1). https://doi.org/10.1186/s40169-017-0175-0

van der Meel, R., Sulheim, E., Shi, Y., Kiessling, F., Mulder, W. J. M., & Lammers, T. (2019). Smart cancer nanomedicine. *Nature Nanotechnology*, *14*(11), 1007–1017. https://doi.org/10.1038/s41565-019-0567-y

Vera Zambrano, M., Dutta, B., Mercer, D. G., MacLean, H. L., & Touchie, M. F. (2019). Assessment of moisture content measurement methods of dried food products in small-scale operations in developing countries: A review. *Trends in Food Science and Technology*, *88*(April), 484–496. https://doi.org/10.1016/j.tifs.2019.04.006

Vetrivel, P., Kim, S. M., Saralamma, V. V. G., Ha, S. E., Kim, E. H., Min, T. S., & Kim, G. S. (2019). Function of flavonoids on different types of programmed cell death and its mechanism: A review. *Journal of Biomedical Research*, *33*(6), 363–370. https://doi.org/10.7555/JBR.33.20180126

Waks, A. G., & Winer, E. P. (2019). Breast Cancer Treatment: A Review. *JAMA - Journal of the American Medical Association*, *321*(3), 288–300. https://doi.org/10.1001/jama.2018.19323

Wan Yusof, W. N. S., & Abdullah, H. (2020). Phytochemicals and cytotoxicity of Quercus infectoria ethyl acetate extracts on human cancer cells. *Tropical Life Sciences Research*, *31*(1), 69–84. https://doi.org/10.21315/tlsr2020.31.1.5

Wang, Z., Deng, X., Ding, J., Zhou, W., Zheng, X., & Tang, G. (2017). Mechanisms of drug release in pH-sensitive micelles for tumour targeted drug delivery system : A review. *International Journal of Pharmaceutics*. https://doi.org/10.1016/j.ijpharm.2017.11.003

Weng, Y. P., Hung, P. F., Ku, W. Y., Chang, C. Y., Wu, B. H., Wu, M. H., Yao, J. Y., Yang, J. R., & Lee, C. H. (2018). The inhibitory activity of gallic acid against DNA methylation: Application of gallic acid on epigenetic therapy of human cancers. *Oncotarget*. https://doi.org/10.18632/oncotarget.23015

Wu, D., Si, M., Xue, H. Y., & Wong, H. L. (2017). Nanomedicine applications in the treatment of breast cancer: Current state of the art. *International Journal of Nanomedicine*, *12*, 5879–5892. https://doi.org/10.2147/IJN.S123437

Xiong, P., & Wei, M. (2016). *Vitamin E TPGS modified liposomes enhance cellular uptake and targeted delivery of luteolin : an in vivo / in vitro evaluation*. https://doi.org/10.1016/j.ijpharm.2016.08.037

Yang, C., Wu, T., Qi, Y., & Zhang, Z. (2018). Recent advances in the application of vitamin E TPGS for drug delivery. *Theranostics*, *8*(2), 464–485. https://doi.org/10.7150/thno.22711

Ye, Y., Zhang, T., Yuan, H., Li, D., Lou, H., & Fan, P. (2017). Mitochondria-Targeted Lupane Triterpenoid Derivatives and Their Selective Apoptosis-Inducing Anticancer Mechanisms. *Journal of Medicinal Chemistry*, *60*(14), 6353–6363. https://doi.org/10.1021/acs.jmedchem.7b00679

Yin, L., Duan, J. J., Bian, X. W., & Yu, S. C. (2020). Triple-negative breast cancer molecular subtyping and treatment progress. *Breast Cancer Research*, *22*(1), 1–13. https://doi.org/10.1186/s13058-020-01296-5

Yuan, Y., Guo, B., Hao, L., Liu, N., Lin, Y., Guo, W., Li, X., & Gu, B. (2017). Doxorubicin-loaded environmentally friendly carbon dots as a novel drug delivery system for nucleus targeted cancer therapy. *Colloids and Surfaces B: Biointerfaces*, *159*, 349–359. https://doi.org/10.1016/j.colsurfb.2017.07.030

Zarrinmehr, M. J., Daneshvar, E., Nigam, S., Gopinath, K. P., Biswas, J. K., Kwon, E. E., Wang, H., Farhadian, O., & Bhatnagar, A. (2022). The effect of solvents polarity and extraction conditions on the microalgal lipids yield, fatty acids profile, and biodiesel properties. *Bioresource Technology*, *344*(PB), 126303. https://doi.org/10.1016/j.biortech.2021.126303

Zhang, J., Chen, D., Han, D. M., Cheng, Y. H., Dai, C., Wu, X. J., Che, F. Y., & Heng, X. Y. (2018). Tannic acid mediated induction of apoptosis in human glioma hs 683 cells. *Oncology Letters*, *15*(5), 6845–6850. https://doi.org/10.3892/ol.2018.8197

Zhou, C., Ma, J., Su, M., Shao, D., Zhao, J., Zhao, T., Song, Z., Meng, Y., & Jiao, P. (2018). Down-regulation of STAT3 induces the apoptosis and G1 cell cycle arrest in esophageal carcinoma ECA109 cells. *Cancer Cell International*, *18*(1), 1–12. https://doi.org/10.1186/s12935-018-0549-4

APPENDIX A
CULTURE MEDIUM PREPARATION

Dulbecco's Modified Eagle's Medium (DMEM) for cell culture

A packet of DMEM powder (10g) was added with 3.7g $NaHCO_3$ and 800ml distilled water in a 1000 ml beaker. The mixture was slowly stirred using the magnetic stirrer to dissolve all the solids. The PH of the mixture was adjusted to 7.2-7.4. Then, distilled water was added to make up the volume to 1000 ml. The prepared medium then was filtered through the nylon filter 0.2µM using the vacuum pam. After that, 0.02% penicillin-streptomycin was added and stored at 4˚C prior used.

Before been used, the prepared medium must be added with sterile Fetal Bovine Serum (FBS) as followed:

For the initial cell culture, 10% FBS was used.

For the sub-culturing cells or cells maintenance, 5% FBS was used.

APPENDIX B
THE PREPARATION OF REAGENTS AND BUFFER SOLUTIONS FOR CELL CULTURE AND CYTOTOXICITY ASSAY

Phosphate Buffer Saline (PBS)

1 PBS tablet was dissolved in distilled water and made up to 200ml and then was autoclaved for sterilization process. The pH of the solution was adjusted to 7.2-7.4 and stored at 4˚C prior used.

Trypan Blue 0.4% (w/v), 10ml

0.04g trypan blue powder was dissolved in distilled water and then made up to 10ml to prepare the trypan blue 0.4% (w/v). The solution then was stored at room temperature prior to use.

Preparation of the *Quercus infectoria* (QI) galls extract and docetaxel for the cell treatment.

The QI galls extract with the concentration of 10mg/ml was prepared by dissolving 10mg of crude extract in 1ml DMSO. For the antiproliferative assay, the serial dilution was conducted, and the final concentration of the extract was 0.39-99µg/ml. The extracts then were stored at 4˚C prior used. The same procedure was repeated for the preparation of cisplatin extracts.

Trypsin-EDTA 0.01% (v/v), 50 ml

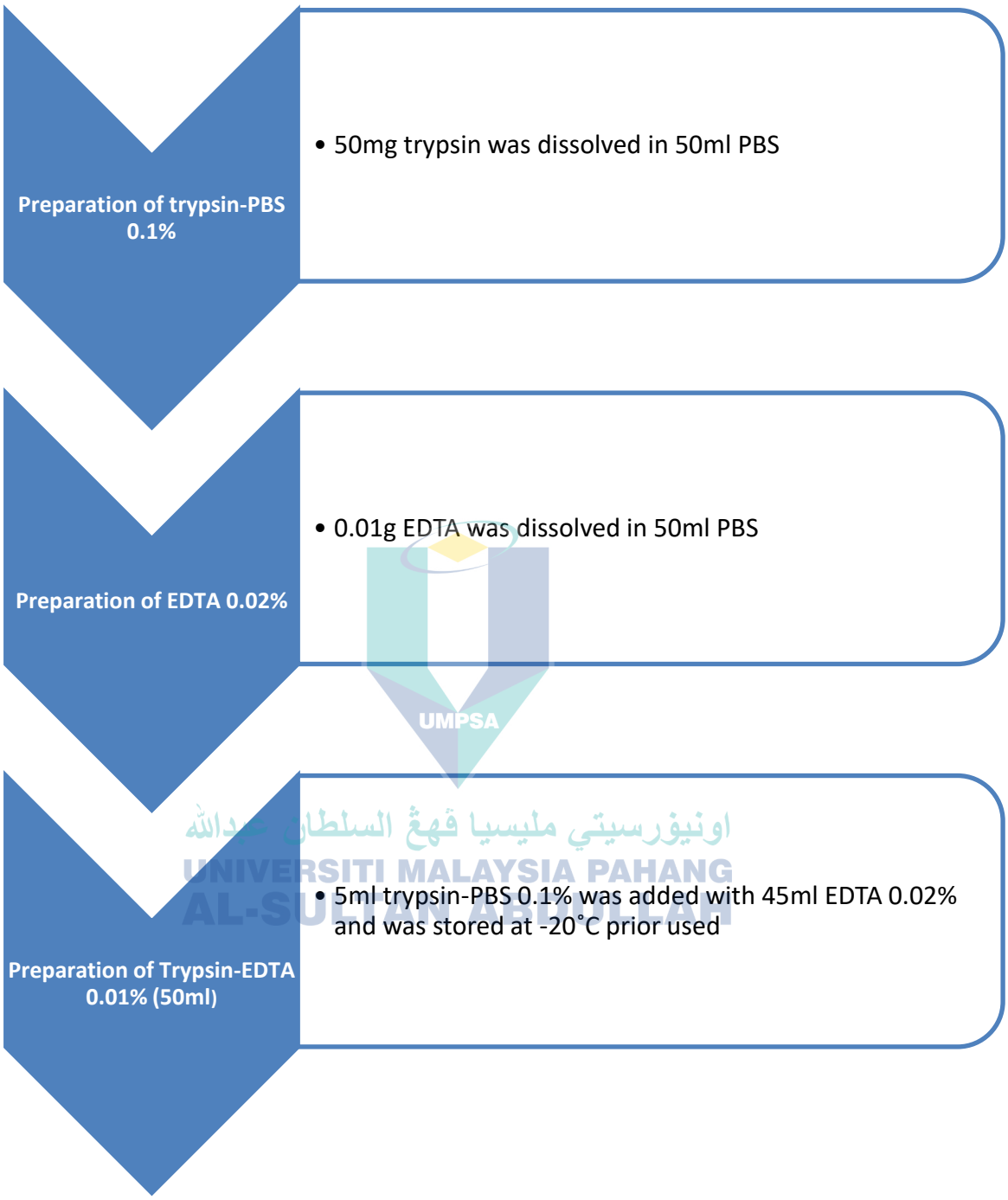

APPENDIX C
PREPARATION OF THE REAGENTS AND BUFFER SOLUTION FOR THE APOPTOSIS ASSAY (FITC-ANNEXIN V/ PROPIDIUM IODIDE DOUBLE STAINING ASSAY)

a) FITC-Annexin V Apoptosis Detection Kit 1 was come with :

1. Binding buffer Annexin V 10X (50ml)
2. FITC Annexin V (0.5ml)
3. The dye of propidium iodide (2ml)

All reagents was stored at 4˚C and protected from lights prior used

b) The preparation of binding buffer Annexin V 10X

1 proportion of the binding buffer Annexin V 10X was dissolved to 9 proportions of distilled water (1:9)

c) Paraformaldehyde 10%

5g of paraformaldehyde was make up to 50ml by dissolving it in PBS and was stirred with the megnetic stirrer untill the solution become clear. The solution was stored at 4˚C prior used. This paraformladehyde was prepared when needed only.

d) TRITON X-100 0.2%

0.1ml Triton X-100 was dissolved with 49.9ml PBS and was stored at 4˚C prior used

APPENDIX D
REVIVING OF THE MDA-MB-231 AND MCF-7 CELL LINES

a) Taking cell line from liquid nitrogen tank (cryopreservation)

b) Thawing process of the cells and thawed cells transferred into complete culture medium

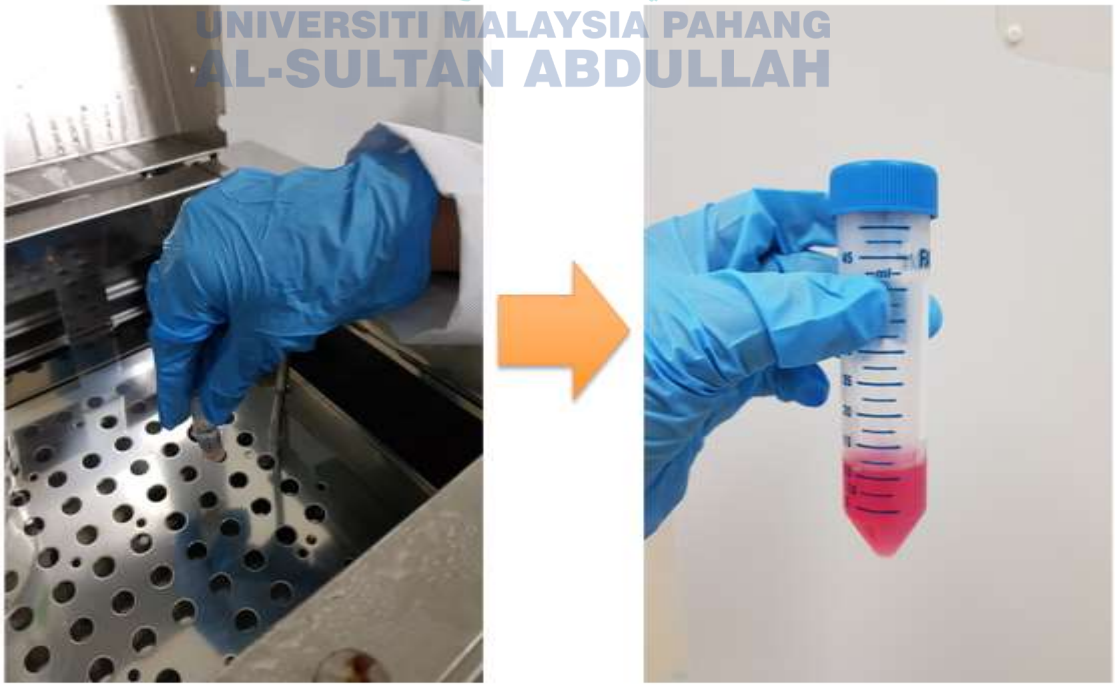

c) Pellet formation through centrifugation process, then cells were transferred into culture flask containing complete culture media and incubated at 37 °C in 5% CO_2 incubator

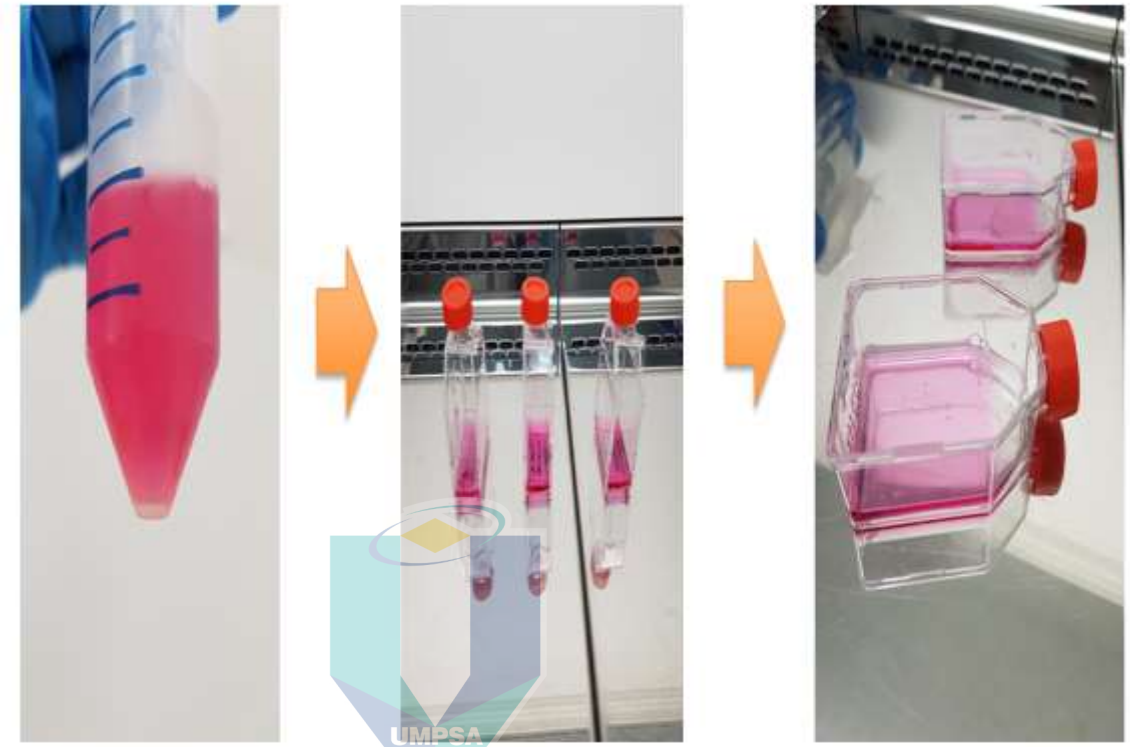

The colorimetric MTT assay is used to measure cell viability (14). The yellow tetrazolium salt (MTT) is reduced by mitochondrial reductase in living and metabolically active cells to purple, water-insoluble formazan crystals, which can then be dispersed using DMSO or other detergents. A decrease in absorbance at 570 nm compared to untreated control cells is then a measure of the cell viability or the amount of apoptosis or necrosis that has been caused by the test material (see Fig. 1).

1. Aspirate the media after the incubation period is over.
2. Prepare the MTT solution by reconstituting the MTT powder in 1× sterile PBS to a final concentration of 5 mg/mL and

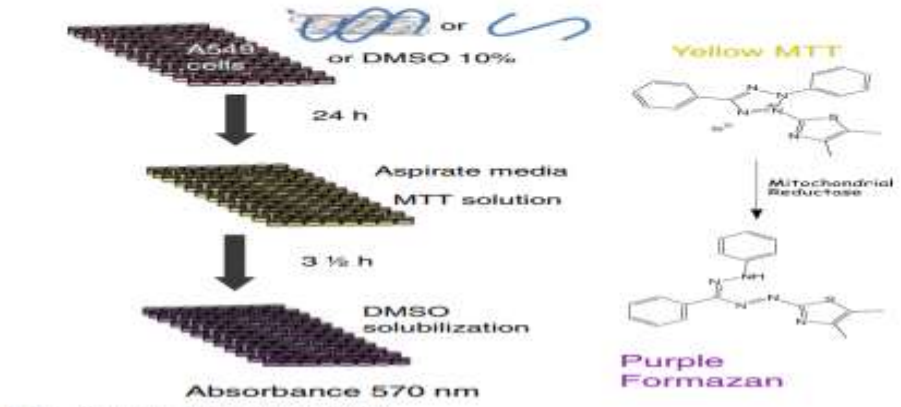

Fig. 1. Schematic of the MTT assay.

subsequently filter and sterilize this solution using a 0.22-µm sterile filter. Store in 2 mL aliquots at −20°C protected from light until use (stable for at least 6 months after reconstitution).

3. Dilute the MTT solution with complete media containing FBS (at a ratio of 1:6) and add 120 µL of this solution to each well.
4. Incubate the cells for 3.5 h at 37°C in a humidified atmosphere (5% CO_2) incubator.
5. Remove the MTT solution by gently inverting the 96-well plate into a paper tissue.
6. Add 150 µL DMSO (100%) to solubilize the formazan crystals and incubate the plate for 15 min at 37°C to remove air bubbles.
7. Read the absorbance at 570 nm in a plate reader and express the results as the percentage cell viability ($n = 8 \pm$ S.D.) compared to untreated control cells (see Fig. 2 and Note 5). The percentage cell viability is calculated using this formula:

$$\% \text{ Cell viability} = \frac{A_{570\,nm} \text{ of treated cells}}{A_{570\,nm} \text{ of untreated cells}} \times 100.$$

APPENDIX E
MORPHOLOGY OF THE MDA-MB-231 AND MCF-7 CELL LINES

a) Morphology of the MDA-MB-231 cell line

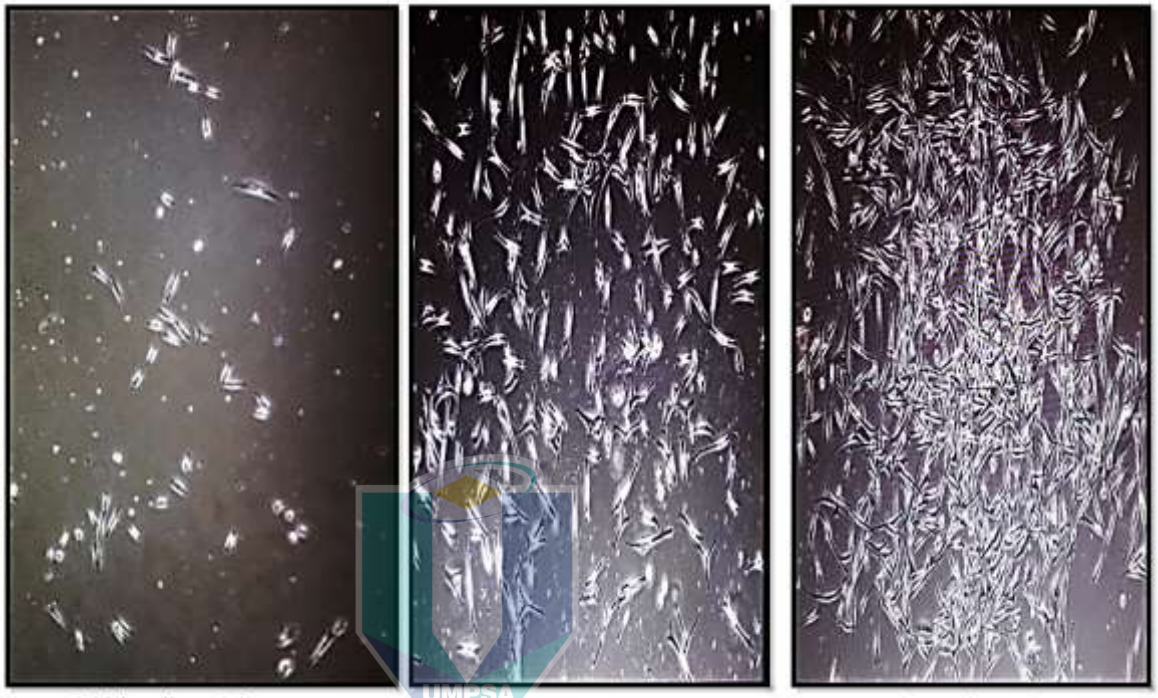

Initial seeding > 24hours | 48-72 hours after seeding | > 72 hours after seeding

b) Morphology of the MCF-7 cell line

Initial seeding > 24hours | 48-72 hours after seeding | > 72 hours after seeding

APPENDIX F
FORMULATION OF THE QUERCUS INFECTORIA (QI) HYDROGEL BEADS

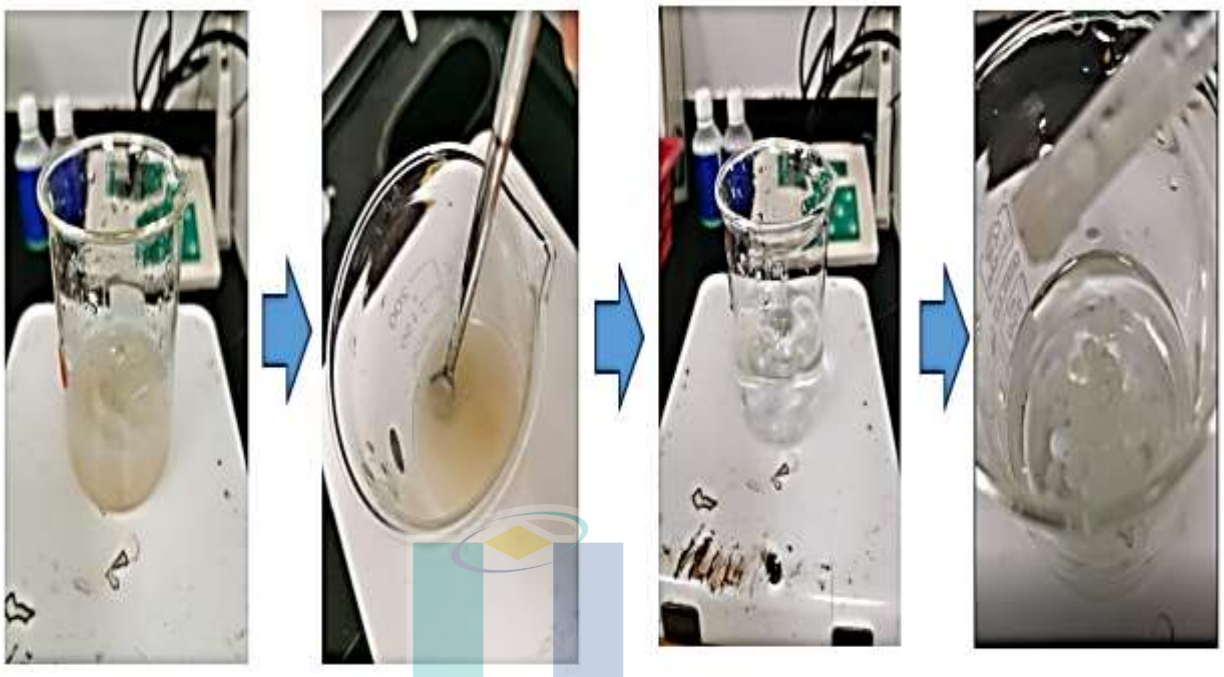

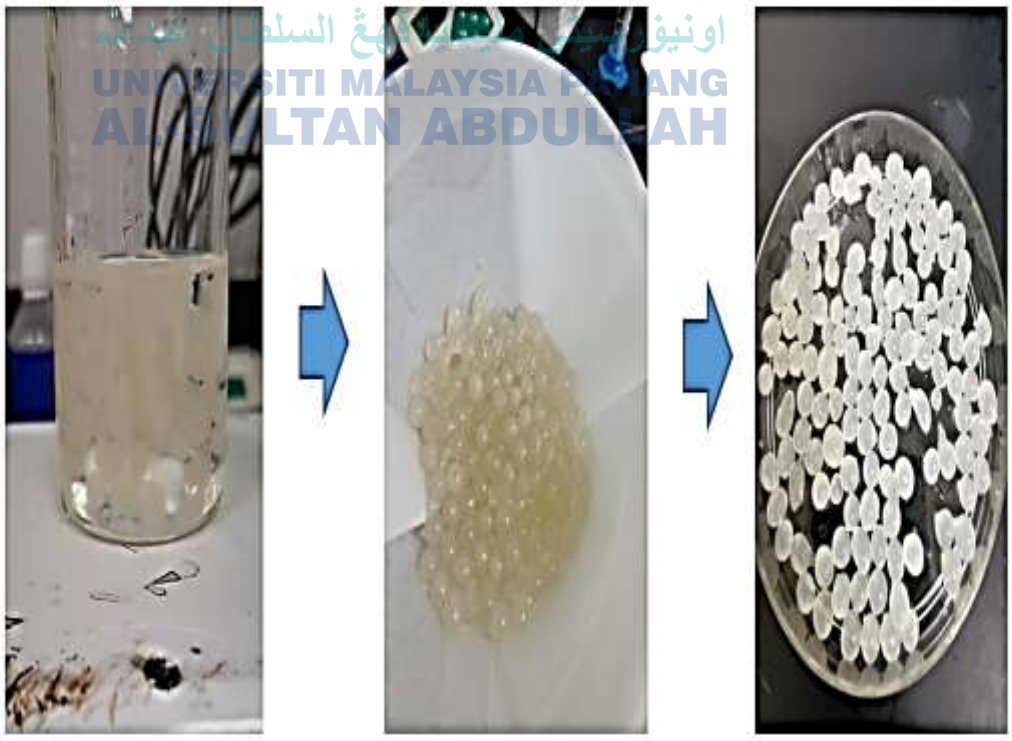

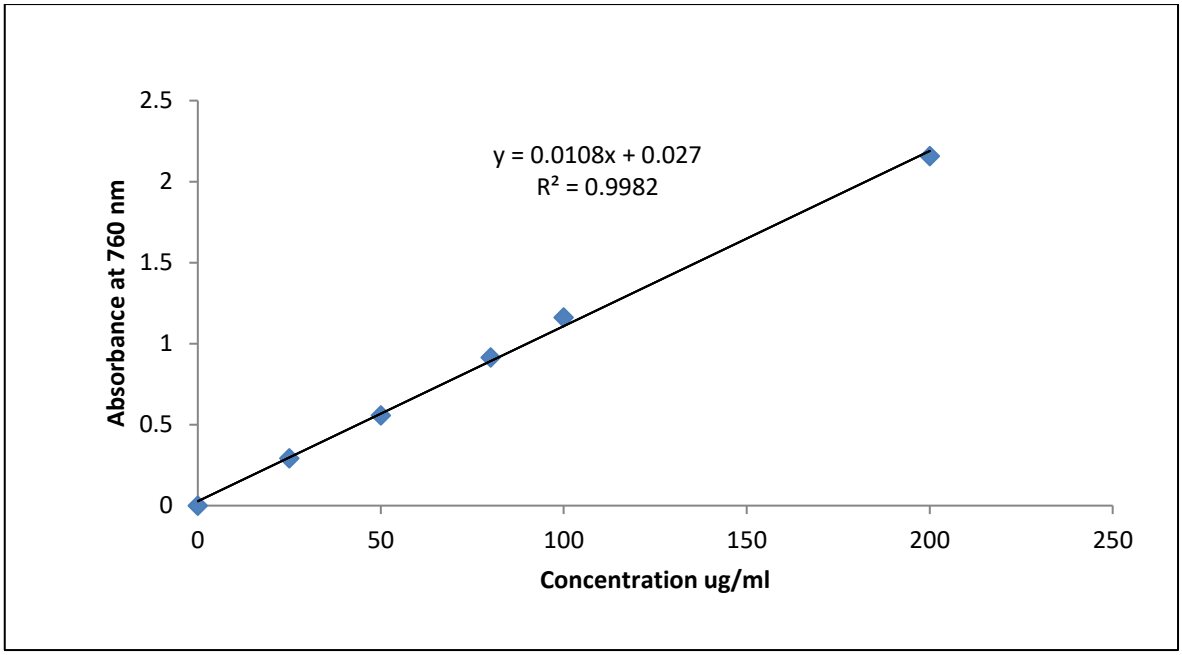

Calibration curve for gallic acid standard

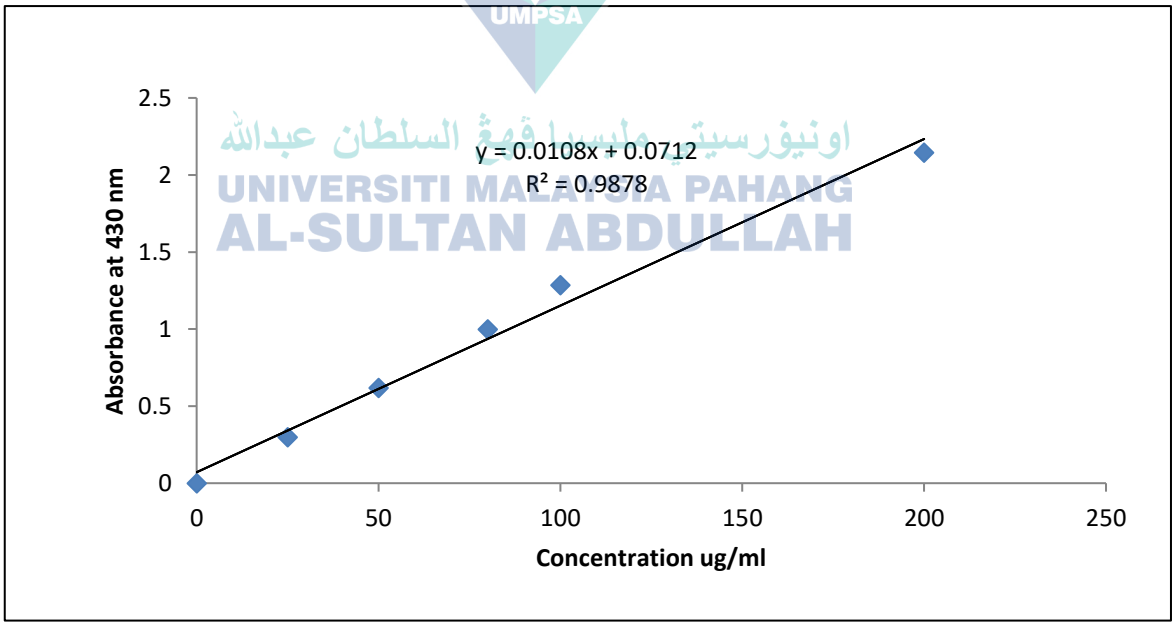

Calibration curve for rutin standard

APPENDIX G
LIST OF PUBLICATIONS

1. Wan Nur Suzilla Wan Yusof and Hasmah Abdullah. Phytochemicals and Cytotoxicity of Quercus infectoria Ethyl Acetate Extracts on Human Cancer Cells. (2020). Tropical Life Science Research 31 (1), 69

2. WY Suzilla, A Izzati, I Isha, A Zalina, VK Rajaletchumy. Formulation and evaluation of antimicrobial herbosomal gel from Quercus infectoria Extract. (2020). IOP Conference Series: Materials Science and Engineering 736 (2), 022030.

3. Wahab, N., Hawa, H., Hassan, M., Nur, W., Wan, S., Jahwi, R. A., Mukriz, M., & Kasim, M. (2022). Physicochemical and microbial analysis of plant-based food waste for potential used as an animal feed Physicochemical and Microbial Analysis of Plant-Based Food Waste for Potential Used as an Animal Feed. 060020(August).

PAPER • **OPEN ACCESS**

Formulation and evaluation of antimicrobial herbosomal gel from *Quercus infectoria* extract

To cite this article: W Y Suzilla *et al* 2020 *IOP Conf. Ser.: Mater. Sci. Eng.* **736** 022030

IOP Conf. Series: Materials Science and Engineering **736** (2020) 022030 doi:10.1088/1757-899X/736/2/022030

Formulation and evaluation of antimicrobial herbosomal gel from *Quercus infectoria* extract

W Y Suzilla[1], A Izzati[1], I Isha[1], A Zalina[1] and V K Rajaletchumy[*]

[1]Faculty of Chemical and Process Engineering Technology, College of Engineering Technology, Universiti Malaysia Pahang, 26300 Gambang, Kuantan Pahang, Malaysia.
[2]Centre of Excellence for Advanced Research in Fluid Flow (CARIFF), Universiti Malaysia Pahang, 26300 Gambang, Pahang, Malaysia.

*vrajaletchumy @ump.edu.my

Abstract. Nowadays, the use of herbal medicine is gaining importance for treating many diseases due to their significant effect and lesser side effects as compared to allopathic medicines. Phytosomal herbal formulations or herbosomes are better absorbed and produce better bioavailability than the conventional botanical extracts. Hence, this study is conducted to formulate the herbosomal gel from QI galls ethanolic extract. The QI gall was extracted using ethanol giving the percentage of yield 17%. For the High-Performance Liquid Chromatography analysis, it was revealed that the QI galls extract contains large amount of tannic acid (1794.18 mg/g) and small amount of gallic acid (76.22 mg/g). The formulation consists of 1.0% of Carbopol 940 were found to be the best formulation since it shows good physicochemical properties. pH value was 6.31 while the viscosity was 3482.3144 cps. Formulated gel showed good stability after 21 days of formulation by not showing significance changes in pH value, viscosity and spreadability. Disc diffusion method was used to determine the antimicrobial activity and the results showed the inhibition zone for P. aeruginosa was greater than S. aureus. As conclusion, the QI galls extract formulated herbosomes was showed promising results to be developed as a new antibacterial gel formulation.

1. Introduction

Herbal medicine or natural based products are gaining importance for treating many diseases due to their significant effect and lesser side effects as compared to conventional medicines [1]. The goal of topical antimicrobial therapy in skin infections is to control microbial colonization and subsequent proliferation thus promoting the healing of the wounds [1]. The emerging technology of drug delivery is being applied to phyto-pharmaceuticals to improve the bioavailability of herbal extracts for medicinal application [2]. Plant extracts can be standardized accordingly and may be formulated as phytosomes for systematic investigation for any improved potential use. Phytosomal herbal formulations are better absorbed, and as a result produce better bioavailability and actions than the conventional phytomolecules or botanical extract [2]. This formulation is also known as herbosomes. This study is conducted to formulate the herbosomal gel from *Quercus infectoria* (QI) galls ethanolic extract.

Quercus infectoria (QI) is a small tree or shrub that falls under Fagaceae (Quercaceae) family [1]. This gall is better known as manjakani among the local people in Malaysia. QI galls was originated from Western Asia and Southern Europe [1]. Galls are irregular plant growth that was produced from the chemical reaction between insects and plant hormones [1]. The QI galls is described in detail in

ethnobotanical and literature to possess various pharmacological actions such as analgesic, antidote, anti-inflammatory, antipyretic, antiseptic, antistomatitis, deodorant, derivative, desiccant, expectorant, germicidal, hypnotic, hypoglycaemic, powerful astringent, sedative, styptic, tonic, tonic to teeth and gum, and wound healing [3]. The main component in QI galls are tannin (50-70%) and small amount of free gallic acid and ellagic acid [3]. The galls also contain gum, sugar and essential oil [3].

Lot of studies were conducted on the potential of this QI galls on their biological activity for medicinal purpose. Previous study showed that the herbosomal gel prepared using QI galls extract exhibited great physical and physicochemical properties [1]. Besides that, another study revealed that hydroalcoholic extract of QI galls can be applied to human body in more effective way when formulated in microemulsion-gel system. In this study, QI galls extract showed acceptable antimicrobial and antifungal activity against selected microbes. Optimized formulations showed acceptable pH, spread ability, in vitro diffusion and percent drug retention [4]. Furthermore, this QI galls extract also was used to prepare the formulation of in-situ herbal gel for the treatment of vagina infection. This study revealed that this QI galls extract was very effective and beneficial in the treatment of vagina infection in the form of herbal gel [5]. Therefore, the purpose of this present study was to formulate the herbosomal gel of QI galls extract and to evaluate the physicochemical properties in term of pH, viscosity homogeneity and spreadability of the herbosomal gel.

2. Methodology

2.1 Preparation of Quercus infectoria (QI) extract

The galls of QI were cleaned and washed with water and air dried. Then, the galls were crushed by using hammer into small pieces and ground to produce fine powder. Ethanolic extract was prepared by maceration extraction process where 100 gram of galls powder was soaked in 600 ml ethanol for 72 hours [8]. Then, the mixture was filtered using filter paper. The filtrates were subjected to rotary evaporation process to remove the ethanol. After rotary evaporation, the extract was stored at -80˚C overnight. Finally, the extract was freeze dried and store at 4 ˚C prior used.

2.2 High Performance Liquid Chromatography (HPLC)

2.2.1 Quantification of gallic acid

Determination of active constituents from extracted compounds was examined using high performance liquid chromatography as described by [6] with a slight modification. In order to evaluate the quality of extracted compounds, all the samples were analysed by using High Performance Liquid Chromatography (HPLC) using gallic acid as standard. Waters 600E System Controller combined with Waters 996 Photodiode Array Detector was used and C18 column was selected as stationary phase. Meanwhile, 0.1% orthophosphoric acid (H3PO4) was consumed as solvent A and 100% acetonitrile (100%) as solvent B. Then, the flowrate of mobile phase was adjusted at 1 ml/min at 280 nm and every injection was set until achieved 10 µL.

2.2.2 Quantification of tannic acid

The concentration of tannic acid from the extracts was determined with slight modification. HPLC was performed by reversed-phase HPLC on a C18 column by using a binary gradient elution with consisting of an aqueous methanol eluent at low pH as mobile phase. The gradient system consisted of solvent A (25 ml acetic acid and 975 ml distilled water) and solvent B (99.8% methanol) pumped at 1 mL/min. The gradient started with 100% solution A and ended with 100% solution B at 30 min. The column temperature was maintained at 30°C. The sample peaks were identified by comparing with standard solution of tannic acid at 280 nm. The percentage of the tannic acid was calculated using the appropriate calibration curves [7].

2.3 *Formulation of herbosomal gel*

Herbosomes are made by reacting the QI gall extract with soy lecithin and cholesterol in a ratio of 1:1 and dissolved them in ethyl acetate. After solubilization completed, the complex compounds formed

was removed by solvent evaporation technique [1]. Herbosomal gel was prepared by using Carbopol 940 as the gelling agent as shown in the table 1 below.

2.4 *Physicochemical evaluation of herbosomal gel*

2.4.1 pH. The pH meter was calibrated using standard buffer solution such as pH 4.0 and 7.0. About 0.5 g gels was weighed and dissolved in 50 ml of distilled water and the pH reading were taken [1].

2.4.2 Viscosity. Viscosity of the formulation was determined by CCT_8_600110 using RST-CC Brookfield Rheometer at 100 rpm [1].

2.4.3. Spreadability. The 0.5 g gel was weighed and pressed between two horizontal plates (20 × 20 cm). Then 500 g weight was put on the upper plate and left for about 5 minutes. Diameters of spread circles were measured in cm. The results obtained were the average of three determinations [1].

2.5 Stability Studies

The optimized formulation of herbosomal gel was selected for stability study. Two other formulations were made as control which was F5 and F6. F5 was formulated without the addition of propylparaben as stabilizer and F6 was formulated without the presence of QI galls extracts as active pharmaceutical ingredients. Stability studies was performed on these three formulations by kept them at three different temperatures, i.e. 45 ± 2˚C, 25 ± 2℃ and 4 ± 2˚C for 21 days [1]. Parameters observed for the herbosomal gel are the determination of the pH value, viscosity, homogeneity and spreadability of the herbosomal gel.

2.6 Centrifugation Test

10g of herbosomal gel was added in a centrifuge tube. During centrifugation, the gel was subjected to a cycle of 3000 rpm for 30 minutes at room temperature. Centrifugation was performed by Model Eppendorf Centrifuge 5820 R [8].

2.7 Agar well diffusion method

Three petri dishes were filled with nutrients agar and 80 µl of bacteria strain in nutrients broth (S. aureus or P. aeruginosa) for each concentration range from 5.00 mg/ml to 0.10 mg/ml using half fold serial dilution. Each concentration for antimicrobial test was done in triplicate. Total concentration for antimicrobial test was 10 concentrations. The nutrient agar was air dried inside fume hood. Then, 5.0 mm^3 of well was bored out using pipette tip. Antimicrobial testing for herbosome gel formulation was run by impregnated 100µl of gel inside the well and incubated the antibacterial assay plate upright for 24 hours at 37 ºC. The area of inhibition was measured using Vernier caliper for each concentration. Then, repeat the test three times for each concentration [9]. The whole step was repeated using QI galls extract. The empty well was used as control to see the natural growth of bacteria under same condition, temperature and environment.

3. Results and discussion

The extraction yield of QI galls with ethanol obtained was 17%. As shown in table 1 below, the QI galls extract contains high concentration of tannic acid and small amount of gallic acid which are 1794.18 mg/g and 76.22 mg/g respectively. From the results, it was revealed that tannic acid is the major bioactive constituents in QI extract. Due to its high concentration, most of the pharmacological properties exhibited by the galls extract can be attributed to tannic acid [10].

Table 1. Concentration of gallic acid and tannic acid in *Quercus infectoria* (QI) galls extract.

Sample	Gallic acid (mg/g)	Tannic acid (mg/g)
Quercus infectoria (QI) extract	76.22	1794.18

Previous study reported lower concentration of gallic acid and tannic acid in ethanolic extract of QI galls which are 37.22 mg/g and 954.03 mg/g respectively [11]. However, this findings were also supported by previous data from past researches, which showed the presence of tannic acid, gallic acid, syringic acid, ellagic acid, β-sitosterol, amentoflavone hexamethyl ether, isocryptomerin, starch, essential oils, anthocyanins, methyl-betulate, methyl- oleanate, hexagalloyl-glucose and polygalloyl-glucose [12] in QI galls extract.. Table 1 to 4 below showed the HPLC chromatogram for the standard and sample tannic and gallic acid in QI galls extract.

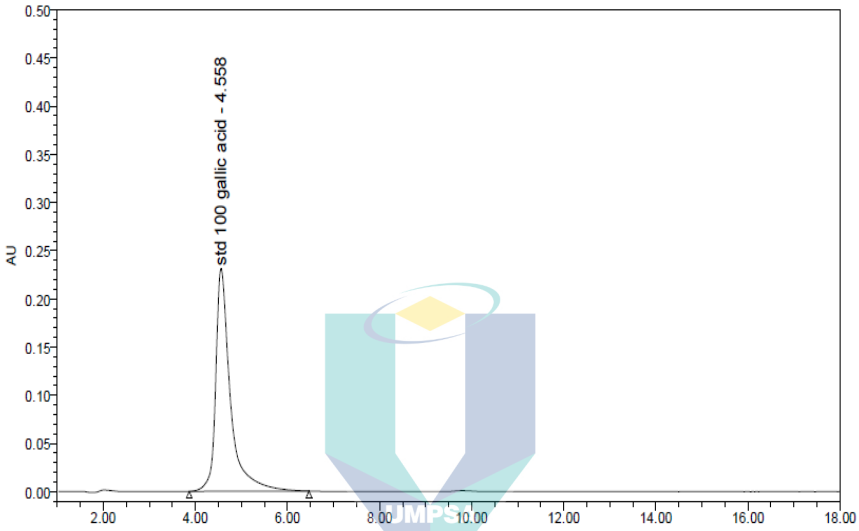

Figure 1. HPLC chromatogram of standard gallic acid

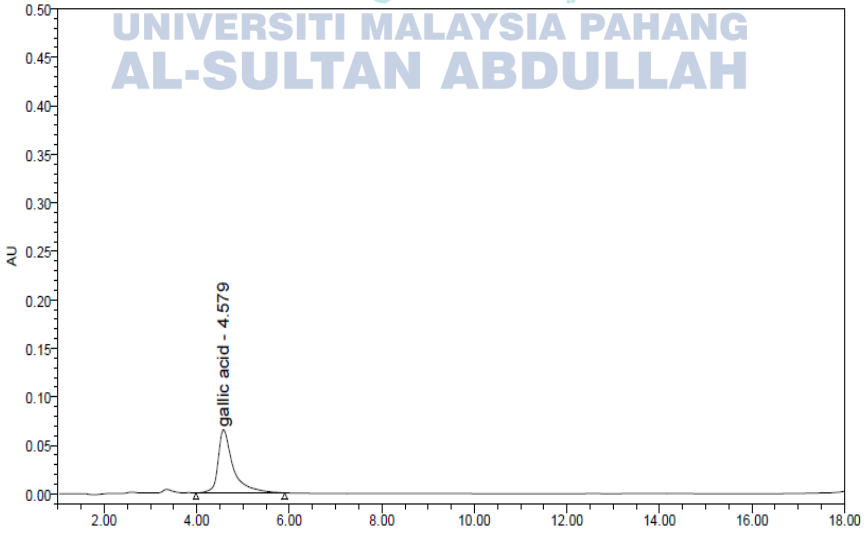

Figure 2. HPLC chromatogram for gallic acid in *Quercus infectoria* (QI) galls extract

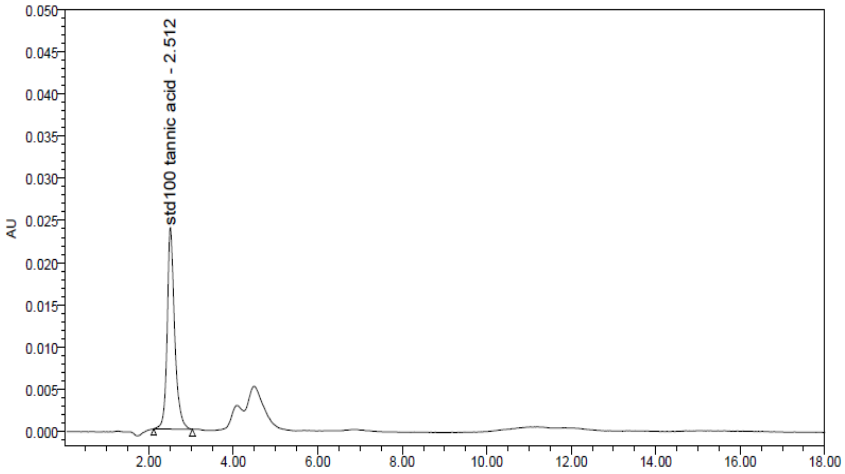

Figure 3. HPLC chromatogram of standard tannic acid.

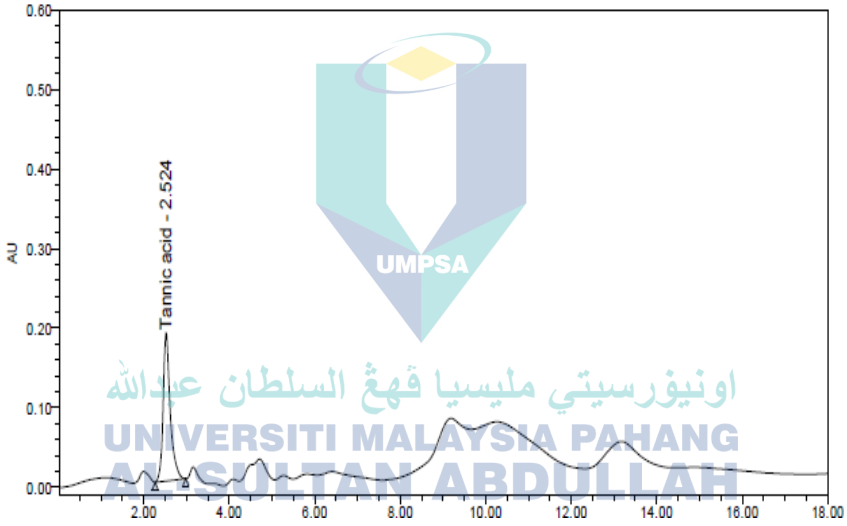

Figure 4. HPLC chromatogram for tannic acid in *Quercus infectoria* (QI) galls extract.

Four different gel formulations (F1, F2, F3 and F4) were prepared using different concentrations (0.5, 1, 1.5 and 2%) of Carbopol 940 polymer as is shown in table 2. Carbopol 940 was used as gelling agent in the formulation as it is biodegradable, bioadhesive, biocompatible, irritation free and not absorbed into body [13].

Table 2. The formulation gel with different concentration of carbopol 940.

Ingredients	Compositions (%)			
	F1	F2	F3	F4
Q. Infectoria extract	0.02	0.02	0.02	0.02
Propylparaben	0.1	0.1	0.1	0.1
Carbopol 940	0.5	1.0	1.5	2.0
Triethanolamine	1.5	1.5	1.5	1.5
Distilled water (mL)	100	100	100	100

The physicochemical evaluation was optimized after preparing the gel with various concentrations of carbopol 940, where the 1.0 % of carbopol 940 containing gels was found to be compatible with the requirements of gel formulations as shown in the figure 2 (a), (b), (c), and (d) for their appearances with different concentration of Carbopol 940. For the physical appearance of four different concentrations of gelling agents, it was found that the formulation with 0.5% of carbopol 940 had changed its colour into yellowish after day one from the gel preparation. Moreover, it was a bit watery compared with other concentrations. The colour changes occurred because of the insufficient of carbopol 940 which is as a gelling agent. Insufficient of carbopol 940 would affect the viscosity value of that gel. Based on the viscosity theory, increase in viscosity of a semi-solid dosage form will lead to an increase in stability. Reasons for instability can be understood from the nature of immiscible phases and their interfacial properties because a gel cannot immobilize the droplet and the droplet can move that lead to the colour changes[14]. The best formulation of the herbosomal gel which is F2 was kept at varying condition of temperature. There was not much change of pH, viscosity, homogeneity and spreadability observed in this formulation.

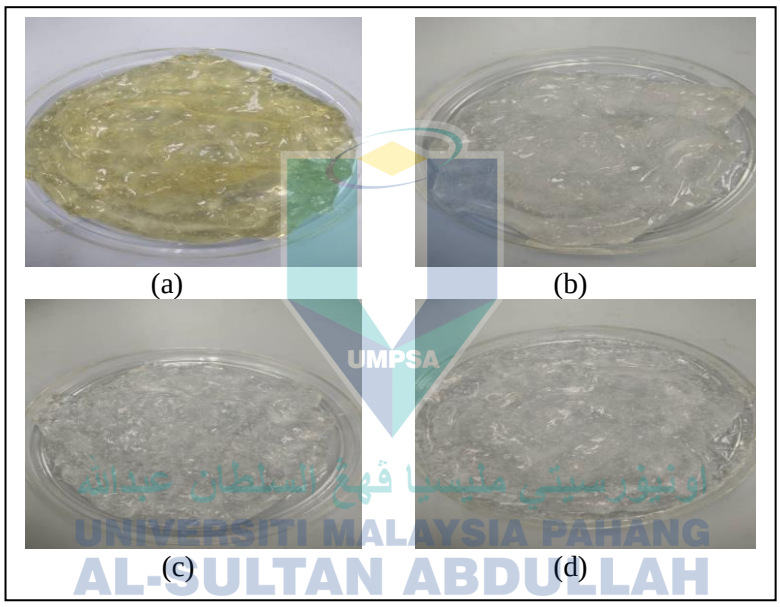

Figure 5. The formulation of gel with different concentration of carbopol 940 for (a) 0.5%, (b) 1.0%, (c) 1.5%, and (d) 2.0%.

For the physical appearance study, it was showed that the formulation with 0.5% of carbopol 940 changed its colour into yellowish after one day of the gel preparation. Besides, this formulation was a bit watery as compared to other formulations. The colour changes occurred might due to the insufficient of carbopol 940 as gelling agent [1]. Insufficient of carbopol 940 can affect the viscosity of the gel. Based on the previous findings, it was revealed that increase in viscosity of a semi-solid dosage form will lead to an increase in stability [1]. Reasons for instability can be understood from the nature of immiscible phases and their interfacial properties because a gel cannot immobilize the droplet and the droplet can move that lead to the colour changes. From the study, it was revealed that the best formulation is F2 because this formulation showed not much change when stored at different condition and temperature.

The pH values of the herbosomal gel is found to be in the range from 6.55 ± 0.03 to 6.91 ± 0.02, which was expected since the carbopol was formulated with pH between 5 to 5.5 and is neutralized using triethanolamine. The pH value showed that QI galls extract gel probably would not cause skin irritation. The QI galls extract gel was evaluated for its physical parameters such as colour, odour and homogeneity. The herbosomal gel formulation has a smooth texture and pale yellow transparent and homogenous and it has characteristic odour of QI galls extract. Table 2 shows data of the stability

studies for antimicrobial herbosomal gel F2. Figure 7 shows the viscosity reading of the herbosomal gel, F2, for 3 consecutive weeks at for 3 different storage temperature. For the formulation with 1.5 and 2.0% of carbopol were found to be compatible to the gel formulation since the physical appearances was in good except the spreadability and viscosity parameters were not meet the requirements of the gel formulation as shown in table 2. This gel formulation was a bit thicker compared with the other concentrations. Therefore, it can be considered that these both concentrations were not giving a good physicochemical evaluation's result since the viscosity and spreadability evaluation were the critical parameter of the gel to have a better absorption because spreadability gives indication of gel to spread on the skin part.

The formulations with 1.5 and 2.0% of carbopol, showed good physical appearance but the spread ability and viscosity did not achieve the gel formulation requirement as shown in table 2. These gel formulations were thicker and viscous as compared to other formulations. Therefore, it revealed that these formulations are not suitable to be developed as herbosomal gel as the physical appearance and viscosity were critical parameter in gel formulation. Four gel formulations (F1, F2, F3 and F4) that prepared using carbopol 940 were evaluated for physical appearance, pH, viscosity and spreadability. The findings showed that the data obtained (Refer table 4) were acceptable for gel formulations. The formulated herbosomal gels showed to be homogeneous, having good physical appearance and consistency. The pH values of all formulations were in acceptable range for gel formulation, pH (6.24-6.45) which is good for human skin. The results for pH determination were shown in figure 6.

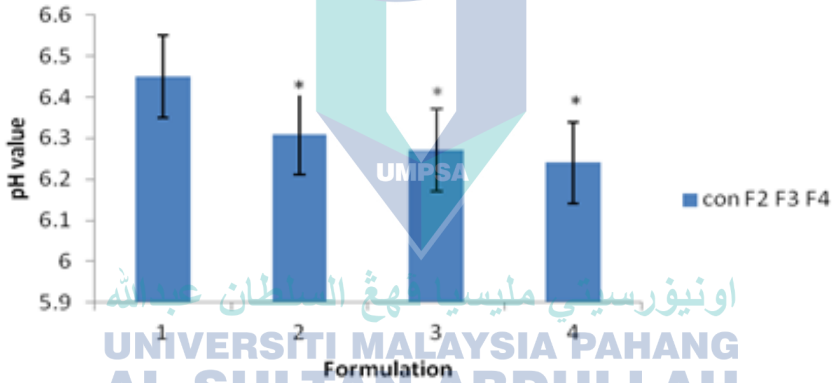

Figure 6. pH value for gel formulation with different concentration of carbopol 940.

The Carbopol 940 was added as thickening gel in order to reach the gel requirements. The values of the viscosity were increased as the concentrations of the gelling agents were increased. Further the value between 2817.96 and 4213.42 centipoises which lies in the acceptable range for topical gel formulation in the figure 4 [15].

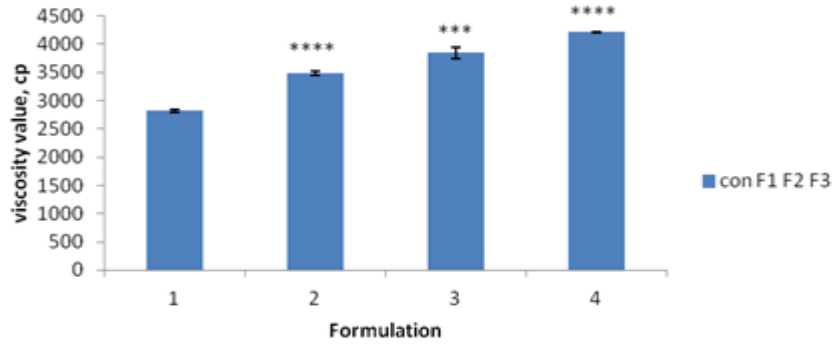

Figure 7. Viscosity value for gel formulation with different concentration of carbopol 940.

Spreadability indicated the gel formulations are easily spreadable on the skin [4]. Among the gel formulations F1 to F4, F2 with 1.0% concentration of carbopol indicating that it has excellent spreadability which is 4.87cm diameter of the gel to spread compared with other formulations shown in the figure 8.

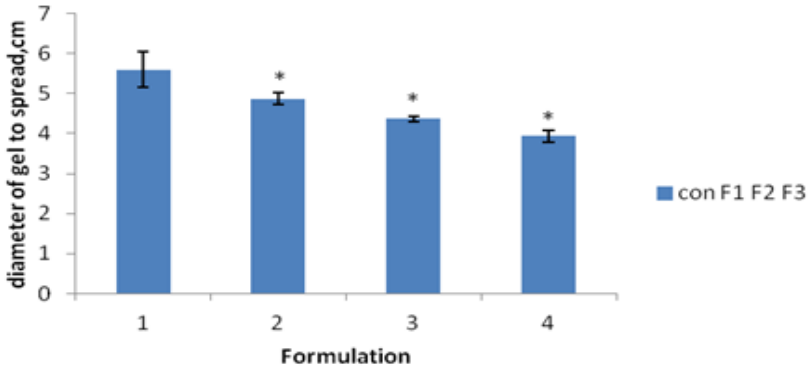

Figure 8. Spreadability value for gel formulation with different concentration of carbopol 940.

F2 was selected as the best herbosomal gel formulation and from now onwards, F2 will be known as F1. In stability study, two other formulations were made as control to observe their stability with different compositions. F2 was formulated without propylparaben as stabilizer and F3 was formulated without the addition of QI galls extracts. After all the formulations of herbosomal gel is completed, stability study was conducted by kept all the formulated gel at three different temperatures; 45 ± 2˚C, 25 ± 2˚C and 4 ± 2˚C for 21 days. In stability study, several testings were conducted such determination of pH value, viscosity, homogeneity and spreadability of the herbosomal gel formulation. The readings were taken for three consecutive weeks. Figure 6, 7 and 8 showed the findings from the stability study of herbosomal gel at 4°C, 25°C and 45°C respectively. Stability study at 4°C showed not much change in pH value, viscosity reading, homogeneity and spreadability throughout three weeks of experiments. The stability of herbosomal gel kept at 25°C was studied because room temperature is the most ideal temperature to store the herbosomal gel. The findings showed no significant changes as well.

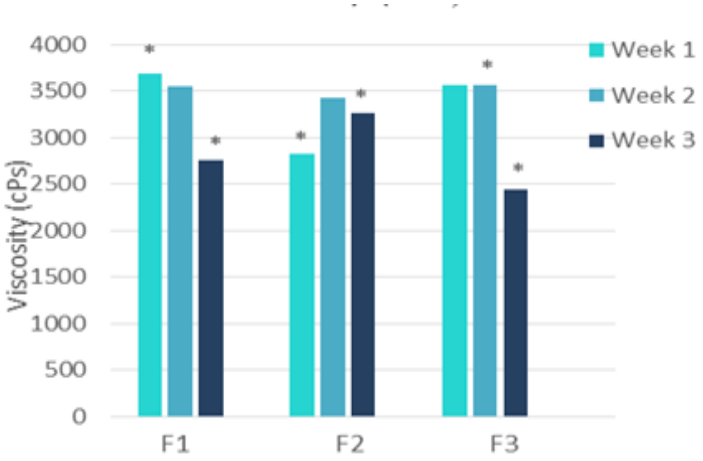

Figure 9. Viscosity of herbosomal gel at 4°C.

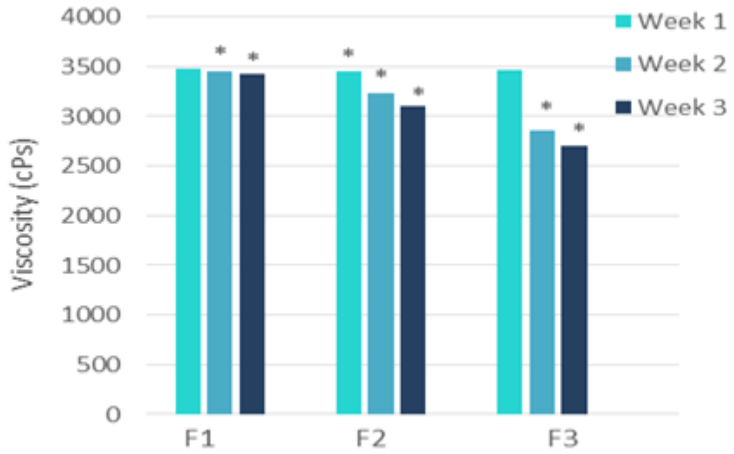

Figure 10. Viscosity of herbosomal gel at 25℃.

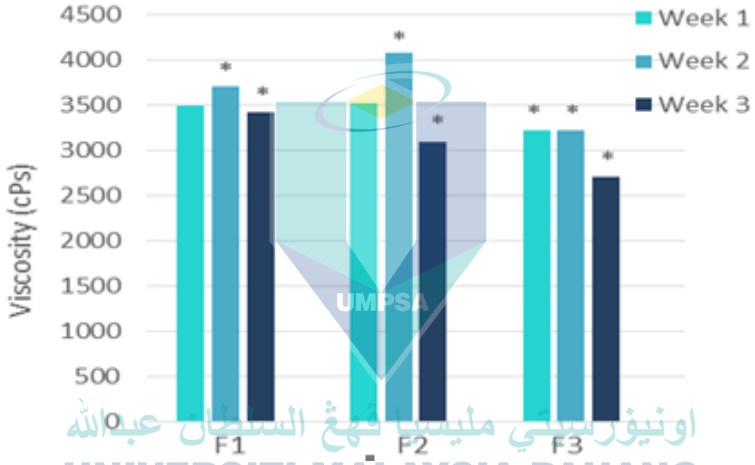

Figure 11. Viscosity of herbosomal gel at 45℃.

Viscosity of the QI galls herbosomal gel varies at different temperature. At 4℃, F1 is gradually decreasing in viscosity reading after three weeks of study. Viscosity of F2 is not consistent every week due to the absence of stabilizer to maintain its structure and stability which is propylparaben. At room temperature, 25℃, herbosomal gel F1, F2 and F3 shows no significant changes and consistent throughout the three weeks of stability study. F1 and F2 continue to show consistency when kept at 45℃ after three weeks. However, F2 shows inconsistency in week 2 and week 3. Generally known that viscosity is affected by the storage temperature variations, so these variations are expected. Acceleration of chemical reactions, alteration of the activity of the active ingredients or components, viscosity, appearance, colour and odour can happen due to higher temperature [16]. Modifications in the formulations structure are not visually noticeable, thus further physical-chemical evaluation is necessary.

During stability study, the herbosomal gels were subjected to centrifugation test to identify its long-term stability. The samples were centrifuged at 3000rpm for 30mins at room temperature. After the centrifugation test is done, all formulated herbosomal gels kept in every temperature show no phase separation. Physical parameters testing was done after the centrifugation test. Centrifugation test is a direct procedure to evaluate the stability of the herbosomal gel when placed in a severe condition [17]. As there is no phase separation after the centrifugation test is done, it shows that the formulation of the herbosomal gel is stable over harsh condition. Figure 12 shows the herbosomal gel before and after the centrifugation test.

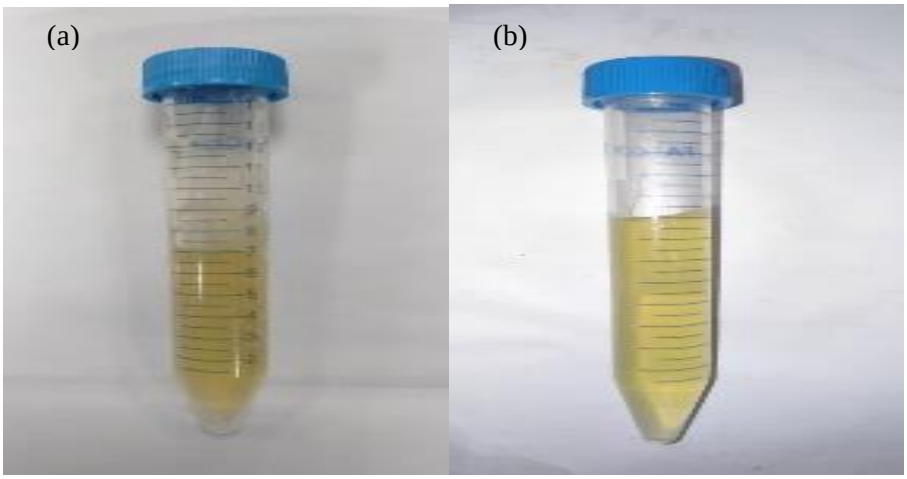

Figure 12. Herbosomal gel before and after centrifugation test, (a) before test and (b) after test.

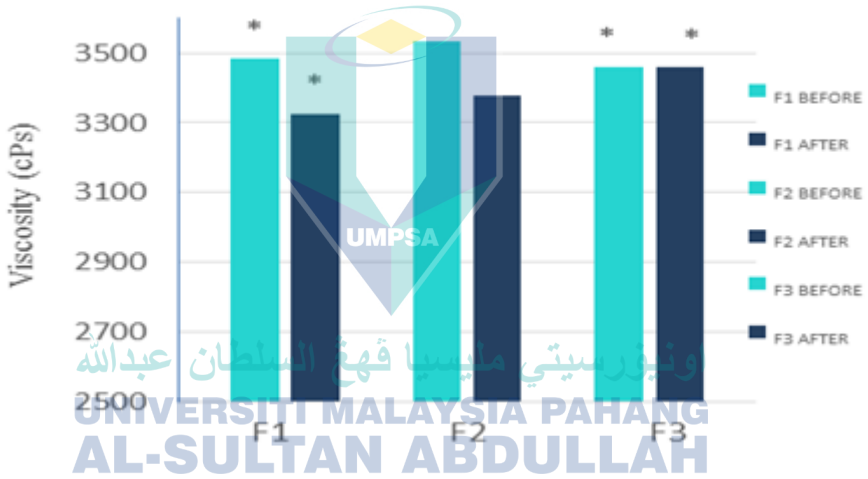

Figure 13. Viscosity for centrifugation test.

Viscosity reading of the herbosomal gel was recorded before and after the centrifugation test. This is to make there is no significant changes in the reading to maintain its stability [16]. However, viscosity reading for F2 which was a formulation without propylparaben has significant changes after the centrifugation test (Refer figure 13). Thus, this herbosomal gel from QI extracts need to have stabilizer to prolong its stability over time.

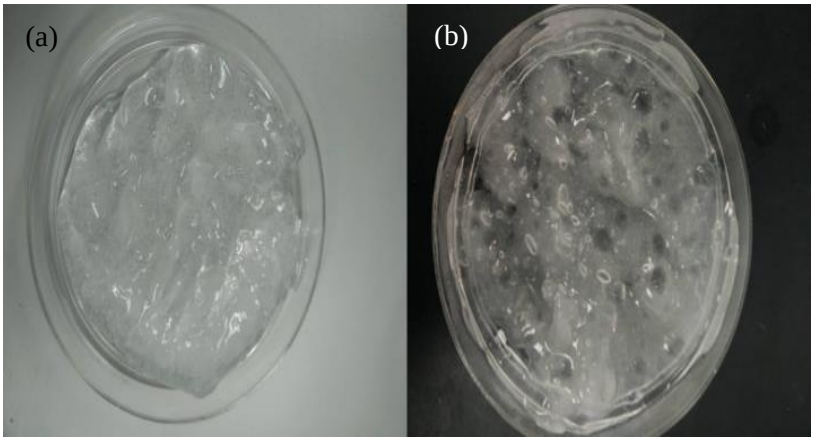

Figure 14. The formulation of antimicrobial gel (a) GWQI, (b) GQI.

The gel was formulated with different concentration of QI galls extract. The concentration used in range of 0.01 mg/ml to 5.00 mg/ml using half-fold concentration calculation which resulted in concentrations of 0.01 mg/ml, 0.02 mg/ml, 0.04 mg/ml, 0.08 mg/ml, 0.16 mg/ml, 0.63 mg/ml, 1.25 mg/ml, 2.5mg/ml and 5.0mg/ml. The main constituent of QI galls extract is tannins which present 1794.18 mg/ml and minor constituents of free gallic acid about 76.22 mg/ml. Both components are responsible for antimicrobial activity. High amount of tannin implied that tannin is the active compound for antibacterial activity in study. Tannin is a phenolic that is soluble in water, alcohol and acetone and provides the precipitates with proteins [18]. The formulation of gel without active ingredient of QI galls extract (Refer figure 14) was formulated to test on the efficiency of QI galls extract as active ingredients to inhibit growth of bacteria. The gel was formulated with excipients such as paraben, triethanol amine and carbopol. Figure 15 and 16 below showed the graph of area of inhibition of the formulated gel against P.aeruginosa and S. aureus.

.

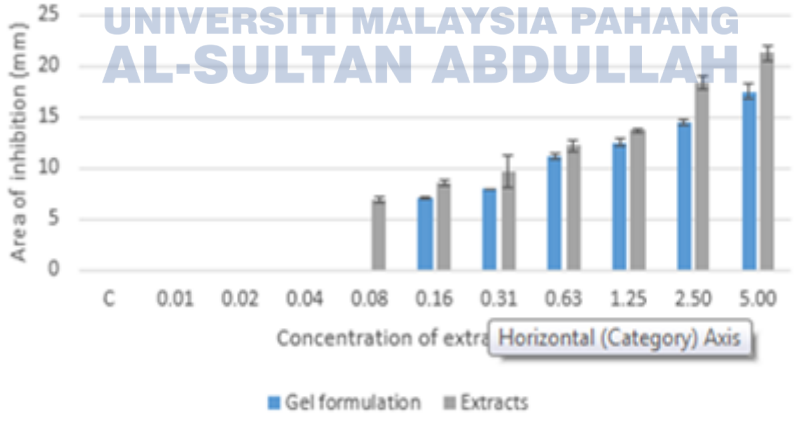

Figure 15. Graph of area of inhibition (P. aeruginosa) (mm) against concentration of extract (mg/ml) for GQI and GWQI.

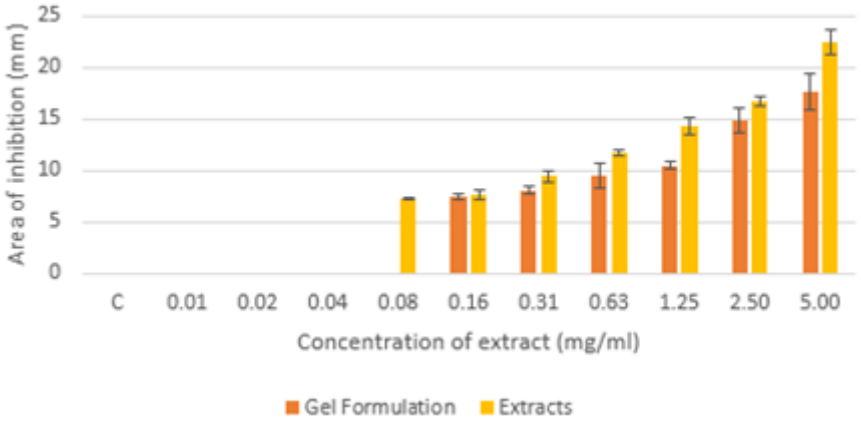

Figure 16. Graph of area of inhibition (S. aureus) (mm) against concentration of extract (mg/ml) for GQI and GWQI.

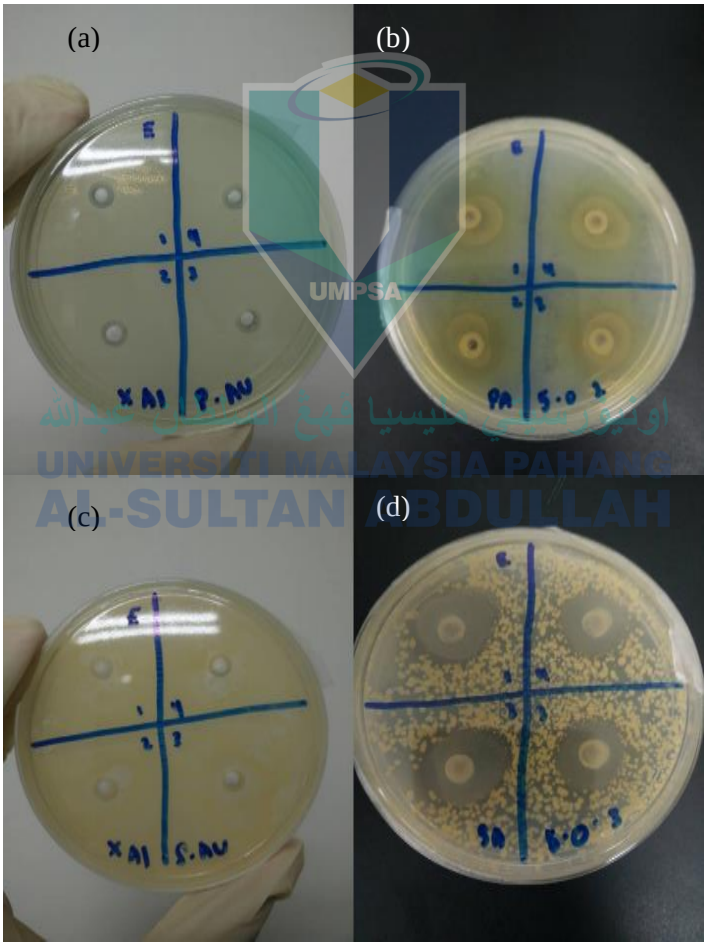

Figure 17. The inhibition zone for (a) Gel without QI extracts (P. aeruginosa), (b) Gel with QI extract (P. aeruginosa), (c) Gel without QI extract (S. aureus), (d) Gel with QI extract (S. aureus).

The agar well diffusion method was carried out by bacteria (S. aureus or P. aeruginosa) spread through the surface of nutrient agar and treated with extract or gel formulation from different concentration which placed in the well bored with tip. The area of inhibition was taken using vernier

caliper in millimeter. The area took included the area of tip borer which was 5mm. Result showed that both gel formulation of QI galls extract, and extract of QI galls extract elicited antimicrobial activities as shown by presence of area of inhibition zones in well agar diffusion method. The antimicrobial effects of formulation from QI galls extract and extract of QI galls extract was dose-dependent as observed that area of inhibition zones increases with increase of concentration of extract.

The result of inhibition zones in figure 17 showed bacterial strains for S. aureus had bigger area than P. aeruginosa at comparable concentration of 5 mg/ml for both parameters. P. aeruginosa antimicrobial activity for gel formulation of QI galls extract was measured 17.57 mm whereas extract of QI galls extract was 21.29 mm. On the other hand, S. aureus, bactericidal effects for gel formulation of QI galls extract was 17.69 mm whereas whereas extract of QI galls extract was 22.47 mm. It demonstrated that agar well diffusion test gives significant difference in supporting dose-dependency of QI galls extract extract on susceptibility of different strains of gram-bacteria. The plate that spread with gram-positive bacteria (S. aureus) has a greater antimicrobial activity compared gram-negative bacteria (P. aureginosa) in comparable concentration of extracts. Gram-negative bacteria have smaller area of inhibition compared to gram-positive bacteria due to present of lipopolysaccharides (LPS) layer on the surface of gram-negative bacteria which had high hydrophobicity and acts as strong barrier against hydrophobic molecules [19]. Consequently, lowering the ability of medication to absorb and pass through the barrier which decreasing the effect of antibacterial formulation gel on bacteria. The antibacterial formulation gel was able to penetrate call wall of gram-positive bacteria and more accessible than gram-negative bacteria due to presence of peptidoglycan and lack of outer membrane [19]. Furthermore, extract have higher affinity due to present of free gallic acid which increases the efficiency of QI galls extract.

The effectiveness of bactericidal between gel formulation of QI galls extract and extract of QI galls prone to depend on the structure and components present on the parameter. The concentration of extract commenced at different concentration range. Gel formulation of QI galls extract evoked at 0.16 mg/ml whereas extract of QI galls extracts at 0.08 mg/ml. The release rate of gel was slower than extract due to gel do not have a direct contact with extract. In virtue of gel formulation of QI galls extract made from gel, the extract effectiveness lowered due to extract necessarily pass through gel first before reaching the inner side of bacteria cell membrane. As for formulation of gel (Refer figure 14) without QI galls extract, the gel formulation was tested on both P. aeruginosa and S. aureus. Both plates exhibit zero area of inhibition. The plates were then contemplated with the plates which treated with formulated gel of QI galls extract. The differences in gowth of bacteria between formulation gel of QI galls extract and formulation gel without QI galls extract proved that the bacterial activity was restrain with present of QI galls extract as active ingredient [20]. Thus, effect of excipients such as paraben, triethanol amine and carbopol was negligible as there was no area of inhibition observed.

4. Conclusion

From the study, it was revealed that the QI galls extract contains large amount of tannic acid which is 1794.18 mg/g and small amount of gallic acid which is 76.22 mg/g. For the physicochemical evaluation, the formulation of herbosomal gel consists of 1.0% of Carbopol 940 were found to be superior to the gel formulations since the physical appearances shows good properties. The reading pH value at 6.31 while the viscosity is at 3482.3144cps. Formulated gel showed good stability after 21 days of formulation, by not showing statistical differences in pH value, viscosity and spreadability before and after test. The antimicrobial testing evaluated by well diffusion method using P. aeruginosa is 17.75mm and S. aureus is 17.69mm. Hence, from all the results it was showed that QI galls extract was well incorporated into carbopol formulation to form herbosomal gel. This developed herbosomal gel using QI galls extract have good pH value, viscosity, spread ability, and stability against vary temperature and storage condition. Besides, the antibacterial activity of the both gel formulation and crude extract also exhibited a good and promising results. Hence, it can be concluded that the QI galls extract has a potential to be developed as a commercial antibacterial gel for medical use with further preclinical and long-term stability study can be conducted.

Acknowledgement
This study was supported by internal grant of Universiti Malaysia Pahang (UMP) (RDU 150379 and RDU1803181), Fundamental Research Grant Scheme (FRGS Ref: FRGS/1/2017/TK05/UMP//1 and RDU 170130). We also would like to thank Faculty of Engineering Technology (FTeK) and Centre of Excellence for Advanced Research in Fluid Flow (CARIFF) for providing the equipment and facilities used in the project.

References

[1] Ganesan V, Kaithavalappil S S, Kannappan M and Vasudevan D T 2014 *Asian J. Res. Pharm Sci. Biotechnol*. 47–54
[2] Dewan N, Chowdhary G, Pandit S, Ahmed P and Dasgupta D 2016 *J. Pharmacog.n Phytochem*. 8-104
[3] Fateh A R F M, Elamin I E, Shayoub M E and Salah E O H 2017 *Int. J. Adv. Pharmacy, Biol Chem*. 346-50
[4] Vaidya V R, Mahendrakumar C B and Bhise K S 2016 *Int. J. Res. Ayurveda Pharm.* 32-128.
[5] Tiwari S S, Gupta S K, Dwivedi S and Dubey R 2018 *J Drug Deliv Ther*. 495–503
[6] Liu M P, Liao M, Dai C, Chen J F, Yang CJ and Liu M 2016 *Sci Rep*. 1–14
[7] Syukriah N, Rahman A, Salleh L, Yaakob H, Adibah F and Majid A 2012 *Int Food Res J*. 26–8
[8] Dantas M G B, Reis S A G B, Damasceno C M D, Rolim L A, Rolim-Neto P J, Carvalho F O, 2016 *Sci. World J*. 1203-12
[9] Wan Nor Amilah W A W, Masrah M, Hasmah A and Noor Izani N J 2014 *Trop. Biomed.* 220 49
[10] Hasmida M N, Liza M S, Nur Syukriah A R, Harisun Y, Mohd Azizi C Y and Fadzilah Adibah A M 2015 *Pertanika J Sci Technol.* 287-95
[11] Nur Syukriah A R, Liza M S, Harisun Y and Fadzillah A A M 2014 *Int Food Res J.* 7-1031
[12] Husna M, Nabilah I and Wan Nor Amilah W A W 2018 *Malaysian J Med Sci.* 42-50
[13] Aiyalu R, Govindarjan A and Ramasamy A 2016 *Brazilian J Pharm Sci*. 493–507
[14] Mariam Joshua J, Anilkumar A, Cu V T, Vasudevan D and Surendran S 2018 *Asian J Pharm Clin Res*. **3** 409
[15] Kim J Y, Song J Y, Lee E J and Park S K 2003 *Colloid Polym Sci*. 122-124
[16] Deuschle V C K N, Norbert Deuschle R A, Bortoluzzi M R and Athayde M L 2015 *Brazilian J Pharm Sci*. **7** 201
[17] Sharma A, Dwivedi S, Mishra G P and Joshi H 2012 *J PharmTech Res*. **2** 4
[18] Gao J, Yang X, Yin W and Li M 2018 *Evidence-Based Complement Altern Med*. 1–9
[19] Bongoni R N 2018 *J. Pharm. Res.* 167–70
[20] Khazaeli P, Goldoozian R and Sharififar F 2009 *Int J Cosmet Sci*. 81-375

TROPICAL LIFE SCIENCES RESEARCH

Phytochemicals and Cytotoxicity of *Quercus infectoria* Ethyl Acetate Extracts on Human Cancer Cells

Authors:

Wan Nur Suzilla Wan Yusof and Hasmah Abdullah*

***Correspondence:** hasmahab@usm.my

DOI: https://doi.org/10.21315/tlsr2020.31.1.5

Highlights

- Qualitative phytochemical analysis revealed the presence of tannin, alkaloids, glycosides, saponins, terpenoids, flavonoids and phenolic compounds.
- QIEA extract exhibited the most potent cytotoxic activity against HeLa cells with (IC_{50} value = 6.33 ± 0.33 µg/mL) and showed cytoselective property against L929 cells
- The cytotoxicity of QIEA extract has exerted DNA fragmentation in treated HeLa cells as hallmark of apoptosis.

Tropical Life Sciences Research, 31(1), 69–84, 2020

Phytochemicals and Cytotoxicity of *Quercus infectoria* Ethyl Acetate Extracts on Human Cancer Cells

Wan Nur Suzilla Wan Yusof and Hasmah Abdullah*

School of Health Sciences, USM Health Campus, Universiti Sains Malaysia, 16150 Kubang Kerian, Kelantan, Malaysia

Publication date: 7 April 2020
To cite this article: Wan Nur Suzilla Wan Yusof and Hasmah Abdullah. (2020). Phytochemicals and cytotoxicity of *Quercus infectoria* ethyl acetate extracts on human cancer cells. *Tropical Life Sciences Research* 31(1): 69–84. https://doi.org/10.21315/tlsr2020.31.1.5
To link to this article: https://doi.org/10.21315/tlsr2020.31.1.5

Abstract: Conventional and modern cancer treatment were reported to manifest adverse effects to the patients. More researches were conducted to search for selective cytotoxic agent of plant natural product on cancer cells. The presences of wide range phytochemicals in *Quercus infectoria* (QI) extract have been implicated with the cytotoxic effect against various types of cancer cell which remain undiscovered. This present study aimed to evaluate cytotoxic effect of QI extracts on selected human cancer cells and then, the most potent extract was further analysed for general phytochemical constituents. QI galls were extracted successively with n-hexane, ethyl acetate and methanol yielded three main extracts; n-hexane (QIH), ethyl acetate (QIEA) and methanol (QIM), respectively. The most potent extract was qualitatively analysed for the present of tannin, alkaloids, glycosides, saponins, terpenoids, flavonoids and phenolic compounds. Next, the extracts were tested to determine the cytotoxic activity against cervical cancer cells (HeLa), breast cancer cells (MDA-MB-231) and liver cancer cells (Hep G2) using MTT assay. Cytotoxic activity of QI extracts against normal fibroblast (L929) cell line was also evaluated to determine the cytoselective property. Meanwhile, DMSO-treated cells served as negative control while cisplatin-treated cells served as positive control. The most potent extract then chosen to be further investigated for DNA fragmentation as hallmark of apoptosis using Hoechst staining. Qualitative phytochemical analysis revealed the presence of tannin, alkaloids, glycosides, saponins, terpenoids, flavonoids and phenolic compounds. QIEA extract exhibited the most potent cytotoxic activity against HeLa cells with (IC_{50} value = 6.33 ± 0.33 µg/mL) and showed cytoselective property against L929 cells. DNA fragmentation revealed QIEA induced apoptosis in the treated cells. The richness of phytochemical constituents in QIEA extract might contribute to the potency of cytotoxic activity towards HeLa cells.

Keywords: *Quercus infectoria* extracts, Phytochemical constituents, Cytotoxic activity, Cytoselective, DNA fragmentation

*Corresponding author: hasmahab@usm.my

Abstrak: Rawatan kanser secara moden dan tradisional dilaporkan telah memberi kesan sampingan kepada pesakit. Banyak kajian telah dijalankan untuk mencari agen sitotoksik yang hanya mensasarkan sel kanser menggunakan produk semulajadi daripada sumber tumbuh-tumbuhan. Kewujudan bahan fitokimia yang pelbagai dalam ekstrak *Quercus infectoria* (QI) memberi kesan toksik terhadap beberapa jenis sel kanser yang belum terungkai. Kajian ini bertujuan untuk menilai aktiviti sitotoksik beberapa jenis ekstrak dan memilih ekstrak yang paling poten untuk dianalisa bahan fitokimia secara umum. Ketuat QI diekstrak secara berperingkat menggunakan n-heksana, etil asetat dan methanol menghasilkan ekstrak: n-heksana (QIH), etil asetat (QIEA) dan methanol (QIM) masing-masing. Ekstrak yang paling poten dianalisis secara kualitatif untuk menentukan kehadiran tanin, alkaloids, glikosida, saponin, terpenoid, flavonoid dan sebatian fenolik. Seterusnya setiap ekstrak diuji aktiviti sitotoksik terhadap sel kanser servik, (HeLa), sel kanser mamari (MDA-MB-231) dan sel kanser hati (Hep G2) menggunakan cerakinan MTT. Aktiviti sitotoksik ekstrak QI juga diuji ke atas sel fibroblast normal (L929) untuk menentukan ciri selektifnya. Sel yang dirawat dengan DMSO bertindak sebagai kawalan negatif, manakala sel yang dirawat dengan sisplatin bertindak sebagai kawalan positif. Ekstrak yang paling poten seterusnya dipilih untuk menyelidik fragmentasi DNA sebagai tanda berlaku apoptosis menggunakan pewarnaan Hoechst. Analisis kualitatif menunjukkan kehadiran tanin, alkaloids, glikosida, saponon, terpenoids, flavonoid dan sebatian fenolik. Ekstrak QIEA adalah paling poten terhadap sel HeLa (IC_{50} = 6.33 ± 0.33 µg/mL) dan menunjukkan ciri sitoselektif terhadap sel L929. Fragmentasi DNA membuktikan QIEA mengaruh apoptosis dalam sel yang dirawat. QIEA yang kaya dengan bahan fitokimia kemungkinan menyumbang kepada kepotenan aktiviti sitotoksik terhadap sel HeLa.

Kata kunci: Ekstrak *Quercus infectoria*, Kandungan fitokimia, Aktiviti sitotoksik, Ciri sitoselektif, Fragmentasi DNA

INTRODUCTION

Cancer is considered as the second cause of death around the world. Cancer is characterised by the abnormality of cell growth resulted in the uncontrolled multiplication of the normal cells to form tumors which in further invades into nearby parts of the body (Gandhiappan & Rengasamy 2012). Among all cancer types, cervical, breast and liver are among the 10 most recorded cancer cases worldwide (Bray *et al.* 2018).

Chemotherapy is the leading approaches in cancer therapies (American Cancer Society 2015) that involves the usage of chosen medications to control the metastasis of cancer cells (Caley & Jones 2012; Massague & Obernauf 2016). However, the drugs used for chemotherapy were reported to manifest adverse effect towards non-cancerous calls (Nurgali *et al.* 2018). Hence, there is an urge for the development of new anticancer medications targeted exclusively on cancer cells. In this regards, natural products from plants are expected to produce candidates for the development of new targeted anticancer drugs. It has been estimated that about 60% of modern drugs were derived from natural origin (Hanahan & Weinberg 2000; Gandhiappan & Rengasamy 2012).

Quercus infectoria Olivier (Fagaceae) or also known as galls of *Quercus infectoria* (QI) is a small tree found in Greece, Asia Minor and Iran (Kottakkal 1995). The main constituents found in the galls of QI are tannin (50%–70%) and small amounts of free gallic acid and ellagic acid (Kottakkal 1995). QI galls locally known as "manjakani" was claimed to be highly beneficial for the Malay Kelantanese postpartum women (Bhattacharjee 2001). There were no reports regarding hazardous effects from the past uses of this herbal preparation. QI galls aqueous extract showed high potential in skin whitening and antioxidant properties as the extract inhibited the superoxide and DPPH radical scavenging activities, and tyrosinase activities (Borgia *et al*. 1981).

Studies indicated that QI galls have a variety of pharmacological properties including being an astringent (Dar *et al*. 1976), antidiabetic (Kaur *et al.* 2007), antitremorine local anesthetic, antiviral (Harborne 1986), potential antibacterial (Hwang *et al*. 2000), antifungal (Baharuddin *et al.* 2015; Magbool *et al.* 2018), larvicidal (Ikram & Nowshad 1977) and anti-inflammation (Mc Clure 1975; Muhamad & Mustafa 1994). Various types of QI extracts were reported to poses anticancer activity on cervical cancer cells (Hasmah *et al*. 2010) and colon cancer cells (Roshni & Ramesh 2013). The main constituents found in QI extracts are tannin and become a major source of gallic and tannic acid (Ong & Nordiana 1999). The presences of various compounds such as flavonoids, polyphenolics, tannins and steroid have been implicated in a number of medicinal properties of the plants (Yoo *et al.* 2018). Thus, this present study was intended to determine the cytotoxic effects of QI extracts and then to analyse the general phytochemical constituents of the most potent extract towards the most sensitive cancer cell lines.

MATERIAL AND METHODS

Plant Materials

Galls of *Quercus infectoria* (QI) was obtained from Chinese herbal outlet in Kota Bharu, Kelantan, Malaysia. To ensure the correct species of the galls used, organoleptic properties investigation based on morphological appearance included external colour, odour, size, surface and texture was conducted as described by Asif *et al.* (2012). Prior to examination of morphological appearance, the same batch of the galls were previously analysed macroscopically and microscopically involving outer and inner part of the plant materials (Hasmah *et al.* 2010). The confirmed of plant materials were proceeded for plant extraction.

Plant Extraction

The QI galls were processed to become powder form and then was successively extracted with organic solvent (n-hexane, ethyl acetate and methanol) by soaking method. Amount of 50 g QI galls powder was homogenised in 1 L beaker containing

200 mL n-hexane and placed in water bath for 24 h with constant temperature at 50°C. After that, the extracts solution was filtered and concentrated by rotary evaporator. The crude extracts then were lyophilised in freeze-drier and stored at −20°C prior used (Fatima *et al*. 2001). The procedures were repeated for the other solvents using the same materials successively and yielded n-hexane extract (HE), ethyl acetate extract (EA) and methanol extract (ME). All extracts were tested against cell cytotoxicity assay.

Phytochemical Screenings of QI Extract

The major groups of phytochemical contents in the extracts were screened qualitatively to determine the presence of alkaloids, tannins, glycoside, flavonoids, terpenoids, saponins and phenolic compounds. The experiments were conducted based on relevant previous study with some modifications.

Alkaloids

Few drops of Mayer's reagent were added to the extract; cream colour precipitate indicates the presence of alkaloids (Rohana *et al.* 2004).

Tannins

1 mL of 5% $FeCl_3$ was added to the extract, presence of tannin was indicated by the formation of bluish black or greenish black precipitate (Rohana *et al.* 2004).

Glycosides

2 mL of glacial acetic acid, few drops of 5% $FeCl_3$ and concentrated H_2SO_4 were added to the extract. Reddish brown color at the junction of two liquid layers and upper layer appears bluish green indicates the presence of glycosides (Siddiqui & Ali 1997).

Flavonoids

Few drops of 10% concentrated sulphuric acid was added to the extract, followed by 1 mL ammonia, formation of greenish yellow precipitate indicates the presence of flavonoids (Rohana *et al.* 2004).

Terpenoids

5 mL chloroform and 2 mL concentrated sulphuric acid was added into 2 mL extract. Reddish brown colorations of interface indicate the presence of terpenes (Soon & Hasni 2005).

Saponins

20 mL water was added to 150 mg extract and shaken vigorously; layer of foam formation indicates the presence of saponins (Rohana *et al.* 2004).

Cell Culture

Different types of cancerous and non-cancerous cells were used in this study, namely, cervical cancer (HeLa), breast cancer (MCF-7 and MDA-MB-231), liver cancer (Hep G2), and normal fibroblast (L929). These cell lines were purchased from American Type Culture Collection (ATCC, Manassas, Virginia, USA). The development medium utilised was Dulbecco's Modified Eagle Medium (DMEM) (Invitrogen, USA) supplemented with 10% Fetal Bovine Serum (FBS) (Gibco, Life Technologies, USA) and 1% penicillin-streptomycin (Invitrogen, USA).

Cryovial containing frozen cells was thawed by gentle agitation in 37°C water bath. Then, the cryovial contents were transfer to a centrifuge tube containing 10 mL growth medium and spinned at 125 xg for 5 min. The supernatant was discarded and cells pellet was gently re-suspended in complete growth medium and dispensed into a 25 cm^3 sterile culture flask (Nunc, Denmark). The cell culture was maintained in 37°C humid incubator with 5% (v/v) CO_2. All procedures were performed under controlled aseptic conditions.

MTT Cytotoxicity Assay

The cytotoxicity assay was performed using MTT assay as previously described with some modifications. Briefly, cells were seeded for 24 h prior to treatment in 96-well plate at 5 × 10^4 cells/well in order to obtain 80% confluent cultures. The extract was dissolved in DMSO (Sigma Chemical Co., St. Louis, Missouri, USA) and added to the culture medium. Cells were treated with QI extract and cisplatin in concentration ranging from 0–99 µg/mL. Control cultures received the same concentration of DMSO. Plated and treated cells were incubated for 72 h at 37°C in a humidified atmosphere with 5% CO_2. At the end of incubation periods, 50 µL of MTT solution (2 mg/mL MTT in plain culture medium; Sigma Chemical Co.) was added to each well. The plate was then incubated for 4 h. After the periods, MTT solution was removed and the purple formazan crystal formed at the bottom of the wells was dissolved with 200 µL DMSO for 20 min. The absorbance was read at 570 nm on a micro plate reader.

Mechanism of Cell Death

Cell cytotoxicity was featured by cell death mechanism. The most potent extract found from the cytotoxicity assay was further studied for mechanisms of cell death. To confirm the cell death by apoptosis, the nuclear morphological changes of the treated cells was observed using Hoechst 33258 stain. Cells with 80% confluence

were washed with PBS and cells trypsinised with 0.25% (v/v) trypsin-EDTA. Next, 5×10^4 cells/ml of cells were cultured in new 25 cm^3 culture flask and incubated in 37°C with 5% CO_2 incubator. The confluence cells were treated with the most potent extract and cisplatin for 24, 48 and 72 h respectively. Untreated cells were utilised as negative control and cells treated with cisplatin served as positive control.

After the treatment hours, cells were trypsinised and centrifuged at 300 xg for 5 min. The supernatant was discarded and cells pellet was dissolved in 10 µL PBS. Next, cells suspensions were smeared on poly-L-lysin slides and air-dried. Then, 10% (w/v) paraformaldehyde was added to fix the cells to the slides. The cells were permeabilised with 0.2% (v/v) Triton-X for 1 min at room temperature. Lastly, cells were stained with 30 µg/mL DNA color Hoechst 33258 stain for 30 min at room temperature and viewed under fluorescence microscope (Zeiss) at magnification 40x.

Statistical Analysis

Data were expresses as mean ± SEM of three independent experiments. Data analysis were performed using Statistical Package of Social Science (SPSS) Software version 20. The Shapiro-Wilk test was used for normality. The statistical significances of differences were determined using one-way analysis of variance (ANOVA) followed by Bonfferoni test and probability values of $p < 0.05$ was considered to be statistically significant.

RESULTS AND DISCUSSION

Organoleptic Properties of *Quercus infectoria* (QI) Galls

The parameters of organoleptic properties of QI galls investigated were external colour, size, surface, texture and odour. All of these parameters are important as the morphological identification (Fig. 1). Morphology of the QI galls used in this study exhibited similar properties (Table 1) as described by Asif *et al*. (2012).

Figure 1: Organoleptic properties of QI galls.

Table 1: Organoleptic properties of QI galls.

No	Organoleptic characteristics	Result
1	External colour	Dark yellowish brownish
2	Odour	Astringent
3	Size	Small (diameter 1–1.5 cm)
4	Surface	Rough and horny
5	Texture	Hard and woody

Phytochemical Screening

The medicinal values of plant lies on bioactive phytochemical constituents of the plant which shows various physiological effects for human body. Hence, phytochemical screening is a tools to elucidate important compound which could be based of modern drugs for curing various diseases (Azad *et al*. 2013) even though latest trends utilise high-throughput screens based on molecular targets which had led to a demand for the generation of large libraries of compounds (Newman & Cragg 2016).

Qualitative phytochemical screening is an essential step towards discovery of new drugs as it provides the information regarding the presence of a particular primary or secondary metabolites in the plant extract of clinical significance (Trease & Evan 1989). Based on the qualitative analysis, the phytochemical evaluation of QIEA extract revealed the presence of tannins, alkaloids, saponins, terpenes, flavonoids, glycosides and phenolic compounds (Table 2).

Table 2: Phytochemical constituents in QIEA.

Phytochemical constituents	Observations	Results
Alkaloids	The formation of the cream color precipitate	Detected
Tannins	The formation of the bluish-black precipitate	Detected
Saponins	Layer of foam formed	Detected
Terpenoids	Reddish-brown color formed	Detected
Flavanoids	The formation of greenish-yellow precipitate	Detected
Glycosides	Reddish brown color between the liquid layer and upper layer turn color to bluish-green	Detected
Phenolic compounds	The formation of the blue-green precipitate	Detected

Our finding was in accordance with previous study which revealed the presence of diverse groups of compounds including saponins, alkaloids, tannins, glycosides, triterpenes, sterols, phenolic mixes, starches and flavonoids in various extracts of QI galls (Shrestha *et al.* 2014). Furthermore, previous study also documented variation of gallic acid and tannic acid distribution in various QI galls extracts. Abdullah *et al.* (2017) reported that polyphenolic compounds constituted by gallic acid derivatives and hydrolysable tannins served as major phytoconstituents present in the QI extract analysed by MS/MS.

The cytotoxic activity possessed by QIEA extract may also be mediated by the unique combination of phytochemicals in the extract (Saxena *et al.* 2013). The cytotoxic activity of phytochemicals in QIEA extract have been documented in some articles (Kanadaswami *et al*. 2005; Okuda & Ito 2011; Lu *et al*. 2012). For example, gallotannic acid (tannin) which present as real constituent of QI galls has been uncovered to show antimutagenic, anticancer and cancer prevention agent properties (Srivastava *et al*. 2000; Gao *et al*. 2018).

Cytotoxicity Activity of QI Galls Extract

The effects of QI galls n-hexane, ethyl acetate and methanol extracts on cells proliferation were determined from IC_{50} value. IC_{50} value is the concentration of the extract or anticancer agent required to inhibit 50% of cells population (Lim *et al*. 2009). Extract that showed best inhibition on the tested cancer cell lines, represented by the lowest IC_{50} value (less than 20 µg/mL) following 72 h treatment was selected as the most potential extract (Zakaria *et al*. 2009).

According to the results, the IC_{50} values calculated in response to QIH treatment for HeLa, MCF-7, MDA-MB-231 and Hep G2 cell lines were in descending cytotoxic activity 47.5 ± 0.58 µg/mL, 49.8 ± 1.46 µg/mL, 95.7 ± 2.51 µg/mL and 97.4 ± 0.88 µg/mL, respectively. In addition, the IC_{50} values in descending cytotoxic activity after treated with QIEA extract was 6.33 ± 0.33 µg/mL for HeLa, while for MCF-7 and Hep G2 were 20.5 ± 1.23 µg/mL and 23.6 ± 2.14 µg/mL, respectively. For MDA-MB-231, QIEA extract showed very low cytotoxicity as the IC_{50} value was ≥ 99 µg/ml. Besides that, the IC_{50} values obtained after treated with QIM

extract was 23.8 ± 0.91 µg/mL for HeLa, while for MDA-MB-231 and Hep G2 were 90.2 ± 0.89 µg/mL and 85.1 ± 0.34 µg/mL respectively. It was found that, QIM extract showed very low toxicity againts MCF-7 cell line as the IC_{50} value obtained was ≥ 99 µg/mL. Within all tested cancer cells, it was demonstrated that QIEA extract exhibited best cytotoxic activity againts Hela cell line as the IC_{50} value obtained was the lowest and ≤ 20 µg/mL.

After incubation of cell lines with QIEA extract for 72 h, the extracts obviously showed cytotoxic effects towards HeLa and MDA-MB in concentration dependent manner. The EA extract exerted higher cytotoxicity effect towards HeLa cells with IC_{50} of 6.33 ± 0.33 µg/mL. However, the QIEA extract was less active against MDA-MB cell line as the IC_{50} value was 90.0 ± 16.9 µg/mL. The extract showed no cytotoxic effect towards normal cells at IC_{50} concentration that inhibit the growth of HeLa cells. Moreover, QIEA exhibited cytotoxic activity towards MCF-7 and Hep G2. Previously QIEA extract exerted cytotoxic activity towards ovarian cancer cells, Caov-3 (Hasmah *et al*. 2010). QIEA exhibited no cytotoxic effect againts normal fibroblast (L929) cell line. The ability to kill cancer cells without affecting normal cells reflects the cytoselective property of QI galls extracts. A survey on traditional usage of QI reported no side effect after the consumption of it herbal preparations (Soon *et al*. 2007). The other study on non-cancerous ovarian (CHO) and normal kidney (Vero) cells also demonstrated no cytotoxic effect of QI galls (Ismail *et al*. 2010). Recently, Hazwani *et al*. (2018) reported moderate cytotoxicity activity exerted by *Q. infectoria* aqueos extract and *Q. infectoria* vaginal cream against HeLa cell with IC_{50} values of 13.90 ± 2.27, and 20.80 ± 1.94, respectively. Both preparation exerted high DPPH radical scavaging activity.

In this study, the cytotoxic effects of QIH, QIEA and QIM extracts againts normal cell line were also investigated. All extracts showed low cytotoxicity activity (IC_{50} ≥ 20 µg/mL) on normal fibroblast (L929) cell line (Table 3).

The most widely used and commercial anticancer drug, cisplatin was used as positive control (Florea & Büsselberg 2011, Hazwani *et al.* 2018). Cisplatin-treated HeLa cell showed lowest IC_{50} value (10 ± 0.67 µg/mL), followed by MDA-MB-231 (11.8 ± 0.67 µg/mL), Hep G2 (14.6 ± 0.34 µg/mL) and MCF-7 (16.9 ± 3.53 µg/mL). However, no significance difference ($P > 0.05$) was observed within the tested cancer cell lines. The cytotoxic activity screening towards normal fibroblast (L929) cell lines demonstrated high cytotoxic activity of cisplatin with IC_{50} value obtained was 18.7 ± 5.73 µg/mL. This showed that cisplatin was well-known not cytoselective agent as it inhibits the proliferation of both cancerous and non-cancerous cells. Cisplatin was used as positive control and the IC_{50} values against HeLa cell lines was 10 ± 0.67 µg/mL. The cytotoxic activities of the extracts and cisplatin were varying in three cancer cell lines tested. In the US NCI plant screening program, a crude extract is generally considered to have in vitro cytotoxic activity if the IC_{50} value (concentration that cause a 50% cell killed) in carcinoma cells, following incubation between 48 and 72 h, is less than 20 µg/mL, while it is less than 4 µg/mL for pure compounds (Umachigi *et al.* 2008).

Table 3: The IC_{50} values for QI galls extracts and cisplatin against non-cancerous cell lines, $P < 0.05$ was taken as significantly different from positive control (cisplatin).

Extracts/compound	L929
QIH	> 99
QIEA	>99
QIM	98.3 ± 2.67
Cisplatin	18.7 ± 5.73

Cisplatin is a broad range of anticancer drugs used for chemotheraphy. The current study revealed the inhibitory properties towards tested of the tested cancer cell lines with potent IC_{50} less than 20 ug/mL (Umachigi *et al*. 2008). However, cisplatin also inhibited the growth of normal cells as well. The non-selective cytotoxic activity of cisplatin is in line with nephrotoxicity effects post chemotherapy as reported previously (Desoize & Madoulet 2002; Florea & Büsselberg 2006; Shah & Dizon 2009; Günes *et al*. 2009; Tsang *et al*. 2009).

Interestingly, QIEA showed the best IC_{50} value as it also demonstrated no cytotoxicity towards normal cells (Table 3). Hence, QIEA extract was selected for further investigations in this study.

Mechanism of Cell Death

Cells undergoing apoptosis usually demonstrated morphological and biochemical components, including chromatin aggregation, nuclear and cytoplasmic condensation, and partition of cytoplasmic and nucleus into membrane-bound vesicles (Kerr *et al.* 1972). Chromatin condensation and nuclear fragmentation served as hallmarks for nuclear morphology of the apoptotic cells, which can be observed under fluorescence microscope through several techniques such as, DNA-binding stains, like 4',6-diaminido-2-phenylindole, Hoechst and others (Ziegler & Groscurth 2004).

Those findings also biochemical alterations served as key players of the apoptotic mechanisms that are responsible of evasion from apoptosis and therefore of tumor development and resistance to therapies. Thus intensive investigation on the molecular mechanisms of apoptosis in cancer cells has led to the identification of the several molecules involved in both the intrinsic and the extrinsic apoptotic pathways (Pistritto *et al*. 2016). The current study employed nuclear fragmentation as early hallmark of apoptosis, as therapeutic target prior to elucidation of apoptotic protein in HeLa cells treated QIEA in future research.

The untreated HeLa cells, stained nuclei were rounded and homogenously stained with Hoechst 33258 stain in the period of 24, 48 and 72 h (Fig. 2). Since the cells were viable and did not demonstrated nuclear morphological changes, no fluorescence were emitted in the untreated HeLa cells.

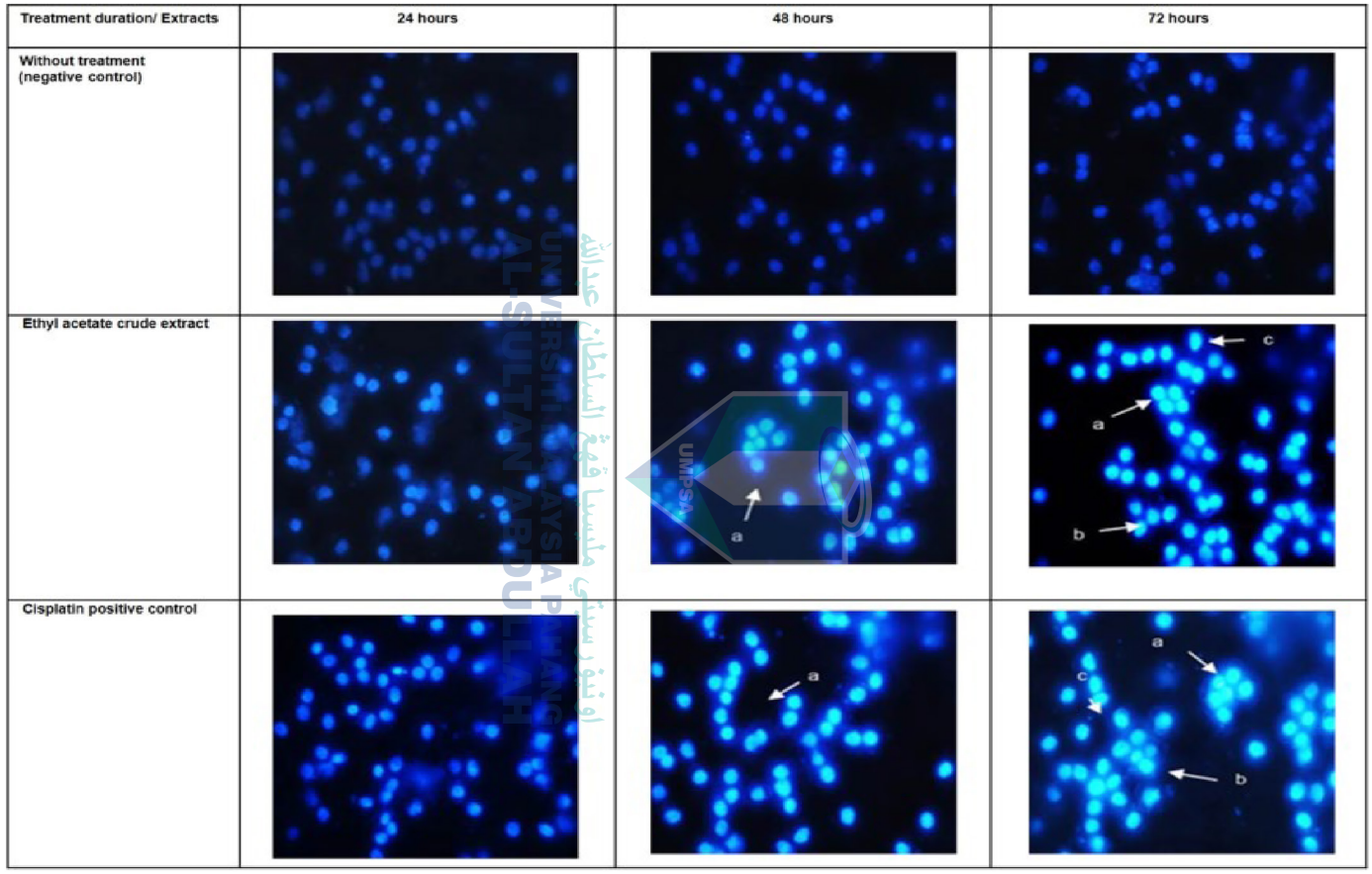

Figure 2: Nuclear morphological changes of HeLa cells stained with Hoechst 33258 stain; (a) nuclear fragmentation, (b) shrinkage of cell nucleus, (c) apoptotic bodies. Magnification: 40X, n = 3.

After 24 h treated with QIEA extract, the morphology of apoptosis began to appear in HeLa cells. It was observed that fluorescence were emitted from the nuclear region of DNA which are the common features of apoptosis (Fig. 2). As the treatment period prolonged to 48 h, chromatin condensation and DNA fragmentation were much more visible (Fig. 2). After 72 h, small fluorescence masses were detected which indicated the presence of apoptotic bodies (Fig. 2).

In addition, the results also showed similar pattern for morphological changes in HeLa cells treated with cisplatin which served as positive control for same treatment period (Fig. 2).

Based on the observations, HeLa cells treated with QIEA, showed the common characteristics of apoptotic cell death such as chromatin and nuclear condensation, DNA fragmentations and formation of apoptotic bodies (Zakaria *et al.* 2009). Chromatin condensations and DNA fragmentations in HeLa cells were started to be visible after 24 h of QIEA treatment. After 48 h, it was observed that the fluorescence was brighter and became more apparent. This showed that, at later stage of apoptosis, the nuclei further condensed and fragmented with intact cell membrane (Majno & Joris 1995). Besides that, the formation of the apoptotic bodies which appeared as small fluorescence spots, further confirmed the occurence of apoptosis in response to 72 h of treatment. As compared to this treated group, it was showed that, no change in nuclear morphology was detected in untreated HeLa cells. This findings is in accordance with previous study by Hasmah *et al.* (2010), in which HeLa cells treated with QI galls ethanolic extract experienced similar apoptotic manifestations.

Meanwhile, the cisplatin-treated HeLa cells also showed nuclear fragmentation and nuclear condensation with similar pattern as observed in QIEA-treated HeLa cells, and this strengthen the current findings (Sedletska *et al.* 2005). Condensed nuclei with fragmented chromatin in the treated cells represented changes in mitochondrial matrix morphology which clearly indicated the role of mitochondria (Jaudan *et al.* 2018) as indicated in HeLa cells treated with Pinostrabin (P_N) a naturally occurring dietary plant bioflavonoid. Induction of cytotoxic cell death through apoptosis in HeLa cells treated QIEA are possibly through DNA damage mechanism (Shang *et al.* 2016) exhibited by DNA fragmentation. However, further investigations are necessary to elucidate full DNA damage mechanism.

CONCLUSION

As conclusion, QIEA extract possessed the most potent cytotoxic activity towards cervical cancer cells (HeLa) with the lowest IC_{50} value among all the tested extract. In addition, cytotoxic activity of QIEA towards normal fibroblast (L929) revealed the cytoselective effect. The cytotoxic activity of QIEA were regulated by apoptosis cell death evidenced by the DNA fragmentation and chromatin condensation in the treated cells. The manifestation of cytotoxic effect and cell death event were might be due to the present of unique range of phytochemicals in the extract including

tannins, alkaloids, flavonoids, glucosides, saponins, terpenoids and phenolic compounds. Thus, the QIEA deserve further study to elucidate the phytochemicals entity and detail mechanism of cell death.

ACKNOWLEDGEMENTS

The authors would like to acknowledge Universiti Sains Malaysia for granted funding to conduct the project under Research University Grant Scheme (1001. PPSK. 813061).

REFERENCES

Abdullah A R, Hapidin H and Abdullah H. (2017). Phytochemical analysis of *Quercus infectoria* galls extracts using FTIR, LC-MS and MS/MS analysis. *Research Journal of Biotechnology* 12: 12. https://doi.org/10.1021/acs.jnatprod.5b01055

American Cancer Society. (2015). How is chemotherapy used to treat cancer? https://www.cancer.org/treatment/treatments-and-side-effects/treatment types/chemotherapy/how-is-chemotherapy-used-to-treat-cancer.html (accessed on 5 July 2019).

Asif M, Ansari S H, Haque M R and Kalam N. (2012). Standardization and contamination studies on nutgalls of *Quercus infectoria* Olivier. *International Research Journal of Pharmacy* 3(8): 149–152.

Azad N, Zahnow C A, Rudin C M and Baylin S B. (2013). The future of epigenetic therapy in solid tumours: Lessons from the past. *Nature reviews Clinical oncology* 10(5): 256. https://doi.org/10.1038/nrclinonc.2013.42

Baharuddin N S, Abdullah H and Abdul Wahab W N. (2015). Anti-Candida activity of *Quercus infectoria* gall extracts against Candida species. *Journal of Pharmacy & Bioallied Sciences* 7(1): 15–20. https://doi.org/10.4103/0975-7406.148742

Bhattacharjee S K. (2001). *Handbook of medicinal plants* (3rd edition) Jaipur, India: Pointer Publishers, 478 p.

Borgia M, Sepe N, Borgia R and Ori-Bellometti M. (1981). Pharmacological activity of an herbal extract: Controlled clinical study. *Current Therapeutic Research* 29: 525–536.

Bray F, Ferlay J, Soerjomataram I, Siegel R L, Torre L A and Jemal A. (2018). Global cancer statistics 2018: GLOBOCAN estimates of incidence and mortality worldwide for 36 cancers in 185 countries. *CA: A Cancer Journal for Clinicians* 68(6): 394–424. https://doi.org/10.3322/caac.21492

Caley A and Jones R. (2012). The principles of cancer treatment by chemotherapy. *Surgery* 30(4): 186–190. https://doi.org/10.1016/j.mpsur.2012.01.004

Dar M S, Ikram M and Fakouhi T. (1976). Pharmacology of *Quercus infectoria*. *Journal of Pharmaceutical Sciences* 65(12):1791–1794. https://doi.org/10.1002/jps.2600651224

Desoize B and Madoulet C. (2002). Particular aspects of platinum compounds used at present in cancer treatment. *Critical Reviews in Oncology/ Hematology* 42: 317–325. https://doi.org/10.1016/S1040-8428(01)00219-0

Fatima S, Farooqi A H, Kumar R, Kumar T R and Khanuja S P. (2001). Antibacterial activity possessed by medicinal plants used in tooth powders. *Journal of Medicinal and Aromatic Plant Sciences* 22(4a): 187–189.

Florea A M and Büsselberg D. (2006). Metals and metal compounds: Occurrence, use, benefits and toxic cellular effects. *Biometals* 19: 419–427. https://doi.org/10.1007/s10534-005-4451-x

_____. (2011). Cisplatin as an anti-tumor drug: Cellular mechanisms of activity, drug resistance and induced side effects. *Cancers* 3: 1351–1371. https://doi.org/10.3390/cancers3011351

Gao J, Yang X, Yin W, and Li M. (2018). Gallnuts: A potential treasure in anticancer drug discovery. *Evidence-Based Complementary and Alternative Medicine* 2018: Article ID 4930371. https://doi.org/10.1155/2018/4930371

Gandhiappan J and Rengasamy R. (2012). Comparative study on antioxidant activity of different species of Solanaceae family. *Advances in Applied Science Research* 3(3): 1538–1544.

Günes D A, Florea A M Splettstoesser F and Büsselberg D. (2009). Co-application of arsenic trioxide (As2O3) and cisplatin (CDDP) on human SY-5Y neuroblastoma cells has differential effects on the intracellular calcium concentration ([Ca2+]i) and cytotoxicity. *Neurotoxicology* 30: 194–202. https://doi.org/10.1016/j.neuro.2008.12.001

Hanahan D and Weinberg R A. (2000). The hallmarks of cancer review. *Cell* 100: 57–70. https://doi.org/10.1016/S0092-8674(00)81683-9

Harborne J B. (1986). Nature, distribution and function of plant flavonoids. In: Cody V, Middleton Jr. E and Harborne J B. (Eds.), *Plant flavonoids in biology and medicine: Biochemical, pharmacological and structure-activity relationships*. New York: Alan R. Liss Inc., 15–24.

Hasmah A, Nurazila Z, Chow C Y, Rina R, and Rafiquzzaman M. (2010). Cytotoxic effects of *Quercus infectoria* extracts towards cervical (Hela) and ovarian (Caov-3) cancer cell lines. *Health and the Environment Journal* 1(2): 17–23.

Hazwani M Y, Hasmah A and Wan Amir Nizam W A. (2018). Cytotoxicity effect of *Quercus infectoria* based vaginal cream on HeLa cells and its preliminary in vivo toxicity evaluation towards female rats. *International Medical Journal Malaysia* 17(2): 99–106.

Hwang J K, Kong T W, Baek N I and Pyun Y R. (2000). α-glycosidase inhibitory activity of hexagalloylglucose from the galls of *Quercus infectoria*. *Plant Medicine* 66: 273–274. https://doi.org/10.1055/s-2000-8569

Ikram M and Nowshad F. (1977). Constituents of *Quercus infectoria*. *Planta Medica* 31: 286–287. https://doi.org/10.1055/s-0028-1097531

Ismail N E, Bustami Effendi T J, Ali A A and Hazizul Hasan M. (2010). Acute toxicity and biochemistry studies of combined aqueous extracts of *Curcuma longa* and *Quercus infectoria*. Paper presented at International Conference on Science and Social Research, Kuala Lumpur, 5–7 December. https://doi.org/10.1109/CSSR.2010.5773882

Jaudan A, Sharma S, Malek S N A and Dixit A. (2018). Induction of apoptosis by pinostrobin in human cervical cancer cells: Possible mechanism of action. *PLoS ONE* 13(2): e0191523. https://doi.org/10.1371/journal.pone.0191523

Kanadaswami C, Lee L T, Lee P P H, Hwang J J, Ke F C, Huang Y T and Lee M T. (2005). The antitumor activities of flavonoids. *In vivo* 19: 895–910.

Kaur G, Athar M and Alam M S. (2007). *Quercus infectoria* galls possess antioxidant activity and abrogates oxidative stress-induced functional alterations in murine macrophages. *Chemico-Biological Interactions* 171(3): 272–282. https://doi.org/10.1016/j.cbi.2007.10.002

Kerr J F, Wyllie A H and Currie A R. (1972). Apoptosis: A basic biological phenomenon with wide-ranging implications in tissue kinetics. *British Journal of Cancer* 26: 239–257. https://doi.org/10.1038/bjc.1972.33

Kottakkal A V S. (1995). *Indian medicinal plants* (Vol. 4). New Delhi, India: Orient Longman Ltd.

Lim S H, Wu L, Burgess K and Lee H B. (2009). New cytotoxic rosamine derivatives selectively accumulate in the mitochondria of cancer cells. *Anti-cancer Drugs* 20(6): 461–468. https://doi.org/10.1097/CAD.0b013e32832b7bee

Lu J J, Bao J L, Chen X P, Huang M and Wang Y T. (2012). Alkaloids isolated from natural herbs as anticancer agents. *Evidence-Based Complementary and Alternative Medicine* 2012: 1–12. https://doi.org/10.1155/2012/485042

Magbool F A R, Elnima E I, Shayoub M E and Hussien E O. (2018). Antifungal potential of *Quercus infectoria* galls against candida albicans-an invitro study. *European Journal of Biomedical and Pharmaceutical Sciences* 5(2): 22–27.

Majno G and Joris I. (1995). Apoptosis, oncosis, and necrosis: An overview of cell death. *The American Journal of Pathology* 146: 3–15.

Massague J and Obernauf A C. (2016). Metastatic colonization by circulating tumor cells. *Nature* 529: 298–306. https://doi.org/10.1038/nature17038

Mc Clure. (1975). *Physiology and function of flavonoids.* New York: Academic Press.

Muhamad Z M and Mustafa A M. (1994). *Traditional Malay medicinal plants*. Kuala Lumpur: Penerbit Fajar Bakti Sdn Bhd.

Newman D J and Cragg G M. (2016). Natural products as sources of new drugs from 1981 to 2014. *Journal of Natural Products* 79(3): 629–661. https://doi/org/10.1021/acs.jnatprod.5b01055

Nurgali K, Jagoe R T and Abalo R. (2018). Adverse effects of cancer chemotherapy: Anything new to improve tolerance and reduce sequelae? *Frontiers in Pharmacology* 9: 245. https://doi.org/10.3389/fphar.2018.00245

Okuda T and Ito H. (2011). Tannins of constant structure in medicinal and food plants—hydrolyzable tannins and polyphenols related to tannins. *Molecules* 16: 2191–2217. https://doi.org/10.3390/molecules16032191

Ong H C and Nordiana M. (1999). Malay ethno-medico botany in Machang, Kelantan, Malaysia. *Fitoterapia* 70(5): 502–513. https://doi.org/10.1016/S0367-326X(99)00077-5

Pistritto G, Trisciuoglio D, Ceci C, Garufi A and D'Orazi G. (2016). Apoptosis as anticancer mechanism: Function and dysfunction of its modulators and targeted therapeutic strategies. *Aging* 8(4): 603–619. https://doi.org/10.18632/aging.100934

Rohana S, Vimala S, Abdull Rashih A and Mohd. Ilham A. (2004). Skin whitening and antioxidant properties of *Quercus infectoria* galls. In: Chang Y S, Mastura M and Nurhanan M Y. (Eds.), *Proceedings of the Seminar on Medicinal Plants. Selangor: Forest Research Institute Malaysia (FRIM),* 188–191.

Roshni P S and Ramesh K G. (2013). Anticancer activity of acetone extract of *Quercus infectoria* Olivier Fagaceae in 1, 2 dimethyl hydrazine induced colon cancer. *International Journal of Cancer Studies & Research* 2(1): 13–16. https://doi.org/10.19070/2167-9118-130002

Saxena M, Saxena J, Nema R, Singh D and Gupta A. (2013). Phytochemistry of medicinal plants. *Journal of Pharmacognosy and Phytochemistry* 1(6): 168–182.

Sedletska Y, Giraud-Panis M J and Malinge J M. (2005). Cisplatin is a DNA-damaging antitumour compound triggering multifactorial biochemical responses in cancer cells: Importance of apoptotic pathways. *Current Medicinal Chemistry-Anticancer Agents* 5: 251–265. https://doi.org/10.2174/1568011053765967

Shah N and Dizon D S. (2009). New-generation platinum agents for solid tumors. *Future Oncology* 5: 33–42. https://doi.org/10.2217/14796694.5.1.33

Shang H, Chang C, Chou Y, Yeh M, Au M, Lu H, Chu Y, Chou H, Chou H, Shih Y and Chung J. (2016). Curcumin causes DNA damage and affects associated protein expression in HeLa human cervical cancer cells. *Oncology Reports* 36: 2207–2215. https://doi.org/10.3892/or.2016.5002

Shrestha S, Kaushik V S, Eshwarappa R S, Subaramaihha S R, Ramanna L M and Lakkappa D B. (2014). Pharmacognostic studies of insect gall of *Quercus infectoria* Olivier (Fagaceae). *Asian Pacific Journal of Tropical Biomedicine* 4(1): 35–39. https://doi.org/10.1016/S2221-1691(14)60205-7

Siddiqui A A and Ali M A. (1997). *Practical pharmaceutical chemistry* (1st Edition). New Delhi: CBS Publishers and distributors, 126–131.

Soon L K and Hasni E. (2005). Consumption of traditional medicines/herbs postpartum among the Kelantanese malay women. 10th National Conference of Medical Sciences (NCMS). School of Medical Sciences, Universiti Sains Malaysia, May 2005 5: 99.

Soon L, Hasni E, Law K, Waliullah S, Farid C and Mohsin S S. (2007). Ultrastructural findings and elemental analysis of *Quercus infectoria* Oliv. *Annals of Microscopy* 7: 32–37.

Srivastava R C, Husain M M, Hasan S K and Athar M. (2000). Green tea polyphenols and tannic acid act as potent inhibitors of phorbol ester-induced nitric oxide generation in rat hepatocytes independent of their antioxidant properties. *Cancer Letters* 153(1-2): 1–5. https://doi.org/10.1016/S0304-3835(99)00400-0

Trease G E and Evans W C. (1989). *Pharmacognosy* (11th edition). London: Bailliere Tindall, 45–50.

Tsang R Y, Al-Fayea T and Au H J. (2009). Cisplatin overdose: Toxicities and management. *Drug Safety* 32: 1109–1122. https://doi.org/10.2165/11316640-000000000-00000

Umachigi K N, Jayaveera C K, Ashok Kumar G S, Kumar B M, Vrushabendra swamy D V and Kishore K. (2008). Studied on wound healing properties of *Quercus infectoria*. *Tropical Journal of Pharmaceutical Research* 7(1): 913–919. https://doi.org/10.4314/tjpr.v7i1.14677

Yoo S, Kim K, Nam H and Lee D. (2018). Discovering health benefits of phytochemicals with integrated analysis of the molecular network, chemical properties and ethnopharmacological evidence. *Nutrients* 10(8): 1042. https://doi.org/10.3390/nu10081042

Zakaria Y, Rahmat A, Pihie A H L, Abdullah N R, and Houghton P J. (2009). Eurycomanone induce apoptosis in HepG2 cells via up-regulation of p53. *Cancer Cell International* 9(1): 16. https://doi.org/10.1186/1475-2867-9-16

Ziegler U and Groscurth P. (2004). Morphological features of cell death. *News in Physiological Sciences* 19: 124–128. https://doi.org/10.1152/nips.01519.2004

Physicochemical and microbial analysis of plant-based food waste for potential used as an animal feed

Cite as: AIP Conference Proceedings **2610**, 060020 (2022); https://doi.org/10.1063/5.0100675
Published Online: 29 August 2022

Nordalilah Wahab, Husna Hawa Mohd Hassan, Wan Nur Suzilla Wan Yusuf, et al.

Physicochemical and Microbial Analysis of Plant-Based Food Waste for Potential Used as an Animal Feed

Nordalilah Wahab[1], Husna Hawa Mohd Hassan[1,b)], Wan Nur Suzilla Wan Yusuf[1,a)], Rabiatul Alawiyah Jahwi[1], Mohd Mukriz Mohd Kasim[2] and Mohd Ridzuan Abdul Rashid[2]

[1]*Department of Food Technology, Politeknik Sultan Haji Ahmad Shah, Semambu, 25350 Kuantan, Pahang,*
[2]*Department of Agrotechnology and Bio-Industry, Politeknik Jeli Kelantan, Jalan Timur-Barat, 17600 Jeli, Kelantan*

[a)] *Corresponding author: wnsuzilla@polisas.edu.my*
[b)] *hawa@polisas.edu.my*

Abstract. Food waste refers to wasted food nutrients of high quality intended for human consumption and it usually has a high nutritional value. As a result of the lower cost of food waste compared to conventional feeds, manufacturing expenses might be reduced. This present study is aimed to evaluate the potential of plant-based food waste such as soybean waste, pineapple waste, and coconut waste to be developed as animal feed. In this study, there were two main analyses conducted which are physicochemical and microbial analysis of the plant-based food waste. The physicochemical analysis conducted was total yield recovery, particle size, and moisture content followed by proximate quantification of fat, protein, crude fiber, and ash. For the microbial analysis, pH, Total Titratable Acidity, and Total Plate Count analysis were conducted. From the results, it was shown that coconut waste gave the highest reading of the total yield recovery which was 43.60%, followed by soybean waste 27.58% and pineapple waste 22.91%. For the particle size determination, it was revealed that all the samples size ranges from 600 µm – 850 µm. Moreover, it was found that all samples have a good moisture content below 10% which was suitable to be used as animal feed. Besides, it was revealed that coconut waste gave the highest fat content (39.17±0.58%) while soybean waste has the highest protein (7.27±0.67%) and fiber content (101.17±0.1%). For the microbial analysis, the soybean waste (soy dreg) was found to have the lowest pH (4.4±0.10) and highest Total Titratable Acidity (TTA) value (14.25±0.69). Meanwhile, for the Total Plate Count (TPC) analysis, it was revealed that the soybean waste has the least growth of the bacterial colony. From the findings, it was shown that the soybean waste has the potential to be used or formulated as animal feed to support the sustainable food waste management system in Malaysia.

INTRODUCTION

Waste management has become an issue of increasing global concern as urban populations continue to rise and consumption patterns change. Generally, waste comes from two major sources, they are from animal and plant-based food waste [1]. The disposal of food waste is a serious environmental problem. In the United Kingdom (UK), approximately 15 million tons of food are wasted each year, mostly disposed of in the landfills, by composting, or maybe via anaerobic digestion (AD). According to European Union (EU) norms, food waste should be utilized preferentially as animal feed; however, this practice is currently forbidden due to disease control issues. [2]. However, interest in the potential diversion of food waste for animal feed is growing, with several East Asian states offering working examples of safe food waste recycling. The low impact of food waste feed as substitution of conventional feed has significant environmental and health impacts [2]

The utilization of by-products is of great importance in rearing livestock, both in developing and developed countries. In India, for instance, various by-products such as rubber seed cake, mango seed kernel, tea waste, and tamarind seed have been recommended for use at 10% to 30% level in the concentrate of livestock ratios [3]. Taking

2nd Energy Security and Chemical Engineering Congress (ESChE 2021)
AIP Conf. Proc. 2610, 060020-1–060020-10; https://doi.org/10.1063/5.0100675
Published by AIP Publishing. 978-0-7354-4378-5/$30.00

Japan as a developed country, the food industries are the major part of the economy, accounting of total 10% of total industrial production and a huge number of industrial by-products are disposed each year [4]. The nutritional characteristics of several food industrial by-products have been investigated in comparison to conventional feeds. Studies in Japan have examined the mixing and ensiling of these by-products with other feed ingredients [4]. One of the most popular sources of supplemental protein for animal feeds is soybean meal and soybean products (dregs). This is derived from its nutritional content, anti-nutritional factor, and other issues [5].

Okara, soy pulp, or soy dregs is a solid non-soluble fraction obtained during soymilk manufacturing. About 1-2 kg of fresh okara is produced from 1 kg of soybean processed for tofu and soy drinks [5]. It is also a natural rich source of dietary fiber and protein, which can be processed to industrial useful forms such as powders, extrudates or pre-gelatinized powders. The main reason behind the limited use of okara as a food ingredient is due to its deterioration if not dehydrated or frozen rapidly [5]. With a world production of more than 18 million tons in 2009, pineapple ranks 12th among fruits crop worldwide. Pineapple waste is produced as a byproduct of pineapple cultivation and processing. Before replanting, the pineapple leaves are simply thrown away at the farm and left to burn in the open [6]. Meanwhile, pineapple debris, including skin, pulp, and rotten flesh, is sent to a dumping site to decay naturally or is burned on-site. Such pineapple waste is being thrown away even though it is still high in sugars, organic acids, and fibre [6]. One alternative use for pineapple waste is to turn it into useful goods such as animal meals [6]. Desiccated coconut is the dried shredded endosperm of the fruit of the coconut palm. Sixty-five percent of the weight of this product is fat with the fatty acid lauric (C_{12}) and myristic (C_{14}) comprising 65% of the total. It is unusual in having low level of unsaturated fatty acid so that it is relatively resistant to oxidative rancidity [7]. The discarded coconut waste included a high proportion of crude fiber [8]. According to crude fibre content, coconut waste, a byproduct of virgin coconut oil (VCO) production, might be utilized as a fiber-source-feed option to address the issue of low pasture supplies during the dry season in Indonesia [8]. Based on this, it is apparent that all of these different forms of food waste contain nutrients that may be utilised as animal feed. This current study aims to evaluate the potential of the selected plant-based food waste such as soybean, pineapple and coconut waste to be used as the potential animal feed.

MATERIALS AND METHOD

Material Preparation

There were three types of food waste samples used in this study which soybean waste (soy peel and dreg), pineapple waste (pineapple peel and dreg) and desiccated coconut. All samples were dried in the oven for 24 to 48 hours at 60°C. Then, all samples were ground to reduce the particle size and stored in bottles at room temperature prior used.

Physical and Chemical Analysis

Particle Size Determination

All samples were ground into a fine powder and separated by a sieve shaker with a series of sieves (0.425mm, 0.600mm, 0.710mm, 0.850mm and 1.400mm). Each sample was placed on top of the sieve and shaken for 10 minutes. Finally, the residue remaining on each sieve was weighed and the reading was recorded.

Moisture Content Analysis

2g of dried samples (soy peel, soy dreg, pineapple peel, pineapple dreg, and desiccated coconut) were weighed in a metal dish. Then the dish containing the samples was placed in an oven for 1 hour at 105 °C. After drying, the metal dish with samples was transferred to a desiccator for the cooling process and weighed. All these steps were repeated until a constant weight was obtained.

Determination of Crude Fat Content

2g of dried samples (soy peel, soy dreg, pineapple peel, pineapple dreg, and desiccated coconut) were weighed in a thimble. 150 ml of petroleum ether was weighed in a round flask and the reflux process was conducted for 8 hours. The extractor and the thimble were removed from the extractor after the distillation process, and the excess petroleum

ether was dried up. Then the flask was placed in an oven (105°C) for an hour. Finally, after the drying process, the flask was cooled down in a desiccator and weighed.

Protein Content Analysis

Food waste samples weighing 0.2 g were weighed in a digestion tube. About 0.8g of protein catalyst and 5 mL of concentrated sulfuric acid (H_2SO_4) were added. The mixture was digested in the digestion unit until the process was completed. All the steps above were repeated for a blank (without sample). Then all the content in the digestion tube was transferred into a distillation tube by the addition of 5 mL of water. Then, 15 ml of NaOH (32%) was added to the tube, followed by the addition of 10 ml of boric acid together with a few drops of protein indicator. The sample was distilled for 15 minutes. Finally, the sample was titrated with 0.02N HCI until the color of the solution turned pinkish.

Crude Fibre Analysis

Half of the sample was put in a thimble, and the top of the thimble was covered with cotton wool. 150ml of petroleum ether was filled into a round-bottom flask and the reflux process was run for 8 hours. Then, 2g of sample and 200ml of H_2SO_4 (0.255%) were added to the flask and the reflux process was continued for another 30 minutes. After that, 200ml of NaOH was added, followed by the reflux process again for 30 minutes. Finally, the sample was rinsed with HCI and ignited using a radiant heater prior to being weighed.

Determination of Ash Content

In a crucible, 10 g of powdered samples were weighed, followed by a slow ignition in a radiant heater until no more fumes were released. Then, the crucible was put in a muffle furnace at 550 C. The samples were incinerated for 2 hours until white powder was obtained and allowed to be cooled in a desiccator prior to weighing.

Microbial Analysis

Determination of pH Value

10 g of food waste samples were weighed in 250 ml conical flask followed by the addition of 90 ml distilled water. pH meter and litmus paper pH were used to determine the pH of the samples.

Determination of Total Titratable Acidity (TTA)

10 ml of the sample was added into a conical flask containing 100 ml of distilled water with ice cubes. Five drops of phenolphthalein were added, followed by titration with 0.1 M NaOH until a light pink colour solution was obtained. The percentage of lactic acid was calculated.

Total Plate Count (TPC) Analysis

A Total Plate Count (TPC) was conducted using the pour plate technique. A 25g sample was mixed with 225ml of buffered peptone water to obtain the stock solution. Then the stock solution was diluted in a series of serial dilutions. 1 ml from each dilution series was taken and put in a petri dish, followed by the addition of culture media. Then, the petri dishes were incubated in the incubator for 24 to 48 hours at 37°C. The number of bacterial colonies growing was counted by a colony counter.

Most Probable Number (MPN) Analysis

All samples were prepared in a 10-fold dilution series, and then 1 ml of samples of each dilution was inoculated into a tube containing broth culture prior to incubation. Following incubation, all tubes were observed for turbidity, and the microbial growth pattern in each tube was recorded in the MPN table.

RESULTS AND DISCUSSION

Determination of Particle Size of Selected Food Waste Samples

Figure 1 shows the particle size distribution (percent of cumulative vs. size of the screen) of the analyzed food waste samples. The highest fine powder with a sizing screen of 0.425mm (425m) was desiccated coconut (77.11%), while pineapple dreg (60.39%) gave the lowest fine powder with a sizing screen of 0.425mm (425m). The highest coarse powder was soy dreg (34.14%) with a sizing screen of 1.4000mm (1400m) and the lowest coarse powder was pineapple dreg (12.19%) with a sizing screen of 1.4000mm (1400m). Normally, more than 95% of coarse powder passes through a number 1400 sieve and less than 40% by mass passes through a number 355 sieve. For fine powder, more than 95% by mass passes through a number 180 sieve and less than 40% by mass passes through a number 125 sieve. The optimum particle size for animal feed should be between 600 and 900 mm [9]. Based on the results, all the plant waste in a range of 600–900 mm which within the acceptable sizing screen and suitable for the food waste to be developed as animal feed. Previous study showed that, the particle size of ground maize for feed formulation in the metropolis was coarser than recommended for poultry (628±1.93 to 1450±2.25 µm) [9]

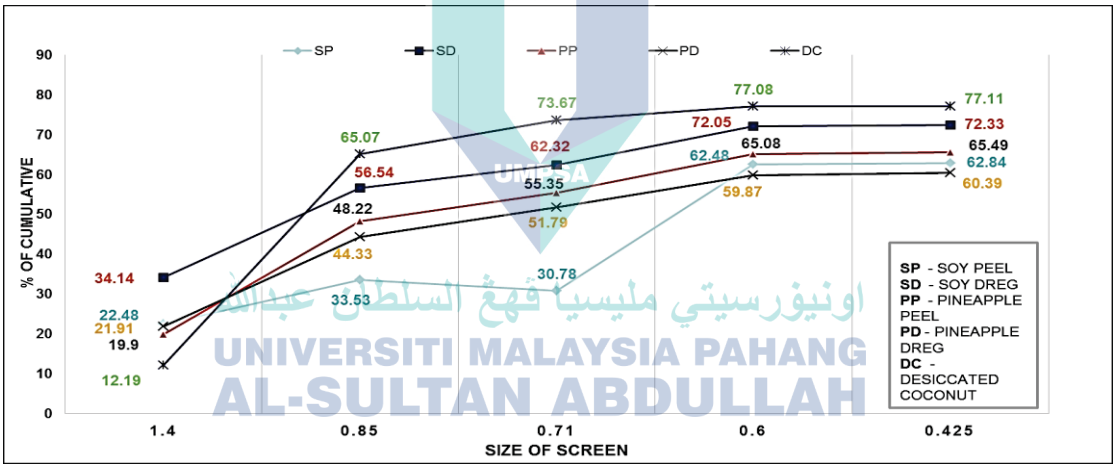

FIGURE 1. Particle size of the food waste samples

The degree of particle size depends both on the size of the fish to be fed and on the technological process to be used for pelleting, but the particle size of dry ingredients should be below 500 µm [10]. Based on the result obtained, it was showed that all waste samples have the potential to be used as fish feed because the size screen of are below 500 µm. However, from the previous study, it was revealed that the particle size intended for larval or juvenile fish should be smaller while the optimal particle size for pig diets is in the range between 500 µm and 1600 µm and the particles size smaller than 400 µm considered as undesirable with high ulcerogenic capacity [11].

Moisture Content Analysis

Determination of moisture content is important in the animal feed industry to determine the nutritional value of food samples. It is because it can display the analytical results of basic analysis tests and compare the compositions of food products or samples. Other than that, the purpose of moisture content is to prolong the shelf life of the product for up to 10 years when it becomes powder, depending on the storage conditions. According to Table 1, the moisture content of various plant wastes after 24 hours of drying at 60 °C differed. Based on Table 1, it was showed that the moisture content for different plant wastes after 24 and 48 hours of drying at 60°C. After 48 hours, it was observed

that all waste samples have moisture content lower than 10% which comply the requirement for animal feed (<13%). According to a previous study, the moisture content of the food waste samples used was higher which 81.32% ± 1.10 [12]. As compared to the current study, it showed lower moisture content, and this is good to prolong the shelf life of the formulated animal feed. Besides that, lower moisture levels can also inhibit the development of other microbes on food waste, thus lowering the quality of the produced animal feed.

TABLE 1. Moisture content of foodwaste samples

Sample	Moisture Content 24 hours	Moisture Content 48 hours
Soy peel	7.46 ± 0.12	6.13±0.12
Soy dreg	7.20 ± 1.73	6.60±0.69
Pineapple peel	13.80±0.35	9.13±0.12
Pineapple dreg	19.06±0.23	8.50±0.87
Desiccated coconut	6.67±0.23	6.47±0.23

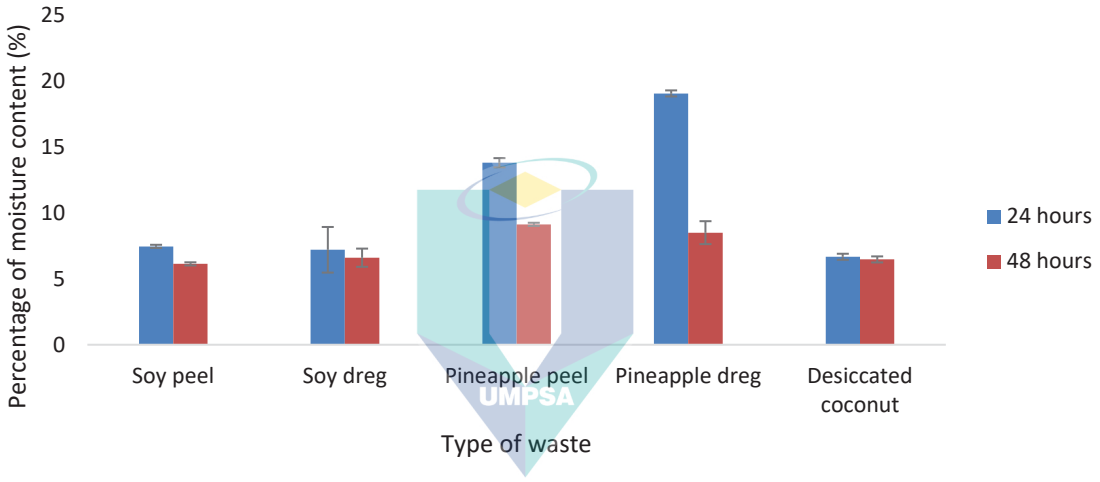

FIGURE 2. Moisture content in the food waste samples

Proximate Quantification of Selected Food Waste Samples

Protein is a source of potential energy for the animal. Protein is one of the important nutrient in food and are necessary ingredient for young developing animals [13]. Crude protein is determined by measuring the nitrogen content of the feed by Kjeldahl method [14]. From Table 2, it was showed that soy peel gave the highest protein content which was 4.2±0.67%. A previous study found that the percentage of protein content in food waste samples was 2.31 ± 0.24 %, which is lower than the proportion found in this study. This study discovered that soybean waste has a higher protein content and may be employed in the formulation of animal feed. According to Kiron et al (2016), protein levels in aquaculture feeds generally average 18-50% while for marine feeds require higher protein. Commonly soybean meal was used due to higher percentage of crude protein (70%) and a favorable amino acid profile. Besides that, soybean meal was also used as source of protein in poultry feed daily basis for maintenance, lactation, growth and reproduction. Sources of protein for animal feeds are many and varied, with considerable opportunities for further diversification and substitutions. More research is required on alternative sources before many of the opportunities can be exploited in practice. The protein requirements of animals are given in terms of an amount of protein and its constituent amino acids per unit of time; usually the amount to be fed each day. However, this value continually changes as the animal grows [15]

Crude fat is an estimation of the total fat content in food samples. Fats are very important in supplying the energy needed by an animal for normal body function. Based on the findings, it was revealed that desiccated coconut has the highest fat content, which was 39.17±0.58 % followed by soy dreg, which was 21.53±0.62 %. The result shows all the food waste samples used have high fat content that meets the requirement as stated in the Poultry Feed Specification. A previous study showed that food waste samples had lower fat content, which was 19.58 ± 1.30 %

[12]. Hence, from this current finding, it was revealed that desiccated coconut and soy dreg can be an alternative protein source due to their high protein content.

The amount of ash is determined by subjecting animal food to high temperatures under laboratory conditions. The main components of ash are usually phosphorous and calcium, but it also normally contains other minerals such as iron and zinc. Total ash content for poultry feed such as sunflower meal and corn is between 4.0 to 7.5% and 2.50% respectively [13]. From the results, it was observed that all food waste samples used in this study such soy peel, soy dreg, pineapple peel, pineapple dreg and desiccated coconut have a potential as animal feed for poultry because it contains 3%, 4.60%, 7.20%, 3.13% and 2.80% ash content respectively which comply the specification of poultry feed (< 10 %).

TABLE 2. Proximate analysis of food waste samples

Sample	Chemical analysis			
	Protein (%)	Ash (%)	Crude Fat (%)	Crude Fibre (%)
Soy Peel	4.2±0.67	3.00±0.20	11.50±0.18	51.17±0.61
Soy Dreg	3.07±0.62	4.60±0.20	21.53±0.62	50.00±0.10
Pineapple Peel	0.85±0.59	7.20±0.02	7.67±0.75	42.60±0.10
Pineapple Dreg	0.96±0.50	3.13±0.12	6.00±0.10	45.50±0.08
Desiccated Coconut	0.18±0.03	2.80±0.00	39.17±0.58	48.67±0.35

The determination of crude fibre is one of the important parameters in food analysis. The crude fibre analysis involved sequential acid and alkali extraction. Crude fibre is primarily measured to comprehend indigestible parts in feeds, and is consisted mainly of a part of lignin, pentosan, chitin, etc., in addition to cellulose. Based on the results, it was observed that soy peel has the highest crude fibre content which was 51.17±0.61% while pineapple peel has the lowest fiber content which was 42.60±0.10%. The optimal crude fiber content proportion for ruminant feed hull is between 31 and 58 percent. As a consequence, all samples in this present study had an acceptable value of crude fibre content and suitable to be used in the formulation of animal feed. From the previous research, it was shown that the crude fiber content in a food waste sample was 2.04 ± 0.45 %, which is much lower as compared to this current study [12]. Hence, it can be revealed that soybean waste is composed of high fibre content and is good as an alternative source of crude fiber.

Percentage of pH and Total Titratable Acidity

Few types of food waste samples were used in this study which were soy peels, soy dregs, pineapple peels, pineapple dregs, and desiccated coconut (raw and powder form). All samples were subjected to pH and Total Titratable Acidity (TTA) analysis. From the results (Figure 3), it was showed that the pH value of raw soy peels is (6.33±0.058) and powder soy peels (4.8±0.20). There are no significant different when compare the pH of raw and powder soy peels. The pH value of raw soy dregs (4.4±0.10) and pH value of powder soy dregs (4.73±0.12). Soy dregs have been fermented before drying process which reduce the pH value of soy dregs. According to Katsuaki Sugiura (2009), food wastes have been fermented before it was been used as an animal feed. Soy dregs might have longer shelf life when used as an animal feed because of the pH value of soy dregs is in acidic condition. Besides that, pH value of raw pineapple peels was 5.3±0.50 and this is higher than pH value of powdered pineapple peels (4.03±0.058). There are significant different between the pH of raw and powdered pineapple peels. Generally, the pineapple fleshes are highly acidic. The pH value of raw pineapple dregs was 3.97±0.058 and pH value of powdered pineapple dregs was 3.833±0.058. Raw desiccated coconut has higher pH value which was 6.37±0.15, while powder desiccated coconut has more acidic pH value (5.07±0.058). Usually, food with lower pH value (below 4.5), pathogens is not expected to survive, somehow this would be limited to yeast, moulds, and a few acids tolerant bacteria. Lower pH value can prolong the shelf life of the animal feed and may contains higher lactic acid bacteria that is crucial in the production of animal feed. The overall acid content in a food is measured by titratable acidity (also known as total acidity). Extensive titration of intrinsic acids with a standard base yields this value. Titratable acidity, rather than pH, is a stronger predictor of acid's influence on flavour [16]. For example, a microorganism's capacity to grow in a specific food type is more dependent on the quantity of free hydronium ions, H3O+, than on titratable acidity. These hydronium ions form in aqueous solution from the reaction of water with hydrogen ions (H+) dissociated from acids. The requirement to quantify free H_3O^+ concentration leads to the second key notion of acidity, pH.

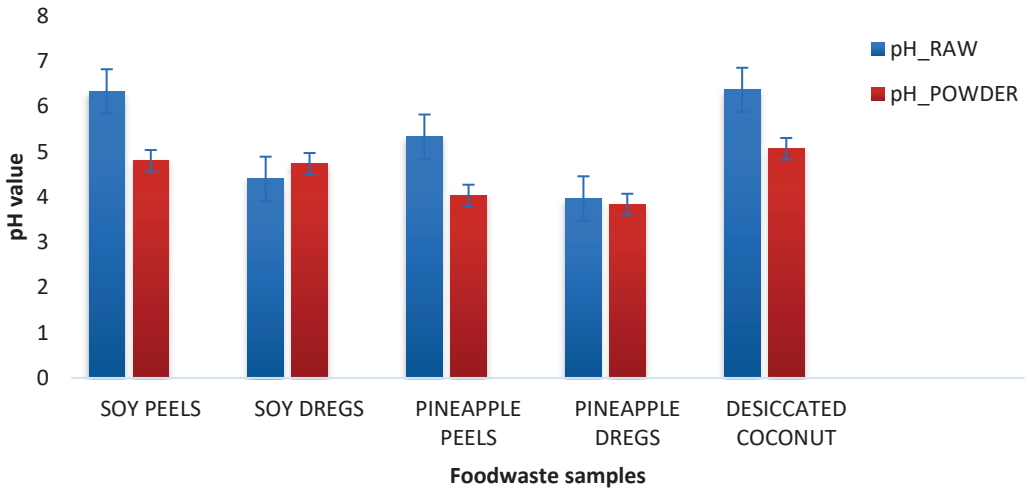

FIGURE 3. pH value of the food waste samples

Furthermore, the TTA analysis of the food waste samples showed that the percentage of total acid in the samples correlated with the pH of the samples. Food waste samples with lower pH (more acidic) gave higher percentage of total acid. From the findings (Figure 4), it was showed that percentage of TTA for raw soy peels was 1.02±0.19, raw soy dregs was 3.63±0.052, raw pineapple peels was 0.067±0.020, raw pineapple dregs was 0.121±0.007 and raw desiccated coconut was 0.69±0.29. From these results, it was revealed that raw soy dregs have a significant different when compared to other samples. This may due to the nature of raw soy dregs which have been naturally fermented for quite period of time and this can increase the pH value gradually. Therefore, the increment in pH will cause the percentage of TTA also increases due to increase in lactic acid content. As for the powdered samples, it was observed that the pH of soy peels was 7.08±0.57, soy dregs was 14.25±0.69, pineapple peels was 1.133±0.058, pineapple dregs was 1.37±0.12 and desiccated coconut was 7.89±1.21. The percentage of TTA for soy dregs have significant different when compared to all samples. This result may due to the ability of soy dregs to ferment itself without addition of any substances thus resulted in increment of pH and total acidity. This cause both raw and powder soy dregs have the highest value of TTA percentage. According to Ambuseivi, (2014), implying the pH range of pineapple waste is 2-5 to 7.0 and he reported a titrable acidity of pineapple waste is 1.86% while the value for the whole fruit ranged from 0.80% to 1.50%. The higher the percentages of TTA are in positive correlation with the lactic acid of samples. The highest lactic acid in samples will give the lower pH value of sample.

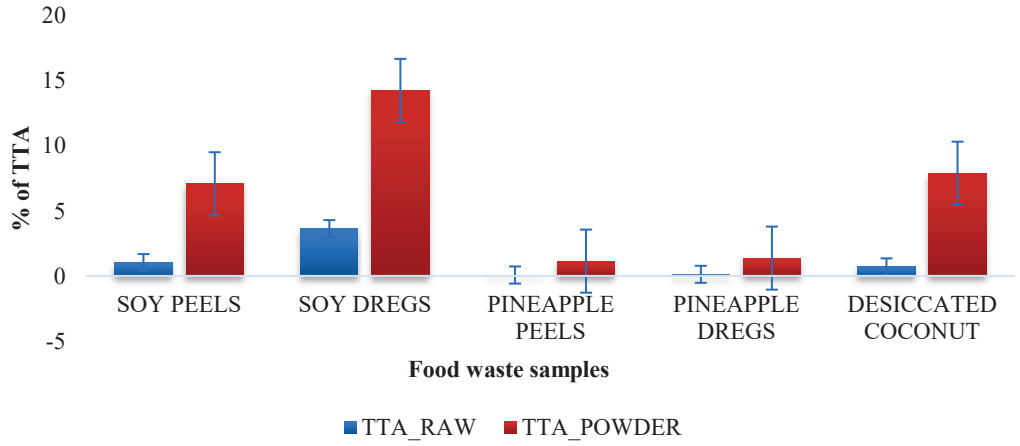

FIGURE 4. Percentage of Total Titratable Acidity of the food waste samples

Total Plate Count (TPC) Analysis

Total plate count (TPC) gives a quantitative estimate of the microorganisms such bacteria, yeast or mold spores in a sample. According to International Organization for Standardization (2002), the count represents the number of colonies forming units (cfu) per g (if sample in solid form) and per ml (if sample in liquid form). General range for viable colony growth on plate is starting from 25 to 250. If more than that, the colony is calculated as too numerous to count (TNTC). Two common methods that usually used are pour plate or spread plate. Serial dilution used is still same which should have 10^{-1} to 10^{-6} [17]. Since the analysis is for non-selected microorganisms, so there is no specific media used, and it is either Nutrient or Plate Count Agar (PCA) and Peptone Water broth (PPW). Obtaining an estimate of the number of microorganisms in an animal feedstuff could be used to evaluate sanitary practices during further processing and handling. It can determine the potential sources of contamination by testing line samples taken at successive stages of receiving, storage, processing and feeding. Next, this count also can sometimes be used to indicate the microbial quality and spoilage level of the feedstuffs [18]. Selective testing for pathogens or other microorganisms is also required in processing of animal feeds but it might be costly, time consuming and time consuming. Therefore, total plate count should be done first, and then proceed with selective microorganisms.

TPC (Total Plate Count) analysis was conducted for non-selected microorganisms followed by confirmation for selected microorganisms such as *Salmonella*, *E. coli* and *Lactobacillus*. Table 3 below shows the confirmation of non-selected microorganisms.

TABLE 3. Confirmation of non-selected and selected microorganisms in foodwaste samples

Samples	Total Plate Count (cfu/g)	*E. coli* (cfu/g)	*Lactobacillus* (cfu/g)	**Salmonella*
Soy peels	$6.1x10^2$	$9.3x10^2$	$<25x10^1$	-
Soy dregs	$4.3x10^5$	$2.4x10^3$	$3.8x10^3$	-
Pineapple peels	$1.4x10^5$	$>1.1x10^4$	$<25x10^1$	-
Pineapple dregs	$1.4x10^5$	$2.9x10^2$	$2.8x10^3$	-
Desiccated coconut	$9.5x10^4$	$4.3x10^2$	$3.7x10^2$	-

*Intensive growth (+++); moderate growth (++); low growth (+); no growth (-)

From the findings, it was showed that soy peel has the lowest microbial growth where the number of colonies was $6.1x10^2$ cfu/g while soy dregs showed the highest colonies growth which was $4.3x10^5$ cfu/g. While for the pineapple peels was $1.4x10^5$ cfu/g and pineapple dregs has approximately $1.4x10^4$ cfu/g colonies growth. There was $9.5x10^4$ cfu/g colonies growth in desiccated coconut. From the results it was observed that all samples showed acceptable value of microbial growth which complied with the International Microbiology Standard where ($3.0x10^5$ cfu/g) for older animals and $5.0x10^5$ cfu/g for younger animals [19]. For this non-selected microorganism's analysis, pour plate method has been applied. Pour plate technique is more accurate and easier compared to spread plate technique. It is because this technique can prevent the agar from lacerated and affects the growth of the microorganisms [20].

As for the selected microorganisms, which was *E.coli,* all samples has positive present of E.coli, but not in each tested tubes. For soy peels, it has number of colonies growth was $9.3x10^2$ cfu/g (MPN value 93) while for soy dregs was $2.4x10^3$ cfu/g (MPN value 240). For the pineapple peels, the number of colonies was $>1.1x10^4$ cfu/g (MPN value >1100) which was the highest among those samples. Pineapple dregs have the lowest colonies growth with $2.9x10^2$ cfu/g (MPN value 29) while for desiccated coconut, the colonies number was $4.3x10^2$ cfu/g (MPN value 43). The acceptable range for *E. coli* is between 10^3 to 10^5. From the results, it was revealed that, the colony number was within acceptable range, hence it is safe to be developed as animal feed. This is very crucial as pathogen such as *E. coli* was responsible for the foodborne disease. For the confirmation of the *E. coli,* all samples were analyzed with the Durham Test. According to a previous study, if there is a presence of *E. coli* in those samples tested, the colour of the McConkey broth will change from purple to yellow. This indicates whether the sample is positive for *E. coli* or not. Another one is by observing each of the tubes, whether there is a bubble present or not. The bubble that appears means there is *E. coli,* or the coliforms, as they show breathing and producing bubbles.

For the confirmation of *Lactobacillus* sp., it was shown that all food waste samples gave positive results where these findings showed that there was lactobacillus growth in each of the tested food waste samples. From the results it was showed that soy and pineapple peel have the lowest number of colonies growth which were $<25x10^1$ cfu/g. Soy dreg has the highest colonies growth which the result was $3.8x10^3$ cfu/g followed by pineapple dreg has $2.8x10^3$ cfu/g

colonies number. For the desiccated coconut it was observed that the number of colonies appear was $3.7x10^2$ cfu/g. However, the presence of these probiotic bacteria in all samples is promising because the acceptable range for *Lactobacillus* in animal feed is below than $1.0x10^9$ cfu/g [21]. This can support our current findings where all food waste samples tested gave lower growth of Lactobacillus sp. Lactobacillus sp. is more prevalent in environments with higher lactic acid content.

For the detection of Salmonella sp, it was revealed that all samples tested negative. This was due to the absence of colonies observed after the test was conducted. The *Salmonella* growth will show a black or dark centre and the colour of the media used (XLD agar) will change to pink. During the observation, only the pink colour of media agar was detected and no black or dark centre was spotted at all, which shows there is no presence of *Salmonella.* Confirmation of this kind of selected microorganism usually requires enrichment media. Enrichment media will help to increase and provide a better outcome for this selected microorganism to grow. Therefore, it was concluded that all samples were free from *Salmonella* contamination. Previous findings stated that animal feed that contaminated with *Salmonella* species had risk of infection to animal's health [22]. Hence, from the findings, soy dreg and pineapple peel have the most suitable acidity and pH value for ruminant feedstuffs. Based on the non-selected microorganisms, soy peel was the least contaminated. In *E. coli* confirmation, soy dreg was the least contaminated with this pathogenic bacterium. Soy dregs were the samples that had the most probiotic *Lactobacillus*. Lastly, the presence of *Salmonella* was not detected in all samples that have been analyzed. This has meant that all samples are acceptable for ruminant feedstuffs.

CONCLUSION

From the findings, it was revealed that soybean waste had the highest crude fiber content as well as protein and fat content. Furthermore, all food waste samples had good ash content, which was within the acceptable range. In terms of microbial analysis, all samples met the Microbiology Quality Standard, with acceptable ranges for pH (5.5–7.0), E. coli (10^3–10^5), Lactobacillus (1.0x109 cfu/g), TPC (3.0x105 cfu/g for older animals) and (5.0x105 cfu/g for younger animals), and Salmonella (Not Detected). Hence, it can be concluded that all these food waste samples have the potential to be developed as animal or fish feed in the future and used as one of the more prominent and nature-friendly food waste handling methods that support the sustainable food waste management system and are suitable for future implementation in Malaysia.

ACKNOWLEDGEMENT

This study was supported by TVET Applied Research Grant Scheme (TARGS) (1001/21). We also would like to thank Department of Food Technology, Politeknik Sultan Haji Ahmad Shah (POLISAS) and Department of Agrotechnology and Bio-Industry, Politeknik Jeli Kelantan for providing the equipment and facilities used in this project.

REFERENCES

1. R. E. Marshall and K. Farahbakhsh, Waste Manag. **33**, 988–1003 (2013).
2. R. Salemdeeb, E. K. H. J. zu Ermgassen, M. H. Kim, A. Balmford and A. Al-Tabbaa, J. Clean. Prod. **140**, 871–880 (2017).
3. A. P. Sulaeman, Y. Gao, T. Dugmore, J. Remón and A. S. Matharu, Cellulose **28**, 687–7705 (2021).
4. T. Hasegawa, "Current Situation of Food Waste in Japan & Food Waste Recycling Law, **1**, 21 (2015).
5. H. K. Dei, "Soybean as a Feed Ingredient for Livestock and Poultry," Recent Trends Enhancing Divers. Qual. Soybean Prod., no. May, 2011, doi: 10.5772/17601.
6. N. Buliah, S. Jamek, A. Ajit and R. Abu, AIP Conf. Proc. *2124*, 1–5 (2019).
7. T. H. Wahyuni, N. Ginting, Yunilas, Hasnudi, E. Mirwandono, G. A. Siregar, I. G. Sinaga and I. Sembiring, IOP Conf. Ser. Earth Environ. Sci. 122, 012129 (2018).
8. M. Muhlisin, C. T. Noviandi, U. G. Mada, and L. M. Yusiati, "The effects of coconut meat waste as feed alternative in sheep ration on cholesterol content and meat quality," in the Proceeding of The 17th Asian-Australasian Association of Animal Production Societies Animal Science Congress, Fukuoka, Japan,. August, 2016.
9. A. Addo, A. Bart-Plange and J. O. Akowuah, ARPN J. Agric. Biol. Sci. **7**, 177–181 (2012).
10. P. Alexander, C. Brown, A. Arneth, C. Dias, J. Finnigan, D. Moran and M. D. A. Rounsevell, Glob. Food Sec.

15, 22–32 (2017).
11. Đ. Vukmirović, R. Čolović, S. Rakita, T. Brlek, O. Đuragić and D. Solà-Oriol, Anim. Feed Sci. Technol. **233**, 133–144 (2017).
12. C. Chun Ng, A. Ismail, M. Zaini Makhtar, M. Fikri Jamaluddin and H. Tajarudin, Int. J. Recycl. Org. Waste Agric. **9**, 33-47 (2020).
13. M. Determination and E. Extract, "Proximate analysis of feedstuff," pp. 1–10.
14. M. Serhan, M. Sprowls, D. Jackemeyer, M. Long, I. Diez Perez, W. Maret, N. Tao and E. Forzani, "Total iron measurement in human serum with a smartphone," AIChE Annu. Meet. Conf. Proc. (2019).
15. E. L. Miller, Protein Sources Anim. Feed Ind. **1**, 1–44 (2002).
16. G. D. Sadler, "pH and Titratable Acidity," in Food Analysis, editted by S. Suzanne Nielsen (Springer, Cham, 2017), pp. 389–406.
17. R. Maio, J. García-Díez and C. Saraiva, Foods **9**, 1–12 (2020).
18. K. Palaniveloo, M. A. Amran, N. A. Norhashim, N. Mohamad-Fauzi, F. Peng-Hui, L. Hui-Wen, Y. Kai-Lan, L. Jiale, M. G. Chian-Yee, L. Jing-Yi, B. Gunasekaran and S. Abdul Razak, Processes **8**, 1–30 (020).
19. J. W. Pepper, PMID **62**, 3185-3191 (2008).
20. E. R. Sanders, J. Vis. Exp. **63**, 1–18 (2012).
21. N. Vieco-Saiz, Y. Belguesmia, R. Raspoet, E. Auclair, F. Gancel, I. Kempf and D. Drider, Front. Microbiol. **10**, 1–17 (2019).
22. O. B. A. Hegazy AI, J. Bacteriol. Parasitol. **5**, 5–7 (2014).